THE UNIVERSITY OF HULL

Applications and Developments of Chemometric Methods for Process Analytical Chemistry

being a Thesis submitted for the Degree of

Doctor of Philosophy

in the University of Hull

by

Ruth Helen Wellock, MChem

(March 2006)

Acknowledgements

This work has been funded by the Engineering and Physical Sciences Research Council (EPSRC) with assistance from the Centre for Process Analytics and Control Technology (CPACT).

I would like to thank my supervisor, Dr. A. D. Walmsley for all his help and guidance during my research. Thanks also go to Dr. Geir Rune Flåten and Tom Dearing for all their advice, discussions and continuous help with my work.

I would also like to thank all those that have made this work possible. This includes the technical staff at the University of Hull, and all those that have helped me in any way. Many thanks go to all my friends at the University of Hull whose friendship and support has been a great help.

My greatest thanks and appreciation go to those friends who have helped me through the writing up process by listening to me, supporting me and who have been incredibly understanding. I couldn't have done it without you.

Also a special thanks has to go to my mum for all her support over the years. Thanks for reading my thesis even though you don't understand most of it!

Abstract

Traditional process monitoring methods of off-line analysis involve removing a sample from the process and taking it to a centralised analytical laboratory. It takes time for the analytical result to be achieved and the result is used retrospectively to determine the yield or quality of a batch, and not to control the process. This leads to batches being produced that do not meet specifications, so may require re-working, wasting time and money. The process should be monitored to allow control of the batch to ensure it meets specifications first time, and every time. The use of at-line or on-line analysis, such as near infrared spectroscopy, provides quicker process analysis and allows the results to be used to monitor and control the process. These techniques are usually non-destructive so less waste is produced, and are safer as they can be located away from the process environment.

Within the analysis of processes, sampling is a key issue. The sample must be representative of the process to ensure the analysis gives a true indication of the batch. This is a problem when the process is heterogeneous as a sample taken from one region of the process may give a different analytical result from a sample taken from another region.

Guided microwave spectroscopy (GMS) has been investigated for its use as an on-line process analyser. The GMS has a sample chamber in which a process can be carried out and this whole chamber is analysed. This removes the sampling issue. This method is not well understood or used in process analysis due to the complicated MW spectra. Near infrared (NIR) spectroscopy is a tried and tested method of process analysis and many examples of applications exist of its use in industry. The spectra are easy to interpret and relate to the process. The main problem with NIR is that a probe must be used for on-line analysis. This produces sampling issues, and any process variation, such as a process upset, must be in the vicinity of the probe to be detected.

In this work, a new process analysis technique, GMS, has been compared to an established technique, NIR, to determine their effectiveness within process analysis. NIR is used as a reference method for the GMS to aid interpretation of the spectra, and relate it to the process.

Various processes have been investigated to determine the effectiveness of NIR and GMS to monitor them. A drying process has been monitored which has a problem of sampling due to huge cakes of several tonnes of material that are dried.

The drying process was first simulated by adding solvent to a material to determine if the process can be monitored and the limits of solvent that can be detected. NIR data was collected using a diffuse reflectance probe. The spectra were found to be unrepresentative of the process as it was reliant on the solvent added being in the vicinity of the probe. GMS was used to monitor the process as it provides a representative measurement. Three different systems were analysed: the addition of water to sand, propanol to ascorbic acid and ethanol to salicylic acid. Simple partial least squares (PLS) models were built to predict the amount of solvent present in the solid sample from MW spectra. Various pre-processing techniques were examined to produce the best model. The models were built using auto-scaled followed by Box-Cox logarithmically transformed data, and allow prediction of the amount of water in sand, and the amount of propanol in ascorbic acid down to 1% w/w with relative errors below 5%. The calibration models can predict up to 30% solvent, so the technique was shown to be very useful for monitoring the drying of a solid. The model for the addition of ethanol to salicylic acid gave relative errors of 32% so seems to be an unsuitable method. However, models built using above 2% ethanol gave relative errors of only 2%, suggesting the MW spectra are not sensitive to levels of ethanol below this.

Propanol was then removed from ascorbic acid by drying to prove that the actual drying method can be monitored. The use of principal component analysis (PCA) scores plotted against time and the residuals (process spectra minus the reference dry spectra) show that the drying process has the possibility of being monitored in a representative way using MW spectroscopy.

An esterification reaction has been monitored and various aspects of this process have been investigated. Traditionally calibration models are built using reference concentration spectra. Ideally process samples should be used to build the model which means a reference method such as GC must be used to give concentration data. These methods take time to develop and within this work it was found difficult to get reproducible results. Calibration free techniques have been used to extract the concentration profiles of the reaction to allow the rate constants of the reaction to be

determined. A calibration free technique has also been used to determine the endpoint of the process, and also detect process upsets. During these processes, it is desirable to be able to predict the endpoint of a reaction, instead of waiting for it to be reached, which may waste time. It is also advantageous to be able to detect process upsets to allow the batch to be corrected.

Multivariate curve resolution (MCR) was used to extract the concentration profiles from the MW and NIR spectra, and these profiles used to calculate the rate constants, k of the reaction. The MW and NIR calculated k values do not agree, suggesting the two techniques do not capture the same process variation. The rate constants have also been calculated using GC measurements as a comparison. These values also do not agree with the spectroscopic methods, but it is unknown which method provides the correct determination of the rate constant. However, it has been found that the use of MW and NIR spectroscopy provides a much more reproducible method to monitor esterification reactions than GC.

An adaptive algorithm called caterpillar has been used to determine the endpoint of an esterification reaction, and also to detect a variety of process upsets. This allows the reaction to be monitored to ensure it proceeds as expected without the need for building a calibration model. The endpoint was detected reproducibly for MW spectra taken for repeat reactions showing the spectra are suitable for monitoring the reaction. The same endpoint was not detected for corresponding NIR spectra, so this does not appear to be as reproducible a method.

MW spectroscopy was found to detect process upsets of addition of incorrect catalyst, addition of water, addition of an interferant and incorrect changing of reactants. The NIR was found to only pick up the addition of water and incorrect charging of reactants. It has been found that the MW spectra are more sensitive to small disturbances in the process variation and it is a better technique for endpoint determination and process upset detection. The NIR spectra does not appear to be as representative of the process, possibly due to the limitations of sampling with the probe used.

Glossary of terms

ALS	Alternating Least Squares
Box-Cox	Box-Cox transformation
EFA	Evolving Factor Analysis
FID	Flame Ionising Detector
GC	Gas Chromatography
GMS	Guided Microwave Spectroscopy
GUI	Graphical User Interface
HPLC	High Performance Liquid Chromatography
ICP-MS	Inductively Coupled Plasma-Mass Spectroscopy
Inter-WS	Inter Window Size
LVs	Latent Variables
MCR	Multivariate Curve Resolution
MLR	Multiple Linear Regression
MSPC	Multivariate Statistical Process Control
MW	Microwave
NIR	Near Infrared
OSC	Orthogonal Signal Correction
PCA	Principal Component Analysis
PCR	Principal Component Regression
PCs	Principal Components

PLS	Partial Least Squares
RMSEC	Root Mean Square Error of Calibration
RMSEP	Root Mean Square Error of Prediction
RSD	Relative Standard Deviation
RSSQ	Residual Sum of Squares
SIMCA	Soft Independent Modelling of Class Analogy
WS	Window Size
X-block	Spectral data
Y-block	Concentration data

TABLE OF CONTENTS

1.0 INTRODUCTION 1

1.1 Aims 1

1.2 Development of process analysis 2

1.2.1 Process analysis 2

1.3 Process analysers 4

1.3.1 Near infrared spectroscopy 6

1.3.2 Microwave spectroscopy 8

1.3.3 Comparison of MW and NIR 11

1.4 Chemometrics 11

1.4.1 Unsupervised modelling 12

1.4.2 Supervised modelling 15

1.4.3 Reaction monitoring 23

1.4.4 Fault detection 24

1.5 Drying process 29

1.5.1 Current methods 29

1.5.2 Advantages of NIR and MW 30

1.6 Esterification 31

1.6.1 Background 31

1.6.2 Current methods 31

2.0 EXPERIMENTAL 33

2.1 Reagents 33

2.2 Equipment 33

2.2.1 Near infrared spectrometer 33

2.2.2 Guided microwave spectrometer 34

2.2.3 Other equipment 37

2.3 Drying experiments 38

2.3.1 Wetting 39

2.3.2 Drying 41

2.3.3 Summary of experiments 43

2.4 Experimental set-up for esterification **43**
2.4.1 Optimum location of the NIR probe 43
2.4.2 Effect of temperature on the collected spectra 44
2.4.3 Effect of volume of liquid in the GMS chamber on the recorded spectra 45

2.5 Esterification reactions **45**
2.5.1 Aim 45
2.5.2 Experimental setup for esterification reactions 46
2.5.3 Characterisation esterification experiments 47
2.5.4 Monitoring of reaction progress by GC 47
2.5.5 Process upsets 50
2.5.6 Summary of experiments 53

2.6 Data analysis **54**
2.6.1 Wetting 54
2.6.2 Drying 56
2.6.3 Esterification 57

3.0 RESULTS AND DISCUSSION **62**

3.1 MONITORING THE DRYING OF A SOLID **62**

3.1.1 Wetting **62**
3.1.1.1 Addition of water to sand 63
3.1.1.2 Addition of propanol to ascorbic acid 89
3.1.1.3 Addition of ethanol to salicylic acid 95
3.1.1.4 Conclusions 100

3.1.2 Drying **102**
3.1.2.1 Drying by the heating of the MW chamber 102
3.1.2.2 Drying by hot air 106
3.1.2.3 Conclusions 109

3.1.3 Overall Conclusions **109**

3.2 EXPERIMENTAL SET-UP FOR ESTERIFICATION REACTIONS **111**

3.2.1 Optimum location of the NIR transmission probe in the GMS chamber **111**
3.2.1.1 Experimental details 111
3.2.1.2 Results and discussion 111
3.2.1.3 Conclusions 114

3.2.2 Effect of temperature on the collected spectra **115**
3.2.2.1 Experimental details 115
3.2.2.2 Results and discussion 115
3.2.2.3 Conclusions 120

3.2.3 Effect of volume of liquid in the GMS chamber on the recorded spectra **120**
3.2.3.1 Experimental details 121
3.2.3.2 Results and discussion 121
3.2.3.3 Conclusions 121

3.3 EXPLORATORY ANALYSIS OF THE ESTERIFICATION REACTION DATA **123**

3.3.1 NIR spectra **123**

3.3.2 MW spectra **126**
3.3.1 Cut-off point 126

3.3.3 PCA **128**

3.3.4 Conclusions **129**

3.4 MONITORING OF AN ESTERIFICATION REACTION **130**

3.4.1 GC Set-up **130**
3.4.1.1 Method development 130
3.4.1.2 Calibration 131
3.4.1.3 Reaction monitoring 134

3.4.2 Reaction spectra **137**

3.4.3 Prediction of k value **139**
3.4.3.1 GC prediction 139
3.4.3.2 Multivariate curve resolution (MCR) 142

3.4.4 Conclusions **148**

3.5 ENDPOINT DETERMINATION OF AN ESTERIFICATION REACTION .. **150**

3.5.1 Experimental set-up **150**

3.5.2 Results and discussion **150**
3.5.2.1 Esterification reaction at 40°C, 1:2 initial molar ratio, 1ml catalyst 151
3.5.2.2 Esterification reaction at 50°C, 1:0.25 initial molar ratio, 1ml catalyst 163

3.5.2.3 Esterification at 40°C, 1:2 initial molar ratio, 4ml catalyst 168

3.5.3 Conclusions **173**

3.6 DETECTION OF PROCESS UPSETS DURING AN ESTERIFICATION REACTION **174**

3.6.1 Experimental set-up **174**

3.6.2 Results and discussion **174**

3.6.2.1 Determination of window size and number of components 175

3.6.2.2 Addition of catalyst 179

3.6.2.3 Charging of half of the reactants 181

3.6.2.4 Addition of water 182

3.6.2.5 Addition of benzoic acid 183

3.6.2.6 Disturbance of stirrer 183

3.6.3 Conclusions **186**

4.0 CONCLUSIONS **187**

4.1 Drying **188**

4.2 Esterification reactions **189**

4.3 Overall conclusions **192**

5.0 FURTHER WORK **194**

6.0 REFERENCES **195**

1.0 Introduction

1.1 Aims

The aim of process analysis and control is to provide continuous monitoring of industrial chemical processes and provide feedback to enable control and optimisation. Traditionally the data has been based upon process variables, such as pressures, temperatures and flow rates, rather then chemical variables, such as reaction composition. This work is aiming to develop a system of chemical feedback, to monitor the progress of a batch process. The data from the progression of the reaction is analysed and can be used to alter the reaction conditions to ensure the reaction is controlled and conditions optimised to push the reaction to completion. Also the data can be used to predict endpoints of full scale reactions to ensure the batch is right first time, and every time.

Two typical processes have been investigated; drying, a solid state process, and esterification, a liquid state process. These reactions have been monitored in-situ, in real time using a combination of process analysers; near infrared (NIR) spectroscopy and guided microwave spectroscopy (GMS). NIR is a proven method for process analysis in a wide range of industries including food analysis, pharmaceuticals and organic reactions [1-5]. MW spectroscopy is a technique that has not been widely used, but does appear to have advantages over NIR [6]. The main advantage of MW spectroscopy is the whole process sample is analysed so giving a truly representative measurement of the process.

The aim of the work was to use this collected data along with chemometric techniques to monitor the processes. Techniques are used which have advantages over current methods, to improve the monitoring of these processes.

A drying process has been monitored. The aim of this work was to monitor the process to allow prediction of the amount of solvent in a sample down to very low levels so it can be determined when the sample is dry. The method needs to be reproducible and allow representative monitoring of the whole process.

A simple esterification reaction has also been monitored. In this research, the aim was to find a method of analysis to monitor the reaction on-line. This method must be

reproducible. Traditional methods of monitoring reactions involve tedious model building. The aim of this work was to investigate methods to monitor the reaction without the need for reference methods or model building. Also it was aimed to be able to detect process upsets in real-time to allow correction of the process.

1.2 Development of process analysis

Traditionally in process monitoring a sample is removed from a process and analysed in a centralised laboratory. The results are used retrospectively to determine the yield obtained or determine if the batch should be re-worked or discarded [7]. This is deemed off-line analysis and is time consuming, and leads to waste. This led to at-line analysis in which a dedicated analyser is located close to the process to provide faster analysis [8].

More recently there has been a move to on-line analysis in which the process is itself measured without needing to remove a sample [7]. The need for this is to reduce costs and increase production by providing fast, real-time monitoring.

The use of process analysis to monitor and control chemical processes is becoming more widespread. In 1984 the Center for Process Analytical Chemistry (CPAC) was established at the University of Washington [9]. Its British counterpart, the Centre for Process Analytics and Control Technologies (CPACT) was founded in 1997 [10]. These are concerned with the devolvement of process analysis techniques for industrial applications.

The increased use of on-line process analysis has been aided by the increase in power of microcomputers allowing more data to be collected and analysed. Also there is increased international competition to produce cheaper products of higher quality [7].

1.2.1 Process analysis

There is increasing pressure to make higher quality products at lower costs and with less waste. In continuous processes the aim is to keep the process composition steady at around the optimum physical and chemical conditions [11]. Traditionally, process samples are sent to a centralised laboratory. The results are obtained after some time, and are not used to adjust the process, but to identify if a final product is within specification, and determine if it must be reworked. Analytical chemistry has an important role in the process control chain. It is more advantageous to use process

analysis immediately for process control. Any abnormalities seen in the process can be corrected [12]. It is important to take corrective action as early as possible to ensure that the product meets specification [13]. The quality of analytical results, expressed in terms of speed, precision and sampling rate, defines the effectiveness of process control [14].

On-line process analysis allows the monitoring of a process from a remote location. By keeping personnel away from the process, safety and industrial hygiene concerns are overcome [13, 15]. Health and safety is a very important aspect in industry, and remote measurements reduce risks.

Process measurements have traditionally included temperature, pressure and flow rate. More efficient process control can be achieved by measuring composition or structural properties, in a way that allows real-time control during the manufacturing process [16]. Chemometrics is used to develop correlations between responses and chemical composition [12]. Critical process parameters must be first established in relation to product quality before process analysis can be implemented [13].

Process analytical chemistry is the application of analytical science to the monitoring and control of industrial chemical processes. Process analysers monitor chemical processes in real time and use this information to control or optimise the process [17]. Spectroscopic techniques are very useful in process analysis, the most widely used being vibrational spectroscopy, including near infrared (NIR), and Raman [18].

For true process control rather than simple process monitoring, analytical information about the process must be in real-time to allow process feedback. It is not always suitable to follow a recipe in which materials are added, stirred and switched off after a specific time, as no two batches will behave in exactly the same way. The quality of the product should be ensured throughout the process instead of just analysing the final product [12]. The aim is to get products right first time, every time. This also minimises the amount of waste that is produced from off-grade products, which has an environmental benefit [15].

The majority of error in process analysis can be attributed to the sampling system [19]. Therefore, a system of on-line, non-invasive monitoring is preferable, to provide the analyser with a sample representative of the process [16, 20, 21].

Calibration models are needed to correlate the process to any measurements made, to allow monitoring of future processes. Calibration is only as good as the reference samples used to build it [21], therefore it is important to choose calibration samples which truly represent the process, and take into account any variation which may be encountered. Often calibration models are constructed using multi-component mixtures of different concentrations which have been prepared in a laboratory. These may not contain intermediates that are formed in a reaction therefore using actual reaction samples gives better modelling of the reaction process [22].

1.3 Process analysers

An ideal process analyser would be non-invasive, non-destructive, chemically selective, robust, cheap and able to monitor a wide range of processes. Many types of process analyser exist that can be used on-line to monitor a reaction. The analyser chosen should be suitable for the application.

Optical spectroscopy is widely used for process analysis. The simplest of these methods is UV-visible spectroscopy. These spectra have absorption peaks which are very broad and overlap which may lead to problems with selective measurement of one component in the presence of another [23]. Usually the wavelength of maximum absorption is used to produce a univariate calibration. The advantages of UV-visible include the fact that water does not absorb significantly between 200 and 750nm so water interferes less with the spectra [21]. Another advantage is that fibre optics can be used to allow remote monitoring of the process. UV-visible spectroscopy is widely used in batch monitoring, for example, Quinn *at al* [24] report using UV-visible spectroscopy to monitor the composition and control of a batch reaction.

Mid-infrared (IR) absorptions are much weaker than those in the UV-visible regions, so is not useful for trace analysis [17]. The bands are quite narrow and characteristic of functional groups so measurements offer better selectivity than UV-visible. The main disadvantage of IR is that the light is highly attenuated by silica fibre optics which limits its length, so the analyser cannot be located as far away from the process [7]. Mid-IR is widely used in industry [25, 26] as it can be correlated to changes in the process.

Raman spectra comprise of vibrational fundamentals so spectra are usually quite simple [17]. Polarizable bands that produce weak absorptions in the IR, produce strong absorptions in Raman spectra, so they can be applied to different applications. Raman has the advantages that it can be used for non-contact analysis of solids and liquids and it can be used with fibre optics [7]. Raman can be used to analyse aqueous samples without the water interfering as water is virtually transparent in Raman, unlike in the NIR and IR where water dominates the absorption [21]. Raman can easily become dominated by other processes such as fluorescence [23], which may limit its usefulness.

Mass spectrometers (MS) separate molecules of a sample according to their masses and measures their quantities [17]. Multi-component analysis can be achieved in seconds making it a useful technique for many environmental monitoring and process control measurement applications [23]. It has become a standard analyser in several industrial applications including steel manufacturing and fermentation off-gas analysis [21]. However, it is an expensive technique and is mainly useful for gas analysis in the field of process analysis.

Nuclear magnetic resonance (NMR) spectrometers are non-contact and non-destructive [7]. Higher resolution Fourier Transform NMR (FT-NMR) is commercially available and is used in the petroleum industry. The linear dynamic range is from ppm to 100%. NMR needs to be made more rugged and cheaper to gain increased use for process analysis. Also precise temperature control is needed for accurate process measurements [21].

Acoustics is a technique which has been used in process analysis. It is non-invasive as transducers are attached to the side of the vessel [7] and they are intrinsically safe. Acoustics provide unique information that can be provided in real-time [27]. Passive acoustics is commonly used in which the source of the acoustic emission is the process itself. Expertise is needed to make sense of the collected acoustic emissions. Applications include monitoring fluidised beds [28] and granulation processes in pharmaceuticals.

In this work two techniques have been examined: near infrared spectroscopy and guided microwave spectroscopy. These techniques fulfil the ideal process analyser criteria to some extent.

1.3.1 Near infrared spectroscopy

Near infrared (NIR) spectroscopy is the measurement of the wavelength and intensity of the absorption of near infrared light by a sample. NIR light spans the range of 4000 – 12 500cm^{-1}. Spectra are due to transitions between vibrational energy levels that occur in the near infrared. NIR is the spectroscopy of the overtones and combinations of the fundamental vibrations seen in the mid-infrared region [29]. NIR spectroscopy is used for measurement of organic functional groups. In practice vibrations of CH, NH and OH species cause the only significant NIR bands [30].

In NIR, peaks are broad and overlapping compared to mid-IR spectra [23]. There are a great number of bands in this region, which cannot always be separated into single peaks. This hinders the assignment of a signal to certain functional groups. Quantitative analysis by NIR requires the use of multivariate calibration.

Different functional groups absorb at different wavelengths. The absorption at a specific wavelength is related to the concentration of the absorbing species according to Beer's Law [17]:

$$A_\lambda = \varepsilon_\lambda dc \qquad \textbf{Equation 1.1}$$

Where A_λ is the absorbance at wavelength λ, ε_λ the molar absorptivity, d the pathlength, and c the concentration. This allows simultaneous determination of several components by calibrating the concentrations of the components with the spectral data.

NIR offers non-invasive chemical analysis of complex processes. The advantages of NIR are its speed, simplicity of sample preparation, the sample is not consumed and the spectra provide enough information to determine the levels of several constituents without the need for re-scanning [31]. A disadvantage is the relative insensitivity of NIR to minor constituents. However, it does mean a complicated matrix can be used without interference from lots of things present in small quantities.

The major advantage of NIR is that remote measurements can be made with the use of fibre optics allowing both at-line and on-line analysis [17]. This allows the spectrometer to be located away from the process being analysed, so improving safety [32] and also more than one point can be sampled with one spectrometer so cutting costs [33]. Real-time information can be obtained to monitor and control a process.

For on-line analysis NIR must be used with a transmission or diffuse reflectance probe located in the process. This means only a small region of the process is sampled and probe fouling may be a problem.

1.3.1.1 Applications

There are many varied examples of NIR being used for process analysis. The industries making use of this technique range from organic synthesis, to food production. Recent examples include the use of NIR for the measurement of total dietary fibre in homogenized meals as reported by Kim *et al.* [1]. A PLS calibration model was built to calibrate the fibre content to the collected spectra. Errors of below 3% were achieved. This compares well to traditional reference methods which take 4 days. Other food examples include the use of NIR for the determination of fatty acid composition and contents of main constituents in a complex food model system reported by Afseth *et al.* [34]. Kasemsumran *et al.* [2] have used NIR for the discrimination and quantification of adulterated olive oils.

Sohn *et al.* [3] have used NIR for determining the linen content in linen/cotton blend products. This offers a quick non-invasive method of analysis. A validation error of 3% was achieved for one model, and 6% for another model for a different fabric.

On-line NIR method has been used for the monitoring of chemical reactions. Norris and Aldride [4] have used NIR for the determination of the steady-state end point of homogeneous and heterogeneous organic reactions for chemical production. The method involves monitoring by NIR at specific time intervals during the reaction. The steady-state point is determined as when the NIR spectra do not change significantly over time.

NIR is also used in the pharmaceutical industry. One example, reported by El-Hagrasy and Drennen [35], is the use of process control for pharmaceutical powder blending. NIR has been used to predict the blending endpoint. Blanco and Alcala [5] have used NIR to test the content uniformity and tablet hardness of intact pharmaceutical tablets. The calibration model encompasses the variation in the tablets due to variation in production, so offering a simpler model. This method has the advantage that intact tablets are tested, so is fully non-invasive, and all tablets can be tested.

NIR is being examined for glucose monitoring in human tissue by Liu *et al.* [36]. A NIR spectrometer has been developed for the tissue sampling on the left palm to give *in vivo* monitoring. This technique offers truly non-invasive glucose monitoring. Currently this technique needs further research to give a good calibration model. Much research is being carried out for the use of NIR for glucose monitoring [37-40] showing what a useful technique this is.

1.3.2 Microwave spectroscopy

The microwave (MW) region lies between 3GHz and 300MHz, which is located between the infrared and radio frequencies. Traditionally MW spectroscopy is defined as "the high resolution absorption spectroscopy of molecular rotational transitions in the gas phase" [41]. MW spectroscopy observes rotational transitions of molecules. Free rotation of molecules occurs only in the low-pressure gas phase. Liquids and solids are not free to rotate which leads to poor spectra. Currently there are few applications for liquid and solid processes.

Small molecules have sharp spectra making it a good fingerprinting technique, and it is mostly used for qualification of products. Much work has been carried out regarding species determination in the gaseous phase. The first experiments on gaseous spectroscopy in the MW region were carried out in 1934 by Cleeton and Williams [42], in which the absorption of ammonia vapour was investigated. There is high accuracy available with MW spectroscopy, allowing much more detailed and exact information to be obtained than with IR spectroscopy [43].

1.3.2.1 Applications

Microwaves have mainly been used for the prediction of moisture content of samples as the technique is very sensitive to water. Many examples exist for moisture determination applications, particularly in the food industry. Thompson [44] describes the different MW methods that can be applied to non-destructive moisture measurement. Meyer and Schiltz [45] used a MW method for the determination of the moisture content of solids, and Kent and Meyer [46] reported a method of using a MW moisture meter for heterogeneous foodstuffs. Trabelsi and Nelson [47] recently reported the use of microwaves for determining the bulk density and moisture content in shelled peanuts. This method is based on the direct relationships between the dielectric constant and dielectric loss, and the moisture content. MW measurements have also been used in

the building industry to measure the moisture content of building materials, as reported by Kaariainen *et al.* [48].

It was predicted as far back as 1990 [23] that MW spectroscopy could be used as a useful technique for process control. Few papers exist describing the application of MW spectroscopy for quantification. This technique has largely been ignored for on-line analysis of liquids and solids as the spectra are often broadband without clear peaks due to the lack of free rotation of the molecules [49]. Multivariate calibration is necessary to correlate the spectra to the process changes.

Guided microwave spectroscopy (GMS) has been used in previous process analysis work. Liang *et al.* [6] reported the use of GMS for the analysis of water and ethanol mixtures. Walmsley and Loades [49] reported a similar application for the determination of acetonitrile in water. Other work includes the determination of moisture in tobacco [50] reported by Dane *et al.*. These papers are preliminary studies and show the possibilities of using microwave spectroscopy for quality control. Daniewicz [51] discusses the use of GMS as an improved method for the measurement of water content in mixtures.

1.3.2.2 Guided microwave spectroscopy (GMS)

In this work a guided microwave spectrometer (GMS), (Epsilon, Texas, USA) has been used. This has been specifically designed for process analysis work. It provides non-invasive analysis of multiple components in liquid, solid and multiphase materials [52], and is not sensitive to the colour of a sample.

It has many advantages over other spectroscopic measurements. The entire process sample fills the GMS chamber and is analysed non-invasively [53] so giving a representative measurement of the sample or process. Pathlengths of several centimetres are used so allowing a greater sample to be measured. This also allows measurements to be made as a material passes through a pipe.

The measurement is made using a single beam which passes through the whole sample. In the presence of MW energy, the polar molecules in the sample, such as water, rotate and align with the electromagnetic field. The movement of the molecules cause the MW signal to be attenuated, and the velocity of the wave decreases as it passes through the sample. The resulting spectrum has two characteristic features, Figure 1.1, [52]. The

cut-off region is the result of the sample attenuating and reducing the velocity of the energy, which changes its wavelength, the dielectric constant. Different components have different dielectric constants, so will result in different spectra. The passband region shows a change in amplitude which is due to the conductivity of the sample and how much energy is lost by the microwaves as they pass through the sample, the dielectric loss. The change in these two regions can be correlated to the change in the concentration of a component of interest. The movement of the frequency of the start of the cut-off region is sensitive to the moisture content, and can be used to correlate to the change in moisture content [53].

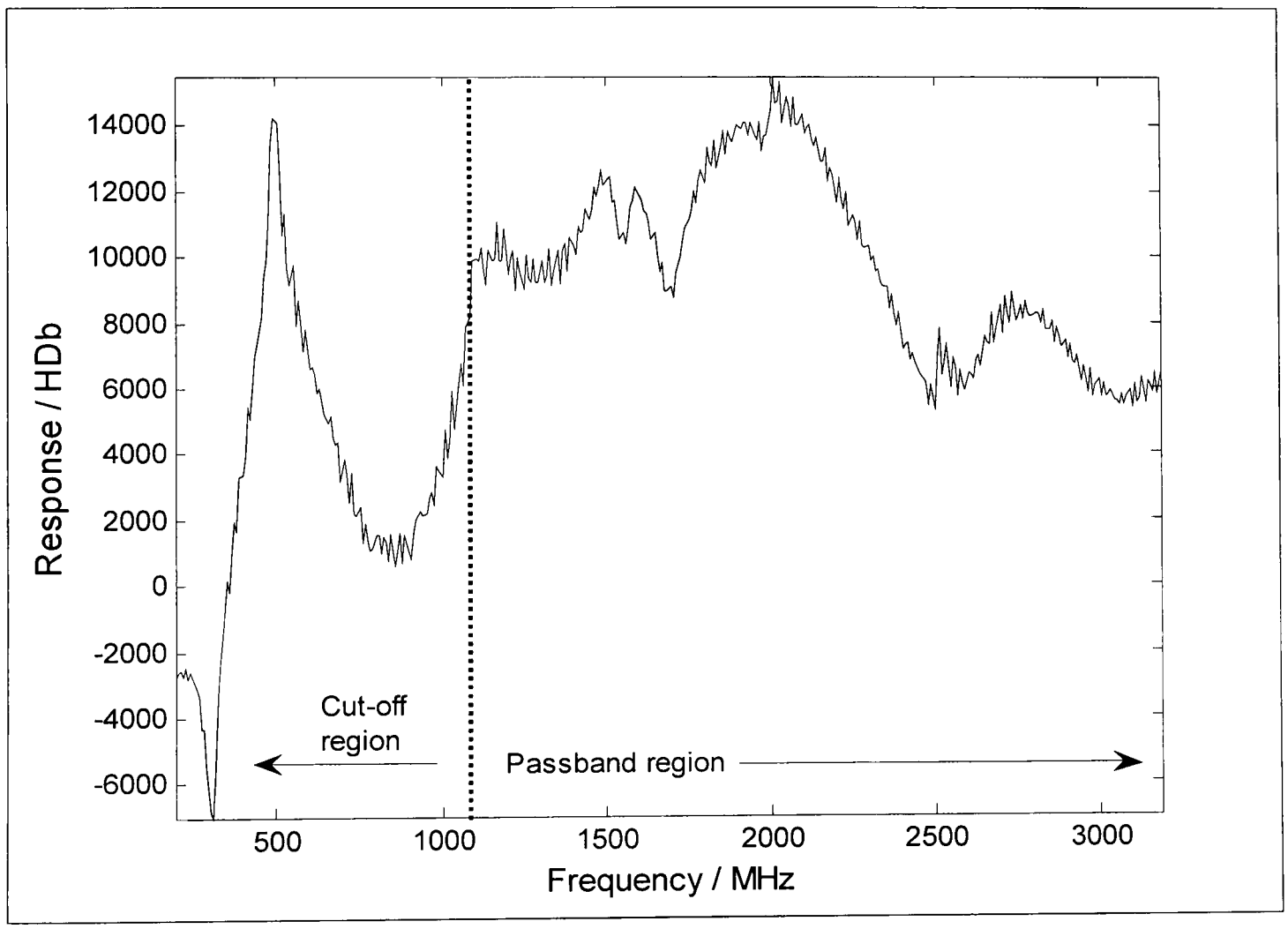

Figure 1.1: MW spectrum of sand and water mixture to show the different parts of the spectra. The cut-off region is due to the sample attenuating and reducing the velocity of the microwaves, the dielectric constant. The pass-band region shows a change due to the MW energy lost as it passes through the sample, the dielectric loss.

Temperature affects the electrical properties of the mixture proportional to the concentration of polar and semi-polar constituents [54], therefore the recorded spectra is affected. The temperature should be fixed to minimise this effect.

1.3.3 Comparison of MW and NIR

GMS and NIR are both wide band instruments, and can be used to simultaneously measure various components of a mixture. The techniques can be used to monitor a process. Multivariate calibration is needed in both cases to calibrate the recorded spectra to the process sample.

NIR is a proven method for process analysis in a wide range of industries. MW spectroscopy is a technique that has not been used much, but does appear to have advantages over NIR. The main advantage of MW spectroscopy is a sample can be analysed in a process pipe, and the whole sample is analysed so giving a truly representative measurement of the sample. NIR relies on the use of a probe to collect spectra on-line during a process. This means only one small area of the process is measured, so the true process may not be measured.

In this work, NIR and MW spectroscopy are to be used to monitor a variety of processes. A variety of chemometric techniques are to be used to relate what is occurring in the process to the spectral data. NIR spectra are much easier to interpret and relate to the process than MW spectra. It is hoped that the NIR data can be used as a reference data to compare to the MW spectra to determine if both sets of data are seeing the same process changes.

1.4 Chemometrics

Chemometrics is often defined as the use of multivariate data analysis and mathematical tools to extract information from chemical data [16]. Due to the production of large amounts of process data, chemometrics is vital to model data for process control. It is used to make sense of, and extract vital information out of complicated spectra. The techniques can be split into two main types: supervised and unsupervised modelling.

Unsupervised modelling are those techniques that cover data visualisation and pattern recognition, including clustering techniques. Only measurements, *X*-block data, taken during a process are used to produce a qualitative model. For example, principal component analysis (PCA) can be used to visualise the progress of a process, and also for data reduction to maximise the variation included in supervised modelling due to the constituents of interest.

Supervised modelling involves calibrating unknown quantitative information, *Y*, with available measurements, *X* [55]. This is the technique of multivariate calibration in which a number of constituents of a process are measured simultaneously, often by spectroscopic techniques such as NIR, and these related to the concentrations of the constituents to allow process monitoring. A calibration model must be built using techniques such as partial least squares (PLS) regression. The calibration must cover the range of variation in both sample composition and process variation, such as inconsistencies in starting material, to produce a robust model [56].

1.4.1 Unsupervised modelling

In this work PCA has been used to explore trends in the collected spectral data, and examine the reaction progress as seen in the data. Multivariate curve resolution (MCR) methods have also been used to monitor a reaction.

1.4.1.1 Principal component analysis (PCA)

The main aim of PCA is to reduce the size of a data set that has a large number of intercorrelated variables, and to retain as much of the information present as possible. PCA reduces the spectral data into principal components (PCs). The first PC accounts for the largest amount of variation in the data, the second the next largest amount of variation and so on [57]. Only a few of the transformed variables are needed. If the rank of the data is three, i.e. there are three independent significant components in the system being measured, then only three PCs should be needed to describe the variation [58]. However, things are never as simple, as noise distorts the picture. It is important to choose a number of PCs which describes all the important variation in the system, but does not include noise.

Before carrying out PCA, it should be decided if each variable in the data should be standardised to zero mean. If it isn't, and one variable has a much larger variance, then this variable will dominate the first PC. Standardising avoids this by making all the variables carry equal weight [57].

Spectral data collected during a reaction can be described as the sum of responses for each significant compound in the data, which are characterised by a concentration profile, *C*, and a spectral profile, *S*, plus experimental noise or instrumental error, *E* [58], as shown in Figure 1.2.

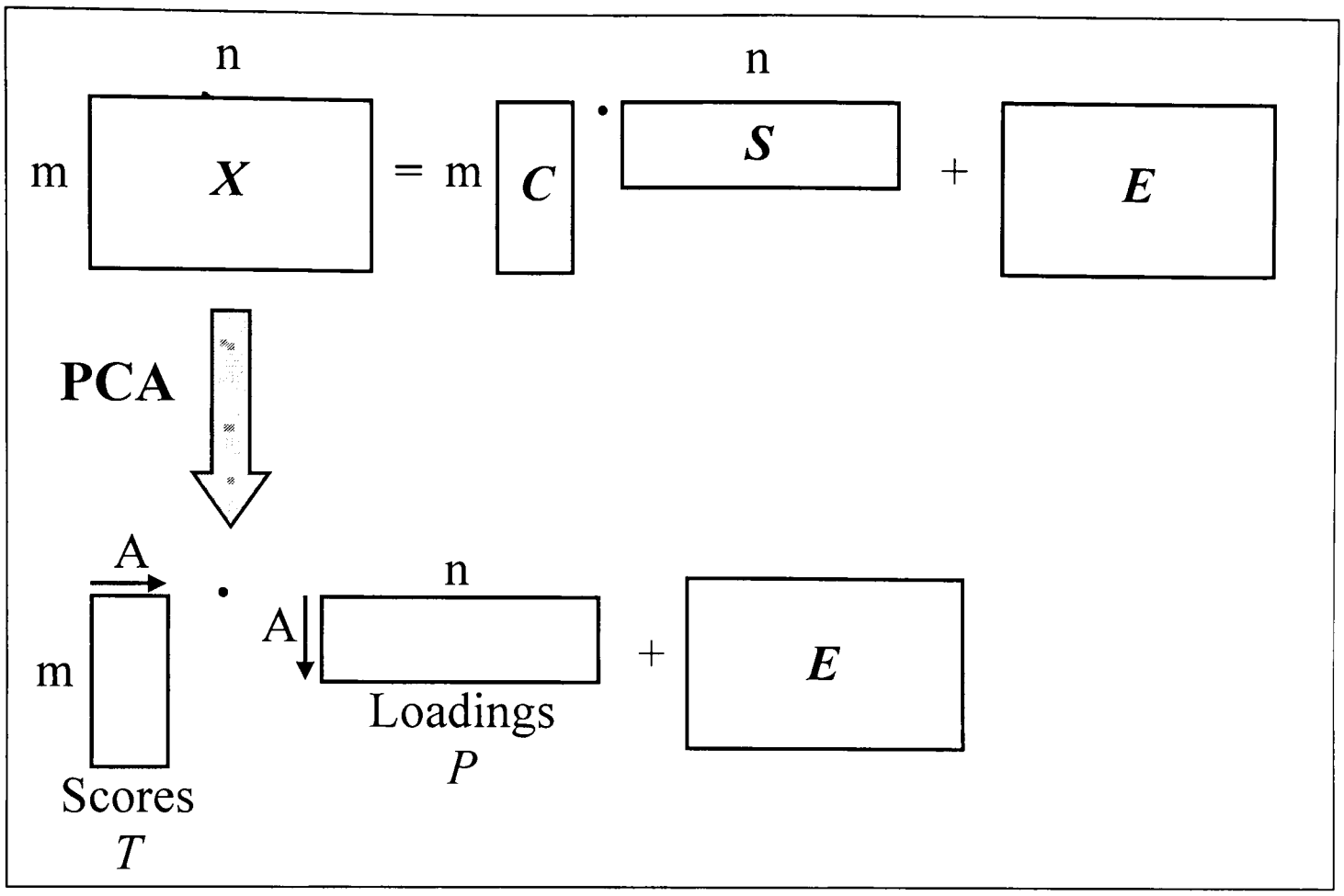

Figure 1.2: Diagram to show chemical factors making up spectral data, and how principal component analysis (PCA) is used to decompose the spectral matrix. *X* is the original spectral data matrix comprising of *m* samples, and *n* variables. This can be described by; *C*, a matrix of the concentration profiles for each component; *S*, a matrix of spectra for each component; and *E*, an error matrix. PCA decomposes the original data matrix, *X*, into scores, *T*, and loadings, *P*. The scores consist of *A* (the number of components) column vectors, and the loadings *A* row vectors.

Using PCA, the data is decomposed into an abstract mathematical transformation of the original data matrix, comprising scores, *T*, and loadings, *P*, as shown in Figure 1.2. The scores show the relationship between the samples, and the loadings the relationship and importance of the spectral variables.

By examining the scores, it is possible to visualise how the samples relate to each other. In the case of reaction spectra, in which there is a meaningful sequential order to the samples as they were collected over time, the scores can be plotted against sample number or time [58]. This makes it possible to see how the samples relate to each other over time, and hence visualise the progression of the reaction.

1.4.1.2 Multivariate curve resolution (MCR)

All the spectral matrix data collected during a reaction has one direction relating to the compositional variation of the system as it evolves over time, and the other direction refers to the variation in the response collected, the actual spectra [59].

The spectral data comprises of the addition of the response of all components in the system. Multivariate curve resolution (MCR) methods decompose the original data matrix, *D*, into the concentration profile, *C* and the pure component spectra, *S*, from the original data matrix *D*, shown in Figure 1.3 .

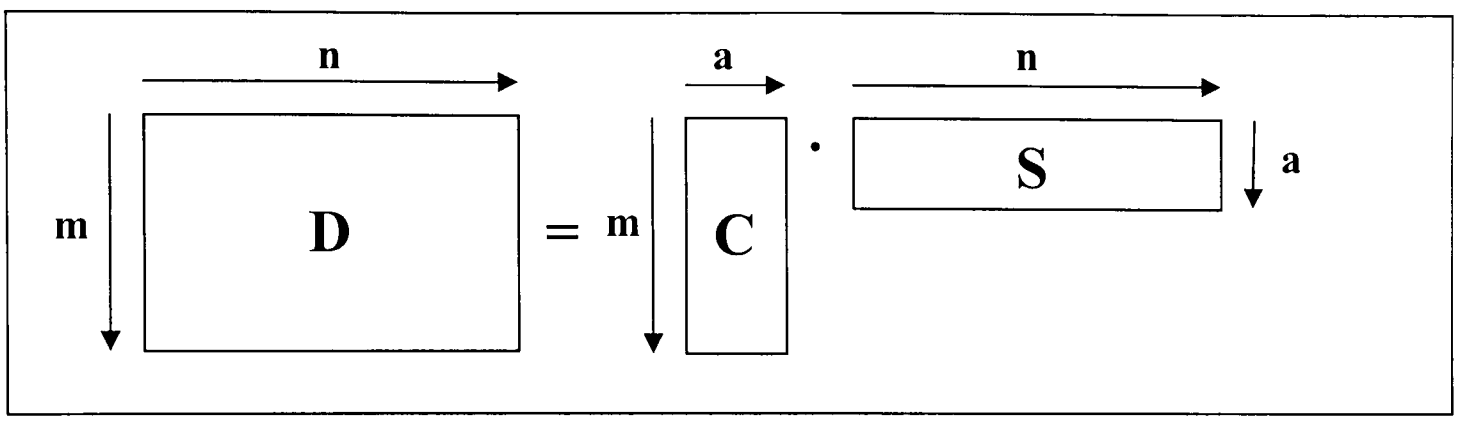

Figure 1.3: Diagram to explain the basis of multivariate curve resolution techniques (MCR). MCR attempts to recover the true value of the concentration profiles, *C*, and the spectral profiles, *S* from a data matrix. Each of the resulting matrices contain a pure profile for each independent component, *a*.

The solutions are not unique, and constraints and initial estimates are used to improve the fit. One such method is the use of evolving factor analysis (EFA) to give an initial estimate of the number of components present in the system. This works by running PCA on a window of data [59]. The window is enlarged by adding rows in the process direction, and subsequent PCA run. EFA is performed by building the windows from the start of the process to the end, the forward direction, and also in the opposite direction, the backward direction. The eigenvalues from PCA are displayed as the process evolves to show how the components in the process emerge and disappear during the process. From this it can be determined how many independent components change during the process and provide initial estimates of their concentration profiles.

The use of alternating least squares (ALS) can be used with these initial estimates to narrow the span of feasible solutions [60]. The initial estimates from EFA are optimised iteratively by ALS until the convergence criteria is reached.

GUIPRO is a graphical user interface (GUI) within MATLAB developed by Paul Gemperline and is based on a new algorithm for multivariate modelling curve resolution that gives improved results by incorporating soft constraints [61]. The method offers a substantial improvement in the ability to resolve time-dependent concentration profiles from mixture spectra recorded as a function of time.

In this work the aim was to minimise the amount of pre-processing and analysis of the data to make the curve resolution techniques as simple and quick as possible, and minimise user prior knowledge and input (see section 2.4.2 for details on GUIPRO and the constraints that can be used).

1.4.1.2.1 Examples

Many examples exist for the use of MCR to solve many different types of problems. Traditionally MCR techniques have been involved in resolving overlapping chromatographic peaks. Some recent examples include the use of MCR to resolve overlapping spectra in high performance liquid chromatography (HPLC) of pesticides in water as reported by Rodriguez-Cuesta *et al.* [62]. Pere-Trepat *et al.* [63] have used MCR to resolve co-eluting peaks of multiple biocide compounds in liquid chromatography-mass spectrometry (LC-MS). Wasim and Brereton [64] discuss the use of different types of curve resolution for the analysis of liquid chromatography coupled with nuclear magnetic resonance (LC-NMR) to resolve the concentration profiles and spectral profiles of mixtures of eight compounds.

Sequential injection analysis (SIA) has been used to generate second order data by Pasamontes and Callao [65]. MCR-ALS has been used to treat the data to allow the determination of several analytes simultaneously both qualitatively and quantitatively without the need to pre-treat the sample.

Work has been reported for the use of curve resolution techniques with NIR spectra to monitor reactions. Spectra collected during curing epoxy resins has been subjected to MCR-ALS by Garrido *et al.* [66] to resolve the reactants and products, and also the intermediate spectra and concentration profiles. The concentration profiles were found to properly represent the system studied. Mercado *et al.* [67] have used NIR with MCR to study the reactivity of silicon-epoxy monomers, and extract the concentration profiles.

1.4.2 Supervised modelling

The aim of multivariate calibration is to build a model that describes the relationship between the dependent variables (concentrations), *Y*-block, and independent variables (spectra), *X*-block of a process.

1.4.2.1 Steps of calibration

To ensure a calibration model is built which suitably relates the *X*-block data to the *Y*-block data various steps should be followed as shown in Figure 1.4. First data must be collected to build the model. Models are only as good as the data used to construct them so this step is important to ensure representative data is collected. *X*-block measurements (spectra) are taken for a variety of samples that have known *Y*-block data (concentrations), either as the samples have been made up to a specific concentration or the values have determined by analysis. This data should cover the range of variation in the *Y*-block expected in real process samples. Experimental design can be used to ensure the maximum amount of information is collected using the minimum number of experiments. The sampling method is also important to ensure a representative sample is used in the data collection.

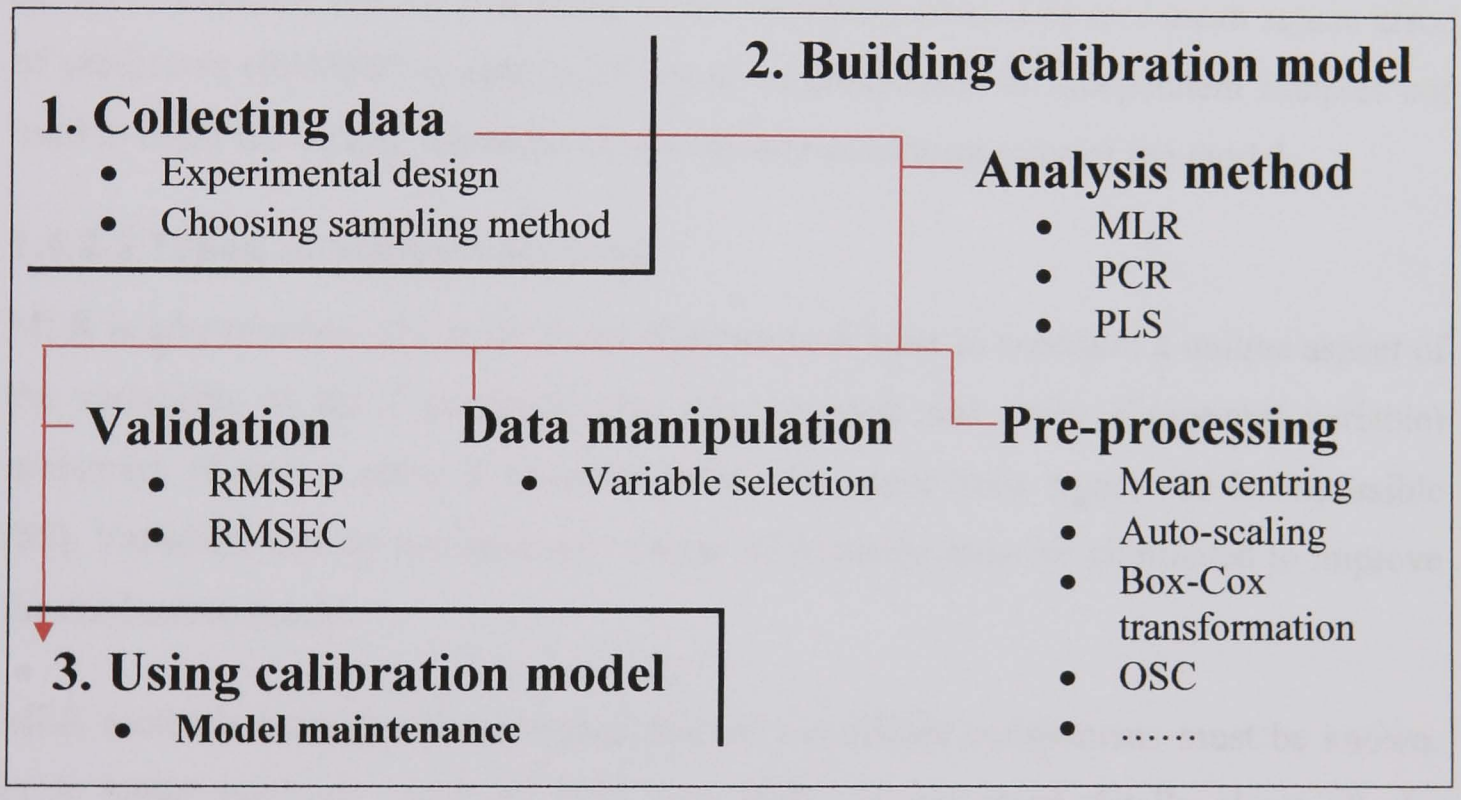

Figure 1.4: Diagram to show the steps involved in calibration model building. The data must first be collected to give a representative sample set that covers the range of data expected to be encountered. The calibration model must then be built, which involves choosing an analysis model, choosing suitable pre-processing for the data to improve the correlation between the *Y* and *X* blocks of data, and finally validating the model to show how well it predicts new samples. Then the model can be used, and it must be maintained to ensure it is still valid if the reaction conditions change.

The next step is the actual model building. An appropriate analysis method must be chosen to relate the *Y*-block to the *X*-block data. There are three main methods for multivariate calibration: multiple linear regression (MLR), principal component regression (PCR) and partial least squares (PLS).

Before the data analysis method is applied, it must be decided if pre-processing of the data is necessary. Pre-processing is defined as anything that alters the data used in the modelling process, and its aim is to improve the correlation between the *X* and *Y* data. Many different types exist, and some knowledge of the data is needed to choose a suitable method or combination of methods to ensure a detrimental effect isn't caused.

Parts of the *X*-block may be uncorrelated to the *Y*-block or may contain noise. Careful variable selection of the *X* data to remove these regions may aid the correlation between the *X* and *Y* block.

Once a model has been built it should be validated to ensure it is suitable for the application and will predict new samples. The root mean square error of calibration (RMSEC) can be calculated to show the calibration error. This uses the samples in the model to calculate the error so is not a true validation error. The root mean square error of prediction (RMSEP) is calculated based on predictions of independent samples not used to build the model, therefore shows the true validation error of the model.

1.4.2.2 Types of analysis method

MLR is an extension of simple linear regression. It aims to ascertain a unique aspect of the variability of the *Y* (concentration data) to each and every *X* (spectral variable) measured. If two or more *X* variables reflect the same basic trend, this is impossible [55]. Variables that do not have any unique information must be eliminated to improve the calibration model.

MLR methods have the disadvantage that all significant components must be known. PCA based methods, such as PCR and PLS, do not need details about all the components in a mixture [58]. However, it is necessary to make a reasonable estimate of how many components are in a mixture to allow the number of components needed to be included in the model to be determined. This number of components or factors to be included has to be decided, which may pose a problem. Including too few means not enough of the variation captured by the original data matrix is included. This leads to under-fitting, and results in a calibration model that is unable to predict new samples that have quite different variation from that included in the model. Including too many may result in information not relating to the concentrations of the components of interest being included. This results in over-fitting of the model which may cause interference and instability on the calibration model.

Principal component regression (PCR) is an extension to PCA. It regresses the *Y*-block onto the scores, *T*, obtained from the PCA of *X* [68]. The principal components are not correlated, so the problem of variables in *Y* being correlated is overcome. PLS aims to find not only the correlation in the data to the concentration data, but also finds the variance in the spectra, so it is often considered to be superior to PCR.

1.4.2.2.1 Partial least squares (PLS)

Partial least squares (PLS) is a method for constructing predictive models when the factors are many and highly co-linear. It is a spectral decomposition technique, which decomposes the data into a small number of relevant factors (latent variables) which explain the most variation in the spectra, *X* and are predictive of the concentration, *Y* data sets [69].

In PLS linear combinations of the predictor variables, *X*, are found. Those that show a high correlation with the *Y* data are given greater weighting, because they are more effective at predicting [57]. This gives linear combinations of *X* which are highly correlated with the *Y*-block and also explain the variation in the *X*-block. The main idea of PLS is to get as much concentration information as possible in the first few loading factors. PLS is taking advantage of the correlation relationship that already exists between the spectral data and the constituent concentrations. Two types of PLS exist: PLS1 is used for prediction of a single variable, and PLS2 for prediction of multiple variables.

During the modeling, the *X* variables are not modeled exclusively, and two models are obtained as shown in Figure 1.5. *q* has analogies to a loadings vector but is not normalized. The spectral data, *X*, is decomposed into *T*, scores, and *P*, loadings, and the concentration data, *Y*, decomposed into *T* and *q*. The scores matrix, *T*, is common to both the *X* and *Y* data. Unique sets of *T* and *P* are obtained for each component of interest, which has corresponding concentration data [58].

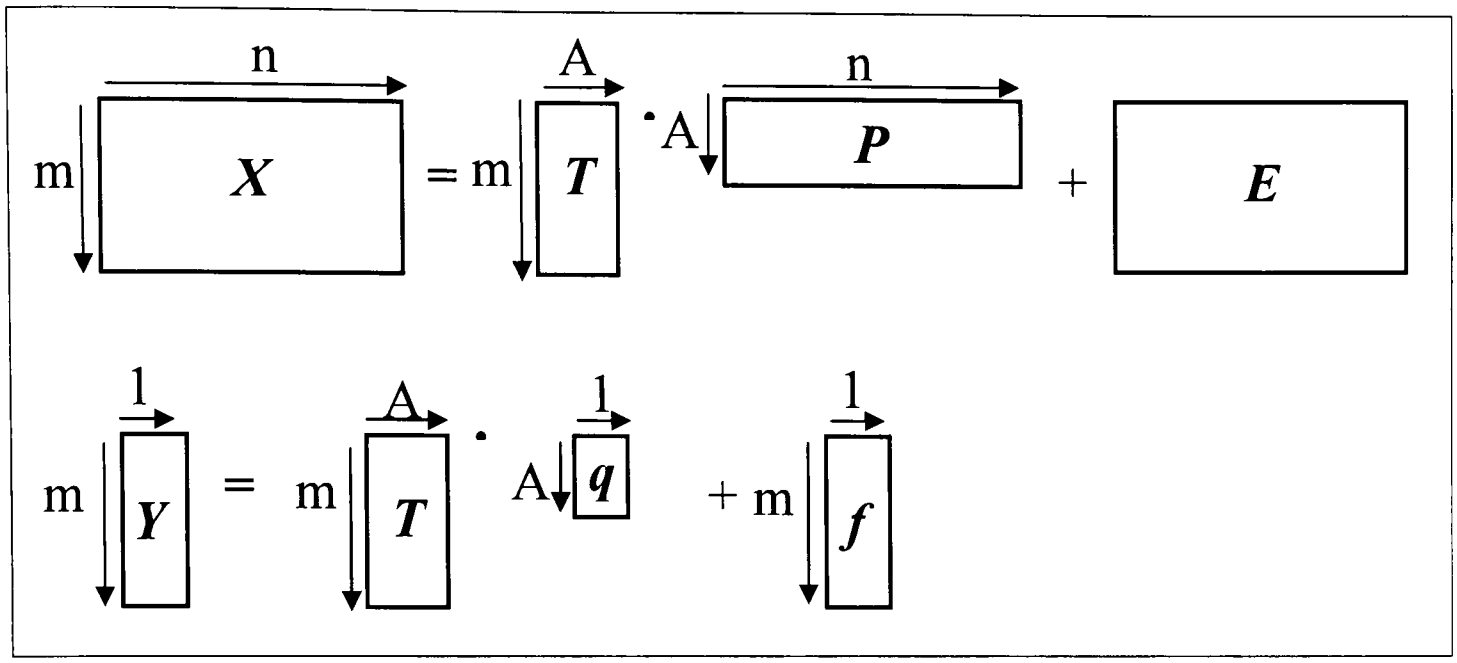

Figure 1.5: Principles of partial least squares (PLS) regression. *X* is the original spectral data matrix which is decomposed into scores, *T*, and loadings, *P*, with an associated error matrix, *E*. *A* is the number of calculated latent variable (LVs). *Y* is the original concentration data, which is decomposed into scores, *T*, and *q* which has analogies to a loadings vector, and also an associated error, *f*. The common link is the scores, *T*.

There are many example of PLS being used successfully for a great variety of applications. It is widely used as it produces high quality calibration models that are easy to implement due to the availability of software [70]. A recent example is the use of PLS modelling for a second order reaction monitored by UV-visible and NIR spectroscopy as reported by de Carvalho, *et al.* [71]. A PLS model was successfully built to predict the concentrations of the reaction components during the reaction. Cozzolino and Moron [72] discuss the potential to use a PLS model to predict soil organic carbon fractions using NIR spectra. Another example is the use of PLS with NIR spectra as a tool for on-line classification of dry-cured ham samples according to their sensory characteristics as discussed by Ortiz et al [73].

1.4.2.3 Pre-processing

Within calibration models the reference concentration data, *Y*, is correlated to the measurement data, *X*. To improve this correlation between the *X* and *Y* data, pre-processing techniques can be used, and any noise present removed. A pre-processing technique can be classed as anything that transforms the data. Within the PLS toolbox in MATLAB (Mathworks), that has been used in this work for data manipulation, several types of pre-processing techniques are inbuilt. Knowledge of the data allows pre-processing techniques to be chosen which will improve the correlation between the spectral and concentration data, and not have a detrimental effect.

NIR data is reported to have a problem with baseline drift which can be corrected for [74]. The collected NIR data in this work is very smooth, with no obvious noise, and no drift in the baseline.

The MW spectra have no baseline, and appear to be quite noisy. However, this noise may be correlated to the concentration data, and any smoothing of the data may be detrimental to the calibration model.

The pre-processing techniques that have been looked at in this work are explained here. If scaling is performed on the *X*-block, then the *Y*-block must be scaled accordingly. New samples must also be scaled before prediction.

1.4.2.3.1 Mean centring

Mean centring is often seen as essential before any data analysis. This involves subtracting the mean of each column (or variable) so that:

$$^{cen}X_{mn} = X_{mn} - \bar{X}_n \qquad \textbf{Equation 1.2}$$

to give mean zero variance. This prevents a variable with large variance dominating the first extracted PC [58].

Seasholtz and Kowalski [75] found that the use of mean centring in data that varies linearly with concentration, has no baseline and has no closure in the concentrations (for each sample the concentrations of all components add to a constant) has a detrimental effect on the predictive ability of the model, therefore should not be used. The NIR data is expected to vary linearly with concentration, and the MW spectra have no baseline, therefore it is expected mean centring will not improve the modelling process.

1.4.2.3.2 Auto-scaling

This involves mean centring the data, followed by dividing by the standard deviation:

$$^{auto}X_{mn} = \frac{X_{mn} - \bar{X}_n}{StdDev} \qquad \textbf{Equation 1.3}$$

Auto-scaling puts all variables on approximately the same scale, so all variables have equal significance [58].

1.4.2.3.3 Box-Cox transformation

For non-linear data the Box-Cox transformation can be used to transform the data [76]. It is transformed using the following equation [77]:

$$Z = \frac{X^{\lambda} - 1}{\lambda} \qquad \textbf{Equation 1.4}$$

Where Z is the transformed data and X is the original data matrix. λ is a parameter set to zero or higher. If λ equals zero the transformation is calculated as $Z = \log(X)$. Setting λ to two performs the square root transformation and setting it to three performs the cube root transformation.

Dieterle *et al.* [78] have used Box-Cox transformation to deal with the non-linearity's present in sensor data.

1.4.2.3.4 Orthogonal signal correction (OSC)

Orthogonal signal correction (OSC) is a filter developed to remove systematic variation in the spectral data (X) which is not correlated to the concentration data (Y). This should aid the correlation between X and Y, and should reduce the number of LVs needed in a PLS model to model all the useful variation.

Wold *et al.* [79] discuss the use of OSC with NIR spectra. It has been applied to four different data sets of multivariate calibration, and the results compared to those of traditional signal correction such as multiplicative scatter correction (MSC) and OSC was shown to give substantial improvements. Fearn [80] also discusses the use of OSC with NIR data and compares this to existing algorithms. The aim was to improve the performance of a PLS model, but little improvement was seen.

1.4.2.4 Experimental design

An experiment is a process by which information is obtained by observing the reaction under certain conditions [81]. The conditions, or factors, that effect a reaction, must be optimised to maximise the reaction. A series of experiments are run to determine these optimum factors, by examining their effect on the reaction, or the response. A well designed plan of experiments will determine the optimum factors in the minimum number of experiments [14]. The plan of experiments will cover the factors, and the levels of these factors that effect the reaction. This is the experimental design.

It is important to design experiments well to minimise cost and time [58]. By using experimental design, the aim is to gain the most information from the minimum number of experiments.

1.4.2.4.1 DoEMan

Within calibration modelling a variety of pre-processing techniques can be used to improve the correlation between the spectral data and the concentration, as discussed previously. Other calibration parameters can also be optimised, including different calibration methods, calibration set selection, and outlier detection. It is possible to choose some suitable parameters based on knowledge of the data. However, to produce the best calibration model, ideally a model should be built using every possible parameter, and combinations, and the errors obtained compared.

DoEMan is a MATLAB graphical user interface (GUI) developed by Andrew Owen of Strathclyde University, based on an idea by Flåten *et al.* [77] that attempts to find the best calibration parameters in a experimental design way. Its use is presented in a paper by Flåten and Walmsley [82].

In this work, the use of different pre-processing techniques has been examined, along with type of regression methods and number of components to use, to produce an optimum calibration model. This method allows a series of calibration models with different parameters to be built simultaneously. The relative merits of the models can be compared by the resulting validation error. This method will not give the ultimate best calibration model to use, but gives an indication of the parameters that will provide the best calibration models, allowing a smaller subset of the models to be examined in more detail.

Details of how this GUI has been used in this work to determine the best calibration model to use are detailed in section 3.1.1.1.2.

1.4.2.5 Validation

Once a calibration model has been built, it should be validated using an independent data set that has not been used to build the model. This allows calculation of the prediction error and shows how good the model is at predicting new samples, allowing comparison of different models. Several types of validation errors can be calculated as described here.

Within the PLS algorithm used in this work, which is inbuilt into the PLS toolbox in MATLAB, the residual sum of squares (RSSQ) is calculated. This is calculated as:

$$RSSQ = \sum_{i=1}^{1} (y_i - \hat{y}_i)^2 \qquad \textbf{Equation 1.5}$$

Where y_i is the actual concentration, $\hat{y}_i$ is the predicted concentration. This is a unitless value and gives an idea of the total error in the model. Its magnitude depends upon the number of samples predicted, so cannot be used to compare the prediction error of different models if different numbers of samples are used in the validation. From this the root mean square error (RMSEP) can be calculated:

$$RMSEP = \sqrt{\frac{RSSQ}{(N-1)}} \qquad \textbf{Equation 1.6}$$

Where N is the number of samples. This error is now the same magnitude as the concentration values, so can be directly compared to the values. Its magnitude relates to the magnitude of the concentration values. If the concentration values are scaled, then this value will be scaled accordingly. Therefore, this number can only be used to examine the error in a particular model, and cannot be used to compare models that are built using different scaling methods.

From this the percentage error can be calculated by using the mean predicted value:

$$\%RMSEP = \frac{RMSEP}{mean(\hat{y}_i)} \times 100 \qquad \textbf{Equation 1.7}$$

This value relates directly to the predicted values, and can be used to compare the errors in the model as it gives a true validation error from an independent validation set.

1.4.3 Reaction monitoring

Reaction monitoring is important in the chemical industry to ensure the progress of the reaction is within the expected limits. Traditionally, a sample is removed from the reaction or process and analysed using high quality analysis methods. These are generally time consuming, and the resulting delay between sampling and analytical result means the reaction can be monitored, but process control is difficult.

On-line monitoring methods, such as NIR spectroscopy, require a calibration model to be built, for example a partial least squares (PLS) model [83]. For these traditional calibration methods, samples are made in the laboratory or a reference method is needed, such as GC or HPLC analysis, to give concentration data for true process samples to be correlated to the acquired spectral data. The model will only be as good as the reference data used to build it. These reference methods are time consuming, and may be unreliable. Model building is a long process and the model must be built which encompasses all expected variation in the reaction. The model is only valid for this reaction whilst occurring within the same process conditions. Any deviation from these conditions, such as change in raw material quality, will cause incorrect prediction of the sample. Calibration models are static and must be updated or rebuilt for each process.

Ideally a technique which requires no reference data, and is batch independent, would be better for process monitoring.

1.4.4 Fault detection

An upset of the reaction can be defined as anything that alters the progress of a batch, and hence deviates its progress from the norm. A process upset, such as the charging of incorrect reactants, may cause the batch to fail to meet the required specification. It also may have to be reacted for longer, which will cost more money. Ideally process upsets should be identified as they occur to allow correction for or abandonment of the batch.

Traditional calibration methods will give a prediction of the reaction progress even if a process upset has occurred. This may give misleading information about the reaction progress. Also the calibration models are only valid for the process whilst it is operating under the same reaction conditions. Ideally a calibration model should be adaptive to any change seen to allow correct determination of the endpoint.

Modelling methods include SIMCA (soft independent modelling of class analogy). This is used as a classification technique with various spectroscopic techniques including NIR spectroscopy [84]. In SIMCA, a reference state, such as the normal operation state of a reaction, is modelled using a principal component model. New samples are compared to this model, and any deviations from it are interpreted as a process change or upset. Any changes in the reaction conditions are also interpreted as an upset,

including expected normal process changes. This technique is only suitable for reactions with a steady state, and not dynamic systems.

MSPC (multivariate statistical process control) can also be used to monitor a process over time and check it stays within the desired limits [85-87]. These models are based on examining the relationship between measured process variables such as temperature and pressure to determine the current performance of the process. Many process variables can be measured at once, and are dependent on each other, so it is necessary to examine them all at once. MSPC models are also based on a steady state reference.

A new adaptive algorithm for detecting process change known as caterpillar [28, 88], has been developed at the University of Hull. This method has been used to track process changes in a fluidised bed using acoustic sensors and can detect the onset of agglomeration events. The idea behind the algorithm is to compare the recent variation to the current variation in order to monitor process change. All abrupt changes are flagged as possible process upsets. The technique appears to be system and batch independent so it has been suggested that it could be applied to different spectroscopic techniques.

Caterpillar is an adaptive algorithm, so for dynamic systems with normal process variation, only true process upsets which cause a significant disturbance to the reaction will be detected. The algorithm adapts to different processes, so remodelling is not necessary if the process alters. It can be used for both endpoint detection and fault detection.

1.4.4.1 Endpoint detection

Caterpillar can be used to determine the endpoint of a reaction. This is important to ensure the batch has finished and saves time by preventing over reacting. Caterpillar is adaptive so will be able to predict the endpoint even if reaction conditions change. It can also be used on-line so the batch can be stopped as soon as the endpoint is reached.

In the endpoint detection caterpillar, two windows are placed in the data (Figure 1.6), with an inter-window-distance (inter-WS) between them. A principal component analysis (PCA) model is calculated for the second, reference window, to describe the "now" variation of the samples in this window. This is compared to the old variation in the samples in the detection window. The windows are moved through the data

stepwise, with the model building repeated at each step, until a steady state in the variation is seen and this determined as the endpoint of the reaction. The windows are separated by an inter-window distance to ensure that a constant variation is due to the actual endpoint of the reaction.

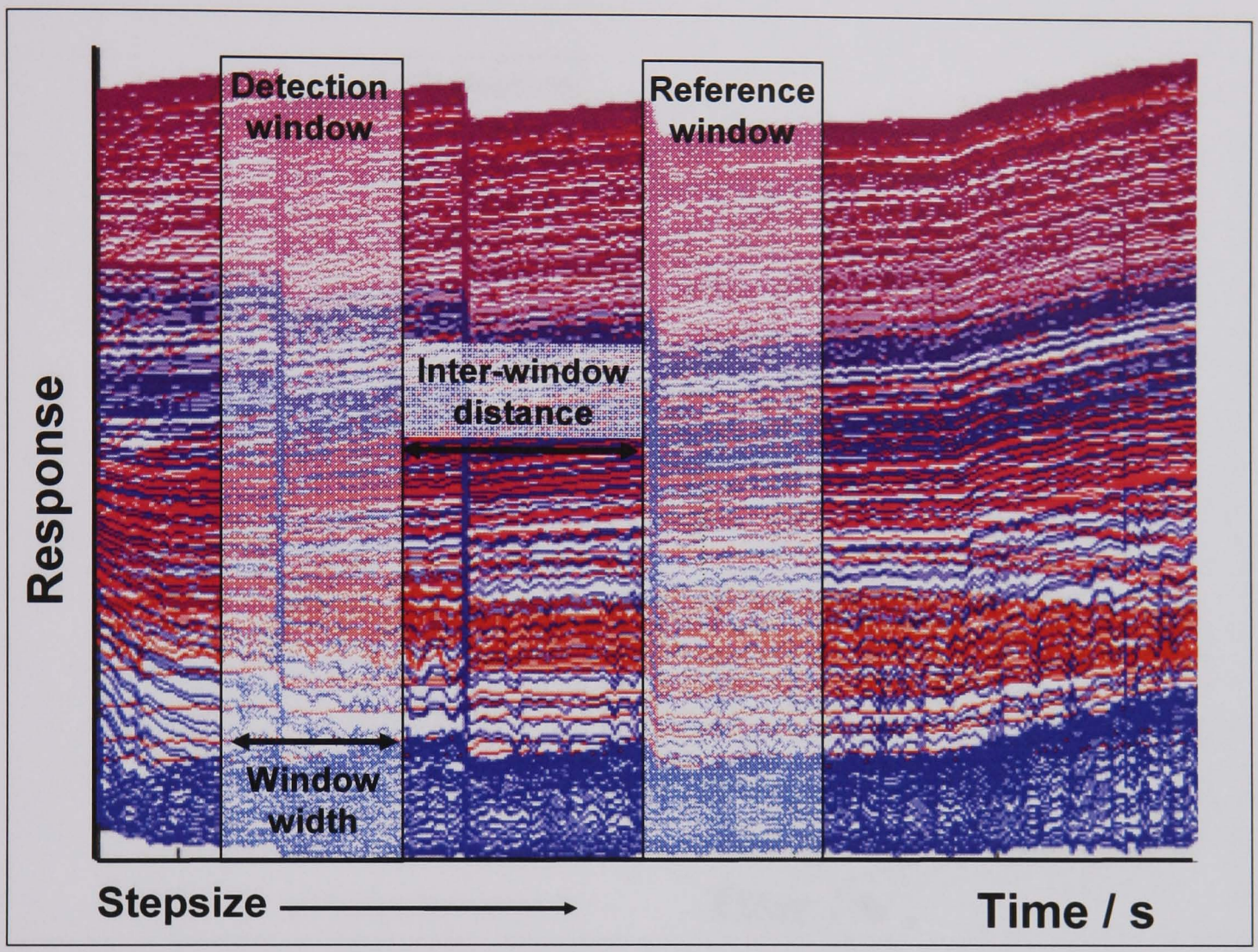

Figure 1.6: Diagram to show how the caterpillar algorithm works for endpoint determination. Two windows are placed in the data, separated by an inter-window-distance. A principal component analysis (PCA) model is calculated for the second, reference window, to describe the "now" variation of the samples in this window. This is compared to the old variation in the samples in the detection window. The windows are moved through the data stepwise, with the model building repeated at each step, until a steady state in the variation is seen and this determined as the end-point of the reaction.

1.4.4.2 Process upsets

In the caterpillar method for process upset detection, two windows are placed side by side and moved step-wise through the data (Figure 1.7). The first window, or reference window, contains "old" samples and a PCA model is built using samples in this window to describe the process variance, and the critical value, d_{crit}, is calculated based on the T^2 statistics (see Equation 1.11). The second window, the prediction window, contains the current samples. The samples in this window are compared to the first reference window. If several samples are significantly different, this is interpreted as a process

change. The number of atypical samples i.e. larger than d_{crit}, are counted and this is shown in an occurrence plot. The occurrence plot allows the operator to clearly see if the reaction is changing. However, it does not indicate the nature of the process change, so other parameters must be examined to decide the necessary action.

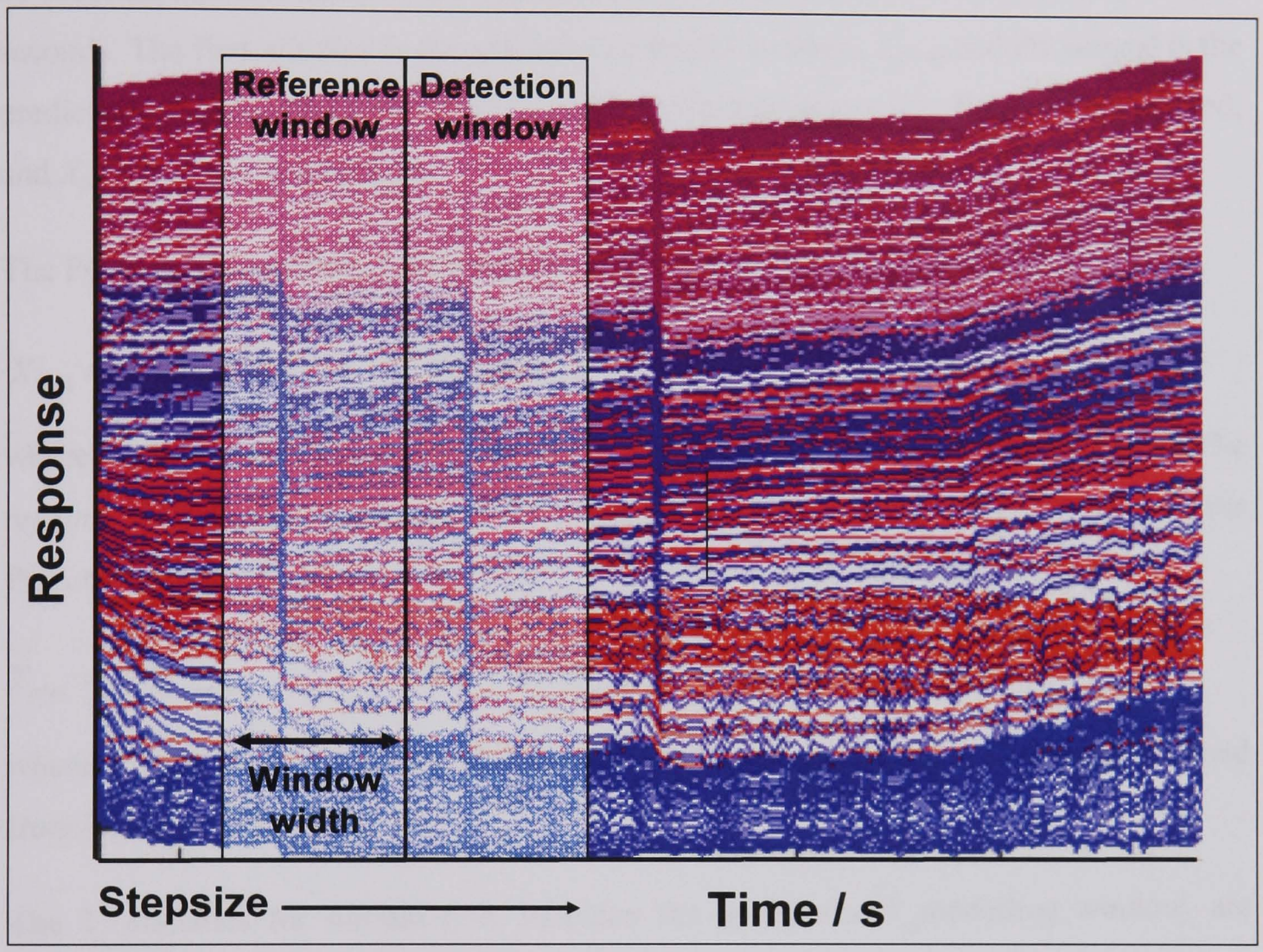

Figure 1.7: Diagram to show how the caterpillar algorithm works to detect process upsets during a reaction. Two windows are placed side by side. A principal component analysis (PCA) model is built using the reference window containing old samples. The samples in the detection window are compared to those in the reference window, and if several samples are significantly different, this is interpreted as a process change.

Within the algorithm, the window size, and number of components, used to describe the variance in the PCA model must be optimised. Ideal reaction data, i.e. with no upsets and only normal process variance, is used to optimise these two variables, see section 8.3.1. This ensures that only true upsets are identified and not normal reaction variation. Once historic data has been examined, and the optimum factors to use determined, it is hoped that the algorithm can be used in real time to detect the onset of upsets and allow correction of the process.

For a detailed account of the theory, see references [28, 88]. The m x n data matrix X contains the spectroscopic data collected for the process. This comprises of m, the

number of measurements made at set time intervals, and *n*, the number of measured wavenumbers, in the case of NIR, and number of frequencies in the case of MW. Caterpillar consists of two windows of width *w* which are *w* x *n* matrices. The window width is determined by the number of samples included. If samples are collected every 60 seconds, and five samples are included in the window, then the window width is 300 seconds. The first window is the reference or model window, X_{mod}, and the second is the prediction window, X_{pred}, which contains the current samples. The X_{mod} is mean centred, and X_{pred} is scaled accordingly.

The PCA model comprising of *k* number of components can be written as:

$$X_{\text{mod}} = T_{\text{mod}} P^{t}_{\text{mod}} + E \qquad \textbf{Equation 1.8}$$

where T_{mod} is the *w* x *k* scores matrix, P^{t}_{mod} is the *k* x *n* loadings matrix, and **E** the residual matrix. The scores for the *w* samples in X_{pred} are calculated by applying the PCA model:

$$T_{pred} = X_{pred} P_{\text{mod}} \qquad \textbf{Equation 1.9}$$

where $\boldsymbol{T_{pred}}$ is the *w* x *k* predicted scores matrix and $\boldsymbol{P_{mod}}$ is the *n* x *k* loadings obtained from Equation 1.8.

The T^2 statistics for sample *i*, d_i, in either the prediction or modelling window, are calculated as:

$$d_i = \frac{t_i t_i^{t}}{\left(\frac{1}{w-1} T_{\text{mod}} T^{t}_{\text{mod}}\right)} \qquad \textbf{Equation 1.10}$$

where t_i is the 1 x *k* scores values for sample *i* and T_{mod} is the *w* x *k* scores matrix obtained from (1).

The critical value for the T^2 statistics, d_{crit}, is calculated as:

$$d_{crit} = \frac{k(w^2 - 1)}{w(w-k)} F_{\alpha,k,w-k} \qquad \textbf{Equation 1.11}$$

where *k* is the number of components used to build the PCA reference model and *w* the number of samples used. *F* is the *F*-statistics at significance level α, which is set to 99%.

1.5 Drying process

The majority of chemistry carried out in industry is in solution phase. The products must then be dried to a set specification. It is an important process and is hard to monitor. Time and money may be wasted by over-drying.

1.5.1 Current methods

Different types of drying processes exist in industry, including the use of a fluid bed dryer, and pressure filtration. The processes are all the same in that water or solvent is removed to achieve a dry product. They all have the same problems of monitoring as huge cakes of wet material are dried in big vessels. The cake must be sampled to ensure it is dry, but the problem is from where should this sample be taken to give a truly representative sample.

In filtration drying, the solid/liquid combination is placed in a huge vessel. This is mixed with an agitator. The agitator is removed, the vessel pressurised and a valve opened. The liquid and small particles drain through a filter mesh located at the bottom of the vessel. The remaining solid is further dried using hot gas to form a 'cake'. The cake is then removed by agitation [89]. The cake must be sampled to ensure it is dry. The problem with this is the cake is thick, so it is difficult to remove a representative sample. Also, as the cake dries it becomes solid, so the agitator has to be used to break up the material before a sample can be removed.

Presently, visual inspection of the cake is used to determine if the material is dry [90]. This is a poor method of control, as only the outer layer of the cake can be seen. Process control would ensure increased yield, quality and reduce the use of raw material, such as gas flow, by accurately predicting the endpoint of the drying process.

York *et al.* [91] have used electrical tomography to model the drying process of a material in a pressure filter dryer. This work has been demonstrated on an industrial scale. Six sections of the cake are modelled for dryness. A 3D model of the cake can be constructed in real-time to give a picture of the drying process.

In fluid bed dryers, the material is contained in a vessel, and hot air is supplied to the bed of material through a specially perforated distributor plate [92]. The air flows through the bed of solids at a velocity sufficient to support the weight of particles in a fluidized state. Bubbles form and collapse within the fluidized bed of material,

promoting intense particle movement. In this state, the solids behave like a free flowing boiling liquid. The problems of sampling exist with this drying method as a large amount is dried at once.

Green *et al.* [93] have investigated the use of in-line NIR monitoring for a fluid bed dryer. The sampling effects on the method accuracy were considered and it was found process heterogeneity plays a large role in the prediction accuracy. The main problem with this work is sampling, as if the process is heterogeneous then the NIR does not measure a representative sample. Ideally the whole sample should be analysed to overcome this.

Paul Dallin, of Clairet Scientific Ltd, presented work carried out on monitoring a fluid bed dryer using NIR [94]. In this work, one wavelength was examined over time. As the drying process occurred, the absorbance at this peak decreased until a steady state occurs as dryness is achieved. Also, the drying of a pharmaceutical active in a filter dryer was monitored using a retractable NIR probe.

1.5.2 Advantages of NIR and MW

The problem with the current drying applications is one of representative sampling. NIR spectra has been used to monitor a drying process, and this too must be representative of the batch [95].

The main advantage of GMS is that it analyses the whole sample simultaneously so removes the need for sampling, and gives a representative picture of the process. As the dielectric constant for water is high, MW spectroscopy should be suitable for monitoring the drying process. It can theoretically measure 0 to 100% moisture content, so is a very useful technique for drying applications.

NIR is a proven technique for monitoring drying processes, and gives easy to interpret spectra that can be related to the process. MW spectra are much more complicated, and less is known how the spectra relate to processes. By monitoring the processes with NIR, alongside the MW, the NIR can be used as a reference method to aid interpretation and correlation of the MW spectra to the process.

When water is added to a dry material, the water is first adsorbed, due to a single layer of water molecules adhering to all surfaces of the solid. Depending on the inner area of

the solid, this adsorbed water can account for the first 2 to 10% of the materials water content. Adsorbed water has two active hydrogen bonds hence it is also known as "bound" water. Once the maximum amount of water is adsorbed by the material, any further water added is free water. The amount of water absorbed by a material is the total amount of water which goes into the solid, both bound and free water in the cavities of the solid [54]. If the full drying process is to be modelled, then both bound and free water must be calibrated for, so a non-linear calibration model may be necessary.

1.6 Esterification

1.6.1 Background

Esterification is the liquid state reaction of an alcohol with an acid to produce an ester and water [96]:

$$ROH + R'COOH \leftrightarrow ROOCR' + H_2O$$

The reaction is an equilibrium reaction and is slow under normal conditions. A strong acid catalyst can be added to speed up the reaction. There are many examples in the literature of the use of process analysis to monitor esterification reactions.

1.6.2 Current methods

Ampiah-Bonney and Walmsley [18] followed the esterification of ethanol by acetic acid, using an acid catalyst, by Raman spectroscopy, using an *in situ* probe. Water is virtually invisible to Raman so this large component does not interfere with the Raman spectra. The data was modelled by PCA, after first mean-centring the data. PC1 was removed from the data as this was found to model the fluorescence spectra. PC2 was found to be the pure Raman spectra, and this was used to give the reaction profiles of the three components, by plotting the response at identified wavelengths. The acetic acid and ethanol are seen to decrease, and the ethyl acetate increase as the reaction progresses, as is the case.

Blanco and Serrano [83] have used NIR spectroscopy for on-line monitoring and quantification of the catalysed esterification of butan-1-ol by acetic acid. PLS was used to construct calibration models based on synthetic mixtures of esterification

components. This model was used to follow the change in composition of an actual reaction, with GC analysis used as a comparison. The relative standard error was less that 3.5%.

McGill *et al.* [97] compared the use of NIR, Raman and UV-Vis to monitor the esterification reaction of crotonic acid and butan-2-ol. Univariate models were constructed for the Raman and UV-Vis and PLS models for the NIR. GC was used as a reference method with laboratory made samples.

Recently work has been published on using MCR-ALS to monitor the esterification reaction of a mixture of caprylic and capric acids with glycerol using NIR spectra [98]. This is a calibration free technique so the need for time consuming model building is removed. The concentration profiles of the components can be extracted from the spectra to give process monitoring. This can be applied in real-time to allow prediction and control of batches. In this work, the inadequate rank of the experimental data matrix was found to restrict the quality of the spectral and quantitative information obtained. The inclusion of concentration data for the components of the system aids the resolution.

In this work, MCR has been used to predict the progress of esterification reactions to provide calibration free modelling using MW and NIR spectra. The spectra collected is rank deficient as the two reactants decrease and the two products increase concentration at the same rate, so effectively there are only two independent components. Paul Gemperlines' GUIPRO [61] has been used with the known kinetics to break rank deficiency to allow prediction of all components present, and predict the rate constants to allow simple comparison of repeat batches.

The reaction of butanol and acetic acid has been examined in this work. This reaction is a good starting point for development of process analysis, as the reaction can be controlled to last a few hours so giving sufficient data for modelling, but without it taking all day to complete. The reaction is well documented, so much is known about the reaction which can be related to the spectra recorded.

This reaction has been monitored by both NIR and MW to give two-way data. NIR is a proven technique so should be able to be used as a reference method to ensure the MW spectra give a representative picture of the process.

2.0 Experimental

2.1 Reagents

Table 2.1: List of reagents used.

Reagent	Grade	Manufacturer	
Acetic acid	Glacial	Fischer Chemicals	UK
L-(+)-Ascorbic acid	99%	Lancaster	UK
Benzoic acid	AnalaR	BDH	UK
Butan-1-ol	GPR	Fischer Chemicals	UK
n-Butyl acetate	99+%	Acros Organics Aldrich	USA UK
Ethanol	GPR	Fischer Chemicals	UK
Methanol	GPR	Fischer Chemicals	UK
4-Methyl-2-pentanone	99.5%, spectrophotometric grade	Aldrich	USA
Pentane	99+%, HPLC grade	Aldrich	UK
Propan-1-ol	GPR	Fischer Chemicals	UK
Salicylic acid	99%	Lancaster	UK
Sand, purified by acid 0.1-0.3mm	GPR	BDH M&B Laboratory Chemicals	UK
Sulphuric acid	97%, AR grade	Phillip Harris	UK
Water	Distilled	In-house	

2.2 Equipment

2.2.1 Near infrared spectrometer

A Buchi, NIRVIS FT-NIR (Fourier Transform Near Infrared) spectrometer (Germany), has been used to collect NIR spectra using NIRcal 3.0 software (BUHLER, Switzerland), run on a PC, with an Intel Pentium III processor, 256MB RAM, running Windows NT workstation 4.0.

The probes used in this work are a 2mm transmission immersion probe (Hellma, Germany) coupled using fibre optics (3m in length) which has been used for liquid reactions (Figure 2.1), and a diffuse reflectance NIR probe (Buchi, Germany) for drying of powder work (Figure 2.2).

Figure 2.1: Near infrared transmission probe with a 2mm sampling port.

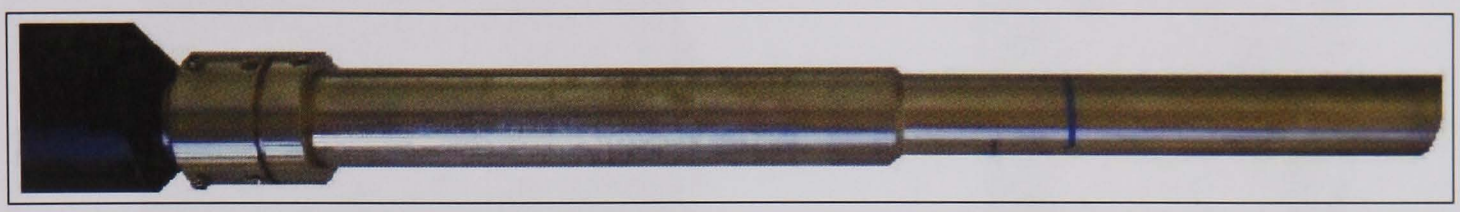

Figure 2.2: Near infrared diffuse reflectance probe.

The NIR spectra are collected over the range 4008 to 9996cm^{-1}, in step sizes of 12cm^{-1}. The spectra are collected in transmission (T) mode and converted to absorbance (A) before data analysis using the following equation:

$$A = \log_{10}\left(\frac{1}{T}\right) \qquad \textbf{Equation 2.1}$$

2.2.2 Guided microwave spectrometer

A guided microwave spectrometer (GMS), (Epsilon Industrial Inc, Austin Texas), has been used in this work to collect microwave (MW) spectra. The spectra are collected using Linefit software version 1.43 (Epsilon Industrial, Austin, Texas) run on a laptop, with an Intel Pentium Processor, with 32MB RAM, running Windows 98. The GMS has a bandwidth of 0.25-3.2GHZ, and covers a dielectric range of 1-85. The MW spectra were recorded over 200 to 3192MHz in steps of 8MHz, giving 375 measurement points in the recorded spectra. The power of the microwave is 5mW, and is powered by a magnetron. The response recorded is the change in power as the signal is attenuated by the sample.

All experimental is carried out within the GMS sample chamber, with internal dimensions of 10.0 x 4.7 x 11.5cm, giving a total volume capacity of 540cm^3 (Figure 2.3). The chamber has a transmitter antenna at one side of the chamber and a receiver antenna at the other side. These are connected to the GMS via two coaxial cables (450cm in length), which transmit microwaves to the transmitter antenna located at one side of the chamber. These pass through the chamber to the receiver, and the response is transmitted back to the GMS via the other cable. The two parallel metal surfaces

between the send and receive antenna act as a waveguide to steer the wave front towards the receive antenna (Figure 2.4).

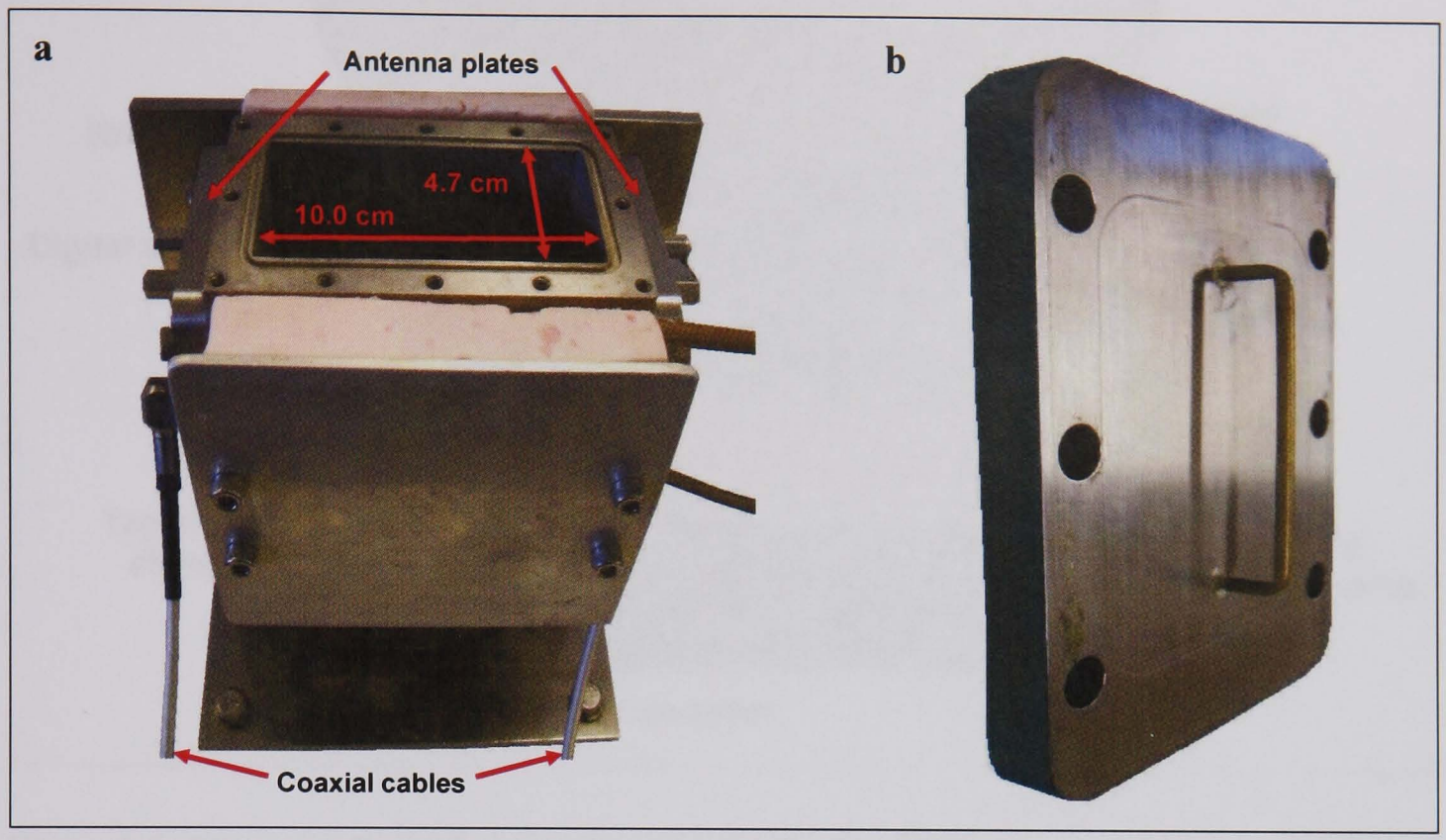

Figure 2.3: a) Guided microwave spectrometer (GMS) chamber showing the location of the antenna plates; b) The antenna plates in detail. There are two of these at either side of the chamber. One acts as a transmitter and the other as a receiver.

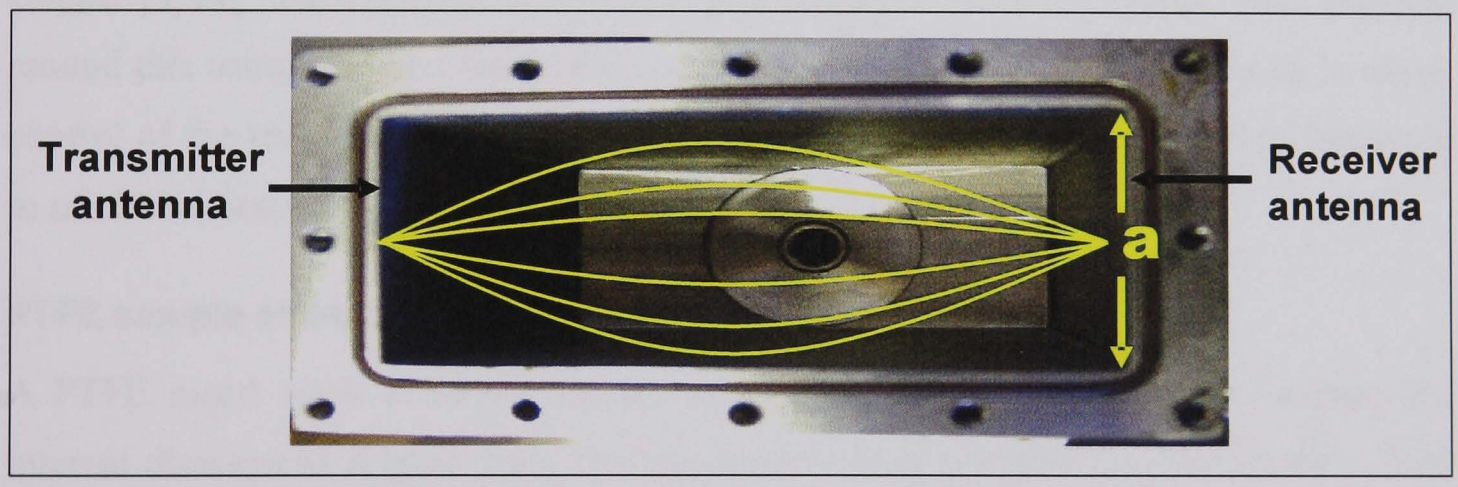

Figure 2.4: Picture of the guided microwave spectrometer (GMS) chamber. The yellow lines show the distribution of microwaves though the chamber. They are transmitted by the transmitter antenna on one side. The two parallel metal plates act as a wave guide and steer the wave front towards the receive antenna, located on the other side. This enables microwaves to pass through the entire chamber.

The GMS chamber is sealed with a lid (Figure 2.5). This contains several inlet ports that serve as an inlet for reagents, a stirrer, a NIR probe and a temperature probe. The NIR transmission probe can be inserted into the chamber to allow MW and NIR spectra to be collected simultaneously. The optimum location of the NIR probe was determined, and the top plate designed accordingly, see section 3.2.1.

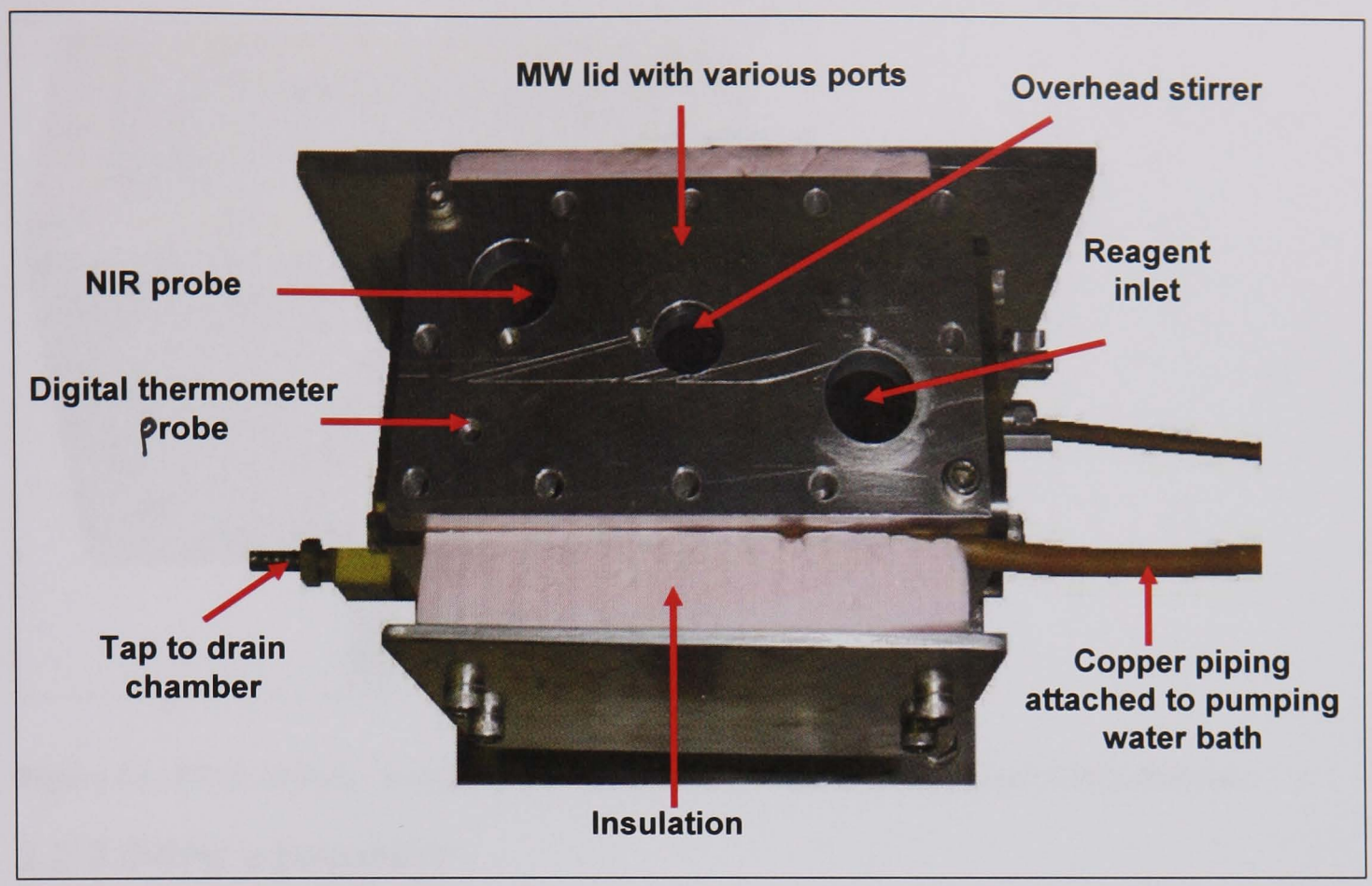

Figure 2.5: Picture of the guided microwave spectrometer (GMS) chamber, showing the lid that seals the chamber. The ports in the lid allow various pieces of equipment to be used in the GMS chamber.

Copper piping (5mm internal diameter) is coiled around the chamber and water pumped around this using a stirred thermostatic circulator water bath (Grant, England) to allow control of the temperature within the stainless steel chamber. The chamber is insulated to minimise heat loss.

PTFE sample chamber

A PTFE insert made in-house can be used within the GMS chamber to reduce the internal dimensions (Figure 2.6). This has been used in the drying experiments to hold the sample and allow air to be passed through it. This has internal dimensions of 5.9 x 8.0 x 4.7cm, giving a maximum volume of 33cm^3.

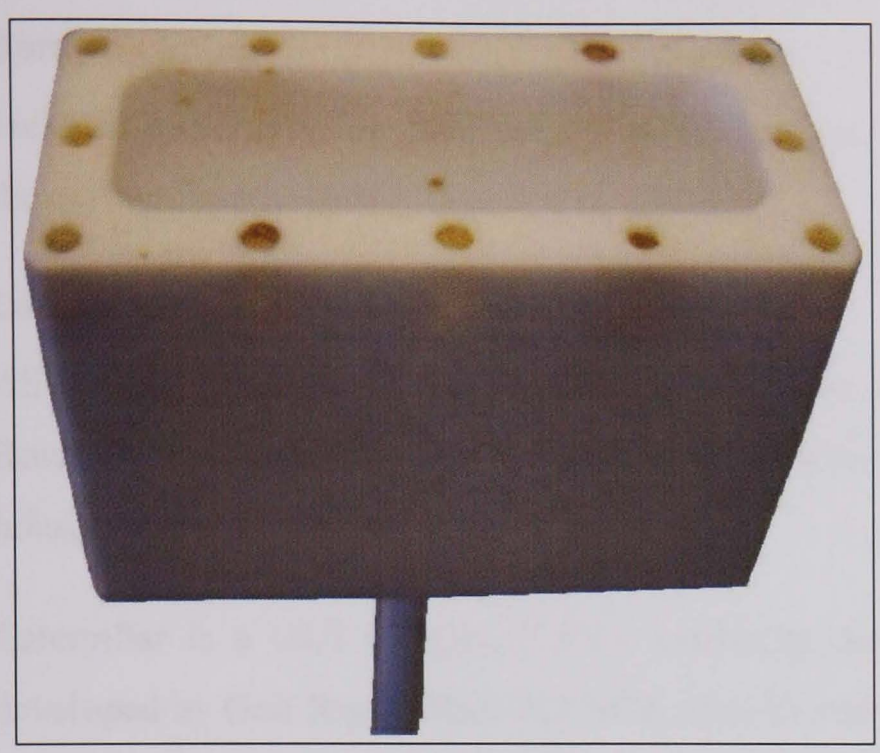

Figure 2.6: PTFE sample chamber for the guided microwave spectrometer (GMS) chamber.

2.2.3 Other equipment

Auto-pipettes

Eppendorf micropipettes, 1-10μl, 10-10μl and 100-1000μl.

Temperature probe

Temperature measurements made using a Kane-May digital thermometer fitted with a temperature probe, 1mm diameter and 10cm length. This covers a range of -50 to +1300°C.

GC

Shimadzu, GC-17A. Auto injector AOC-20i. This uses a flame ionising detector (FID). Hydrogen (99.995%, Energas Ltd, Hull, UK) and air are used.

A VF-5ms FactorFour capillary column (Varian, USA) is used for all analysis. This contains 5% phenyl-methyl low bleed stationary phase, which is equivalent to 5% phenyl, and 95% dimethylpolysiloxane. The column length is 30m, and width 0.25mm. Helium (99.99%, Energas Ltd., Hull, UK) is used as a carrier gas.

Stirrer

Janke and Kunkel, IKA-Werk. Variable speed 1-10. Set on 1 for all experiments (60 rpm).

Spray chamber

Jacketed cyclonic spray chamber, (Glass Expansion, Australia), used for heating air in the drying experiments.

Data processing

All spectra collected are transferred into MATLAB versions 6.5 or 7.0 (Mathworks). Routines from the PLS-Toolbox version 3.0.4, were used along with ones created in-house.

Caterpillar is a GUI (Graphical User Interface) that operates within MATLAB 7.0, developed by Geir Rune Flåten (CPACT, Hull University, UK).

DoEMan is a GUI for the determination of the best parameters to use to build a calibration model. This has been developed by Andrew Owen (CPACT, Strathclyde University, UK) and uses routines from the PLS-Toolbox. It uses a design of experiment approach to build a series of calibration models using different types of pre-processing, and these models can be compared to determine the optimum combination of pre-processing to use. The idea is based on a paper by Flåten and Walmsley [77].

GUIPRO is a MATLAB program for performing multivariate curve resolution (MCR) analysis of spectroscopic data, developed by Paul Gemperline of East Carolina University, USA [61]. Various settings can be used within this GUI to aid the modelling. Kinetic profiles can be used to break rank deficiency and allow the calculation of the kinetic profiles of a reaction.

2.3 Drying experiments

Dying a solid material is a widely used step in industry. The main problem with it is determining when the sample is dry. If a sample is to be removed to determine the degree of dryness, the main problem is where in the process the sample should be taken to ensure it is representative of the entire batch. Also there is a problem of how to take a sample, as physically removing a sample may cause the process to have to be stopped, so delaying it.

An ideal situation would be if the entire process could be monitored on-line, so eliminating the need to remove a sample and give a truly representative picture of what is happening in the process.

GMS is ideal as a sample can be placed in the chamber, and the whole sample is analysed at once. The aim of the work is to simulate a drying process within the GMS chamber, and monitor it by MW spectroscopy. The process is also to be monitored using a NIR diffuse reflectance probe. This only samples a small region of the material.

This has been split into wetting experiments, in which the drying process is simulated by adding solvent to a material, and drying in which solvent is removed from the material.

2.3.1 Wetting

2.3.1.1 Aim

The first experiments involve wetting the material to simulate a drying process. The aim is to monitor the increasing amount of solvent in a material using MW and NIR spectroscopy. The feasibility of monitoring a drying process using these techniques can be determined and also the limits of detection. The two techniques can be compared to determine if MW is the superior technique for this application as is expected.

2.3.1.2 Experimental setup for wetting experiments

The material to be dried is placed within the PTFE insert which has been made in-house. The insert is cuboid in shape which fits in the GMS chamber, and rests on the bottom of the chamber (Figure 2.7). The PTFE insert has an inlet tube at the top and an outlet at the bottom to allow liquid to flow through. The outlet tube must have filter paper put over it to keep the material within the insert. The NIR diffuse reflectance probe can be inserted in one of the ports of the lid of the GMS chamber.

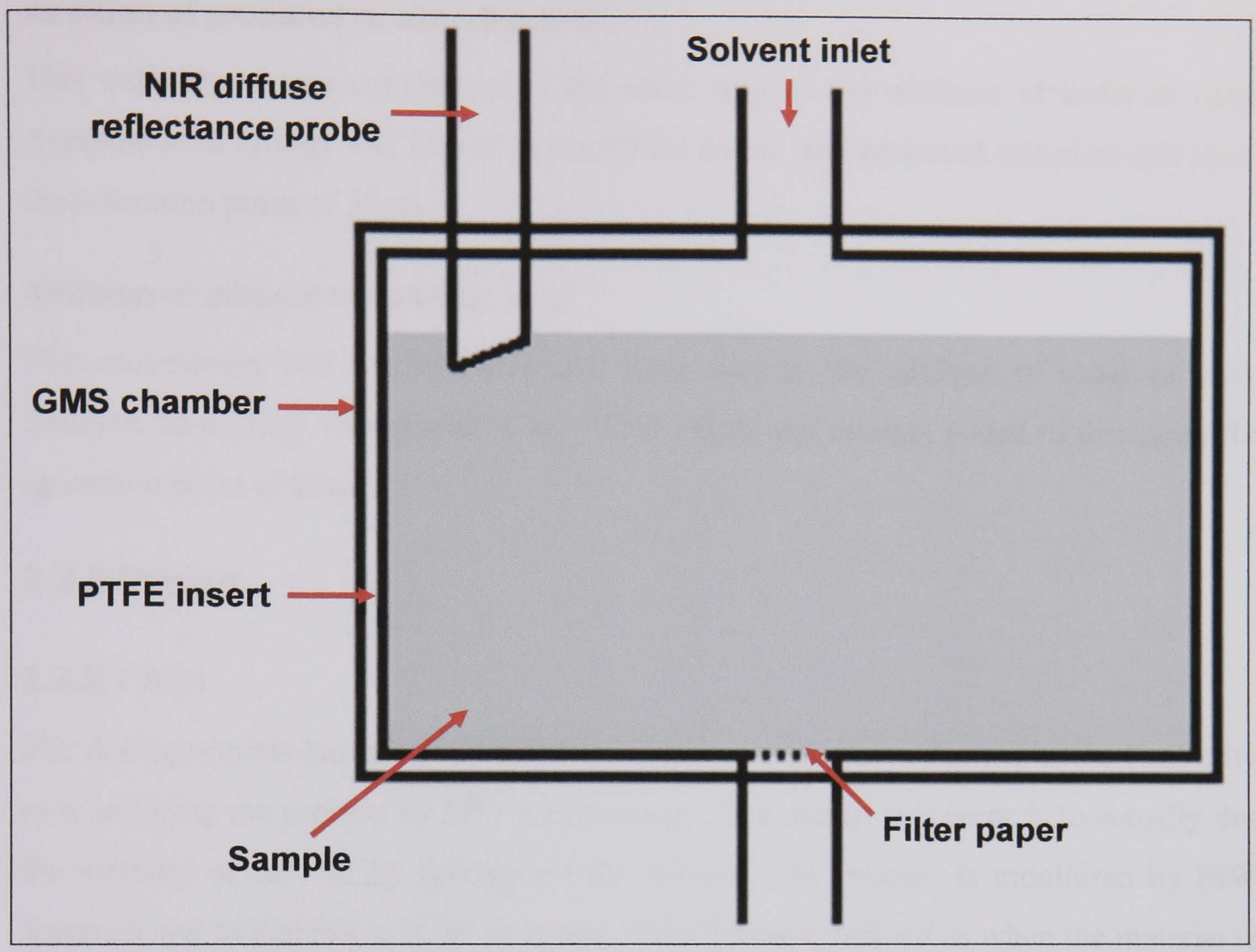

Figure 2.7: Basic set-up for the drying experiments. The PTFE insert sits on the bottom of the GMS chamber.

2.3.1.3 Experimental details for wetting experiments

Each experiment was repeated in triplicate. Repeats of MW and NIR spectra were collected. These repeats were averaged out to give one spectrum for each addition before data analysis was performed.

Addition of water to sand

Sand (150g) was placed in the PTFE insert. Distilled water was added in 0.1ml steps until 1.0ml total volume was reached using an autopippette, and then in 1.0ml steps until 10ml and 5.0ml steps until 35ml of water had been added in total. This gave full saturation of the sand. After each addition of water, two minutes were allowed to elapse to allow the water to soak through the material, and then 20 repeat MW scans and 40 repeat NIR scans were recorded. These repeat spectra were averaged to give one MW and one NIR spectra for each addition.

Addition of propanol to ascorbic acid

This experiment was carried out in the same way as the addition of water to sand. Ascorbic acid (100g) was placed in the PTFE insert, and propanol added to this up to the saturation point of 30ml.

Addition of ethanol to salicylic acid

This experiment was carried out in the same way as the addition of water to sand. Salicylic acid (83g) was placed in the PTFE insert, and ethanol added to this up to the saturation point of 25ml.

2.3.2 Drying

2.3.2.1 Aim

The drying process has been simulated by wetting a material to determine the feasibility of monitoring the process by MW spectroscopy. The aim of this work is to actually dry the material of solvent by driving off the solvent. The process is monitored by MW spectroscopy to determine if the endpoint of the process, defined as when the material is dry, can be identified.

2.3.2.2 Experimental setup for drying experiments

The experimental set-up was almost the same as for the wetting experiments, except a system to pass air though the material was used which meant no NIR probe was used due to lack of space for it in the chamber. The material is placed in the PTFE insert placed inside the GMS chamber. The experimental setup for the different methods of drying is described in the following experimental details section.

2.3.2.3 Experimental details for drying experiments

Drying of propanol from ascorbic acid by heating

Ascorbic acid (100g) is placed within the PTFE insert in the GMS chamber. The chamber is heated to approximately 52°C by the pumping water bath. Propanol (25ml) is added to the ascorbic acid and the solvent allowed to evaporate off for five hours. MW spectra are taken at intervals to monitor the progress of drying.

Drying of propanol from ascorbic acid by hot air

Ascorbic acid (100g) is placed in the PTFE insert within the GMS chamber, and propanol (10ml) is added. Air is flowed though a gas nebuliser into a jacketed cyclonic spray chamber used in ICP-MS. The spray chamber is connected to the water bath, and water is circulated around at 80°C to heat the air as it passes through. The air is then flowed into PTFE sample held in the GMS chamber (Figure 2.8).

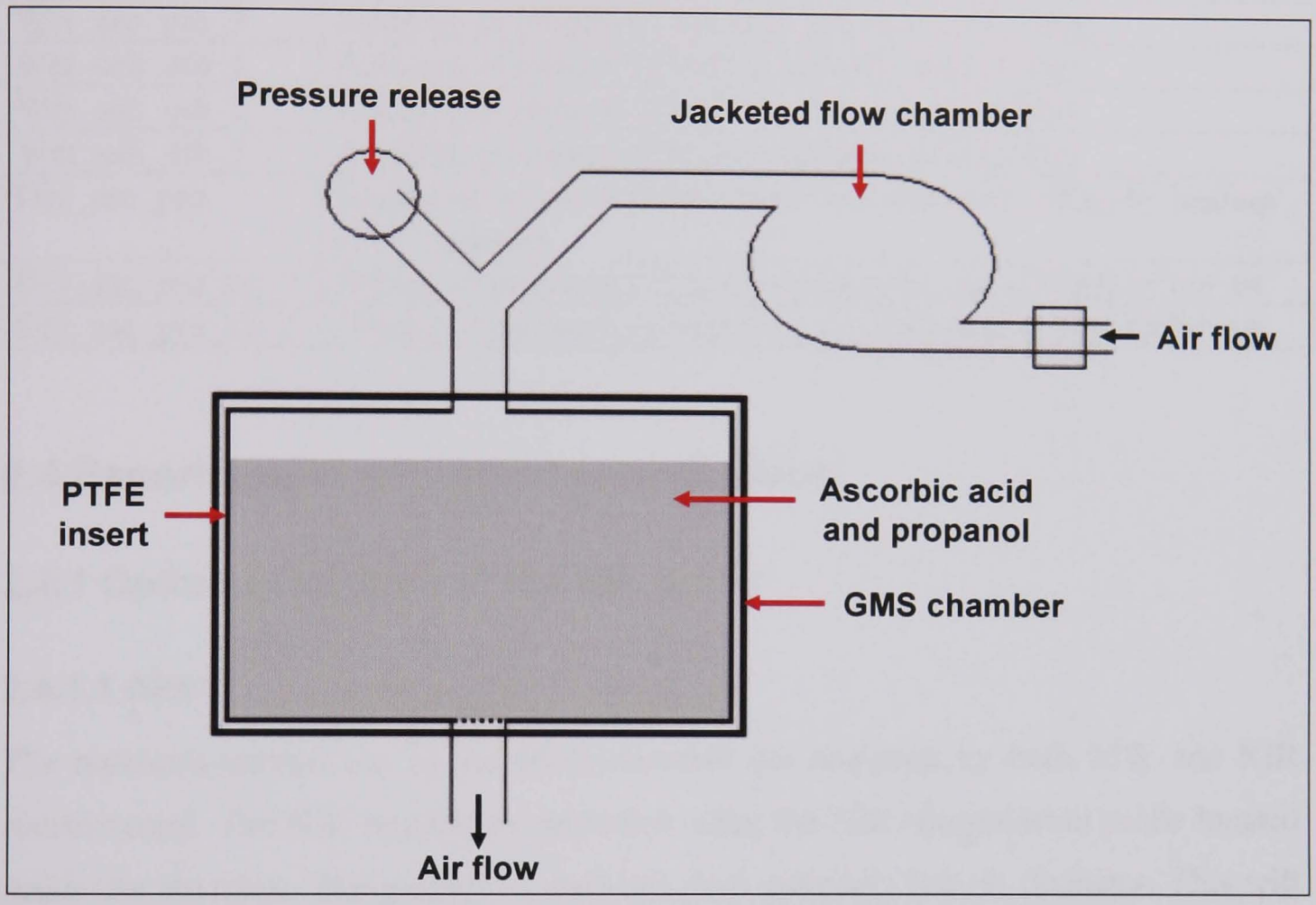

Figure 2.8: Equipment set up for the drying of propanol from ascorbic acid using hot air.

The flow rate was controlled using a gas flow control valve set to approximately 1l min^{-1}. The air temperature in the GMS chamber was approximately 23°C. The air was flowed through the system to allow the ascorbic acid to dry over time. MW spectra were taken at intervals. The experiment was carried out twice. The first experiment was left for 5h 30min, the heating stopped and the sample left overnight after which time further spectra were taken. The second experiment was left for 7h after which time the material appeared to be dry.

2.3.3 Summary of experiments

Table 2.2: List of drying experiments.

Experiment name	Description
Wet_sand_water_1	Addition of water (35ml) to sand (150g)
Wet_sand_water_2	Addition of water (35ml) to sand (150g)
Wet_sand_water_3	Addition of water (35ml) to sand (150g)
Wet_asc_pro_1	Addition of propanol (30ml) to ascorbic acid (100g)
Wet_asc_pro_2	Addition of propanol (30ml) to ascorbic acid (100g)
Wet_asc_pro_3	Addition of propanol (30ml) to ascorbic acid (100g)
Wet_sali_eth_1	Addition of ethanol (25ml) to salicylic acid (150g)
Wet_sali_eth_2	Addition of ethanol (25ml) to salicylic acid (150g)
Wet_sali_eth_3	Addition of ethanol (25ml) to salicylic acid (150g)
Dry_asc_pro	Drying of propanol (25ml) from ascorbic acid (100g) by heating GMS chamber
Dry_asc_pro_air_1	Drying of propanol (10ml) from ascorbic acid (100g) by hot air
Dry_asc_pro_air_2	Drying of propanol (10ml) from ascorbic acid (100g) by hot air

2.4 Experimental set-up for esterification

2.4.1 Optimum location of the NIR probe

2.4.1.1 Aim

The reactions carried out in the GMS chamber are analysed by both MW and NIR spectroscopy. The NIR spectra are collected using the NIR transmission probe located inside the chamber. The probe is a stainless steel cylinder, 2cm in diameter. This will cause reflectance of the microwaves when placed in the chamber, so affecting the MW spectra collected. This reflectance needs to be minimised. The probe must be located in an optimum position which causes least interference to the MW spectra, whilst giving representative NIR spectra. An experiment has been carried out to determine this optimum position. A plate will then be made for the top of the chamber to hold the probe in position. This location may have to be a compromise for ease of construction of the plate.

2.4.1.2 Experimental details for location of the NIR probe experiments

The chamber has been split into areas in which the probe could be located. The probe is 2cm in diameter, so the cross section of the chamber is split into regions to accommodate the probe. The width of the chamber is 4.7cm so some of the positions overlap. The probe must be inserted into the chamber to a depth of at least 3.5cm to

ensure the transmission slit is covered by the reaction mixture. Therefore, the depth of the chamber has been split into 3 sections of 3.5 / 4cm (Figure 2.9).

The chamber is filled with water (500ml) and the chamber heated to 32°C, to give a constant temperature. Ten repeat MW scans were taken with the NIR probe in each position (A1-15, B1-15, C1-15), along with ten NIR spectra, ensuring the transmission slit was facing into the chamber to ensure maximum contact with the liquid.

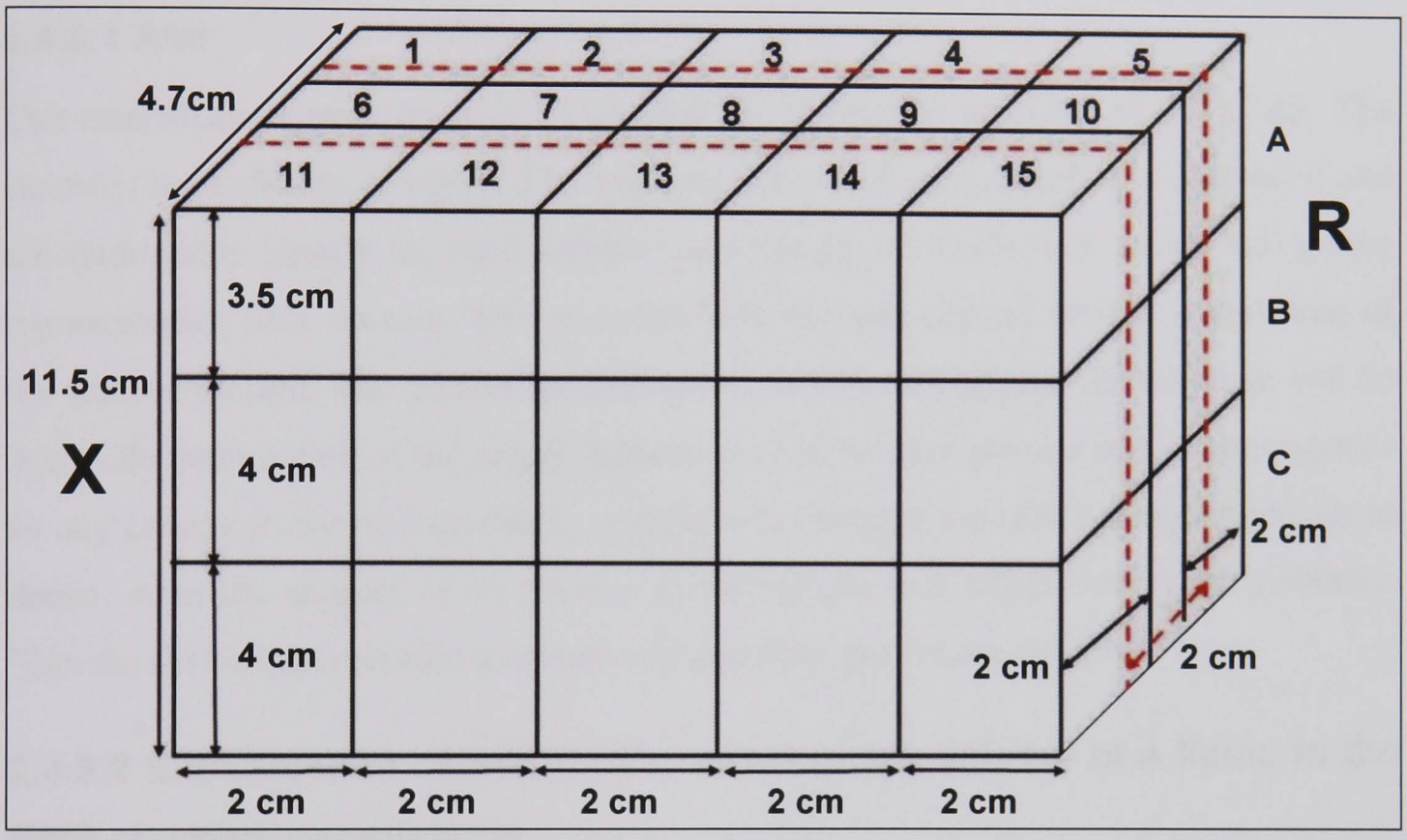

Figure 2.9: Possible locations of the NIR transmission probe within the GMS chamber. The red dashed line indicates the overlap of some of the possible probe positions. X indicates the location of the transmitter antenna and R the location of the receive antenna.

2.4.2 Effect of temperature on the collected spectra

2.4.2.1 Aim

The temperature of a sample affects both the NIR spectra of the sample, and also the MW spectra. This experiment was carried out to show the effect the temperature has on the collected spectra of the components in the esterification reaction. This will show the importance of keeping the temperature as constant as possible.

2.4.2.2 Experimental details for the effect of temperature experiments

The GMS chamber was heated to a variety of temperatures (25, 35, 40, 50 and 60°C). The reagents to be used in the esterification reaction (butanol and acetic acid) and the products formed (water and butyl acetate) were heated to the same temperature as the

GMS chamber and 450ml placed in the chamber. 20 repeat MW scans were taken for each reagent at each temperature, along with 40 repeat NIR scans using the transmission probe placed in the GMS chamber. The spectra were averaged to give one spectrum for each temperature.

2.4.3 Effect of volume of liquid in the GMS chamber on the recorded spectra

2.4.3.1 Aim

The esterification reaction is to be carried out inside the chamber of the GMS. The chamber holds 540ml of liquid. The reagents to be used are expensive to dispose of and are flammable. Ideally the total volume used should be minimised, whilst still giving representative MW spectra. The recorded MW spectra respond to the composition of the sample present. The greater the amount of sample, the greater the response will be due to the attenuation of the signal. Spectra is required that gives a maximum response so any change in the spectra due to a change in composition of the sample is easier to detect. Also the amount of air present in the sample will affect the recorded spectra. This should be kept constant to ensure reproducible spectra are collected.

2.4.3.2 Experimental details for the effect of the volume of a liquid in the GMS chamber experiments

The chamber is filled with 50ml of water, and ten repeat MW scans taken of this volume of water. The water used is at room temperature, the same as the chamber, to minimise temperature effects. A further 50ml is added, and again spectra are taken. This is repeated until the chamber is filled to 500ml. The spectra for each volume of water are averaged before data analysis.

2.5 Esterification reactions

2.5.1 Aim

The aim of this work was to monitor a simple reaction by MW and NIR spectroscopy, and compare the relative merits of each technique. The reaction studied is the esterification of butan-1-ol by acetic acid which is catalysed by sulphuric acid:

$$CH_3CH_2CH_2CH_2OH + CH_3COOH \leftrightarrow CH_3COOCH_2CH_2CH_2CH_3 + H_2O$$

This reaction was chosen as it is a simple, quick reaction which is relatively safe and uses cheap, easily obtainable reagents.

It was proposed that the use of different chemometric techniques with the collected spectra could allow the monitoring of the reaction progress, and determine properties of the reaction such as the endpoint, and any upsets that may occur during the reaction that alter its progress.

2.5.2 Experimental setup for esterification reactions

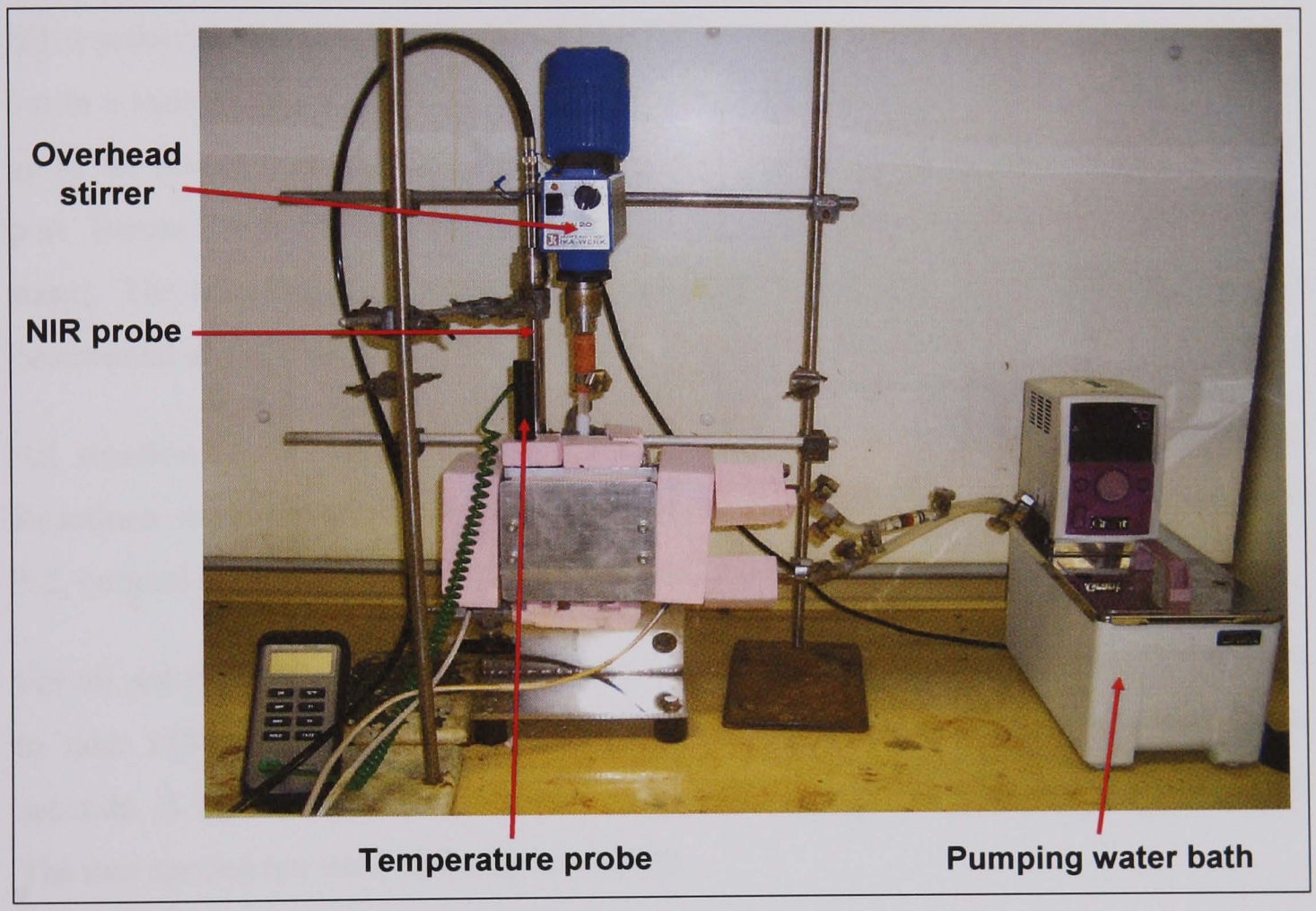

Figure 2.10: Equipment setup for the esterification reactions.

All experiments are carried out in the GMS chamber with the NIR probe inserted. The optimum location of the probe has been determined, see section 3.2.1. The chamber is thermostated using a pumping water bath. Figure 2.10 shows how the equipment has been set up.

The base plate of the GMS has a tap attached to allow easy emptying. The top plate has been made in-house and this contains ports for different pieces of equipment (Figure 2.5). An overhead stirrer is located in the central port. There is also a temperature probe inserted to monitor the reaction temperature. The NIR probe is located in another port, and there is a port for the inlet of reagents.

2.5.3 Characterisation esterification experiments

2.5.3.1 Aim

A set of standard characterisation reactions were monitored by MW and NIR spectroscopy, to give good data sets which can be used with various chemometric techniques. The reactions were repeated to determine if reliable and reproducible spectral data can be collected to monitor the reaction.

2.5.3.2 Experimental details for characterisation reactions

All reactions were carried out within the GMS chamber. The reagents were measured out in a measuring cylinder, and placed in volumetric flasks. The reagents were heated up to the reaction temperature before being placed in the GMS chamber via the inlet port. Butanol was added first, followed by the acetic acid. Spectra were taken at all stages. The acid catalyst was measured out using an auto-pipette, and added last. t_0 is determined as the time at which the catalyst is added.

All reactions were stirred using an overhead stirrer set to a speed of 1 (60rpm). Reactions were carried out at 40°C, thermostated by the water bath. A molar ratio of 1:2, butanol (200ml) to acetic acid (250ml) was used, with 1ml of catalyst.

For all reactions, MW spectra were taken every minute. The NIR spectrometer was set to take 1500 single spectra. One spectrum is recorded approximately every seven seconds. A spectrum relating to every minute is extracted for use in data processing. The raw spectra are used in the data analysis.

There is a summary of all experiments carried out in section 2.3.7. Reactions that differ from the standard characterisation reactions are described in the following sections.

2.5.4 Monitoring of reaction progress by GC

2.5.4.1 Aim

The standard data sets can be used with multivariate curve resolution techniques to predict the concentration profiles of the reactants and products during the reaction. A reference method is needed to compare the prediction profiles to what is actually occurring in the reaction. GC has been used to monitor some of the reactions to give this reference data. The GC method was first developed and calibrated. This was then

used with real samples taken from reactions to predict the concentrations and hence monitor the reaction.

2.5.4.2 Experimental details for GC work

GC set-up and calibration

A GC method was developed to resolve the components in the reaction mixture, and then a calibration built to allow the prediction of the composition of reaction samples.

An internal standard was chosen which has a different retention time from the components of interest, but is near enough so the analysis time is minimised. This allows correction of any variation that may occur in the injection volume. 4-Methyl-2-pentanone was chosen.

Method optimisation

First calibration samples 1, 4 and 8 (see Table 2.3) were made up in 5ml volumetric flasks, made up to 5ml with pentane. The pentane elutes before the other components so will not interfere with the analysis. 1.0ml was injected using a split of 1:85 to ensure the column was not overloaded with sample. The injector temperature was set to 250°C to ensure the sample is vaporised fully, and the detector also set to 250°C. The column temperature was set to 100°C to ensure a good separation was achieved.

Table 2.3: Volumes of components used to make up GC calibration samples. 1ml of internal standard (4-Methyl-2-pentanone) was added to each mixture.

	Butanol		Acetic Acid		Butyl Acetate		Water	
	Vol. / µl	Moles	Vol. / µl	Moles	Vol. / µl	Moles	Vol. / µl	Moles
1	889	0.00971	1111	0.01943	0	0.00000	0	0.00000
2	777	0.00850	1041	0.01820	160	0.00121	22	0.00121
3	666	0.00728	971	0.01698	319	0.00243	44	0.00243
4	555	0.00606	901	0.01576	479	0.00364	65	0.00364
5	443	0.00485	831	0.01454	638	0.00485	87	0.00485
6	330	0.00361	760	0.01330	800	0.00607	109	0.00607
7	217	0.00238	689	0.01206	962	0.00730	131	0.00730
8	105	0.00114	619	0.01082	1123	0.00853	154	0.00853

Calibration

Once a suitable method was obtained, a calibration was constructed to allow prediction of future, unknown samples. A set of eight calibration samples were made up, covering the range of concentrations of the components expected to be found in the reaction samples (see Table 2.3). Auto-pipettes were used to measure out the components. These were made up to 5.0ml with methanol, as the water dissolves better in methanol then pentane as used in the method optimisation and still elutes at a different time from the other components. The samples were made up with the final addition of acetic acid and stored in the fridge immediately to try to minimise any reaction which may occur. The calibration samples were run on the GC in a random order, and each sample was run in triplicate. The samples were made up fresh and the whole calibration repeated twice to ensure reproducibility of the method.

GC monitored reactions

Reactions were carried out in the same way as the standard reactions. A sample was removed (~1ml) at 10 minute intervals for GC analysis. The sample was put into a vial held in ice, to reduce the temperature as quickly as possible to try to stop the reaction. 2ml of the sample was taken using an auto-pipette, and placed in a 5ml volumetric flask (Grade A). 1ml of internal standard was added and this made up to 5ml with methanol. The mixture was kept on ice at all times. A small amount was placed in a GC vial, and this immediately analysed by GC.

The reactions were carried out at 40°C. A list of the reactions is shown in Table 2.4. A molar ratio of 1:2, butanol (200ml) to acetic acid (250ml) was used, with 1ml of catalyst.

Table 2.4: Esterification reactions followed by GC analysis.

Name	Molar ratio	Temp. / °C	Catalyst / ml
Ester_GC_40_1_1	1:2	40	1
Ester_GC_40_1_2	1:2	40	1
Ester_GC_40_1_3	1:2	40	1

2.5.5 Process upsets

2.5.5.1 Aim

The esterification reaction was carried out in which process upsets were stimulated, monitored by NIR and MW spectroscopy. These are to simulate process upsets that may occur in industry. The aim was to detect these process upsets from the NIR and MW spectra using chemometric techniques.

2.5.5.2 Experimental details for process upset reactions

All reactions were carried out in the standard way, with a molar ratio of 2:1, glacial acetic acid (250ml) to butanol (200ml). 4.0ml concentrated sulphuric acid (97%) was used as a catalyst in all but the catalyst addition reaction.

Ester_upset_cat: Addition of catalyst

1.0ml of catalyst is added at the start of the reaction. Further additions of catalyst (1.0ml) were added at 1790, 3590 and 5450s into the reaction, to give a total of 4.0ml of catalyst.

Ester_upset_charging: Charging of half of the reagents

The reaction chamber was charged with the butanol and approximately half of the acetic acid. The remaining acetic acid was added 2460s into the reaction.

Ester_upset_water_1: Addition of water

Water was added to the reaction at 1860 (1ml), 3660 (2.5ml), 5460 (5ml) and 6660s (7.5ml).

Ester_upset_water_2: Addition of water

Water was added to the reaction at 1800 (5ml), 2990 (7.5ml) and 4790s (10ml).

Ester_upset_benzoic: Addition of benzoic acid

Benzoic acid (2g/0.02mol) was added to the reaction at 3800s to simulate the charging of incorrect reactants.

Ester_upset_stirrer: Disturbance of stirrer

The following disturbances were made to the stirrer:

Table 2.5: Disturbances made during the process upset reaction (*ester_upset_stirrer*), in which the stirrer was disturbed.

Time / s	Disturbance	Time / s	Disturbance
2760	stirrer turned down to 1	4440	stirrer switched off
3120	stirrer switched off	6660	stirrer switched on
3720	stirrer switched on	7260	stirrer turned up to 2

Ester_upset_stirrer: Disturbance of stirrer

The following disturbances were made to the stirrer:

Table 2.6: Disturbances made during the process upset reaction (*ester_upset_stirrer2*), in which the stirrer was disturbed.

Time / s	Disturbance	
1200	stirrer switched off	stirrer off for 3 min
1380	stirrer switched on	
1980	stirrer switched off	stirrer off for 5 min
2280	stirrer switched on	
2880	stirrer switched off	stirrer off for 6 min
3240	stirrer switched on	
3840	stirrer switched off	stirrer off for 7 min
4260	stirrer switched on	
4860	stirrer switched off	stirrer off for 8 min
5340	stirrer switched on	
5940	stirrer switched off	stirrer off for 9 min
6480	stirrer switched on	
7260	stirrer switched off	stirrer off for 10 min
7860	stirrer switched on	
8460	stirrer switched off	stirrer off for 15 min
9360	stirrer switched on	

Table 2.7 summarises the process upsets stimulated in each of the experiments.

Table 2.7: Table of process upset reactions giving details of the process upsets stimulated.

Name	Experiment	Time upset stimulated / s		
Ester_upset_cat	Addition of catalyst (1ml) at intervals.	1790	3590	5450
Ester_upset_charging	Charging of butanol and half acetic acid. Remaining acetic acid added during reaction.	2460		
Ester_upset_water_1	Addition of water at intervals, 5ml, 7.5ml, 10ml.	1800	2990	4790
Ester_upset_benzoic	Addition of benzoic acid (2g / 0.45%w/v) during reaction.	3800		
Ester_upset_stirrer_1	Stirrer switched off at intervals for different time periods.			
Ester_upset_stirrer_2	Stirrer switched off at intervals for different time periods.			

2.5.6 Summary of experiments

Table 2.8: Table of esterification reactions carried out.

Name	Molar ratio	Temp. / °C	Catalyst / ml	
Ester_40_1:2_1_1	1:2	40	1	Characterisation reaction.
Ester_40_1:2_1_2	1:2	40	1	Characterisation reaction.
Ester_40_1:2_1_3	1:2	40	1	Characterisation reaction.
Ester_40_1:2_4_1	1:2	40	4	Characterisation reaction.
Ester_40_1:2_4_2	1:2	40	4	Characterisation reaction.
Ester_50_1:0.25_1_1	1:0.25	50	1	Characterisation reaction.
Ester_50_1:0.25_1_2	1:0.25	50	1	Characterisation reaction.
Ester_50_1:0.25_1_3	1:0.25	50	1	Characterisation reaction.
Ester_GC_40_1_1	1:2	40	1	Reaction followed by GC.
Ester_GC_40_1_2	1:2	40	1	Reaction followed by GC.
Ester_GC_40_1_3	1:2	40	1	Reaction followed by GC.
Ester_upset_cat	1:2	40	4	Addition of catalyst (1ml) at intervals.
Ester_upset_charging	1:2	40	4	Charging of butanol and half acetic acid. Remaining acetic acid added during reaction.
Ester_upset_water_1	1:2	40	4	Addition of water at intervals, 5ml, 7.5ml, 10ml.
Ester_upset_benzoic	1:2	40	4	Addition of benzoic acid (2g / 0.45%w/v) during reaction.
Ester_upset_stirrer_1	1:2	40	4	Stirrer switched off at intervals.
Ester_upset_stirrer_2	1:2	40	4	Stirrer switched off at intervals.

The experiments carried out have been given a code to aid identification of the conditions used. For all standard reactions the code is as follows:

Ester_a_b_c_d

Where ester indicates an esterification reaction, *a* the temperature the reaction was run at, *b* the molar ratio of butanol to acetic acid, *c* the amount of catalyst used and if *d* is present it indicates a repeat reaction.

So *Ester_40_1:2_1_2* is an esterification reaction carried out at 40°C, with a molar ratio of 1:2, butanol:acetic acid, with 1ml of catalyst, and this is the second repeat of the reaction.

For reactions followed by GC the code is:

Ester_GC_a_c_d

The GC indicated that is has been followed by GC, and the molar ratio is not included as all GC reactions were performed with a molar ratio of 1:2. *a*, *c* and *d* are the same as in the standard reactions.

For process upset reactions, the following code is used:

Ester_upset_z

The ester and upset indicate an esterification reaction with an upset stimulated. The type of upset is indicated by *z*.

When individual data sets are being referred to, the name of the reaction will be used with _MW or _NIR at the end to indicate if it is the MW or NIR data sets being used.

2.6 Data analysis

2.6.1 Wetting

2.6.1.1 Aim

MW and NIR spectra have been collected during the addition of solvent to a sample. The percentage mass of solvent present in the sample is known for each spectrum taken. Therefore, data sets exist with corresponding reference concentration data.

The aim of the data analysis of these data sets is to use simple multivariate calibration techniques to correlate the collected spectra to the reference concentration data. Once a model had been built, unknown samples can be predicted against it to predict the relative "wetness" of the sample. A model is built for each type of solvent and sample.

Various pre-processing techniques exist which can be used on the spectra to improve the correlation between the spectra and the concentration data to give the best model. Proper pre-processing of the data can help in the development of better predictive

DoEMan is a GUI within MATLAB which uses a design of experiment approach to calculate a series of calibration models using different pre-processing techniques. The aim of this work is to use DoEMan to determine the optimum model to use for prediction of the percentage by mass of solvent in the sample.

2.6.1.2 Experimental details

The data sets to be used are:

Wet_sand_water_1, 2 and 3

Wet_asc_pro_1, 2 and 3

Wet_sali_eth_1, 2 and 3

Models are built for each set of solvent and sample, for both MW and NIR spectra. DoEMan is used to build models using various pre-processing techniques and allow comparison of the techniques.

The models can be built using different calibration techniques: PCR, PLS1 and PLS2, and the prediction abilities of each one compared. In this work, PLS1 and PLS2 have been used as only one component concentration is to be calibrated, PLS1 should be sufficient, and it is expected using PLS2 will not improve the predictive ability of the calibration.

DoEMan uses the pre-processing algorithms in the PLS toolbox. Depending on the type of spectra to be used, only some of these are useful, and some knowledge of the techniques is needed. The pre-processing that is to be looked at is mean centring, Box-Cox transformation, orthogonal signal correction (OSC) and auto-scaling.

The predictive ability is assessed based by the root mean error of prediction (RMSEP) of the model, and how well the concentrations have been correlated to the spectra by the root mean square error of calibration (RMSEC). The models are built using two of the three repeat data sets, the calibration data, and the other data set is used as an independent validation set.

Global model

DoEMan, a Matlab GUI for determining the optimum calibration model (see section 1.4.2.5 for details) was applied to the calibration data set using the pre-processing

techniques stated. The calibration models that appeared to be the best were then used with the validation data to determine the predictive ability of the model.

Local models

The data collected appears to be non-linear, therefore building one large global calibration model may decrease the predictive ability of the spectra. The data was split into two linear ranges, 0.1 to 1.0ml, and 2.0ml to the maximum amount added. Again DoEMan was used to determine the optimum calibration models to use for each linear range based on the calibration data. The best models were validated and compared to determine the best overall model.

2.6.2 Drying

2.6.2.1 Aim

The drying of propanol from ascorbic acid has been monitored by MW spectroscopy (data sets *dry_asc_pro*, *dry_asc_pro_air_1* and *2*). The only reference available is the spectra of the dry ascorbic acid, before any solvent was added to it. The aim of the work is to analyse the data and see if it is possible to determine when the ascorbic acid is dry by comparison to the reference spectrum.

2.6.2.2 Experimental details

PCA

Principal components analysis (PCA) is performed on the data sets, after first mean centring the data. The scores containing the most amount of variance are examined to see if they reach a point at which no more variation is occurring between the samples. This point would be the point at which the material is dry and no more solvent is being removed.

Residuals

The reference dry spectrum can be subtracted from the process spectra to give the residual spectra. When this residual is zero, or very close, then the difference between the process spectra and the reference spectra of the dry material is negligible, therefore the material can be determined to be dry. The residuals were calculated for all data sets, and these examined to determine if it is possible to detect when the material is dry.

2.6.3 Esterification

2.6.2.1 Reaction progress prediction

Aim

Multivariate curve resolution (MCR) is a technique which is used to extract concentration profiles and pure component spectra from data with no reference concentration data. The majority of esterification reaction data collected in this work had no concentration information. Therefore, MCR has been performed on the reaction data to extract the concentration profiles and allow the reaction progress to be monitored. From these profiles the kinetic constant, *k*, is calculated. This value indicates the rate of reaction. For reactions run with the same conditions, except at different temperatures, the *k* value will be different. The same is true for reactions run with different molar ratios. This constant can be compared to assess the effectiveness of predicting the reaction progress.

Experimental details

A variety of the standard esterification reaction data has been used, *ester_40_1:2_1_1, 2* and *3*. MW and NIR data have both been used. GUIPRO is a GUI within MATLAB developed by Paul Gemperline [61]. A variety of constraints can be used within this GUI to aid the resolution of the data. In this work the aim was to minimise the amount of pre-processing and pre-analysis of the data to make the MCR techniques as simple and quick as possible, and minimise prior knowledge and user input.

The spectral data is loaded into the GUI, with corresponding time and wavelength data. A wavelength range can be selected so any regions not relating to the reaction or containing noise can be excluded. The range 4000 to 9000cm^{-1} was used for the NIR and the full frequency range for the MW data. The time range is also selected and for all data this is set so the first spectrum used in the calculation is that relating to the addition of the catalyst, t_0. The data is visualised using calculated PCA scores and any obvious outliers removed.

The first type of pre-processing that can be applied is baseline correction. There are various types that can be applied depending on the baseline effect that needs to be corrected for. The MW data does not have a baseline so no correction can be applied. The NIR data collected is of high quality with no shift in baseline, so no baseline

correction is needed. The second type is normalization. This corrects for any drift in the spectra which is seen when a region of the data, which is expected to remain constant, changes over time. There is no change seen of this kind in the collected spectral data, so this pre-processing was not used.

The number of components to be searched for in the data using MCR must be selected. This can be done manually or using an F-test. In either case some knowledge of the system is needed. In this data there are four components present, acetic acid, butanol, butyl acetate and water. However, there are only two independent components as the two reactants are decreasing at the same rate and the two products are increasing at the same rate, so they contribute the same amount of variance to the system and are not distinguished between. Therefore the number of components is set to two. This rank deficiency can be overcome by using kinetic constraints in the curve resolution, which will be discussed later.

The approximate locations of peaks in the composition profiles are determined. This can be done using a needle search [99] or EFA [59]. A needle search is performed automatically by performing a least-squares fit of a very narrow peak function, a needle, on each spectrum. When the location of the needle peak coincides with a maximum concentration of a component, a local minimum is often observed in the residual sum of squares. The results are displayed and some of the local minima selected. This technique may require some user knowledge as a local minima for each component is needed. If the correct number is not automatically chosen within the algorithm, then the user must decide which to use. EFA calculates initial estimates of the concentration profiles and the pure component spectra, and from this automatically approximates the location of the peaks. EFA has been used as it requires less user knowledge, so making the process simpler.

A scaling constraint can be applied to the reaction data. A maximum of one for the total concentration of the components can be used or a mass balance scaling. The mass balance scaling has been used as in most cases the reaction is a closed system with nothing being added or removed during the reaction. In the reactions monitored by GC, a small volume of sample is removed at intervals; however the mass balance constraint has still been applied to allow comparison of the results from all types of reactions.

There are two types of curve fitting that can be applied; constrained P-ALS (penalty alternating least squares) and non-negative ALS [61]. P-ALS requires user knowledge and input so complicating the curve resolution. Within this non-negative constraints can be applied to the concentration profiles and/or the spectral profiles for each component individually. Spectra of the pure components can also be included to aid resolution. Non-negative-ALS simply applies non-negative constraints to the pure component spectra and the concentration profiles for all components. It is expected that the concentration should be non-negative so this method has been used.

The final option within GUIPRO is the use of a kinetic fit [99]. Non-linear least squares uses the known reaction equation to aid resolution by breaking the rank deficiency of the data. The initial concentrations of the components are also used to give a starting concentration in the extracted concentration profiles. Concentration profiles for all components are predicted and this allows the calculation of the rate constant, *k*. This option has been used in GUIPRO for all the reactions looked at. It is this *k* value that is compared to determine the predictability of curve resolution.

The rate constants have also been determined for the GC reactions *ester_GC_40_1_1, 2* and *3*, run under the same conditions to compare the experiments.

2.6.2.2 Endpoint determination

Caterpillar is an adaptive algorithm which can be used to predict the endpoint of a reaction, by comparing the now variation to recent variation.

In caterpillar, two windows with a set window width size (WS) are placed in the data (see section 1.4.4.1 in introduction), with an inter-window-distance (inter-WS) between them. A principal component analysis (PCA) model is calculated for the second, reference window, to describe the "now" variation of the samples in this window. This is compared to the old variation in the samples in the detection window. The windows are moved through the data stepwise, with the model building repeated at each step, until a steady state in the variation is seen and this determined as the end-point of the reaction. The windows are separated by an inter-window distance to ensure that a constant variation is due to the actual endpoint of the reaction.

Optimization of variables to use in caterpillar algorithm

Aim

The variables within the algorithm, WS, inter-WS, stepsize, and number of PCs to use in the model must be defined. The aim of this experiment was to use a reference data set to optimise these variables. Once these are determined for a reaction with specific conditions, the same variables can be used for subsequent reactions with the same conditions.

Experimental details

The step-size of the movement of the windows through the data can be changed, this was set to one for all analysis due to the data sets being relatively small (~180 samples). The significance level below which the reaction must fall before it is deemed to have reached stability and hence the endpoint, can also be altered. This was set to 0.99 for all analysis to ensure the reaction is truly at its endpoint.

These variables have been optimised using the *ester_40_1:2_1_3* MW and NIR data sets. All the combinations of the different variables to be used can be examined. A minimum WS of five and a maximum of ten, with a minimum inter-WS of ten and a maximum of 20 are examined. It is convenient to use an inter-WS double that of the WS.

Once the optimum variables to use for these reaction conditions were chosen, the algorithm was applied to the spectra collected for the repeat reactions, using the same experimental conditions, *ester_40_1:2_1_1* and *2*. The endpoint should be the same for all the repeats.

2.6.2.3 Process upset detection

The caterpillar algorithm can also be used to detect process upsets in a reaction. This works in a similar way to the endpoint determination, but this time the windows are placed side by side. The first window is used as a reference window and the second as a detection window. A PCA model is calculated for the reference window to describe the variation of the samples in this window. The newest samples, contained in the detection window, are then compared to this model. If several of the samples in the prediction window are significantly different from the reference PCA model, this is interpreted as process change. Both windows are moved through the data stepwise allowing the

reference model to adapt to any process changes. This means the caterpillar algorithm will detect the onset of new phases in the process data as they occur.

Aim

The variables of WS and number of PCs to use in the PCA model must be optimised to ensure correct determination of process upsets. It is important, that only true process upsets are detected and not normal reaction variation as this would lead to false alarms.

Once the optimum variables have been chosen, the algorithm can be performed on spectra collected from reactions with stimulated process upsets to determine if these process upsets can be detected.

Experimental Details

The characterisation reaction spectra, data sets *ester_40_1:2_4_1* and *2,* were used to determine the WS and the number of PCs to be used in the PCA model within the caterpillar algorithm. This data is representative of the reactions performed, and contains only normal process variation.

The reference data was analysed using a range of window sizes and number of PCs and the number of atypical samples determined for each combination. The number of atypical samples is counted and displayed in an occurrence plot. The significance level must also be chosen, but this was set high (0.99) to minimise the number of false alarms.

Generally it is suggested to use a wide WS to ensure that the best representation of the variation in all stages of the process is captured. The data examined comprises of only around 180 samples, therefore, the WS is limited. A range of five to ten samples in the window was looked at. The smallest WS must always be one greater than the maximum number of components. One to four components were examined.

3.0 Results and Discussion

3.1 Monitoring the drying of a solid

Drying processes are widely used in industry, and the process must be carefully monitored to ensure the desired endpoint is achieved in the shortest time possible. One method to monitor a drying process is to physically remove a sample and test it. This is inefficient as the process may need to be stopped to take a sample, and it may be necessary to take several samples to ensure the analysis is representative of the whole material being dried, which is difficult if the sample is large.

GMS has the advantage that the whole sample is analysed at once, so a more representative measurement of the process is taken. It is also very sensitive to water and solvents as they have relatively large dielectric constants, whereas solid materials have a low dielectric constant. NIR is used to monitor some drying processes with the use of a diffuse reflectance probe. These probes are placed in the solid and analyse a certain depth of the material. This has the disadvantage that only one small area of the process is sampled, so a representative measurement may not be taken. NIR is to be used in this work to monitor a drying process to give a direct comparison to MW spectroscopy, and to determine if either method is suitable for the monitoring of the drying of a solid.

The process of wetting a material with solvent was initially monitored to simulate the drying process in reverse i.e. the order of the spectra is collected in reverse order, from dry to wet. This is to ensure a change in the amount of solvent in a material can be detected by the two techniques and also to give an indication of the limits of detection that can be achieved. The actual drying process has also been monitored to show the possibilities of using these techniques for monitoring a true drying process.

3.1.1 Wetting

Three types of wetting experiment have been performed; the addition of water to sand, propanol to ascorbic acid and ethanol to salicylic acid. Reference data exists in the form of the quantity of solvent added to the material, quoted as percentage weight for weight. The aim of the work is to correlate the concentration information to the spectra to monitor the process, and allow the prediction of the dryness of new samples. A calibration model is to be built which gives the best prediction of new samples.

The collected NIR spectra should be linear with respect to the amount of solvent added, as according to Beers Law, the absorption is directly proportional to the amount of absorbing species present. This should mean simple linear models will be needed for the calibration of the NIR spectra to the amount of solvent present.

The collected MW spectra are expected to be non-linear with respect to the amount of solvent added. When the solvent first comes into contact with the dry material, a single layer of water is adsorbed. Depending on the inner area of the solid, adsorbed water can account for the first 2 – 10% of a solids water content. Once the maximum amount of water has been adsorbed, this amount is constant, and no longer affects the measurement. The remaining water is absorbed which has a different affect on the collected MW spectra. For applications that cover a range from low to high water contents, a non-linear calibration method or local calibration models that cover linear ranges are needed to handle these two different types of solvent affects.

3.1.1.1 Addition of water to sand

Water was added to sand in 0.1ml steps to 1ml, then 1ml steps to 10ml and 5ml steps until the saturation point of 40ml was reached. MW (20 replicates) and NIR (40 replicates) spectra were recorded at each step. The spectra were averaged before data analysis to give one representative spectrum for each step. The process was repeated three times to give three replicates. The data sets recorded are *wet_sand_water_1*, *2* and *3*, for MW and NIR.

3.1.1.1.1 MW spectra for the addition of water to sand

Exploratory analysis of the data

Spectra for one of the process repeats are shown in Figure 3.1.1. These clearly change over the course of the process. The dry spectra can be distinguished from the other spectra. The first ten spectra, below 1ml of water added, are very close together. It can be seen that below 300MHz there appears to be noise in the spectra. It is expected that using frequencies above 300MHz only will result in a better calibration model as the noise that appears to be in the spectra will not be included.

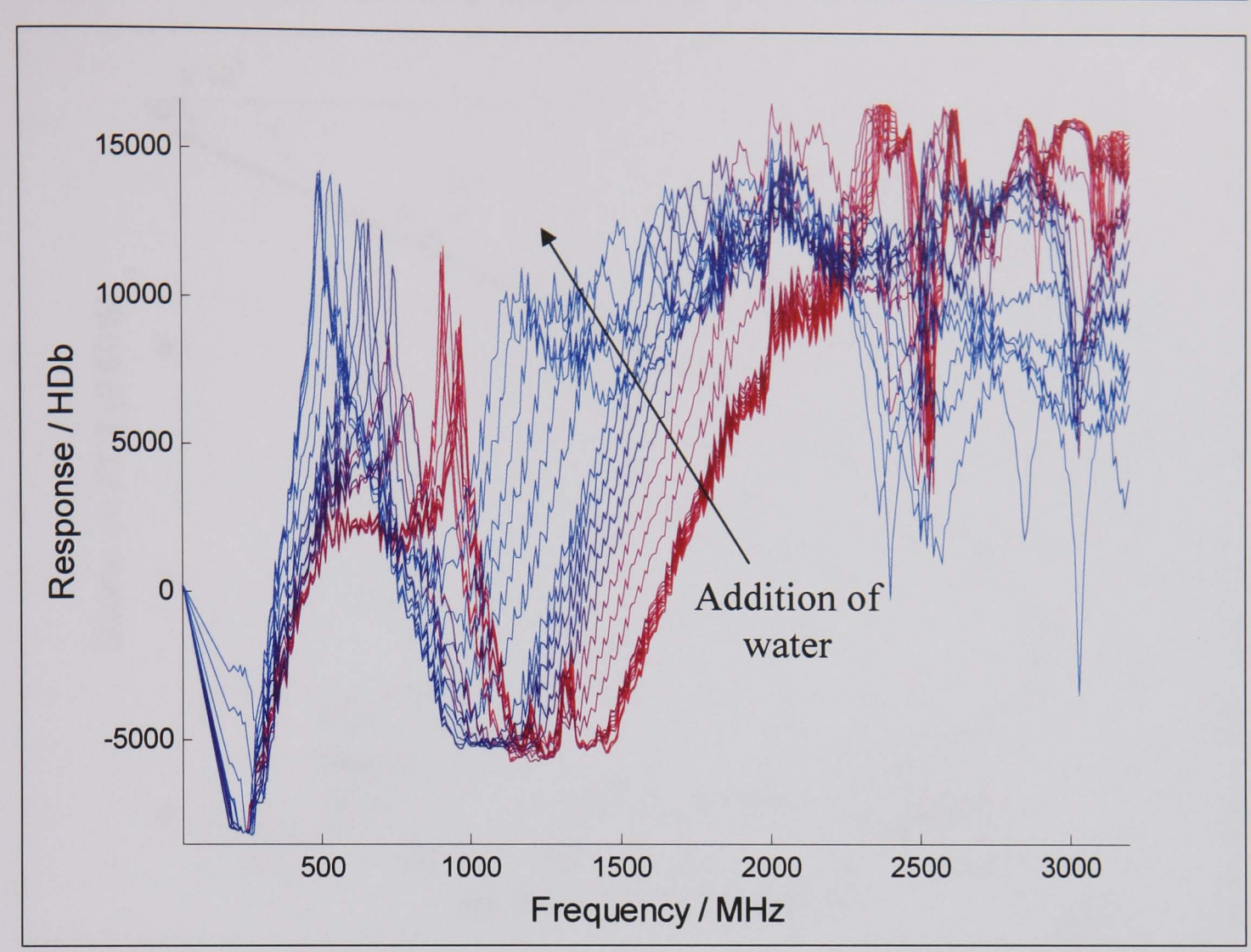

Figure 3.1.1: MW spectra for the addition of water to sand. The spectra go from red (dry sand) through to blue (40ml water).

PCA has been performed on all three replicates of the process and the scores on PC1 vs. PC2 are shown in Figure 3.1.2. The scores show the variation between the samples. There appears to be three clusters in the scores. The water was added in three different step sizes, 0.1ml, 1ml and 5ml, and these three clusters could be due to these different step sizes giving different variation.

The second and third data sets were recorded on the same day, and the first on a subsequent day. The scores for the second and third data set (red and green respectively) have less variation between them. These two sets are to be used as calibration data as they should have similar experimental variation as they were recorded on the same day. The first data set is to be used as a true validation set as it will have slightly different experimental variation so will test the robustness of the calibration model to experimental variation.

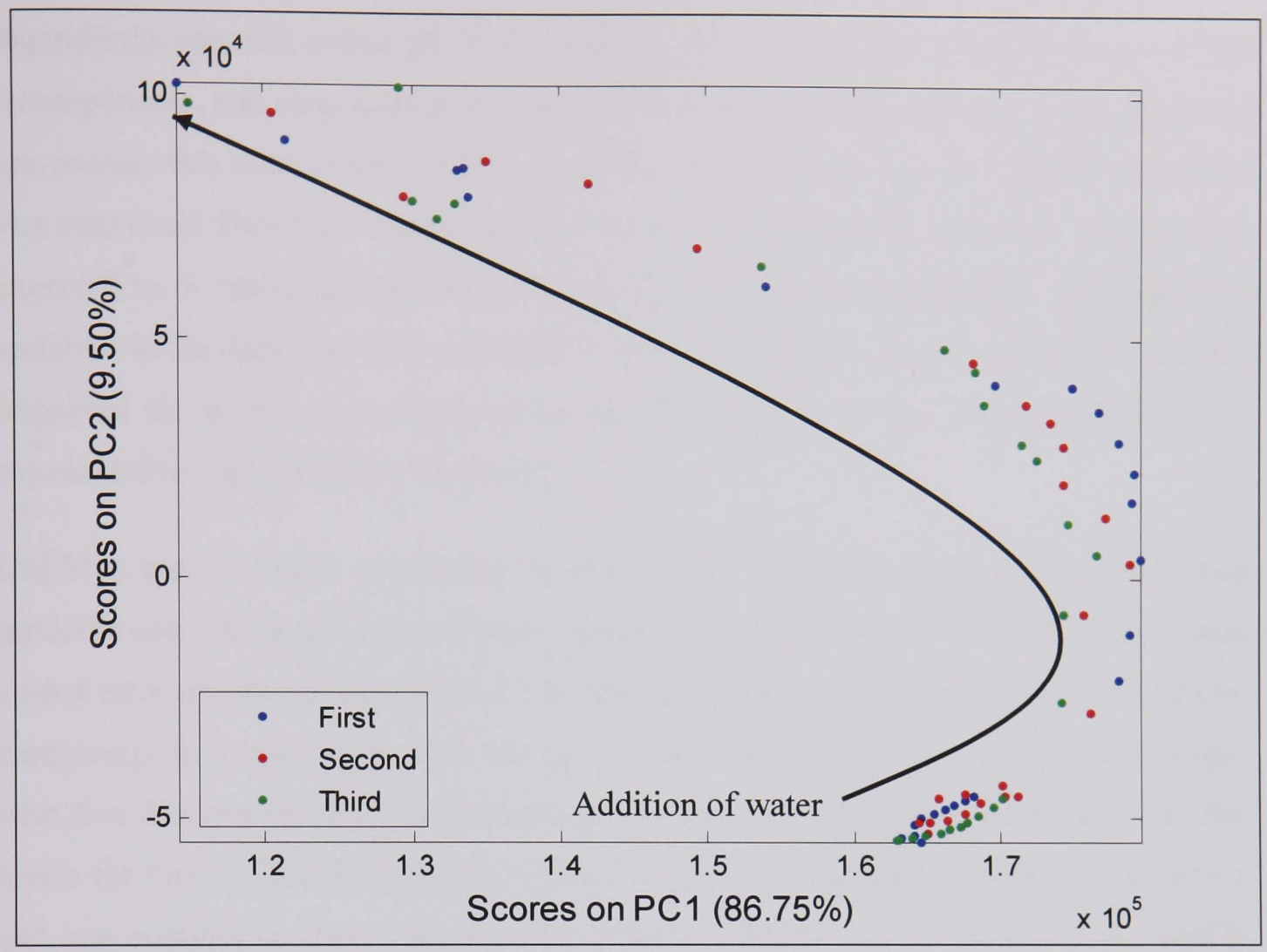

Figure 3.1.2: Scores on PC1 vs. PC2 for MW spectra recorded during the addition of water to sand. The process was monitored three times to give three replicate sets of MW spectra.

Optimisation of calibration method

A variety of pre-processing techniques can be used within a calibration model to improve the correlation between the spectral and concentration data. Some pre-processing techniques will have a detrimental effect on the calibration model, therefore it is important to choose pre-processing techniques carefully. Ideally a model should be built using each of the techniques and the models compared. DoEMan is a GUI in MATLAB which allows a range of models to be built with various types of pre-processing and the predictive ability of the models compared. This gives a reasonable idea of how the pre-processing techniques will affect the modelling, and is much quicker than building all possible variations of models manually.

There are several types of pre-processing available to use in the GUI. They are all inbuilt MATLAB functions within the PLS toolbox. Some techniques are not useful for the type of data being looked at. It is therefore necessary to choose the techniques most likely to improve the calibration using knowledge of the data and the techniques. The techniques chosen to be examined are mean centring, Box-Cox transformation using

logarithmic, squared, cubed and to the power four transformations, OSC, using 1, 2 and 3 components, and auto-scaling. It was decided these techniques are the most suitable to pre-process this data. Mean centring is usually performed as standard so this technique was examined. Box-Cox transformations improve the linearity of data and as the data is expected to be non-linear this was tried using different transformations. OSC removes variation in the data that isn't correlated to the concentration, so this was tried to see if it improved the model. Auto-scaling puts all the variables on the same scale so it was expected this might improve the model.

DoEMan uses a design of experiment approach to determine the optimum calibration model to use. The response, root mean square error of prediction (RMSEP) or root mean square error of calibration (RMSEC) is examined when going from a low level, no pre-processing, to a high level, with the use of pre-processing. It is a mixed level design, with five discreet factors (pre-processing and type of calibration model) varied at two levels for three of the factors, four levels for one factor, and five levels for one factor, and one continuous factor, the number of latent variables (LVs) to use in the model, varied at ten levels.

A calibration model is built using each of the chosen pre-processing techniques individually, and using a combination of the pre-processing techniques. The error of calibration (RMSEC) and error of prediction (RMSEP) are calculated to allow comparison of the models. The RMSEP is calculated by using an independent data set, so gives the true validation error (see section 1.4.2.5 in introduction).

DoEMan does not give the ultimate best parameters to produce the best calibration model, but it does give an indication of which pre-processing will improve the model and which will have a detrimental effect. This then allows the user to build a smaller series of models using the pre-processing techniques expected to improve the calibration model. These models can be fully validated using an independent validation set of data, and the best calibration model determined.

The chosen response of the design of experiment is RMSEC and RMSEP, a matrix of the response is plotted (Figure 3.1.3 and Figure 3.1.4 respectively) to allow ease of comparison. The plots along the main diagonal show the main effects of the pre-processing techniques as labelled on the axis. The other plots show the interaction effects between the pre-processing variables. The abscissas in the subplots relates to the

response, either RMSEC or RMSEP. The lower the error in the model, the better the fitting of the model.

In the subplots the response, RMSEC or RMSEP, for the variables are indicated by points that are connected with lines. The ordinate of the subplot indicates the level of the pre-processing used. In the majority of cases, 1 indicates the pre-processing is not used, and this is termed the low level. 2 indicates the pre-processing has been used, and this is referred to as the high level. In the cases where there are more levels, the pre-processing technique has been used with several different parameters. In the case of the Box-Cox transformation, 1 indicates the pre-processing is not used, 2 indicates it is used with power = 0, logarithmic transformation; 3 indicates power = 1, square root transformation, 4 indicates power = 2, cube root transformation and 5 power = 3, root to the power four transformation. In the case of OSC, 1 indicates OSC isn't used, 2 indicates 1 OSC component is used, a 3, 2 OSC components are used and 4, 3 OSC components are used.

The type of pre-processing labels the row. In the subplots with two lines, the interaction effects are shown. The lines correspond to the level of pre-processing used, blue for off, low level, and green for on, high level. The pre-processing examined is labelled at the foot of the column. The rows and columns have also been labelled with letters to aid identification when describing a plot.

The bottom row of plots (g,a) through to (g,f) show the error for the models built with different numbers of LVs. It is important to include the correct number of LVs so that all the relevant variation in the data is modelled, without including noise. The number of LVs to use is a compromise between low error, and a low number of LVs.

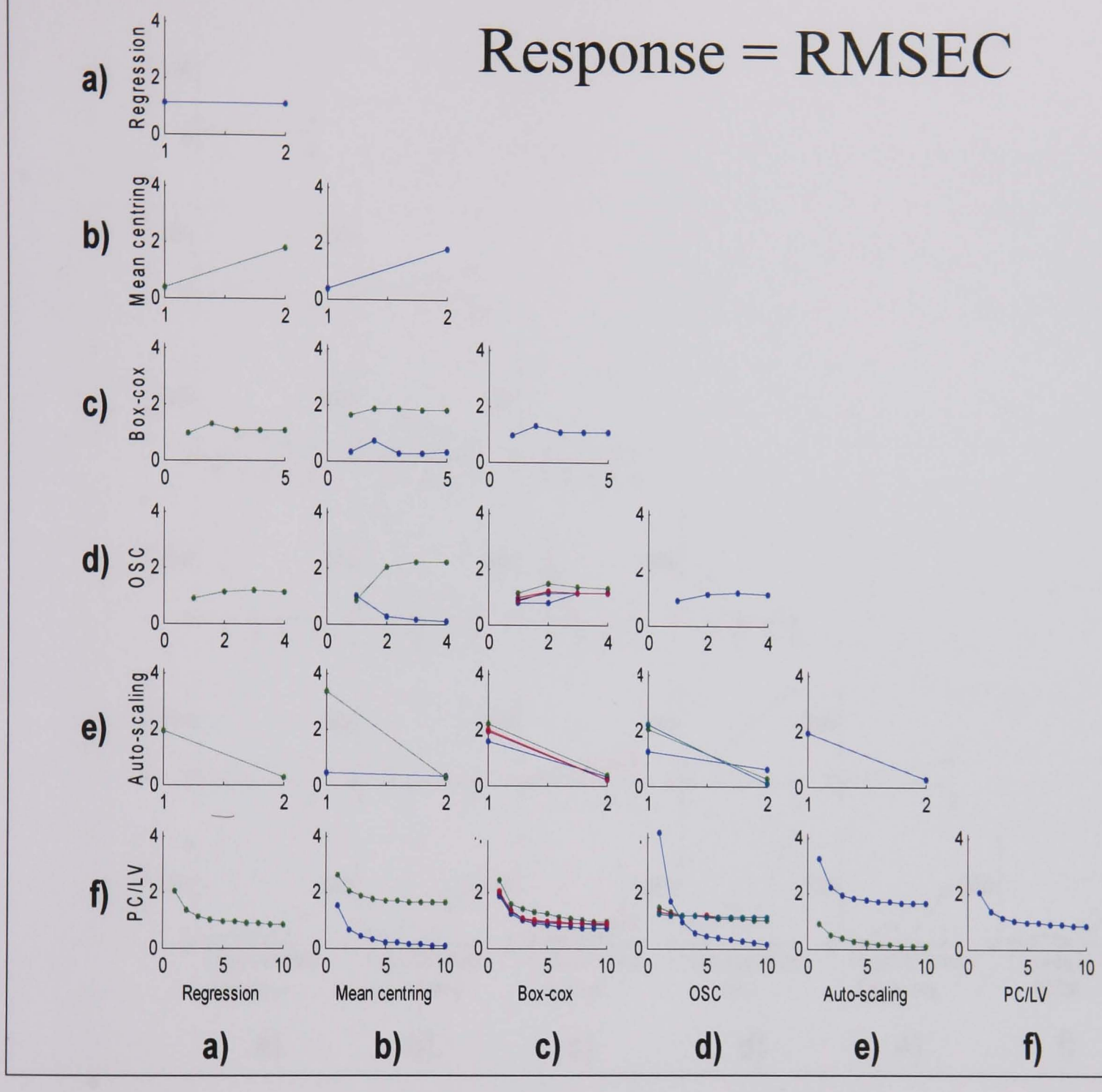

Figure 3.1.3: Results of DoEMan using the second and third data sets showing the effects of the different pre-processing used. The error shown is the RMSEC. The plots along the main diagonal show the main effects of the pre-processing techniques as labelled on the axis. The other plots show the interaction effects between the pre-processing variables. In the subplots the RMSEC for the variables are indicated by points that are connected with lines. The ordinate of the subplots indicate the level of the pre-processing used. The type of pre-processing labels the row. 1 indicates the pre-processing is not used, and this is termed the low level. 2 indicates the pre-processing has been used, and this is referred to as the high level. In the subplots with two lines, the interaction effects are shown. The lines correspond to the level of pre-processing used, blue for low, and green for high. The pre-processing examined is labelled at the foot of the column. The rows and columns have also been labelled with letters to aid identification when describing a plot.

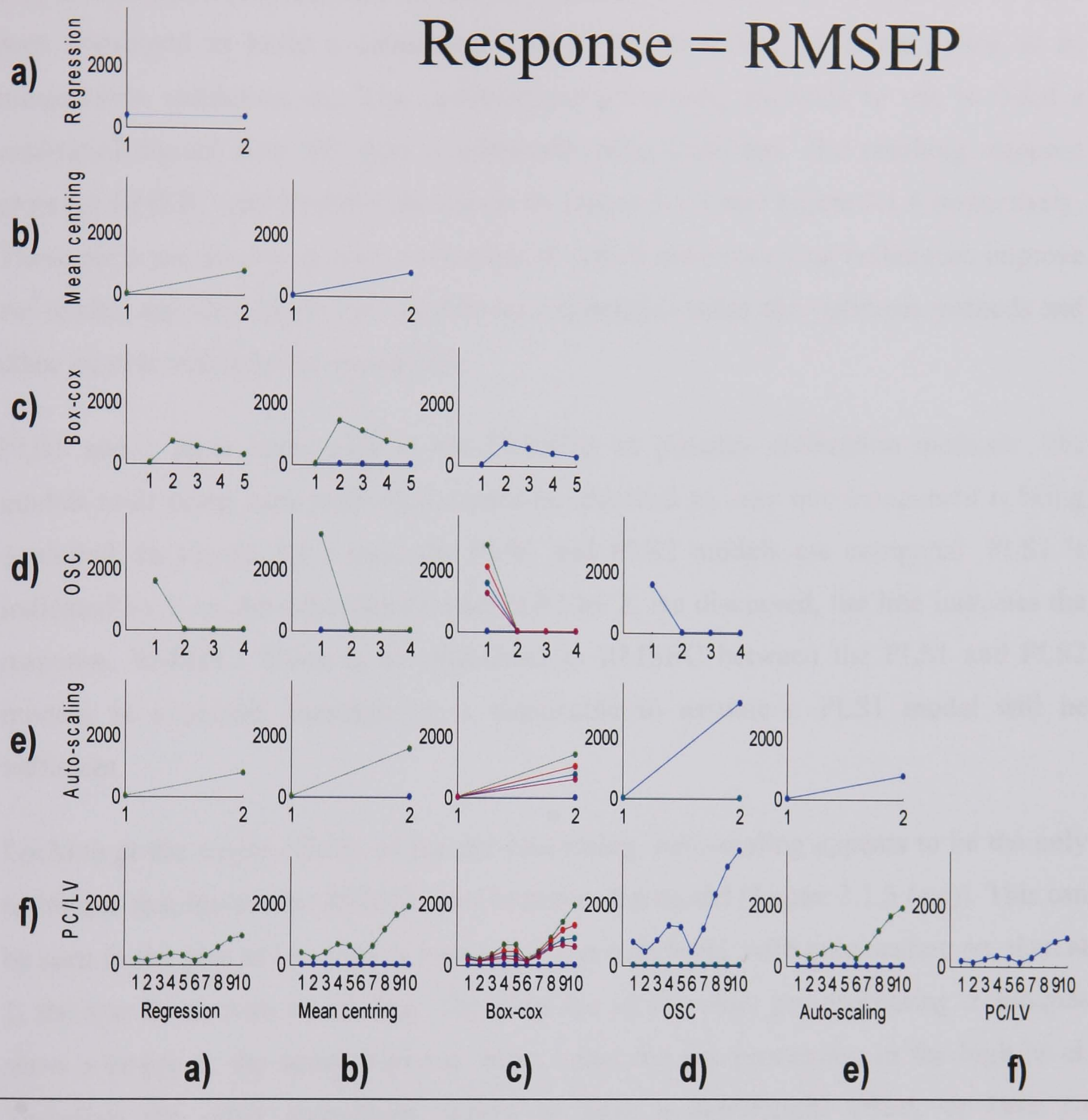

Figure 3.1.4: Results of DoEMan using the second and third data sets showing the effects of the different pre-processing used. The error shown is the RMSEP. The plots along the main diagonal show the main effects of the pre-processing techniques as labelled on the axis. The other plots show the interaction effects between the pre-processing variables. In the subplots the RMSEP for the variables are indicated by points that are connected with lines. The ordinate of the subplots indicates the level of the pre-processing used. The type of pre-processing labels the row. 1 indicates the pre-processing is not used, and this is termed the low level. 2 indicates the pre-processing has been used, and this is referred to as the high level. In the subplots with two lines, the interaction effects are shown. The lines correspond to the level of pre-processing used, blue for low, and green for high. The pre-processing examined is labelled at the foot of the column. The rows and columns have also been labelled with letters to aid identification when describing a plot.

Optimisation of the calibration model using the second and third data sets

The second and third data sets for the MW data (*wet_sand_water_2* and *3_MW*) have been combined to build a calibration model. The first data set is then used as an independent validation set. The optimum pre-processing methods to use to build a calibration model with this data is examined using DoEMan. The resulting response plots for RMSEC and RMSEP are shown in Figure 3.1.3 and Figure 3.1.4 respectively. These plots are used to give an indication of which pre-processing techniques improve the model, and then individual models are constructed using the optimum methods and these models validated independently.

PLS1 and 2 have been used in the DoEMan as possible calibration methods. The models built using each technique should be identical as only one component is being modelled. In Figure 3.1.3 (a,a) the PLS1 and PLS2 models are compared. PLS1 is indicated by 1 on the subordinate, and PLS2 by 2. As discussed, the line indicates the response, RMSEC. There is no difference in RMSEC between the PLS1 and PLS2 models as expected, therefore it is reasonable to assume a PLS1 model will be sufficient.

Looking at the major effects of the pre-processing, auto-scaling appears to be the only technique that lowers the RMSEC and improves the model (Figure 3.1.3 (e,e)). This can be seen in the plot as the error is lower at 2, the high level, with auto-scaling on, than at 1, the low level, with no scaling. The plots for all the other pre-processing techniques show a larger or the same response when using the pre-processing in the high level. Therefore the other techniques appear to have a detrimental effect, or have no improvement on the model.

The minor effects need only be looked at between auto-scaling and the remaining pre-processing techniques, as it has been shown only auto-scaling improves the model. These are shown in plot Figure 3.1.3 (e,a) through to (e,d). The blue line indicates the secondary pre-processing, as shown at the foot of the column, is not used, and the green line indicates the pre-processing is applied to the data, so for the Figure 3.1.3 (e,b), the blue line at point 1 had no pre-processing, and the green line at 2 has auto-scaling applied followed by mean centring, The pre-processing is applied in the order of that of the row header followed by that of the column label. Looking at the remaining plots

From these plots it appears that only auto-scaling will improve the fitting of the model, and the use of PLS1 is sufficient. The RMSEP plots, Figure 3.1.4, are also examined to identify which pre-processing techniques will improve the prediction error of the model. The models built are not validated with an independent data set, therefore this prediction error is only an indication of what can be expected. It is important to test the optimum calibration models with an independent data set.

Looking at the major effects in the RMSEP plot (Figure 3.1.4), there is no difference in the models built using either PLS1 or PLS2. From the RMSEP it seems that the use of OSC will give a better calibration model, and using one, two or three OSC components will give the same error. However, from the RMSEC the use of auto-scaling looks promising. From the RMSEP using no Box-Cox transformation gives the lowest error. Using a power=1 gives the highest error, and this decreases from power=2 onwards. The data is expected to be non-linear so the use of Box-Cox is to be investigated.

The use of auto-scaling, OSC and Box-Cox transformation as pre-processing techniques for the calibration of percentage water in sand were investigated. Box-Cox will be examined using a power of 0 and 1 to see what difference this makes to the model. This involves building a series of models using the different pre-processing techniques, as well as a combination of the techniques, using the second and third data sets as the calibration data (*wet_sand_water_2* and *3_MW*). When applying two pre-processing techniques, two calibration models must be built with each technique applied first, as the order in which the pre-processing techniques are applied will affect the resulting calibration model. The models were validated using the first data set (*wet_sand_water_1_MW*), which is an independent data set.

Global Calibration models

No pre-processing

As discussed earlier, only frequencies above 300MHz are to be examined in the data analysis. A PLS model has been built using the raw MW spectra, which has had no pre-processing applied to it. This is preformed in MATLAB using the PLS toolbox. The percentage variance captured in each LV is given in Table 3.1.1 for both the *X*-block (spectra) and *Y*-block (concentration) data. It is important to choose the number of LVs to use in the model which show a high correlation with the concentration data and also explain the variation in the spectra. Enough variables must be included to ensure all the

(spectra) and *Y*-block (concentration) data. It is important to choose the number of LVs to use in the model which show a high correlation with the concentration data and also explain the variation in the spectra. Enough variables must be included to ensure all the relevant variance is included, but inclusion of too many will cause over-fitting of the data. The percentage variance captured by each block for each latent variable calculated can be represented visually (Figure 3.1.5).

With 3 LVs 98.08% of the *X*-block is captured and 98.36% of the *Y*-block. With 4 LVs, only a further 0.37% variance of *X* is captured and 1.14% of *Y*. This is reduced to 0.22% in *X* and 0.29% in *Y* for 5 LVs. It is difficult to determine from looking at the percentage variance captured how many LVs need to be included in the model, so other methods must also be examined.

Table 3.1.1: Percentage variance captured by PLS model built using raw MW spectra, data sets 2 and 3, collected for the addition of water to sand. The percentage variance captured is shown for both the *X*-block (spectra) and *Y*-block (concentration).

	X-Block		Y-Block	
LV	**This LV**	**Total**	**This LV**	**Total**
1	84.79	84.79	41.40	41.40
2	11.57	96.36	47.56	88.96
3	1.67	98.03	9.40	98.36
4	0.37	98.40	1.14	99.50
5	0.22	98.63	0.29	99.79
6	0.26	98.88	0.04	99.83
7	0.10	98.99	0.08	99.91
8	0.20	99.18	0.02	99.93
9	0.14	99.33	0.02	99.95
10	0.07	99.40	0.01	99.96

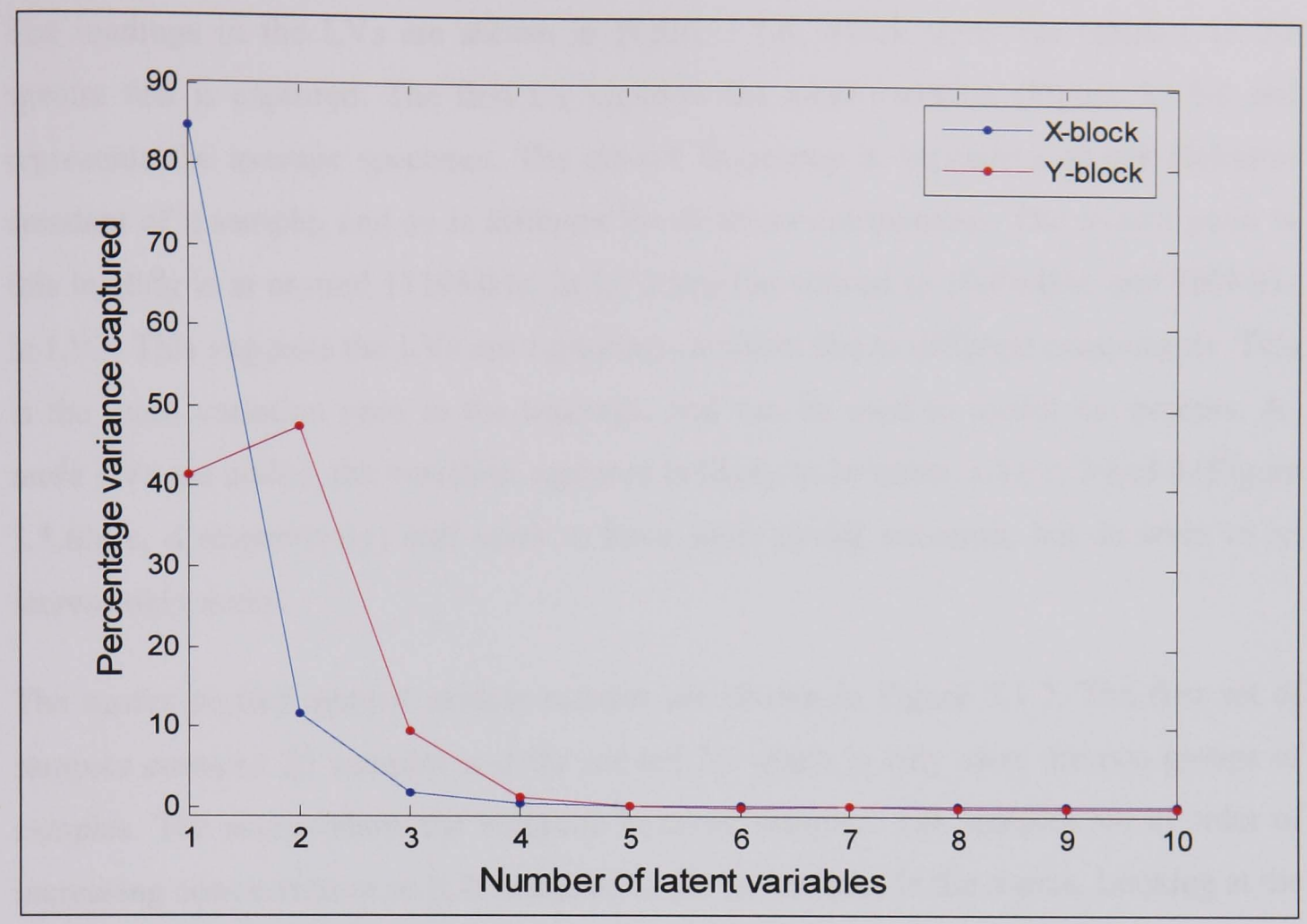

Figure 3.1.5: Scree plot for the PLS model built using raw MW data sets 2 and 3, for the addition of water to sand. The percentage variance captured for the *X* (spectra) and *Y* (concentration) blocks are shown for each latent variable calculated.

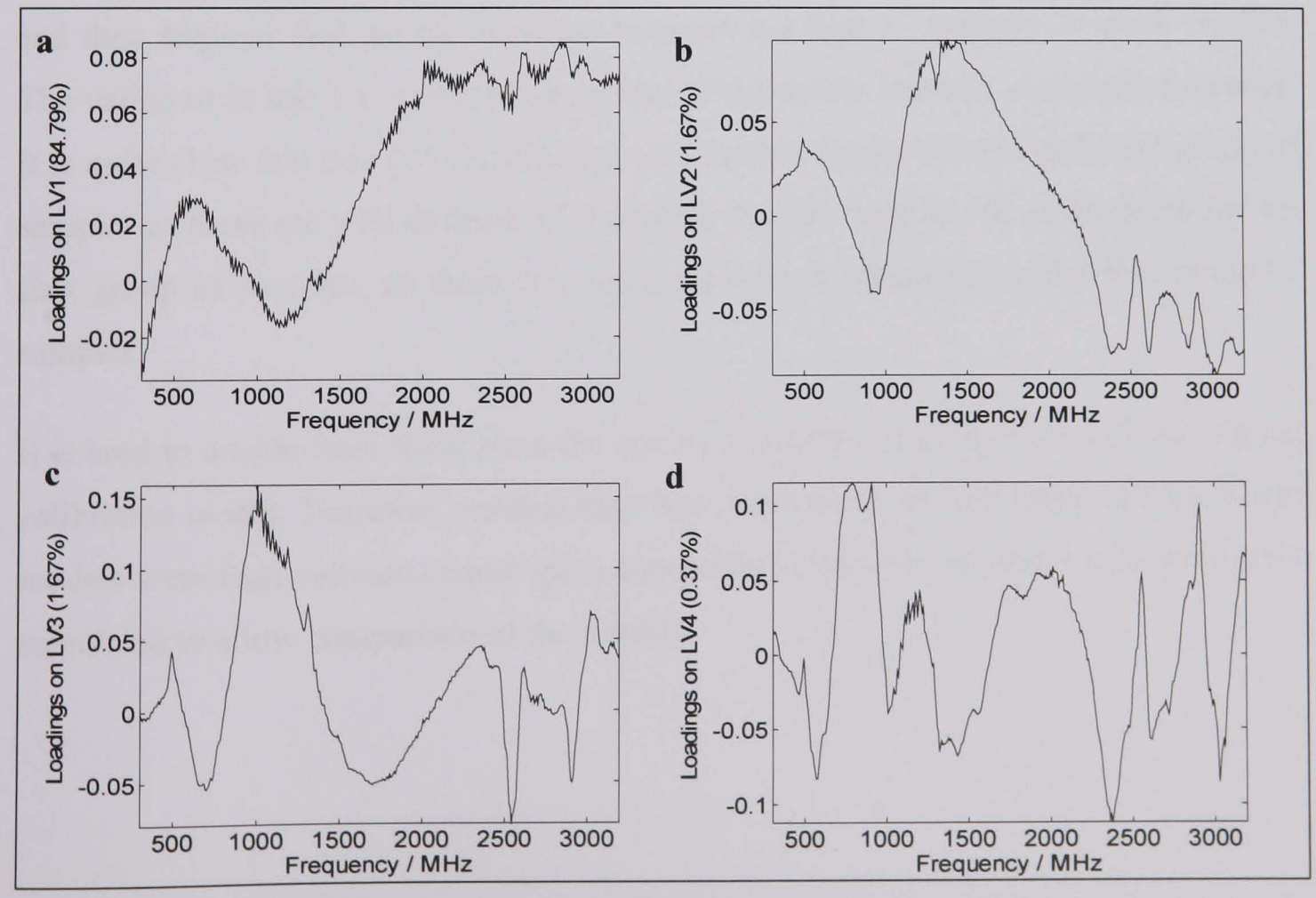

Figure 3.1.6: Loadings for the PLS model built using raw MW data sets 2 and 3, for the addition of water to sand, in the first four LVs; a) LV1; b) LV2; c) LV3; d) LV4.

The loadings in the LVs are shown in Figure 3.1.6, which show the variance in the spectra that is captured. The first LV captures the most variation (Figure 3.1.6a) and represents the average spectrum. The cut-off frequency is dependent on the dielectric constant of a sample, and so is different for different components. The cut-off point in this loading is at around 1110MHz. In LV2 this has moved to 1000MHz, and 700MHz in LV3. This suggests the LVs are capturing variation due to different components. This is the main variation seen in the loadings, and can be used to model the process. As more LVs are added, the variation captured is likely to be noise. LVs 2, 3 and 4 (Figure 3.1.6b, c, d respectively) still seem to have some useful variation, but do seem to be increasingly noisy.

The scores plotted against sample number are shown in Figure 3.1.7. The first set of samples contains 25 samples and the second 26 which is why there are two groups of samples. The scores show the variation between samples. The samples are in order of increasing concentration so it is expected to see an increase in the scores. Looking at the scores on LV2 (Figure 3.1.7b) there appears to be one group from 1 to 11 samples, and then a group from 12 to 20, and a further group for the last five samples. This is because for the first 11 samples, the water was added in steps of 0.1ml, after this in steps of 1ml, and then steps of 5ml, so the variation between the first 11 samples is much smaller. The variation in this LV seems quite regular as the scores increase in a regular manner. It is quite clear that this LV contains the information for the second and third group of samples as these are well defined. LV1 (Figure 3.1.7a) contains the information for the first group of samples, as there is a large amount of variation for the first group of samples.

It is hard to decide from these plots the optimum number of LVs to use to build a good calibration model. Therefore, models have been built using the full range of LVs. These models were then validated using the independent validation set, and a validation error calculated to allow comparison of the models.

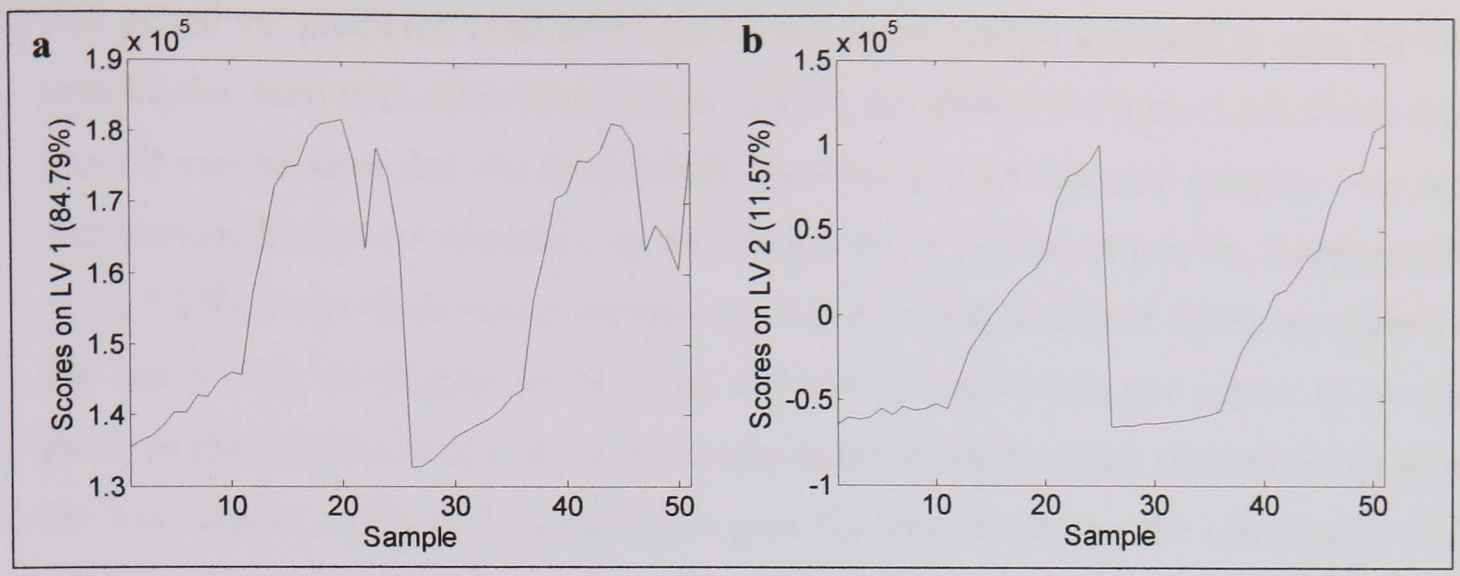

Figure 3.1.7: Scores for the PLS model using raw MW data sets 2 and 3, for the first two LVs plotted against sample number; a) LV1; b) LV2.

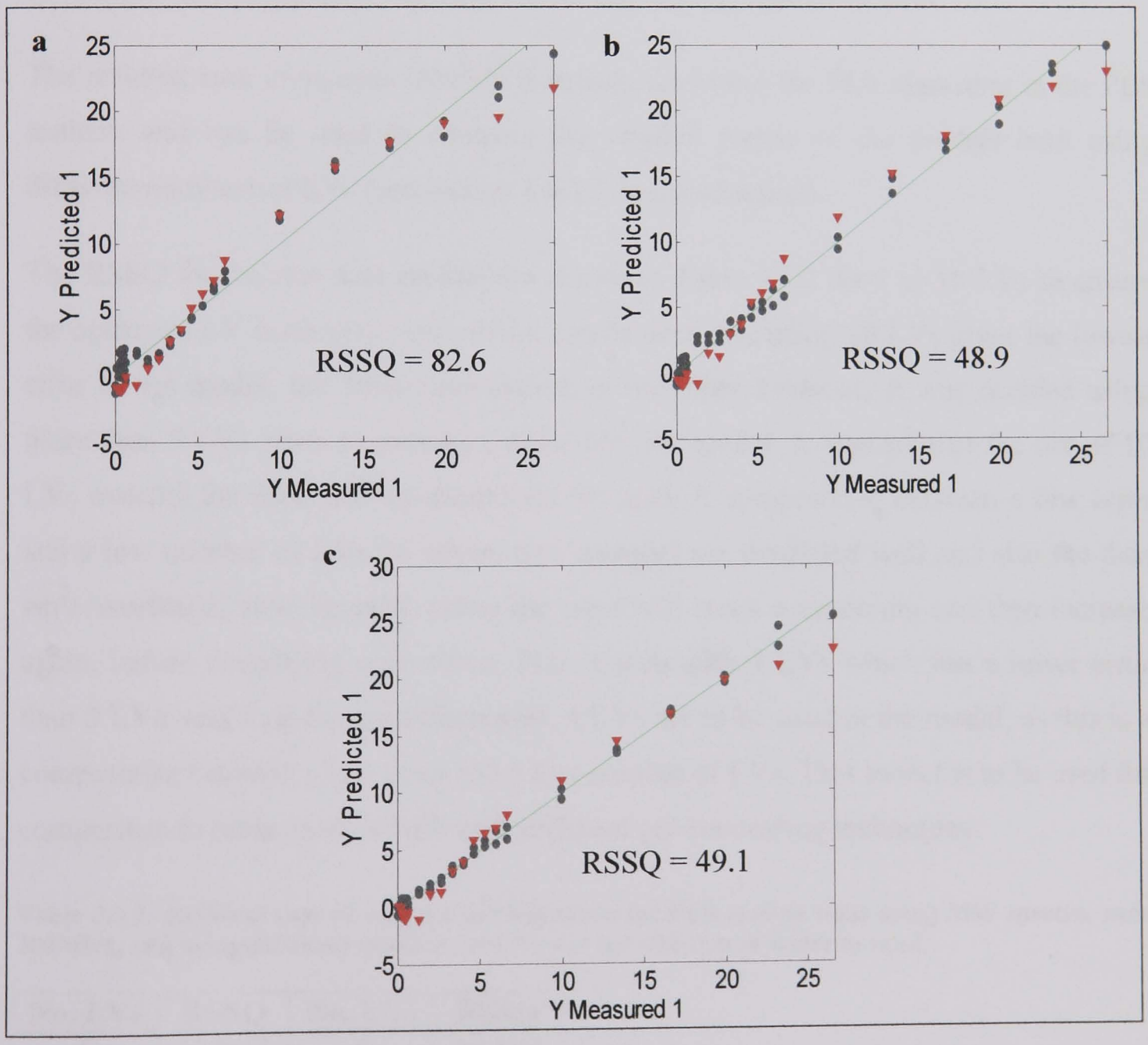

Figure 3.1.8: Plots of actual vs. predicted concentration of water in sand, % weight for weight, for the models built using different numbers of LVs using raw MW spectra. The black dots represent the samples included in the model, and the red triangles are the independent validation data set samples; a) model built using 3 LVs; b) model built using 4 LVs; c) model built using 5 LVs.

The actual vs. predicted concentrations for the three models expected to give the best predictions, built with different numbers of LVs, are shown in Figure 3.1.8. From these plots it can be seen that the model built does not predict the new samples very well (represented by the red triangles), as they do not sit on the line of best fit. It appears that using 5 LVs in the model gives the best prediction, as the predicted values are closest to the line of best fit (Figure 3.1.8c). The models themselves do not appear to be very good, as the samples used to build the model (represented by black circles) do not sit on the line. Again, using 5 LVs seems to give the best model as the samples fit well; however there is a possibility that the samples have been over fitted by including noise in the model. It is hard to decide from these plots which model gives the best prediction. A calculation of the prediction error allows the models to be compared.

The residual sum of squares (RSSQ) is calculated within the PLS algorithm in the PLS toolbox and can be used to compare the relative merits of the models built using different numbers of LVs (see section 1.4.2.5 in introduction).

The RSSQ for the raw data models are shown in Table 3.1.2 for 1 to 10 LVs to ensure the optimum LV is chosen. From this it can be seen that using 10 LVs gives the lowest error in the model, but from examination of the other evidence, it was decided using more than 5 LVs starts to introduce noise into the model. It appears that the use of 10 LVs overfits the data, and so should not be used. A compromise between a low error and a low number of LVs, to ensure new samples are predicted well and also the data isn't overfitted, must be used. Often the error will reach a minimum and then increase again, before decreasing once more. This is seen with 4 LVs which has a lower error than 5 LVs, and then the error decreases. 4 LVs are to be used in the model, as this is a compromise between a low error and a low number of LVs. This model is to be used for comparison to other models built with different pre-processing techniques.

Table 3.1.2: Residual sum of squares (RSSQ) error for PLS models built using MW spectra, over 300MHz, and using different numbers of LVs, for the addition of water to sand.

No. LVs	RSSQ	No. LVs	RSSQ
1	1385.7	6	40.898
2	299.33	7	21.962
3	82.634	8	17.598
4	48.872	9	16.441
5	49.068	10	16.209

The final model was also built using all frequencies, and compared to the validation error, to ensure that no useful information had been removed. The errors are shown in Table 3.1.3. Using 9 LVs gives the lowest error. However, as discussed before, using too many LVs introduces noise into the system, and it is likely the data will be overfitted. Therefore a compromise of 5 or 6 LVs should probably be used, but it is hard to decide the optimum to use. This shows that including the whole frequency range gives a different error in the model, and this is slightly lower in this example. For the rest of the models, the models will be built with the full frequency range and frequencies above 300MHz to examine the difference.

Table 3.1.3: Residual sum of squares (RSSQ) error for PLS models built using raw MW spectra, all frequencies and using different numbers of LVs, for the addition of water to sand.

No. LVs	RSSQ	No. LVs	RSSQ
1	1404.6	6	35.166
2	299.10	7	20.011
3	80.764	8	16.416
4	48.271	9	16.211
5	46.393	10	16.450

Auto-scaling

The second set of models was built using MW spectra and concentration data that were first auto-scaled. The validation set was scaled accordingly. The determination of the optimum number of LVs to use was carried out in the same way as for the raw data models, by using the validation set to determine the RSSQ for the model. Models were built using spectra covering the whole frequency range, and also just above 300MHz. It was determined to use a model built with 5 LVs for all frequencies, and 8 LVs for above 300MHz.

Box-Cox transformation

This set of models was built using MW spectra and concentration data pre-processed using the Box-Cox transformation using a power equal to 0 (logarithmic transformation) and 1 (square root transformation). The determination of the optimum number of LVs to use was carried out in the same way. For the model built using power = 0, it was decided to use 4 LVs for all frequencies, and 3 LVs for models built with spectra with frequencies above 300MHz. For the model built using power = 1, it was

5 LVs for both types of model. The use of power = 0 gave the lowest error, so this is used in the pre-processing for the following models.

Auto-scaling followed by Box-Cox

The spectra were first auto-scaled then transformed using logarithmic Box-Cox. The optimum number of LVs for the model built with all frequencies was found to be 3, and also for the model built with frequencies over 300Mz.

Box-Cox followed by auto-scaling

The spectra were first subjected to Box-Cox logarithmic transformation, then auto-scaled. The optimum number of LVs for the model built with all frequencies was found to be 7, and 2 LVs for the model built with frequencies over 300Mz.

OSC

OSC was used in the model to reduce the number of LVs needed to model the data. Models were built using one and two OSC components. It was decided to use 5 LVs for both one and two OSC components, for both models built using all frequencies and above 300MHz.

Conclusions

Table 3.1.4 gives a summary of the errors associated with each model constructed. The RMSEP can be calculated using the predicted values (see equation 3.1.1). This error is now in the same magnitude as the concentration values so can be directly compared to the values. RMSEP allows comparison of the models. From this it can be seen that using no pre-processing gives a comparatively large RMSEP of 1.2 and 1.4 for the model built with all frequencies and over 300MHz respectively, therefore pre-processing should be used to improve the model. It was hoped to get as small an RMSEP as possible.

The use of Box-Cox logarithmic transformation alone, and Box-Cox (logarithmic) followed by auto-scaling give a small RMSEP in the region of 0.4 for the models constructed with all frequencies, and 0.5 for over 300MHz. Using Box-Cox square root transformation gave much higher errors of 1.1 and 2.1 for all frequencies and above 300MHz respectively. Due to the poor prediction ability of these models, the Box-Cox logarithmic transformation was used for the remaining model building.

The lowest error in these models is with the use of auto-scaling followed by Box-Cox (logarithmic) which gives an RMSEP of only 0.05 when using all frequencies of the spectra in the model, and 0.06 when using only frequencies over 300MHz.

The use of one and two OSC components gave similar results. The RMSEPs are relatively poor, 0.7 for all frequencies, and 0.6 using frequencies above 300MHz. Due to the poor prediction ability of using OSC, this method was not used as a pre-processing technique for the subsequent model building.

Table 3.1.4: Summary of errors for all the global models built for the MW spectra of the addition of water to sand.

Preprocessing technique		No. LVS	RSSQ	RMSEP
Raw	All freq	6	35.17	1.210
	over 300 MHZ	4	48.87	1.427
Auto-scaling	All freq	5	0.136	0.075
	over 300 MHZ	8	0.246	0.101
Box-Cox, logarithmic	All freq	4	3.626	0.389
	over 300 MHZ	3	6.616	0.525
Box-Cox, square root	All freq	5	28.95	1.098
	over 300 MHZ	5	101.6	2.057
Auto-scaling and Box-Cox, (logarithmic)	All freq	3	0.061	0.050
	over 300 MHZ	3	0.099	0.064
Box-Cox (logarithmic) and auto-scaling	All freq	7	4.479	0.432
	over 300 MHZ	2	7.606	0.563
1 OSC component	All freq	5	13.42	0.748
	over 300 MHZ	5	10.27	0.654
2 OSC components	All freq	5	12.62	0.725
	over 300 MHZ	5	8.857	0.608

From the errors it appears that using all frequencies gives a better model than using just frequencies above 300Mz, except when OSC is used in the modelling. This region below 300MHz may relate to the non-linearity of the data, so would aid the correlation of the spectra to the concentration data.

The lowest error for the global calibration model was achieved by using auto-scaling followed by Box-Cox logarithmic transformation as pre-processing techniques, using the full spectral frequency range. This is a global model that covers a wide range of concentrations, 0 to 27%. To check the calibration model predicts well over the entire range, the percentage error, %RMSEP, is calculated for each validation sample (see section 1.4.2.5 in introduction).

This is shown against the actual concentration of the sample in Figure 3.1.9. This gives a clearer indication of the magnitude of the prediction error over the whole calibration range than simply looking at the RMSEP. The prediction error at the lower end is close to 7%. This is a reasonable error as the concentration values predicted are very small. At the higher end the error is near 3%, and is fairly consistent for values over 10% water in sand. This is a very acceptable level of error. The %RMSEP increases with decreasing concentration of water, but is still acceptable over the whole range of concentrations.

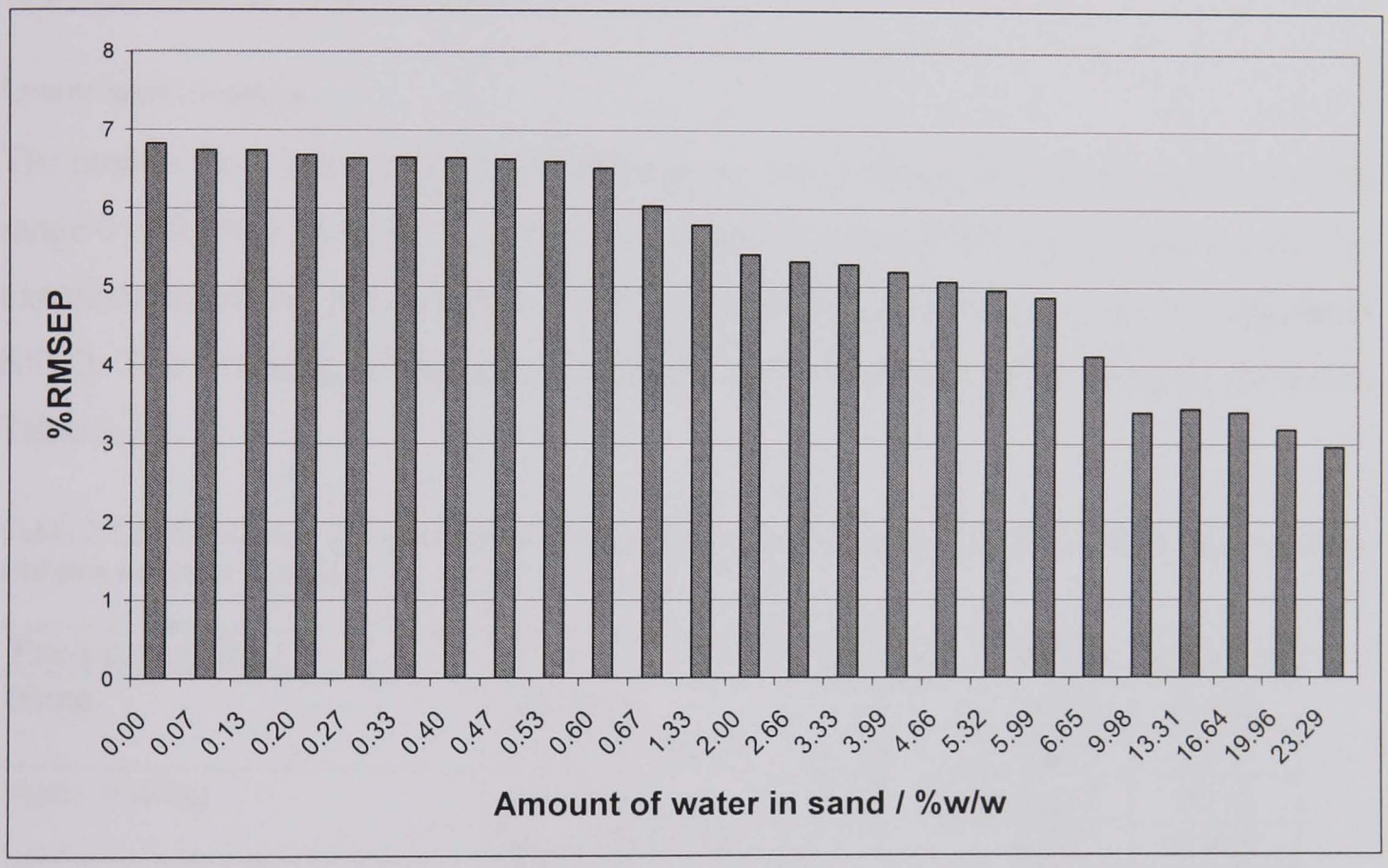

Figure 3.1.9: Plot of the percentage RMSEP for the validation set predicted against the global model built for the prediction of amount of water in sand (%w/w) using auto-scaling and Box-Cox logarithmic transformation to pre-process the MW spectra covering the whole frequency range.

These models have been built using the entire concentration range to give a global model covering the whole range. It was suggested that the whole range may not be linear, but there may be two linear ranges present, due to the non-linearity expected from the addition of water. The sample first adsorbs the water, and then absorbs it giving two different responses, and possibly two different linear ranges. Therefore the models were built in the same way, but using two local models, one from 0 to 0.7% (lower level), and the other encompassing the remaining concentrations (higher level).

Local calibration models

The same types of pre-processing were considered as with the global models. It appears from the global models that some are detrimental to the model building but this could be due to the data being non-linear, therefore when the data is split into linear ranges the pre-processing may have more use. DoEMan has been used with both local data sets, and only auto-scaling was predicted to have any use in the model building. This was also suggested for the global model, but the use of auto-scaling followed by Box-Cox logarithmic transformation proved to give the best model. Therefore the different types of pre-processing were compared.

Lower level models

The models have been built in exactly the same way as the global models, and cover the range 0 to 0.7% w/w water in sand. The optimum number of LVs to use was decided by examination of the percentage variance captured in the LVs and also the calculated RSSQ. The resulting calculated errors associated with each model built are shown in Table 3.1.5.

Table 3.1.5: Summary of errors for all the lower level local models built for the MW spectra of the addition of water to sand.

Pre-processing		**No. LVS**	**RSSQ**	**RMSEP**
None	All freq	3	0.018	0.045
	over 300 MHZ	3	0.018	0.045
Auto-scaling	All freq	2	0.232	0.161
	over 300 MHZ	2	0.227	0.159
Box-Cox transformation (logarithmic)	All freq	2	2.946	0.572
	over 300 MHZ	2	2.012	0.473
Auto-scaling and Box-Cox (logarithmic)	All freq	2	12.61	1.184
	over 300 MHZ	2	12.62	1.184
Box-Cox (logarithmic) and auto-scaling	All freq	3	1546	41.45
	over 300 MHZ	2	322.5	5.986

The use of no pre-processing techniques produced the best model with a RMSEP of only 0.045 for the use of all frequencies and for over 300MHz. This error is slightly lower than that achieved for the global model with the use of auto-scaling and Box-Cox logarithmic transformation for the full spectral frequency range, which gave an RMSEP of 0.050. These models are built with 3 LVs which seems a reasonably low number.

The errors for the models built using Box-Cox (logarithmic) followed by auto-scaling are huge at 41.45 compared to previous low errors seen below 1, for all frequencies, and 65.986 for above 300MHz. The Box-Cox (logarithmic) models give errors similar to that achieved with the global model. The auto-scaling followed by Box-Cox (logarithmic) was found to be the best global model, but gives higher errors here with 1.184 for both models compared to 0.05 achieved for the global model.

There is little difference in the errors produced for the majority of models built using spectra covering the full frequency range and those built using only frequencies over 300MHz. This suggests there is no information below 300MHz which aids the modelling, but there is also no noise present which would decrease the modelling ability.

Higher level models

These models have been built in the same way as the lower level models, and encompass the range 1 to 27% w/w water in sand. The resulting calculated errors associated with each model built are shown in Table 3.1.6.

Table 3.1.6: Summary of error for all the higher level local models built for the MW spectra of the addition of water to sand.

Pre-processing		No. LVS	RSSQ	RMSEP
None	All freq	6	16.54	1.087
	over 300 MHZ	6	16.68	1.091
Auto-scaling	All freq	2	0.172	0.111
	over 300 MHZ	4	0.378	0.164
Box-Cox logarithmic transformation	All freq	3	0.262	0.137
	over 300 MHZ	3	0.504	0.190
Auto-scaling and Box-Cox (logarithmic)	All freq	3	0.020	0.037
	over 300 MHZ	3	0.020	0.038
Box-Cox (logarithmic) and auto-scaling	All freq	3	0.059	0.065
	over 300 MHZ	2	0.138	0.099

The lowest RMSEP in these models is for those built using spectra which is auto-scaled, then subjected to Box-Cox logarithmic transformation. The same error of 0.020 is achieved when using the full spectral region and also just frequencies above 300MHz. These models are built with 3 LVs which seems a reasonably low number. This is a lower error than the best achieved for the global models, and is equivalent to a 3%

prediction error in the concentration values. When looking at the error in the global model for this region, a 3% error was achieved, so is a very similar error.

The models built using Box-Cox (logarithmic) followed by auto-scaling have low errors of 0.065 and 0.099 for all frequencies and above 300MHz respectively. This is in contrast to the previous models built for the lower region and the global models using this pre-processing, which had much larger errors compared to the other pre-processing techniques.

A lower error has been achieved when using the entire frequency range of the spectra, instead of just frequencies over 300MHz, to build the models. This is not true for the models built using raw data, and data which is subjected to auto-scaling followed by Box-Cox logarithmic transformation, in which the errors achieved were the same in each case. Generally this suggests there is useful information contained in the spectra below 300MHz which needs to be included in the modelling process to aid correlation between the spectra and concentration data.

Conclusions

The MW data sets for the addition of water to sand has been split into two regions which are expected to be linear. These are 0 to 0.7% w/w water in sand, the lower level, and 1 to 27% w/w water in sand, the higher level. Local calibration models have been built for each region using a variety of pre-processing techniques to optimise the model.

The errors for the best models for the two local models and the global model are shown in Table 3.1.7. The RMSEP is quoted as this allows comparison of the models, and the percentage error has been calculated to give a clearer indication of how the RMSEP relates to the actual concentration predicted.

Table 3.1.7: Summary of errors for the best models built for the MW spectra for the addition of water to sand, using different ranges of the data.

Model	Pre-processing		No. LVS	RMSEP	% error
Global	Auto-scaling and Box-Cox (logarithmic)	All freq	3	0.050	5
Local lower	Raw	All freq	3	0.045	7
Local higher	Auto-scaling and Box-Cox (logarithmic)	All freq	3	0.037	3

It has been found that the use of raw data with the entire frequency range gives the lowest error of 7% for the lower level models. The use of auto-scaling followed by Box-Cox logarithmic transformation gave the lowest error of 3% for the higher level range. The same error was produced for both the entire frequency range and above 300Mz. The higher level has a lower error than the best achieved for the global model, but the lower level model has a slightly worse error. This suggests that the data for the lower level is not as well correlated to the concentration data. This could be due to the data being non-linear or could be due to the MW spectra not being able to detect such a low water content. However, the lower level model did not require any pre-processing to achieve the best model, so producing a simpler model.

The best model for the global model and higher level uses Box-Cox logarithmic transformation in the pre-processing. This is useful to aid calibration of non-linear data. This suggests that the higher level data range is non-linear and it may be helpful to break the data into smaller linear regions if possible.

Building one global model is much simpler than several local models. In this example the global model gave an error of 5% which is very reasonable so would be suitable for the application. When the error is examined in detail for each local region, an error of 6 - 7% was achieved for the lower level, and 3 - 5% for the higher level, so the models are very comparable. Therefore, for its simplicity and low error, the global model is a suitable compromise.

Generally a lower error is achieved when using the entire frequency range of the spectra, instead of just frequencies over 300MHz, to build the models. Therefore for all further model building, the entire spectral range was used.

3.1.1.1.2 NIR spectra for the addition of water to sand

Exploratory analysis of the data

The NIR data collected for the addition of water to sand is shown in Figure 3.1.10, the experiment was repeated three times, and the spectra for each repeat are shown.

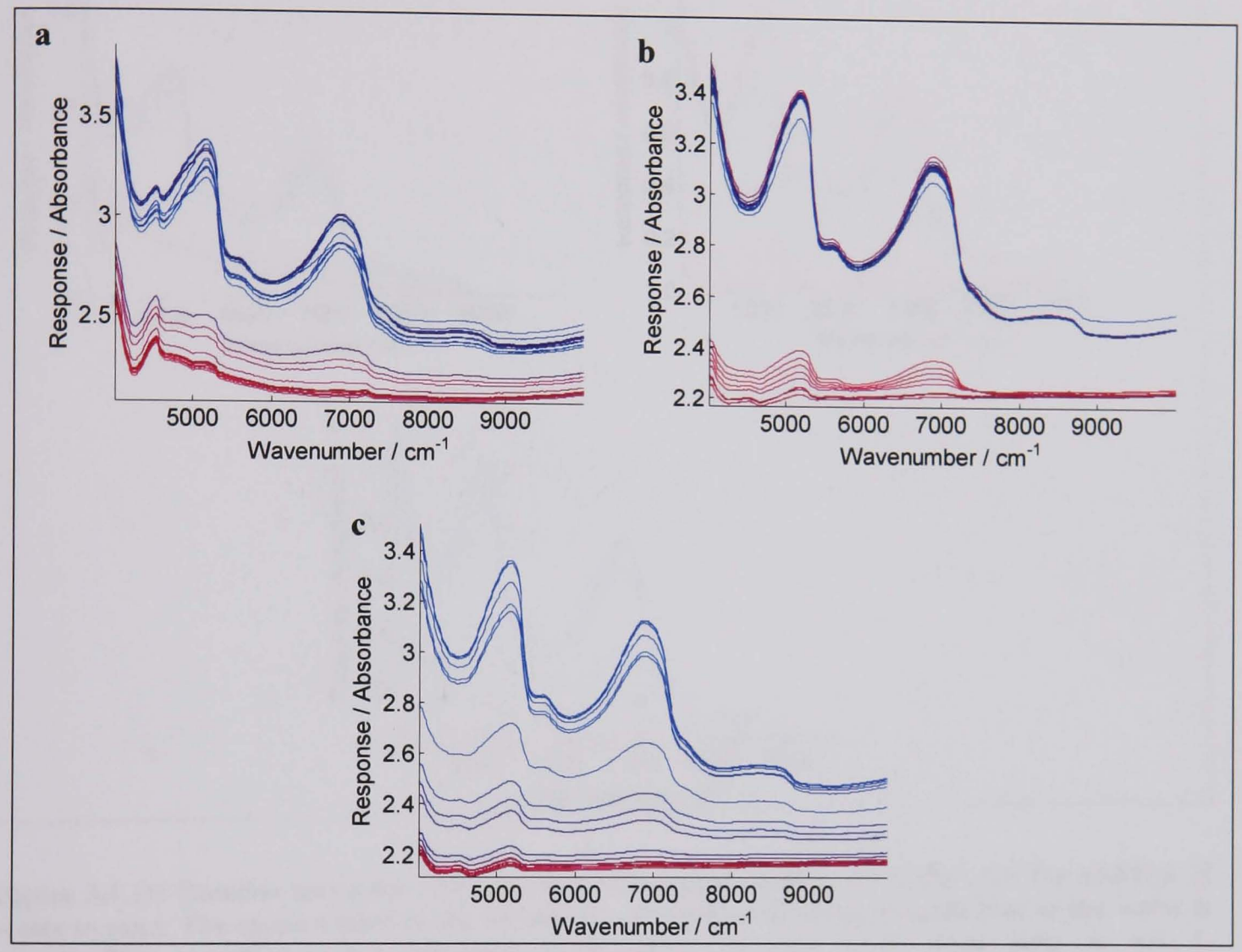

Figure 3.1.10: Raw NIR spectra for the addition of water to sand. The spectra start in red for the dry material, and move towards blue as the water is added. The experiment was repeated three times to give three data sets; a) set 1, *wet_sand_water_1_NIR*; b) set 2, *wet_sand_water_2_NIR*; c) set 3, *wet_sand_water_3_NIR*.

The NIR is collected using a diffuse reflectance probe. This sits in the sample and is static; therefore the spectra collected only represent a small area of the total sample. The water is added in drops, placed on the sample surface, and it takes time for the water to spread though the sample and to reach the sampling area of the probe. Therefore the true process may not be captured by the probe. This can be seen in the spectra collected, as the spectra for each repeat are quite different, so it seems a different process is being captured. There is a general increase in response seen in all spectra as water is added, but the baseline also increases. The baseline in NIR spectra should be constant. To

improve the spectra, the baseline has been corrected by normalisation against a region where the baseline should be zero, i.e. 9048 to 9996cm^{-1}. The corrected spectra are shown in Figure 3.1.11.

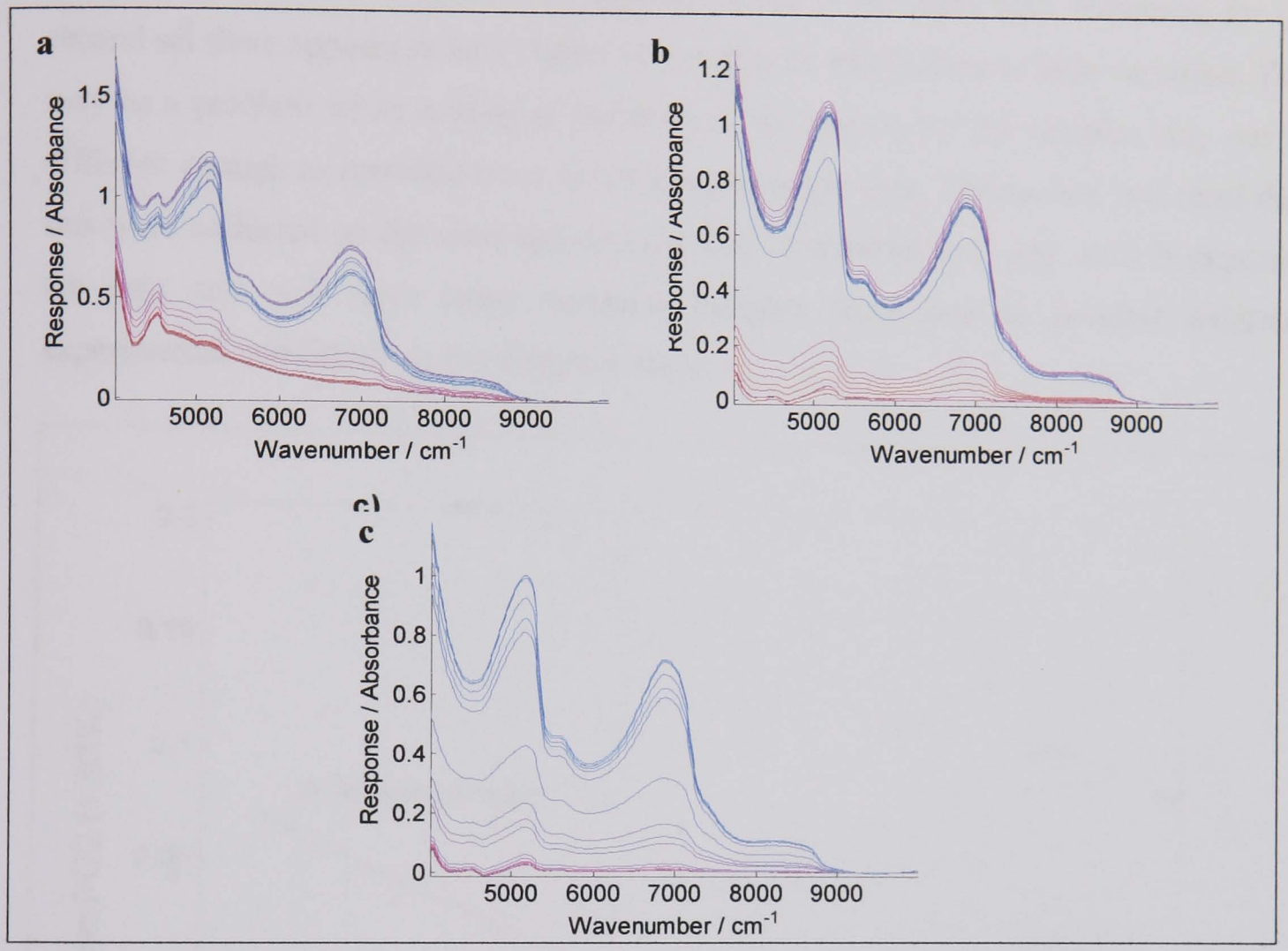

Figure 3.1.11: Baseline corrected NIR spectra in the region 9048 to 9996 cm^{-1}, for the addition of water to sand. The spectra start in red for the dry material, and move towards blue as the water is added. The experiment was repeated three times to give three data sets; a) set 1, *wet_sand_water_1_NIR*; b) set 2, *wet_sand_water_2_NIR*; c) set 3, *wet_sand_water_3_NIR*.

With the baseline corrected spectra the spectra still show a general increase as the water is added, but are still very different for each repeat. Repeat 1 and 2 (Figure 3.1.11 a and b) have two distinct clusters of spectra, and the spectra do seem to change in respect to the water being added. However, it appears the spectra are not in order of increasing water concentration in the upper cluster of spectra, and there are spectra coloured purple with a higher absorbance than the blue spectra which represent the highest concentration of water in the sand. The third data set (Figure 3.1.11c) seem to be much more regular spectra, with a regular increase in absorbance as the water is added.

PCA was performed on the three sets of spectra and the scores on PC1 vs. PC2 are shown in Figure 3.1.12. From this it can be seen that the three data sets are very different as can be seen in the spectra. This suggests there is experimental variation,

possibly due to the way in which the water was added and then how it spread through the sample for each experiment, which may lead to the spectra collected being different. The first set is the most different. The second and third data sets are similar, and the variation between the samples does seem to change in the same way. However, for the second set there appears to be a cluster of samples in which there is little variation. This may be a problem when modelling the data, as the spectra for the samples may not be different enough to correlate them to the concentration data. The second and third data sets were collected on the same day and the first on a subsequent day, so it is expected the data sets will have some variation between them due to possible different experimental conditions on the different days.

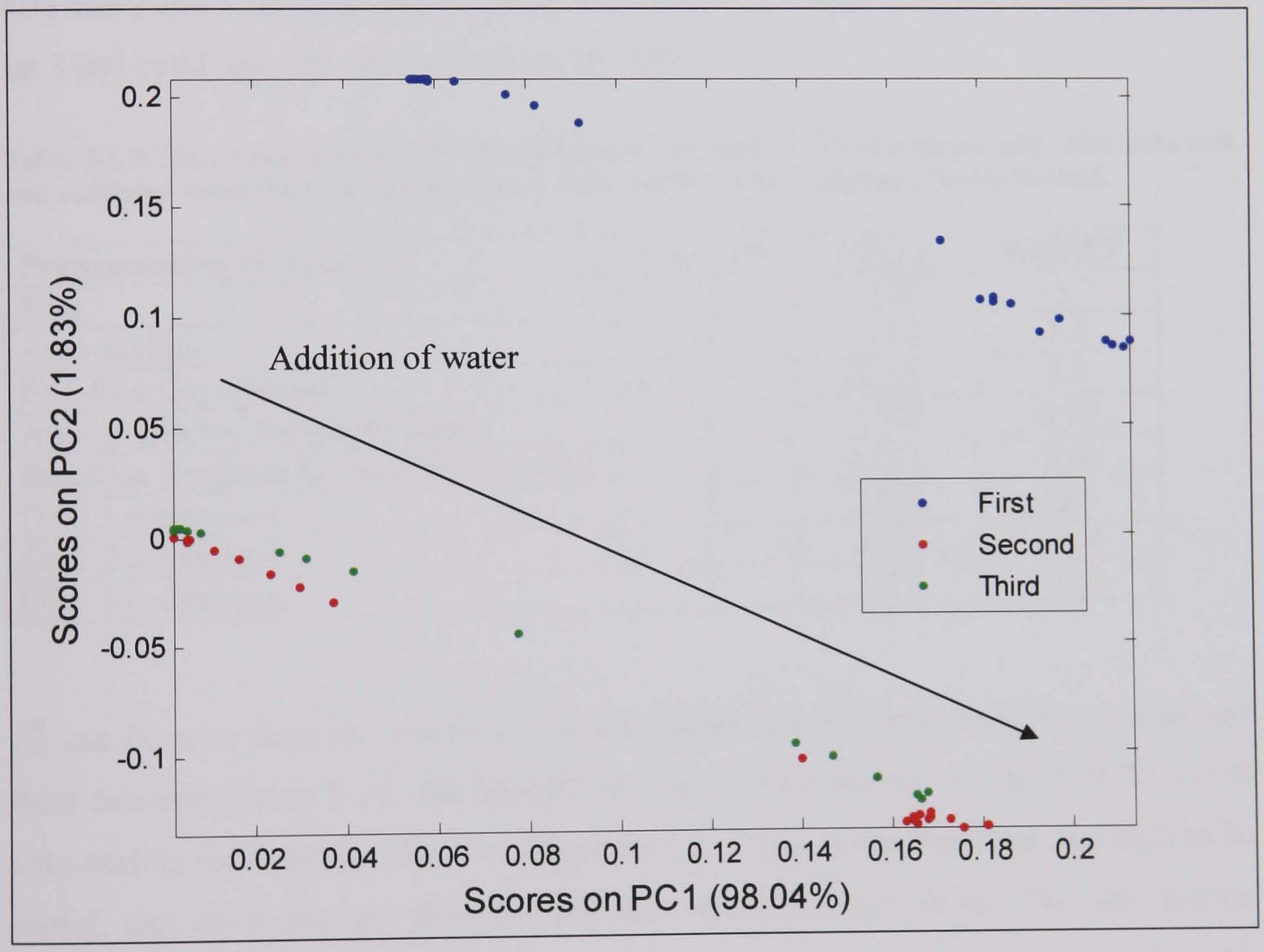

Figure 3.1.12: PCA scores, PC1 vs. PC2, for all three NIR data sets recorded for the addition of water to sand.

Calibration models

A calibration model was built using the second and third data sets as the calibration data and the third set as the validation, although it was not expected that this would produce a good model as the data sets appear to be so different. Models have also been built

using the third data set as the calibration data and the second data set as the validation set, as these data sets are more similar so it was expected this will give a better model.

DoEMan was used on the data sets to give an indication as to which pre-processing techniques may improve the modelling. The same pre-processing techniques were looked at as with the MW data. The Box-Cox logarithmic transformation is used. All NIR wavenumber have been included in the calibration models, as from the spectra there does not appear to be noise in the data in any wavelength region.

The calibration models were built, the optimum number of LVs to use determined, and the RSSQ and RMSEP calculated for each model. The results for the models built using data sets 2 and 3, and validated with set 1 are shown in Table 3.1.8 and those built using set 3 and validated with set 2 are shown in Table 3.1.9.

Table 3.1.8: Summary of errors for the various models built using the second and third data sets, and validated using the first data set for the NIR spectra of the addition of water to sand.

Preprocessing technique	No. LVS	RSSQ	RMSEP
Raw	3	4118	13.7
Auto-scaling	9	44.04	1.4
Box-Cox (logarithmic)	2	22.95	1.0
Auto and Box-Cox (logarithmic)	5	2.792	0.36
Box-Cox (logarithmic) and auto-scaling	8	67.71	1.8
OSC 1 component	1	2372	10.4
OSC 2 component	1	2374	10.4
OSC 3 component	1	2374	10.4

As can be seen from the errors for the calibration models built using the second and third data sets (Table 3.1.8) the RMSEP is over 1 for all models, except with the use of auto-scaling followed by Box-Cox (logarithmic). These errors are much too high to be useful, and show that the data has not been modelled well at all. The auto-scaling followed by Box-Cox (logarithmic) gives a reasonable error of 0.36 but is still much higher than that achieved with the MW spectra in which the best model gave an RMSEP of 0.05.

With the use of the third data set as the calibration data, the errors are still very high, with the majority over 1 (Table 3.1.9). Again, the use of auto-scaling followed by Box-Cox (logarithmic) gives the lowest error of 0.51. This is higher than that achieved for

the models using data sets 2 and 3, so no improvement has been made by selecting the data sets thought to be more similar.

Table 3.1.9: Summary of errors for the various models built using the third data set, and validated using the second data set for the NIR spectra of the addition of water to sand

Preprocessing technique	No. LVS	RSSQ	RMSEP
Raw	3	1980	14.1
Auto-scaling	4	30.66	1.8
Box-Cox (logarithmic)	3	11.02	1.05
Auto-scaling and Box-Cox (logarithmic)	2	2.592	0.51
Box-Cox (logarithmic) and auto-scaling	4	10.05	1.00
OSC 1 component	3	1364	7.9
OSC 2 component	2	1666	8.7

Conclusions

The NIR data has been used to build a calibration model to predict the amount of water contained in sand. All the models built gave very high errors when compared to the equivalent models built using MW spectra. The spectra collected is not good enough to build a good calibration model. This is due to the use of a diffuse reflectance probe which only samples a small area of the material, and so the true process is not captured.

For the remaining experiments the NIR spectra collected is also not very good, and does not appear to be representative of the process. Therefore, only the MW data is to be used for calibration.

3.1.1.2 Addition of propanol to ascorbic acid

Propanol was added to ascorbic acid (100g) in steps of 0 to 1ml, as 0.1ml additions, 2 to 10 ml as 1ml additions and 15 to 30ml as 5ml additions, at which point the material was saturated with solvent. 20 repeat MW spectra, and 40 repeat NIR spectra were taken at each addition. These spectra were averaged before data analysis. This was repeated three times. The concentration data is quoted as percentage w/w propanol in ascorbic acid. The data sets collected are *wet_asc_pro_1, 2* and *3*.

3.1.1.2.1 MW spectra for the addition of propanol to ascorbic acid

Exploratory analysis of data

The data consists of three repeat data sets. The first one recorded on one day, and the second and third on a second day. Typical spectra collected are shown in Figure 3.1.13.

From the spectra it can be seen there is an obvious change in the spectra as propanol is added. The change is not as large as seen for the addition of water to sand (see Figure 3.1.1). The dielectic constant of water is large, 80.4 at 20°C, compared to that of propanol, 21.8 at 20°C, so an increase in water will have a larger effect of the spectra than propanol.

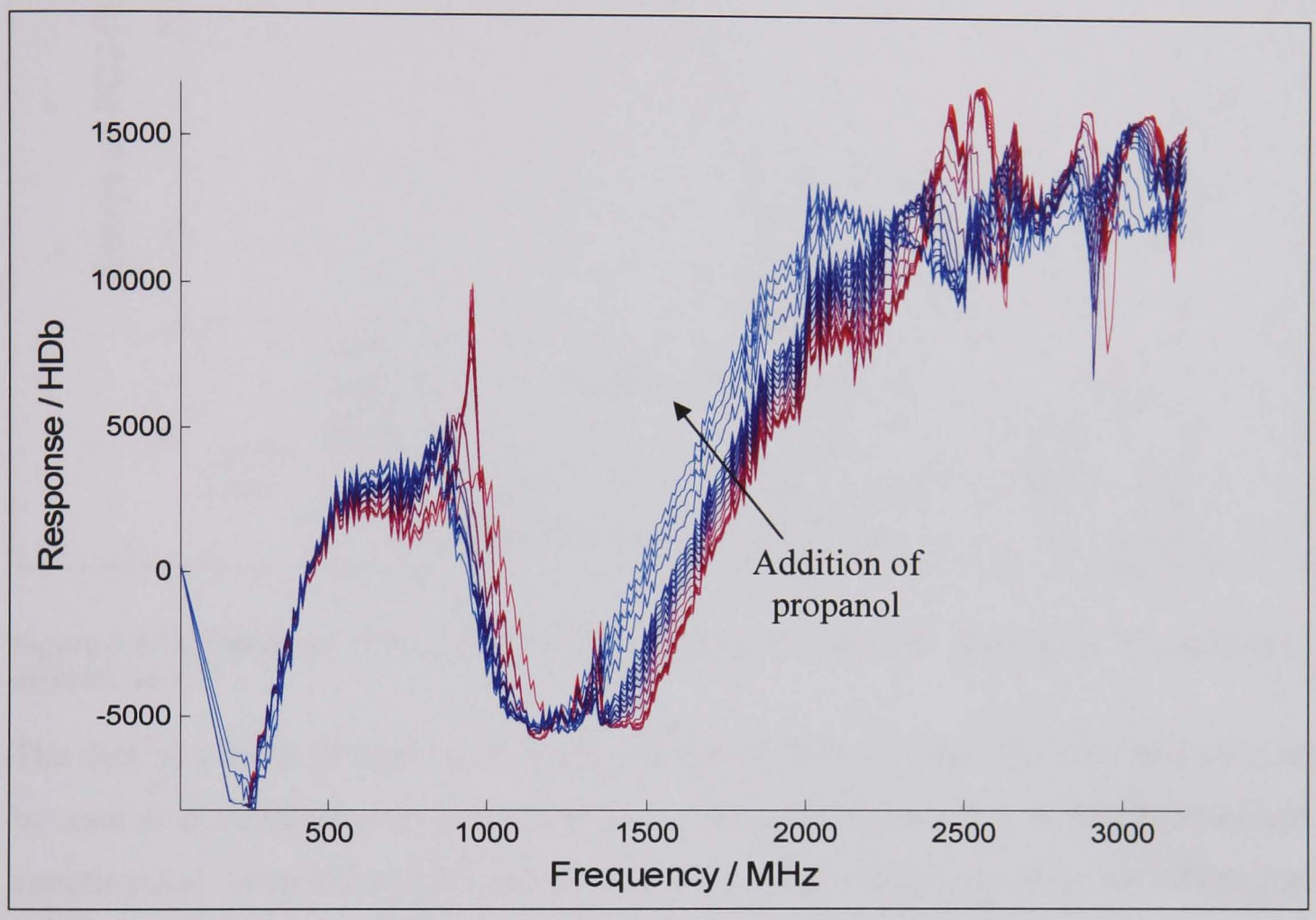

Figure 3.1.13: Example MW spectra for the addition of propanol to ascorbic acid. The spectra start red when the material is dry and go to blue as propanol is added.

PCA was performed on all three sets of data and the scores on PC1 vs. PC2 are shown in Figure 3.1.14. This plot shows how the variation between the samples, in each data set changes. The scores for each set of data are similar, and follow a similar shape, therefore the variation within the sets is similar.

There may be three ranges present as there appears to be three groups of samples. However, this seems to be due to the fact the propanol was added in three different steps, 0.1ml, 1ml and 5ml additions. This may lead to a difference in variation in the samples and hence the three regions. This makes it difficult to decide if the data can be split into smaller linear ranges.

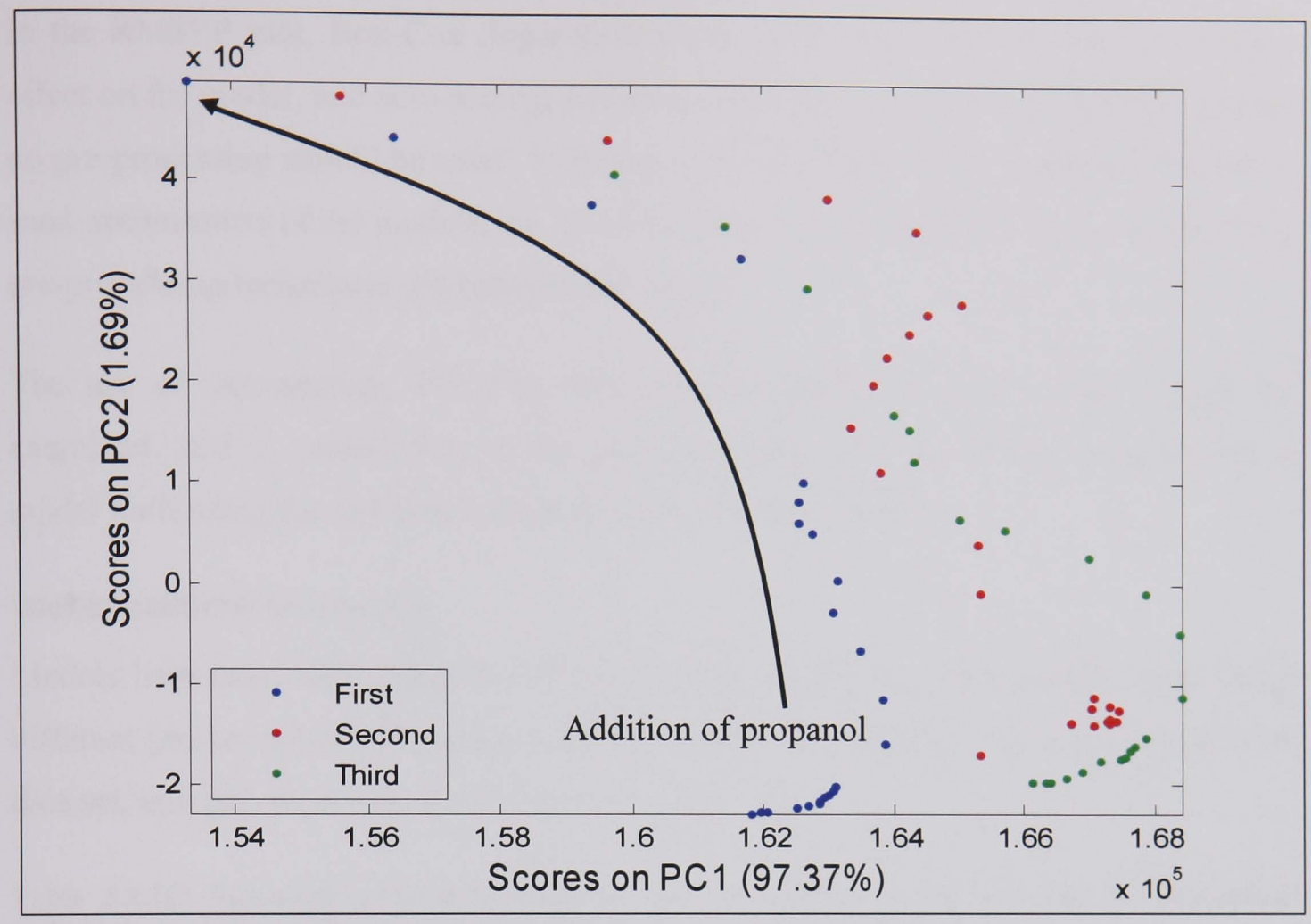

Figure 3.1.14: Scores on PC1 vs. PC2 for PCA of the MW spectra for the addition of propanol to ascorbic acid.

The data sets are to be split up as in the addition of water to sand. The first data set is to be used as a validation set as this was recorded on a different day so has independent experimental variation, and the second and third sets are to be used to as the calibration data.

Optimisation of PLS model

DoEMan was used with the calibration data to decide which pre-processing techniques it was worth examining in the PLS model building. The results were analysed in the same way as in the water added to sand experiments.

From the RMSEC plots it was found that the use of PLS1 or PLS2 makes no difference to the model, also mean centring was found to have a negative effect on the model building. Box-Cox (logarithmic) and auto-scaling were both found to have a positive effect on the model as seen in the previous example, and the use of auto-scaling followed by Box-Cox (logarithmic) also improved the model. In this case, OSC was found to improve the model, as well as the use of OSC and Box-Cox (logarithmic), and auto-scaling and OSC.

In the RMSEP plot, Box-Cox (logarithmic) and OSC were found to have a negative effect on the model, and auto-scaling and mean centring to have no effect. This suggests no pre-processing should be used. A similar thing was found in the addition of water to sand optimisation of the models, but when the individual models were built, some of the pre-processing techniques did improve the model.

The use of auto-scaling, Box-Cox logarithmic transformation and OSC should be examined, and a combination of the pre-processing, and the results compared to a model built using the raw data to determine the best model to use.

Global calibration models

Models have been built using the MW spectra for the entire concentration range, using different pre-processing techniques. Theses models are validated using an independent data set, and the errors calculated (Table 3.1.10).

Table 3.1.10: Summary of errors calculated for models built using different pre-processing techniques to calibrate the amount of propanol added to ascorbic acid.

Preprocessing technique	No. LVS	RSSQ	RMSEP
Raw	5	2.415	0.317
Auto-scaling	8	0.002	0.010
Box-Cox (logarithmic)	6	0.065	0.052
Auto-scaling and Box-Cox (logarithmic)	3	0.011	0.021
Box-Cox (logarithmic) and auto-scaling	8	0.003	0.011
OSC (2 components)	8	1301	7.364

The use of no pre-processing gives a fairly high RMSEP of 0.317. This suggests some sort of pre-processing is necessary to increase the correlation between the spectral and concentration data to build a better model.

The lowest RMSEP is achieved for models built using auto-scaling and Box-Cox (logarithmic) followed by auto-scaling, which both give an error of 0.010. This is a low error, but both models have been built using 8 LVs, which is a large number to use. This suggests that noise is included in the model, and it has been over-fitted to produce a lower error.

The use of OSC gives a very high RMSEP of 7.364, and uses a large number of LVs, 8. The amount of variance in the concentration data captured by this PLS model was much less. Therefore more LVs were needed to be included in the model to include the

relevant variation. This defeats the object of OSC as it aims to reduce the number of LVs needed, therefore this method will not be used in further model building.

The use of auto-scaling followed by Box-Cox (logarithmic) also gives a low RMSEP of 0.021. However, this model only uses 3 LVs so it is more likely to have less noise included in the model and generally be a better model. To ensure this model predicts well over the entire concentration range, the percentage error for each validation sample is calculated and this is shown against the actual concentration in Figure 3.1.15. From this is can be seen that the model predicts much better at the higher concentration range, over 10% propanol in ascorbic acid, with around a 1.5% error. At the lower end of the range, the error is still below 3% which is still very good. The concentrations predicted cover a large range, down to low level and it is expected it is harder to predict accurately such low levels.

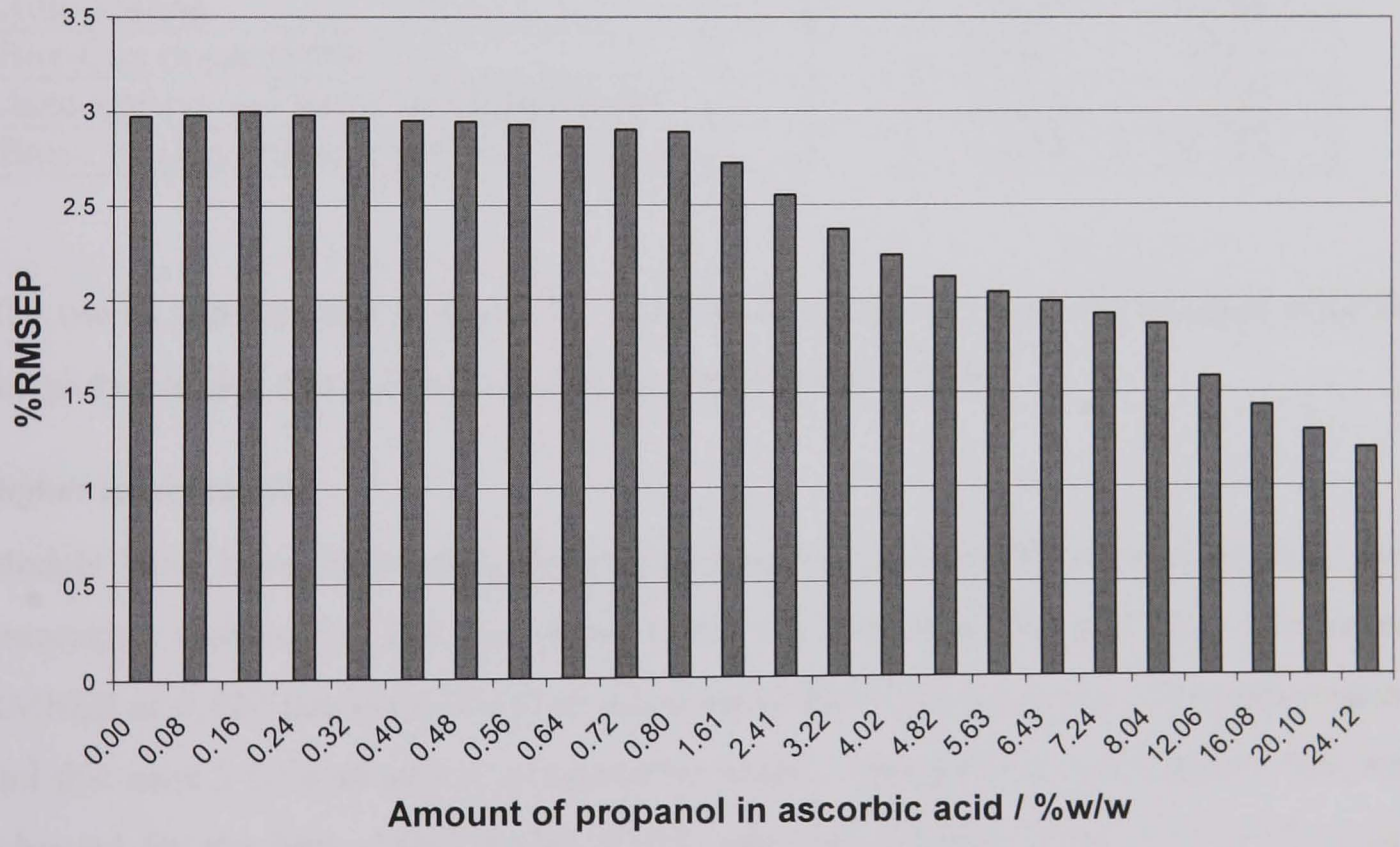

Figure 3.1.15: Plot of the percentage error for the validation set predicted against the global model built for the prediction of amount of propanol in ascorbic acid (%w/w) using auto-scaling followed by Box-Cox logarithmic transformation to pre-process the MW spectra.

Local calibration models

From the scores plots it seems that the data is not linear, however it is difficult to determine where linear regions are in the data. Therefore the data is to be split into two regions as previously. Therefore the lower level covers the range 0 to 0.8% w/w, and the higher level 1.6 to 24% w/w.

Lower level models

A series of models were built using the lower concentration range, and a range of pre-processing techniques. The RMSEP was calculated and these values quoted in Table 3.1.11. From this it can be seen that the lowest error of 0.070 was achieved when the raw data was used. However this model uses 5 LVs which seems a bit on the high side, and the model may be over-fitted. The use of Box-Cox logarithmic transformation gives a low error of 0.097 and this uses only 2 LVs so should have less noise included in the model and be a better model. This error is considerably larger than that achieved for the best global model, which gave an RMSEP of 0.021 using auto-scaling and Box-Cox (logarithmic).

Table 3.1.11: Summary of errors calculated for the lower level local models built using different pre-processing techniques to calibrate the amount of propanol added to ascorbic acid.

Pre-processing technique	No. LVS	RSSQ	RMSEP
Raw	5	0.049	0.070
Auto-scaling	2	0.656	0.256
Box-Cox (logarithmic)	2	0.095	0.097
Auto-scaling and Box-Cox (logarithmic)	4	32.01	1.789
Box-Cox (logarithmic) and auto-scaling	2	0.379	0.195

The use of auto-scaling followed by Box-Cox (logarithmic) gave the smallest error for the global model, but here has the largest error here of 1.789.

Higher level models

Models have been built using the higher range of concentrations and different pre-processing techniques. The calculated errors are shown in Table 3.1.12. The lowest RMSEP of 0.330 has been achieved when using Box-Cox (logarithmic) transformation and this uses 3 LVs so seems a reasonable model. This error is much higher than that achieved for the best global model, 0.021, and also the best lower level local model, 0.097.

Table 3.1.12: Summary of errors calculated for the higher level local models built using different pre-processing techniques to calibrate the amount of propanol added to ascorbic acid.

Pre-processing techniques	No. LVS	RSSQ	RMSEP
Raw	2	49.41	1.879
Auto-scaling	2	17.34	1.113
Box-Cox (logarithmic)	3	1.523	0.330
Auto-scaling and Box-Cox (logarithmic)	2	20.07	1.197
Box-Cox (logarithmic) and auto-scaling	8	8.958	0.800

The use of Box-Cox logarithmic transformation followed by auto-scaling gives a reasonable error of 0.800, but this uses 8 LVs suggesting noise is being included. Auto-scaling and auto-scaling followed by Box-Cox (logarithmic) also give higher errors of 1.113 and 1.197 respectively, and only use 2 LVs so seem to be reasonable models.

Conclusions

The errors for the global and local models which give the lowest validation error are shown in Table 3.1.13. The RMSEP has been quoted to allow comparison of the models, and the percentage error calculated based on the mean predicted value to give the error in real terms.

Table 3.1.13: Summary of errors for the best models built for the MW spectra for the addition of propanol to ascorbic acid, using different ranges of the data.

Model	Pre-processing	No. LVS	RMSEP	% error
Global	Auto-scaling and Box-Cox (logarithmic)	3	0.021	2
Local lower	Box-Cox (logarithmic)	2	0.097	11
Local higher	Box-Cox (logarithmic)	3	0.356	16

The best model produced is a global model which has only a 2% error when using auto-scaling and Box-Cox logarithmic transformation as pre-processing. As seen in Figure 3.1.15 this prediction is good across the whole range of concentrations. This model is built with 3 LVs so is a very acceptable model.

The two local models give much worse models with prediction errors of 11 and 15%. This is unusual, as it would be expected to give similar errors as the global model as the same data is used. It seems that modelling the whole data set together improves the correlation between the concentration data and the spectra.

3.1.1.3 Addition of ethanol to salicylic acid

Ethanol has been added to salicylic acid (83g) in steps of 0.1ml for 0 to 1ml, 1ml steps for 2 to 10ml and 5ml steps for 15 to 25ml, at which point the material was saturated. MW spectra (20) were taken at intervals, and these averaged to give one spectrum for each addition before analysis. The experiment was carried out three times to give three replicate sets of spectra. The data sets used are *wet_sali_eth_1_2* and *3*.

3.1.1.3.1 MW spectra for the addition of ethanol of salicylic acid

Exploratory analysis of spectra

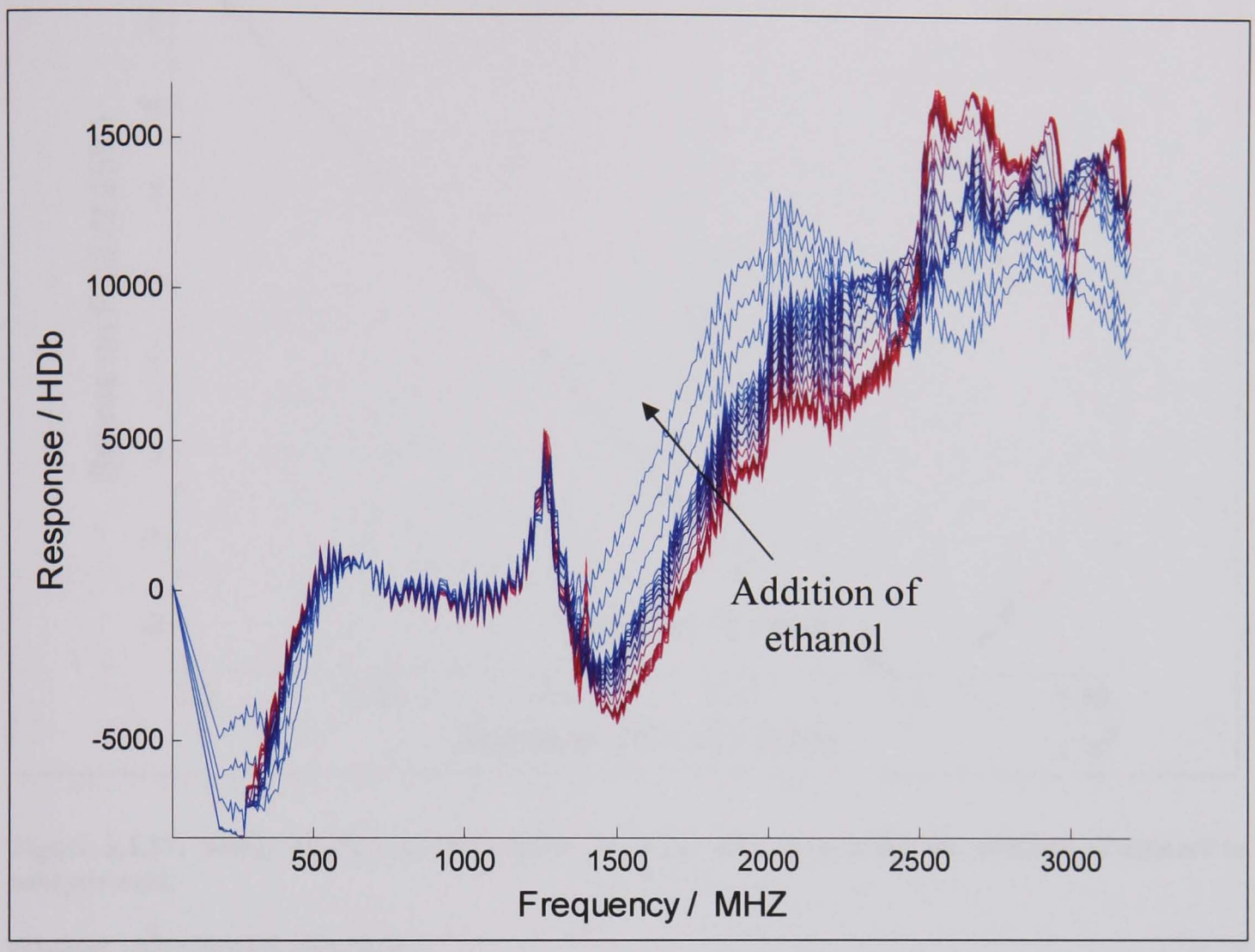

Figure 3.1.16: Example MW spectra of the addition of ethanol to salicylic acid. The spectra start red, dry salicylic acid, to blue, maximum amount of ethanol (24% w/w).

From the MW spectra, Figure 3.1.16, it can be seen that the spectra clearly change as the propanol is added to the salicylic acid. It is a fairly significant change, so it is expected that the amount added can be correlated to the spectra. The change in the process is similar to that seen in the addition of propanol to ascorbic acid (Figure 3.1.13). The dielectric constant of ethanol is 24.3 at 25°C, which is similar to that of propanol (21.8 at 20°C), so similar spectra are expected.

PCA was preformed on the three replicates of the MW spectra, and the scores on PC1 against PC2 are shown in Figure 3.1.17. From the scores, the three data sets appear to be somewhat different. The variation between the scores within each data set is similar. The three different additions of ethanol (0.1, 1 and 5ml steps) seem to give three clusters of samples in the scores. The second and third replicates were preformed on one day, and the first on a separate day. Therefore, the first set will be used as an independent validation set to test calibration models built on the other two sets of data.

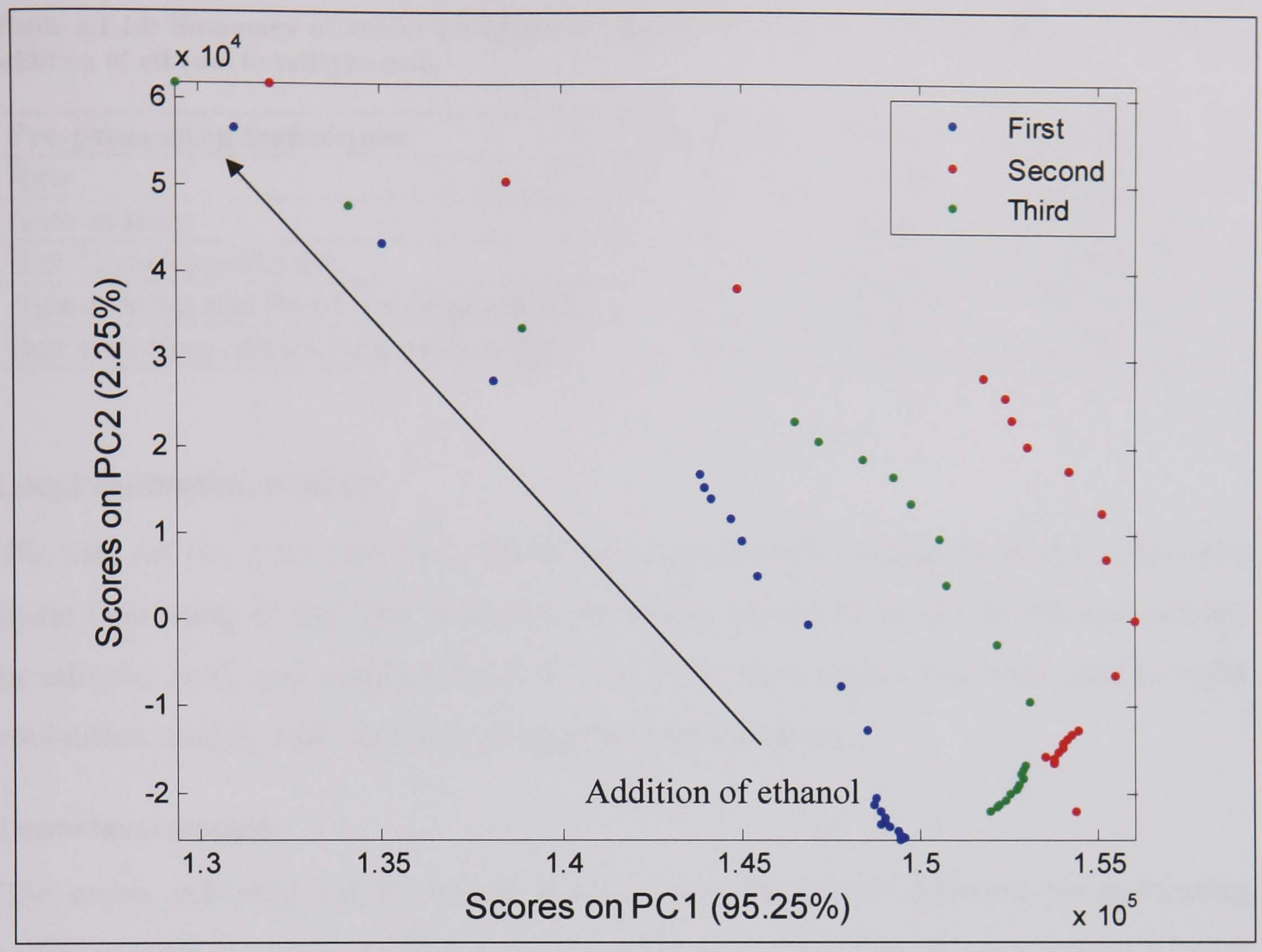

Figure 3.1.17: Scores on PC1 vs. PC2 for PCA of the MW spectra for the addition of ethanol to salicylic acid.

Global calibration models

PLS models have been built using the second and third data set, and the first used as a validation set. Different types of pre-processing techniques have been used to build the best model. DoEMan was used to determine the pre-processing techniques expected to improve the model. None were shown to improve the calibration models, so the same pre-processing techniques as examined for the previous examples have been used here.

Table 3.1.14 shows the validation errors for each model built. From this it can be seen that the lowest RMSEP, 0.330, is achieved using Box-Cox logarithmic transformation followed by auto-scaling. 4 LVs were needed to build this model, which may be too many, and the data may be over-fitted. Auto-scaling followed by Box-Cox (logarithmic) gave a similar error of 0.408 and this was built using 3 LVs so perhaps is a better model, with less noise included. Box-Cox logarithmic transformation alone also gave a reasonable error of 0.503, and this was built with 3 LVs.

Table 3.1.14: Summary of errors for global models built using the MW spectra collected for the addition of ethanol to salicylic acid.

Pre-processing techniques	No. LVS	RSSQ	RMSEP
Raw	2	61.04	1.666
Auto-scaling	6	11.71	0.730
Box-Cox (logarithmic)	3	5.558	0.503
Auto-scaling and Box-Cox (logarithmic)	3	3.669	0.408
Box-Cox (logarithmic) and auto-scaling	4	2.397	0.330

Local calibration models

The data set has been split into two smaller concentration ranges expected to be more linear than using all the data. This comprises of the lower level of 0 to 1% w/w ethanol in salicylic acid, and a higher level of 2 to 24%. Each region has been used to build calibration models with the same pre-processing techniques.

Lower level models

The errors achieved for the lower level models built with different pre-processing techniques are shown in Table 3.1.15. The RMSEP for these models are generally lower than those achieved for the global models. The lowest RMSEP is 0.180, achieved using Box-Cox logarithmic transformation. This model is based on 2 LVs so is a good model. Using no data processing also gave a low error of 0.208, but this uses 5 LVs so noise may have been included in the model. All the other models gave an error, RMSEP, over 1 which is quite high.

Table 3.1.15: Errors achieved for local models built using the lower region of concentration data, for the MW spectra of the addition of ethanol to salicylic acid.

Pre-processing techniques	No. LVS	RSSQ	RMSEP
Raw	5	0.431	0.208
Auto-scaling	2	15.31	1.237
Box-Cox (logarithmic)	2	0.326	0.180
Auto-scaling and Box-Cox (logarithmic)	4	98.88	3.144
Box-Cox (logarithmic) and auto-scaling	4	163.1	4.039

Higher level models

The errors for the models built are shown in Table 3.1.16. The lowest RMSEP is achieved with auto-scaling followed by Box-Cox (logarithmic), which gave an error of 0.033. This was built with 3 LVs so is a good model. This is a much lower error than

the best achieved for the global model, 0.391. The use of Box-Cox (logarithmic) followed by auto-scaling gave a low error of 0.214 but this was built with 5 LVs.

Table 3.1.16: Errors achieved for local models built using the higher region of concentration data, for the MW spectra of the addition of ethanol to salicylic acid.

Pre-processing techniques	No. LVS	RSSQ	RMSEP
Raw	2	34.23	1.689
Auto-scaling	6	3.337	0.527
Box-Cox (logarithmic)	3	4.107	0.585
Auto-scaling and Box-Cox (logarithmic)	3	0.013	0.033
Box-Cox (logarithmic) and auto-scaling	5	0.547	0.214

Conclusions

The errors for the models for the global model and the two local model regions, which gave the lowest prediction error, are shown in Table 3.1.17. The percentage error based on the mean predicted value is also shown to put the errors into context.

Table 3.1.17: Summary of errors for the best calibration models for the global and local models, built using MW spectra collected for the addition of ethanol to salicylic acid.

Model	Pre-processing	No. LVS	RMSEP	% error
Global	Auto-scaling and Box-Cox (logarithmic)	3	0.391	32
Local lower	Box-Cox (logarithmic)	2	0.180	23
Local higher	Auto and Box-Cox (logarithmic)	3	0.033	2

The only reasonable model is the local higher level model which has a percentage error of 2%. This suggests this region is linear so the spectra are well correlated to the concentration data. 3 LVs are used to build the model which is a reasonable number, and system noise should not be built into the model.

The global model and local lower level model give poor prediction of 32 and 23% error respectively. The poor prediction in the lower level model, below 2% ethanol in salicylic acid, suggests the MW spectra are not sensitive to such small amount of ethanol, and the limits of detection of the MW spectra have been reached.

3.1.1.4 Conclusions

Three processes of the wetting of solids with solvents have been studied with MW and NIR spectroscopy; the addition of water to sand, propanol to ascorbic acid and ethanol to salicylic acid. These experiments were carried out to determine the suitability of the techniques to monitor such a process, and how small an amount of solvent can be detected.

Calibration models were built to correlate the spectra to the concentration data. A variety of pre-processing techniques were examined to determine the best model to build. Models were built, and an independent data set used to validate the models and test the robustness.

The NIR spectra collected was of poor quality due to the use of a diffuse reflectance probe which only samples a small area of the sample. The solvent is added to the surface of the sample and must spread through the sample. If it does not reach the sampling area of the probe the true process won't be captured. This was reflected in the calibration models produced which did not predict very well at all. Therefore, this method was found not to be suitable for this process. For the true drying process, the solvent is removed from the sample at a fixed rate. Therefore, NIR would be more suitable for the true drying process.

The MW spectra captured the process much better, and both global and local models were built. It was thought the data may be non-linear, therefore smaller local models were built using regions expected to be linear to try to produce a better model. The global models gave comparable errors for the addition of water to sand and propanol to ascorbic acid. These models are much easier to build, as only one model is built, and also easier to use as there is no choice of which model to use when predicting new samples. The errors for the best models built are shown in Table 3.1.18. The error for the model above 2% ethanol in salicylic acid is shown.

Table 3.1.18: Summary of results for the calibration models built for each process studied. The results are shown for the global models, and above 2% for the ethanol in salicylic acid, constructed using all the frequencies in the MW spectra.

Process	Pre-processing	No. LVs	RMSEP	% Error
Water / sand	Auto-scaling and Box-Cox (logarithmic)	3	0.050	5
Propanol / ascorbic acid	Auto-scaling and Box-Cox (logarithmic)	3	0.021	2
Ethanol / salicylic acid	Auto-scaling and Box-Cox (logarithmic)	3	0.033	2

The use of auto-scaling followed by Box-Cox logarithmic transformation was found to be the best pre-processing technique to use with the MW spectra for all examples. Auto-scaling scales the data to mean zero unit variance. This removes the scale of the measured values, and so different data sets, scaled in the same way, are now on the same scale. This aids calibration using different data sets. The MW spectra were expected to be non-linear. Box-Cox improves the linearity between X and Y, so it was expected that this transformation of the data would improve the linear fit.

The errors show that very good models have been built for the addition of water to sand and propanol to ascorbic acid. When the predictions were looked at in detail, it was found that the models predict well over all concentrations, down to very low levels. This shows that the use of MW spectroscopy for monitoring the addition of solvent to a material is very acceptable in most cases. For the addition of ethanol to salicylic acid, a model built with concentrations above 2% gave only a 2% error using auto-scaled and Box-Cox logarithmic transformed data. This suggests the limits of detection have been reached. The use of Box-Cox transformation suggests the data is non-linear.

These models were built with spectra collected for two repeats, and validated with an independent validation data set. The validation sets show different variation compared to the calibration sets as they were collected on different days, but low prediction errors are still achieved. This shows the robustness of the calibration models to experimental variation.

3.1.2 Drying

It has been proved in the wetting experiments that the amount of propanol in ascorbic acid can be determined using MW spectra. In these sets of experiments propanol was added to ascorbic acid contained in the PTFE insert placed in the GMS chamber. The propanol was evaporated off by two different methods. The first method involved heating the chamber and the second passing heated air though the material.

The recorded spectra has been analysed using PCA and visual examination of the residual spectra, to determine if the end of the drying process can be identified.

3.1.2.1 Drying by the heating of the MW chamber

In this experiment propanol (25ml) was added to ascorbic acid (100g) contained in the PTFE sample chamber which is placed in the GMS chamber. This was allowed to evaporate by heating the chamber, with MW spectra recorded at intervals. This was monitored for five hours, and ten replicate spectra were taken at seven time points during the process. These were averaged to give data set *dry_asc_pro*. The ascorbic acid was not completely dry at the end of the recorded period so the endpoint was not reached. Therefore, the data analysis can show the possibility of monitoring the reaction, but the endpoint will not be determined. A spectrum of the dry ascorbic acid was also recorded as a reference. The results produced provide a qualitative example of using MW spectra to monitor such a drying process.

The recorded spectra are shown in Figure 3.1.18. The spectrum at the start of the process is in red, and this moves through to blue for the last spectrum recorded. The spectrum of the dry ascorbic acid is plotted in pink as a comparison. The last spectrum recorded is not at all similar to the dry spectra as would be hoped if the end of the process was achieved. The cut-off frequency is at around 1250MHz for the first spectrum taken during the process and is at around 1500MHz in the dry spectrum. The cut-off frequency changes due to the change in dielectric constant. This is due to the change in composition of the material as the amount of solvent present during the process changes. The cut-off frequency moves in the direction of that of the dry spectrum, so showing there is a possibility with this technique to detect the end point of a drying process just by examination of the spectra.

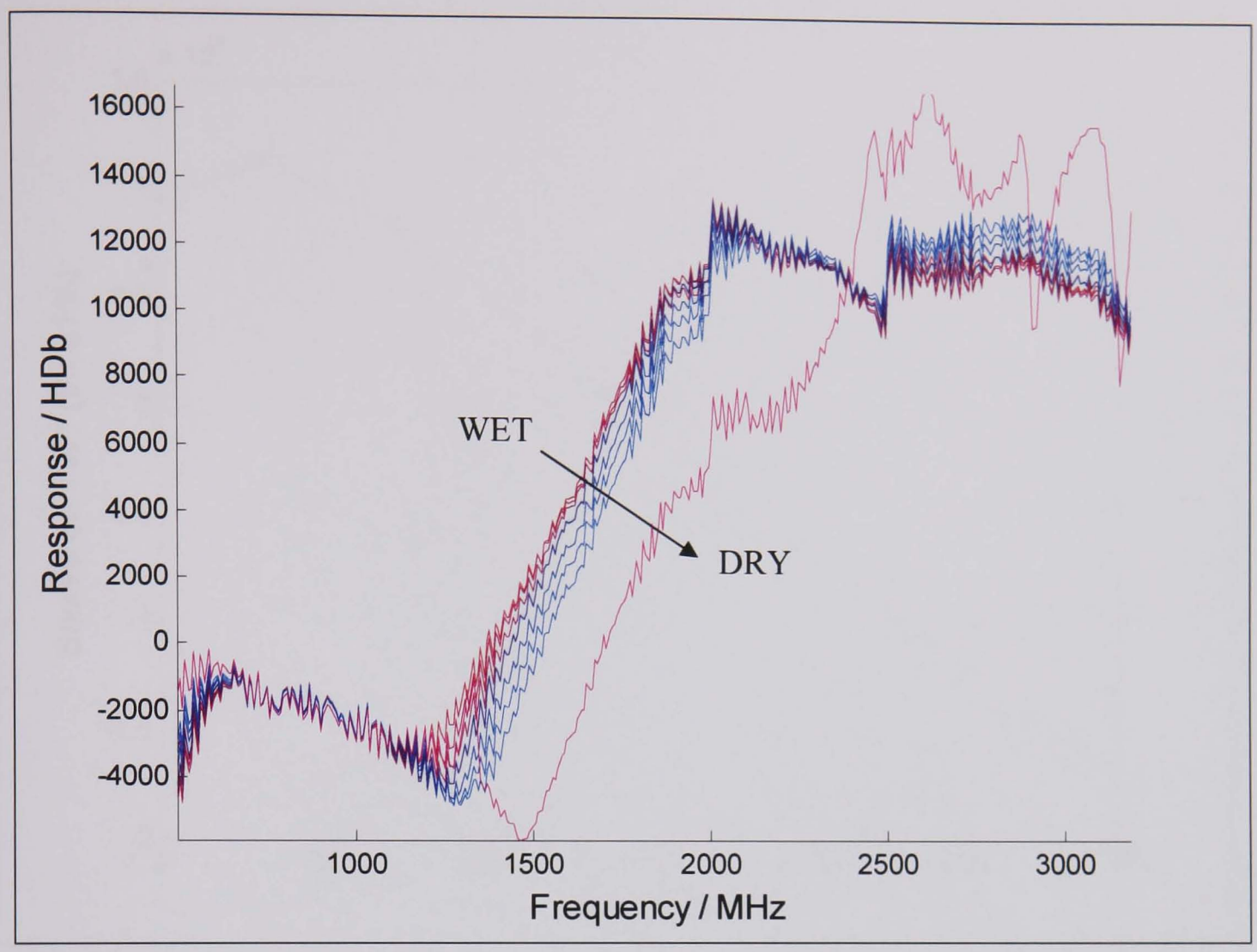

Figure 3.1.18: MW spectra of the drying of ascorbic acid by evaporation of propanol. The spectra go from red as the propanol was added, to blue at the end of the monitoring period. The pink spectrum is the actual dry ascorbic acid.

PCA was preformed on the spectra, and the scores in the first PC, which contains the most information, plotted against time are shown in Figure 3.1.19. This shows how the samples vary over time, and how they relate to each other. When the material is dry and the process has ended, the samples will no longer change and there will be no variation between them. Therefore it is expected that the scores will stop changing. For this process, the scores decrease over the time period and do not stabilise. This shows that the samples are changing but the end of the process has not been reached, as was clear from the spectra. Again this shows the possibility of detecting the material once dry.

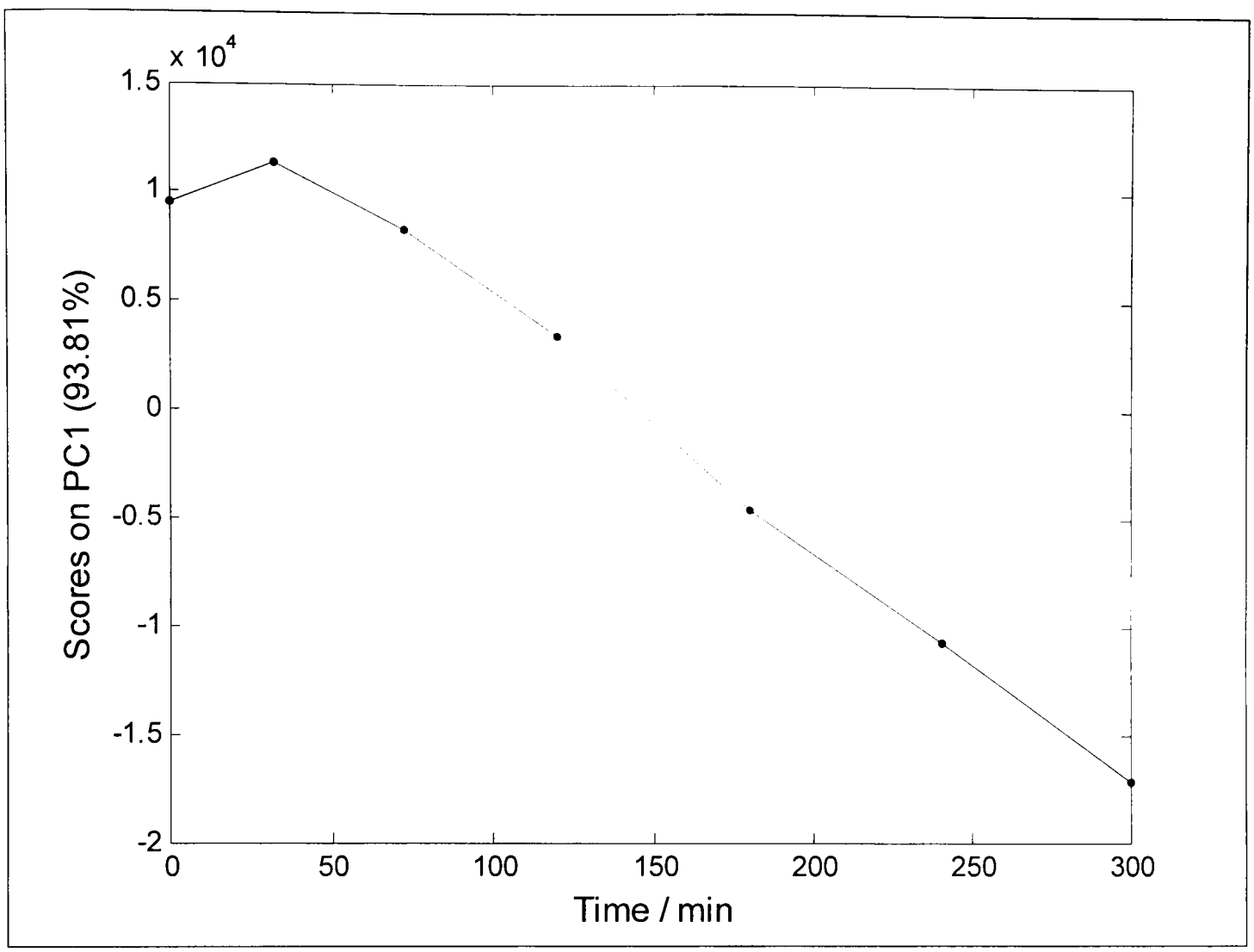

Figure 3.1.19: Scores on PC1 against time for the MW spectra of the removal of propanol from ascorbic acid by evaporation.

The residuals have been calculated by subtracting the dry spectrum from each of the MW spectra (Figure 3.1.20). When the process has reached the end, and the material is dry, the recorded spectra will be the same as the dry spectrum, therefore the residual should be 0. It is clear from the residuals for this reaction that the endpoint is not reached. The residuals are moving towards 0 during the course of the process so again showing the possibility of this technique.

The residual response at 1600MHz has been plotted against time, Figure 3.1.21, to give a clearer indication of how the residual changes as the process proceeds. This shows that the residual increases at the start of the process, but then moves towards zero as the process proceeds.

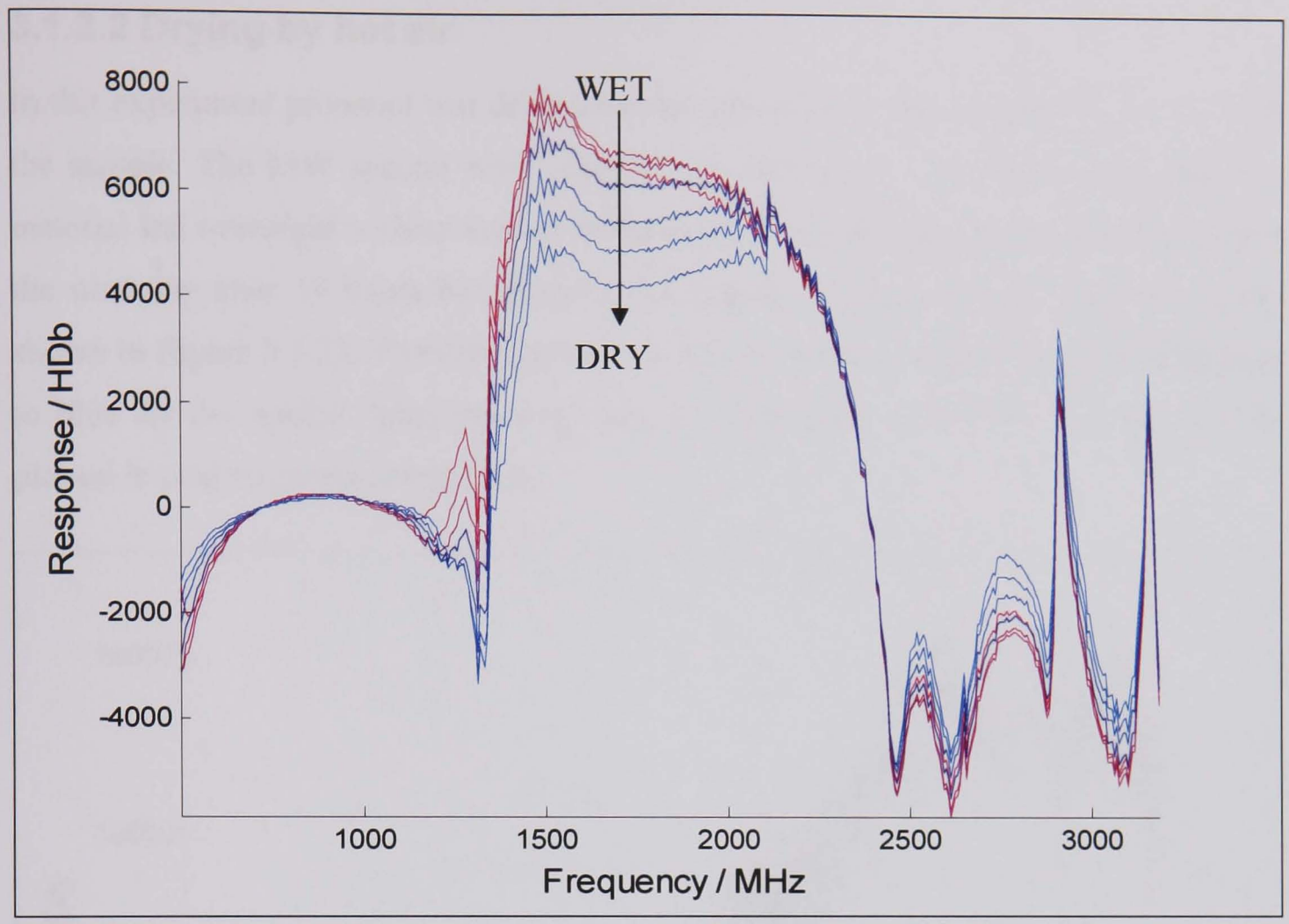

Figure 3.1.20: The residual spectra of the removal of propanol from ascorbic acid by evaporation. This is calculated by subtracting the dry ascorbic acid spectrum from each process MW spectra. The spectra go from red for the first sample, to blue for the final spectrum.

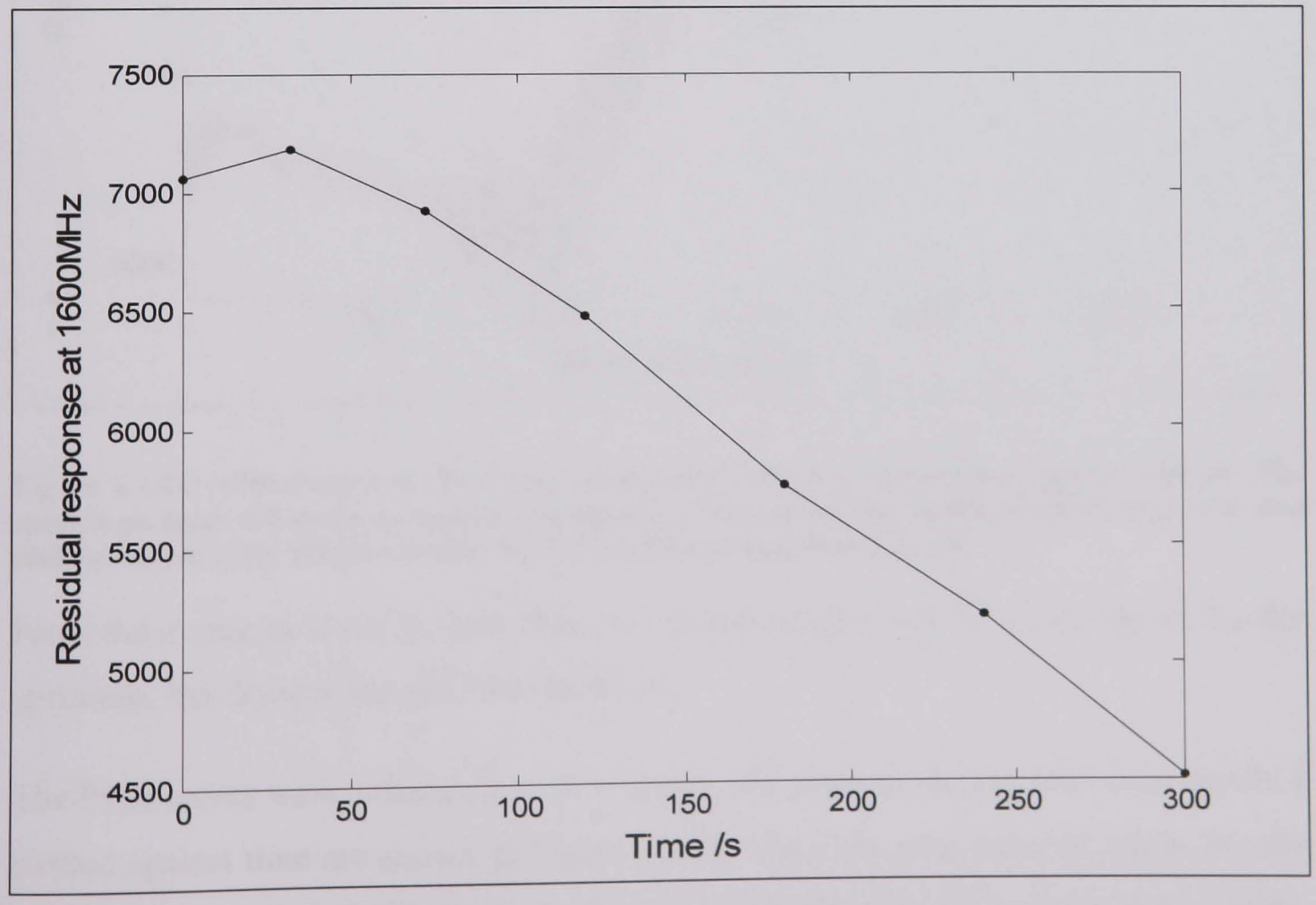

Figure 3.1.21: Plot of the residual response at 1600MHz against time for the MW spectra collected during the removal of propanol form ascorbic acid by evaporation.

3.1.2.2 Drying by hot air

In this experiment propanol was dried from ascorbic acid by blowing heated air through the sample. The MW spectra were recorded at intervals for five hours, and then the material left overnight without any air being passed through and another spectrum taken the next day after 19 hours had passed. The spectra, data set *dry_asc_pro_air_1*, are shown in Figure 3.1.22. The first spectrum is in red, and the spectra are plotted through to blue for the spectra taken the next day. The spectrum of the dry ascorbic acid is plotted in pink to give a comparison.

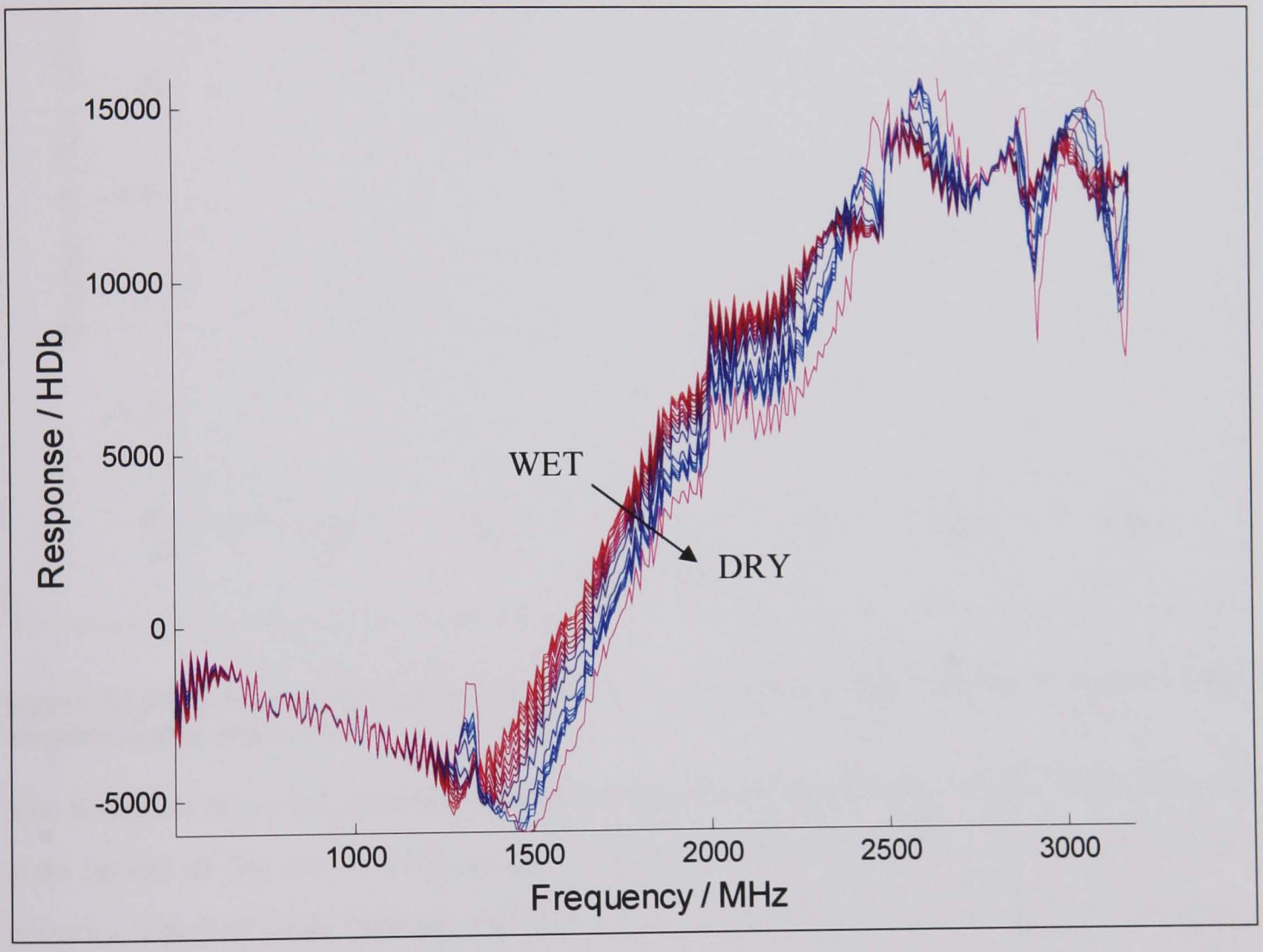

Figure 3.1.22: MW spectra of the drying of ascorbic acid by evaporating propanol with air. The spectra go from red as the propanol was added, to blue at the end of the monitoring period. The pink spectrum is the actual dry ascorbic acid, before propanol was added.

From these spectra it can be seen that the last spectra are very similar to that of the dry spectrum, but dryness has not been achieved.

The PCA scores were calculated as for the previous experiment, and the scores for PC1 plotted against time are shown in Figure 3.1.23. The final measurement, taken the day after is not included in this analysis. There is a decrease in the scores value over the time the process was monitored, and the amount of variation between the samples

decreases over the time period. Again this experiment does not appear to reach the endpoint of the material being fully dry, but it does show the possibilities for monitoring the process.

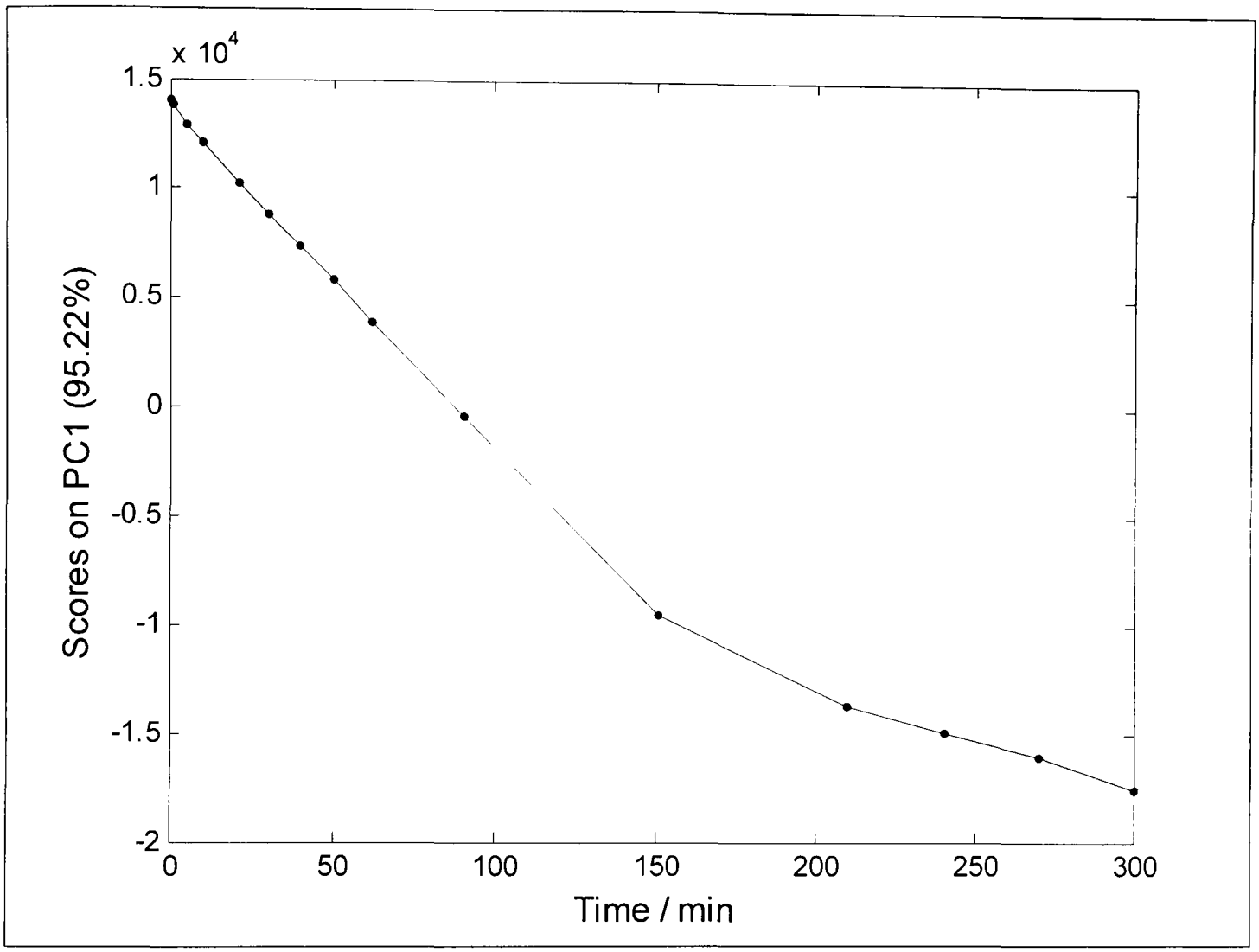

Figure 3.1.23: Scores on PC1 against time from the MW spectra of the removal of propanol from ascorbic acid by evaporation.

The residuals were calculated (Figure 3.1.24) as in the previous example. The residuals start in red at the start of the process and move through to blue for the end of the process. The residuals become closer to 0 as is expected as the material is becoming drier, and so the spectra recorded should become increasing similar to the reference dry spectrum.

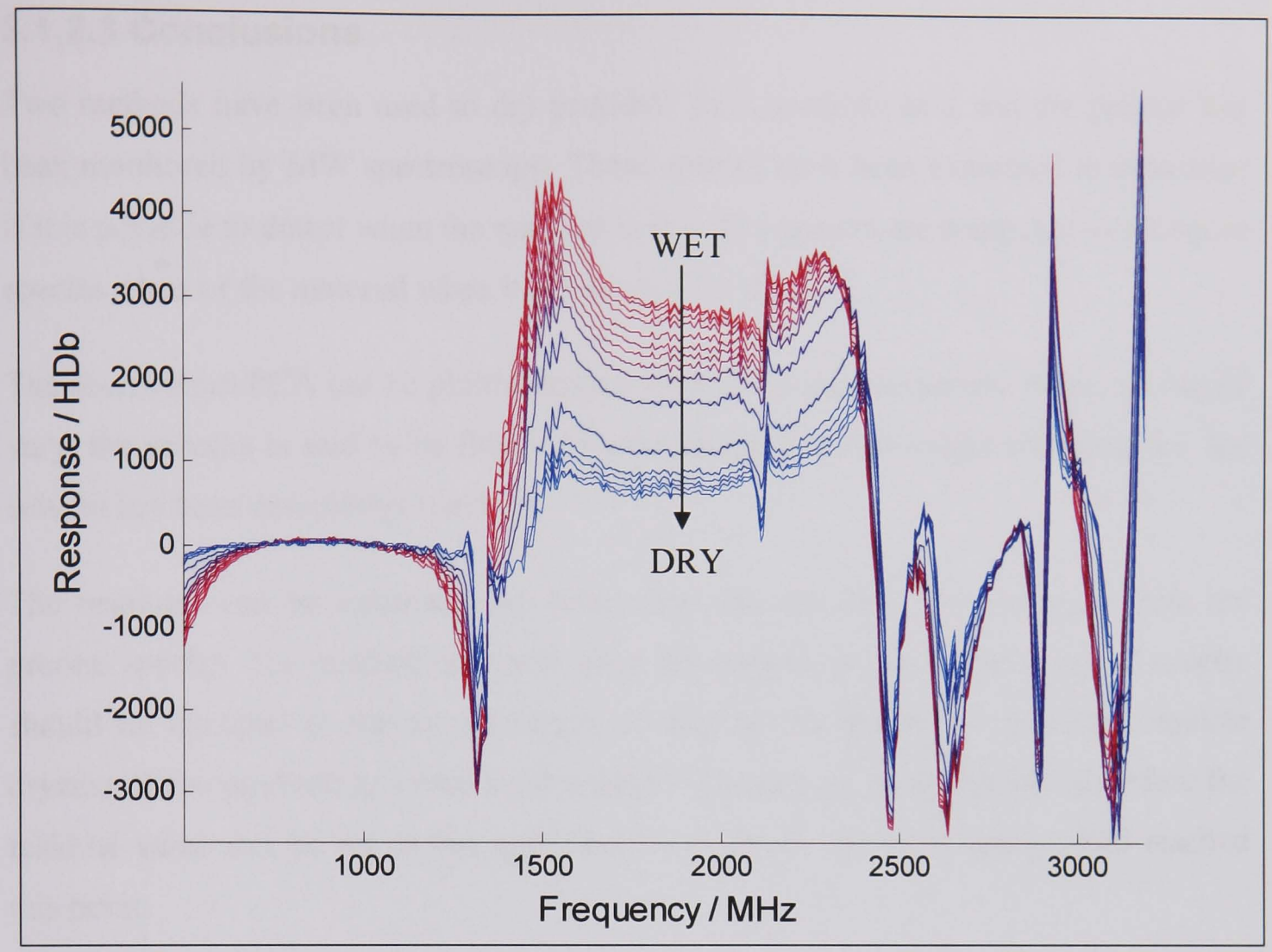

Figure 3.1.24: The residual MW spectra of the removal of propanol from ascorbic acid by drying with air. This is calculated by subtracting the dry ascorbic acid spectrum from each process spectra.

This experiment was to determine if the reaction is reproducible. The spectra, data set *dry_asc_pro_air_2*, are similar to that of the previous experiment, and show the final measurement, taken after seven hours, is very similar to the reference dry spectra. This experiment got closer to the endpoint of the drying process than the previous experiment.

Again the scores were calculated and these show a general decrease over time as in the previous experiments. The samples are varying less by the end of the time period suggesting the process is slowing down.

The residuals were been calculated in the same way. The residual of the final spectrum is very close to 0 in the region 1500-2000MHz. This shows the spectrum is very similar to that of the dry spectrum. It shows the possibility of using this technique to detect the endpoint of a drying process.

3.1.2.3 Conclusions

Two methods have been used to dry propanol from ascorbic acid and the process has been monitored by MW spectroscopy. These spectra have been examined to determine if it is possible to detect when the material is dry. The spectra are compared to reference spectra taken of the material when it is known to be dry.

The scores from PCA can be plotted against time and when the sample scores no longer vary, the process is said to be finished as the samples are no longer changing, i.e. the solvent has been completely removed.

The residuals can be calculated by subtracting the reference dry spectrum from the process spectra. The residual will be 0 when the material is dry, as the recorded spectra should be identical to the dry spectrum. It may not be necessary to reach complete dryness of the product; however a percentage wetness may be acceptable, therefore the residual value can be set to this specification to detect when the process had reached this point.

None of the experiments carried out actually reached the endpoint. The experiments need to be repeated for a longer period to ensure it is possible to detect when the material is dry. This has not been done due to time and equipment constraints. However, these experiments do show the possibility of monitoring a drying process. The MW spectrum of dry material is quite obviously different to the wet material spectra, so a distinction can be made when the endpoint is reached.

3.1.3 Overall Conclusions

The drying process has been simulated by wetting a material with solvent. Calibration models have been built using the recorded MW spectra to predict the amount of solvent present in the material. This shows the possibility of monitoring a drying process with this technique, and shows how little solvent can be detected.

The MW spectra were successfully used to predict the amount of solvent in a sample down to very low amounts (below 1% w/w). Global calibration models were built using the entire spectral range. The use of a variety of pre-processing techniques was examined. The use of auto-scaling followed by Box-Cox logarithmic transformation was found to give the best model. This worked well for the prediction of water in sand and propanol in ascorbic acid, which gave prediction errors of 5 and 2% respectively.

The global model was not as successful for the prediction of ethanol in salicylic acid which gave a prediction error of 32%. However a local model for above 2% ethanol in salicylic acid gave a 2% error, suggesting the limit of detection is at 2%.

The NIR spectra were also collected and these found to not be representative of the process as a diffuse reflectance probe was used. This only measures a small area of the sample and is reliant on the solvent spreading through the sample to the area the probe is measuring. The NIR should be capable of measuring a true drying process as the solvent is being removed in a more continuous manner. Unfortunately the NIR probe could not be used to monitor the drying process due to limitations of space in the GMS chamber.

An actual drying process was also monitored by MW spectroscopy to show that the true process can be monitored. These experiments lack reference concentration data, so can only give an indication of the possibility of monitoring the process. The use of the PCA scores plotted against time and the calculated residual spectra showed the possibility of monitoring the drying process using MW spectroscopy. These experiments did not reach completion, but do show the possibility of the technique.

Monitoring of the drying process was found to be very successful. This occurs as a continuous process. During the wetting process, the solvent is added in steps and it must then seep through the material. Effectively two processes are occurring and both are monitored. The wetting experiments have shown the possibility of building calibration models to predict the amount of solvent present, and the drying has shown the true drying process can be monitored.

3.2 Experimental set-up for esterification reactions

For the esterification reactions, certain aspects of experimental set-up need to be examined to ensure the optimum set-up is used to get the most representative and reproducible results. NIR and MW spectra were collected simultaneously for the reactions. The reactions were contained in the GMS chamber as this is the easiest way to collect the MW spectra. The NIR transmission probe can be placed inside it. It is important to determine the optimum location of this probe. It is also important to consider how large a volume of sample should be used in the chamber to give the best spectra. The last consideration for experimental set-up is the temperature that the reactions are run at, and if this should be keep constant.

3.2.1 Optimum location of the NIR transmission probe in the GMS chamber

The NIR probe to be used to collect spectra is placed inside the GMS chamber, and this will cause reflectance of the microwaves, so affecting the MW spectra collected. This reflectance needs to be minimised. The probe must be located in an optimum position which causes least interference to the MW spectra, whilst giving representative NIR spectra.

3.2.1.1 Experimental details

The chamber has been split into areas in which the probe could be located as detailed in section 2.3.1 of the experimental chapter. The chamber is filled with water (500ml) and the chamber heated to 32°C, to give a constant temperature. Ten repeat MW scans were taken with the probe in each position (A1-15, B1-15, C1-15), along with ten NIR spectra, ensuring the transmission slit was facing into the chamber to allow maximum contact with the liquid.

3.2.1.2 Results and discussion

The average NIR spectra for each location are shown in Figure 3.2.1. From this it can be seen that locating the NIR probe in different places in the GMS chamber does not significantly alter the collected spectra of water. There is some difference in the spectra but this is minimal.

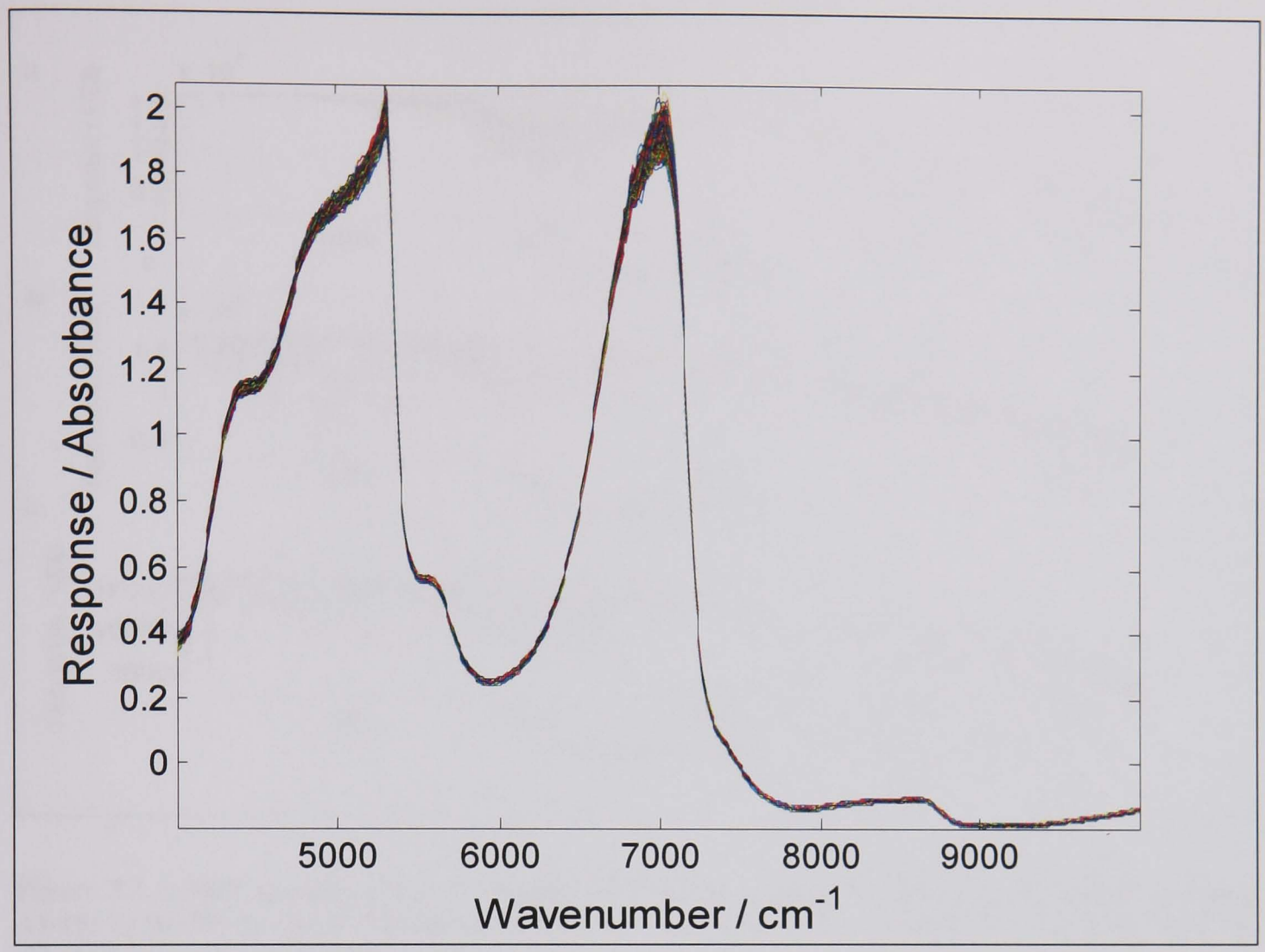

Figure 3.2.1: NIR spectra of water contained within the GMS chamber, with the probe located at different positions.

The MW spectra collected were examined for each location and any obvious visual outliers removed. The ten spectra for each location were averaged (Figure 3.2.2). It can clearly be seen that the NIR probe has a large effect on the MW spectra. The smallest effect is seen when the probe is located in the A position, Figure 3.2.2a.

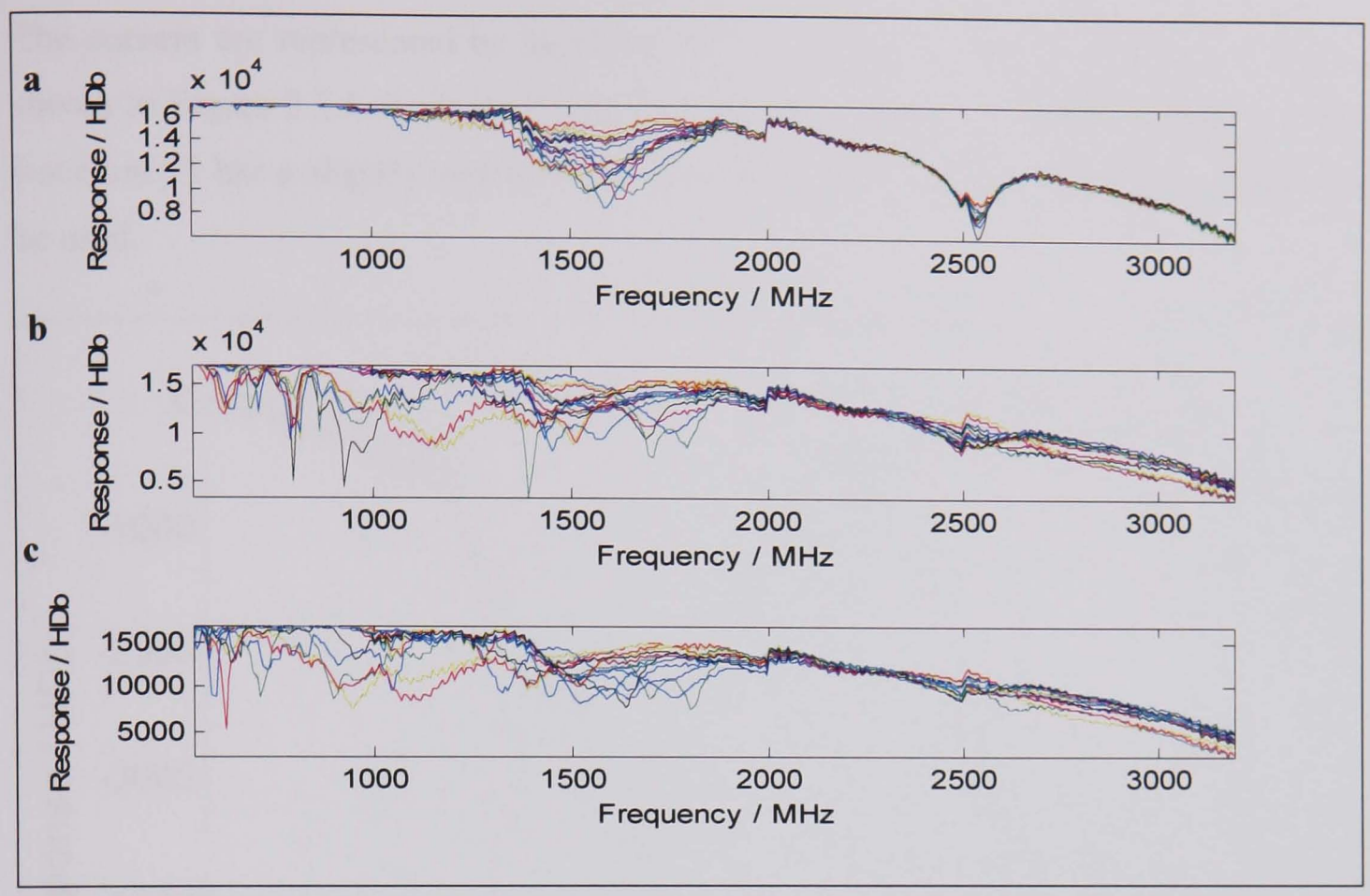

Figure 3.2.2: MW spectra of water with the NIR probe located in different positions; a) locations A1-15; b) B1-15; c) C1-15. The actual positions are not labelled, but this gives an indication of the effect of the probe of the MW spectra.

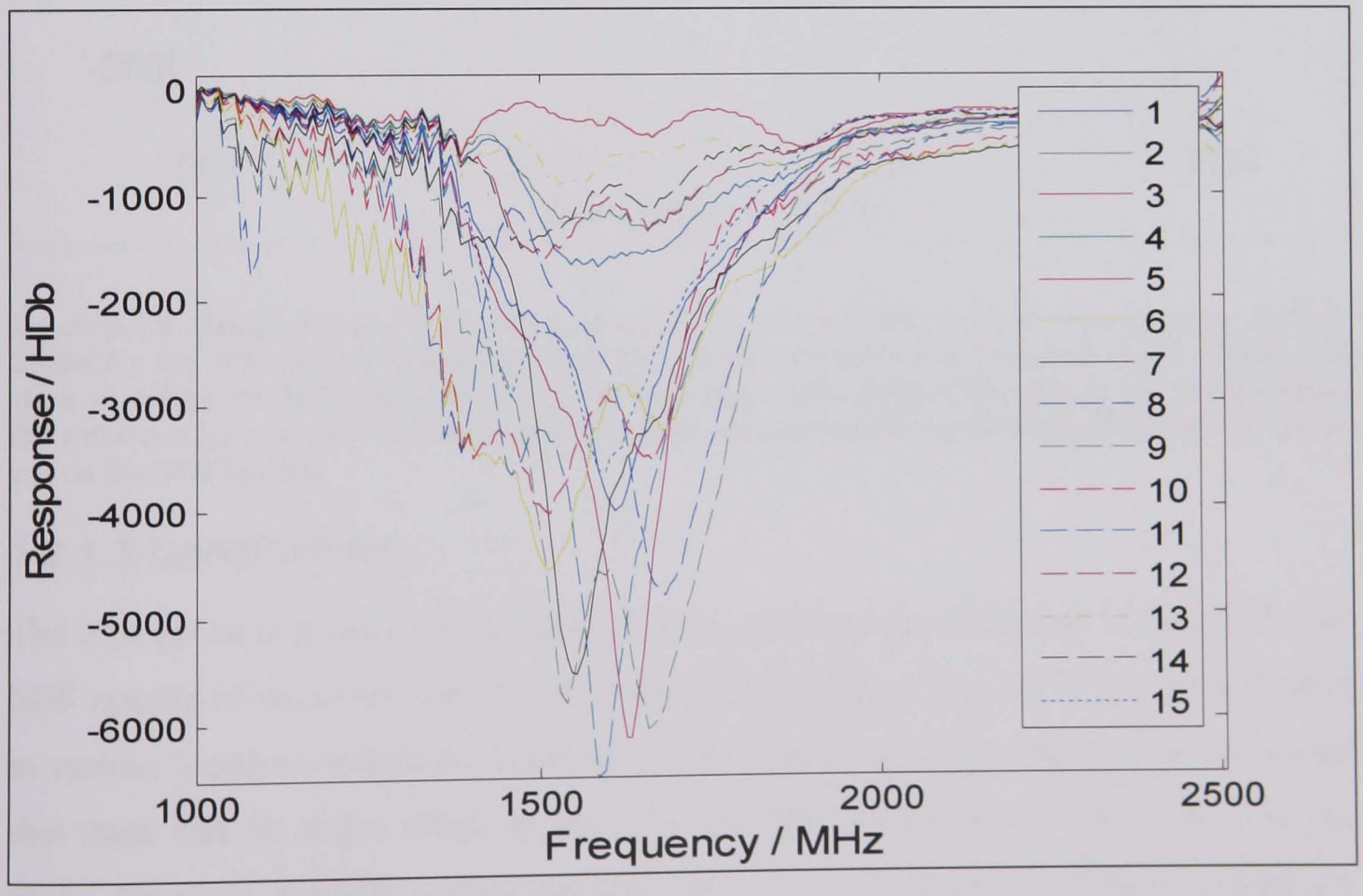

Figure 3.2.3: Residual plots (MW spectra minus the reference water spectra) over the range 1000 to 2500MHz for MW spectra collected with a NIR probe located in the A position, to show the effect the NIR probe has on the MW spectra. The smaller the residual, the more similar the reference spectra and the collected MW spectra, and hence the smaller the effect the NIR probe has on the MW spectra.

The corners are represented by locations 1, 5, 11 and 15. The residuals for these are shown in Figure 3.2.4. Location 1 and 15 have the smallest residuals, and are similar. Location 15 has a slightly smaller residual so this is the compromise location that is to be used.

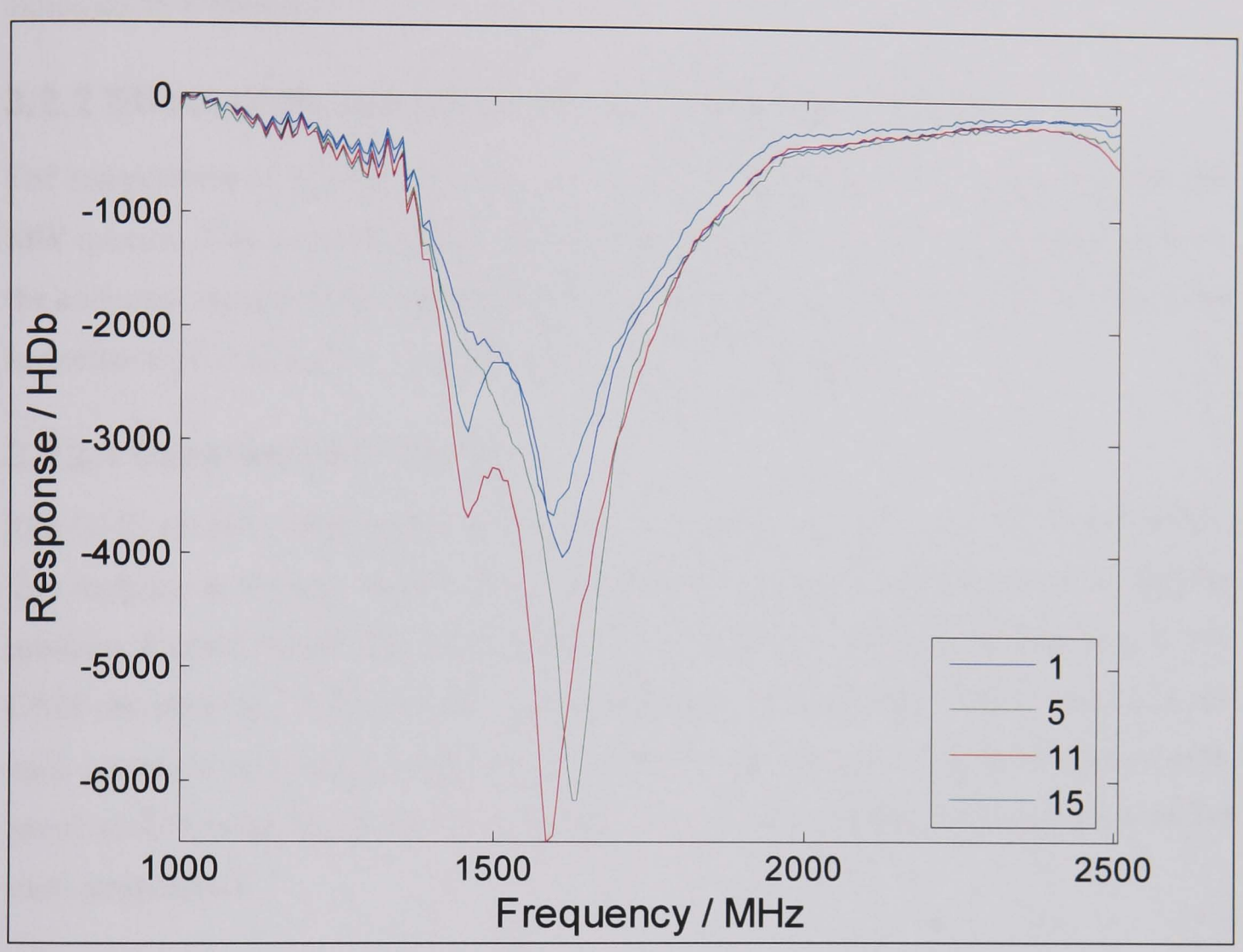

Figure 3.2.4: Residual plots (MW spectra minus the reference water spectra) over the range 1000 to 2500MHz for MW spectra collected with a NIR probe located in the corners in the A position, to show the effect the NIR probe has on the MW spectra. The smaller the residual, the more similar the reference spectra and the collected MW spectra, and hence the smaller the effect the NIR probe has on the MW spectra

3.2.1.3 Conclusions

The NIR probe is located in the GMS chamber to allow the collection of both NIR and MW spectra of reactions carried out in the GMS chamber. The probe has been located in various locations within the chamber and the spectra of water collected. It was found that there was no major effect on the collected NIR spectra due to the location of the probe. However, the MW spectra collected with the probe located in different places are affected greatly by the NIR probe. The optimum location was determined by examination of the residuals, calculated by removing reference water spectrum, with no probe in the chamber, from the collected spectra. The location of the probe has to be a

compromise between the least interference on the MW spectra, and ease of location with respect to other equipment in the chamber (overhead stirrer). Therefore, the best location for the NIR probe within the GMS chamber was determined to be in one corner, next to the transmitter antenna, with the probe 3.5cm into the chamber, as indicated by position 15 .

3.2.2 Effect of temperature on the collected spectra

The temperature of a sample affects both the NIR spectra of the sample, and also the MW spectra. This experiment was carried out to show the effect the temperature has on the collected spectra of the components in the esterification reaction. This will show the importance of keeping the temperature as constant as possible.

3.2.2.1 Experimental details

The GMS chamber was heated to a variety of temperatures (25, 35, 40, 50 and 60°C). The reagents to be used in the esterification reaction (butanol and acetic acid) and the products formed (water and butyl acetate) were heated to the same temperature as the GMS chamber, and 450ml placed in the chamber. 20 repeat MW scans were taken for each sample at each temperature, along with 40 repeat NIR scans using the transmission probe placed in the GMS chamber. The spectra were averaged to give one spectrum for each temperature.

3.2.2.2 Results and discussion

The MW spectra for the components at different temperatures are shown in Figure 3.2.5 to Figure 3.2.8. The spectra of acetic acid (Figure 3.2.5) look to have the same shape but a slightly different response, so the change due to temperature is small. The butanol spectra (Figure 3.2.6) show a large change in response. The spectra are affected by the change in temperature suggesting the dielectric constant of butanol varies greatly over the temperature range used. The spectra of butyl acetate (Figure 3.2.7) have little variation over the temperatures used. The spectra for the temperatures 25, 35 and 40°C are very similar, as are the spectra for 50 and 60°C. The spectra for water (Figure 3.2.8) have a varied response with a change in temperature. The variation in response increases as the frequency increases.

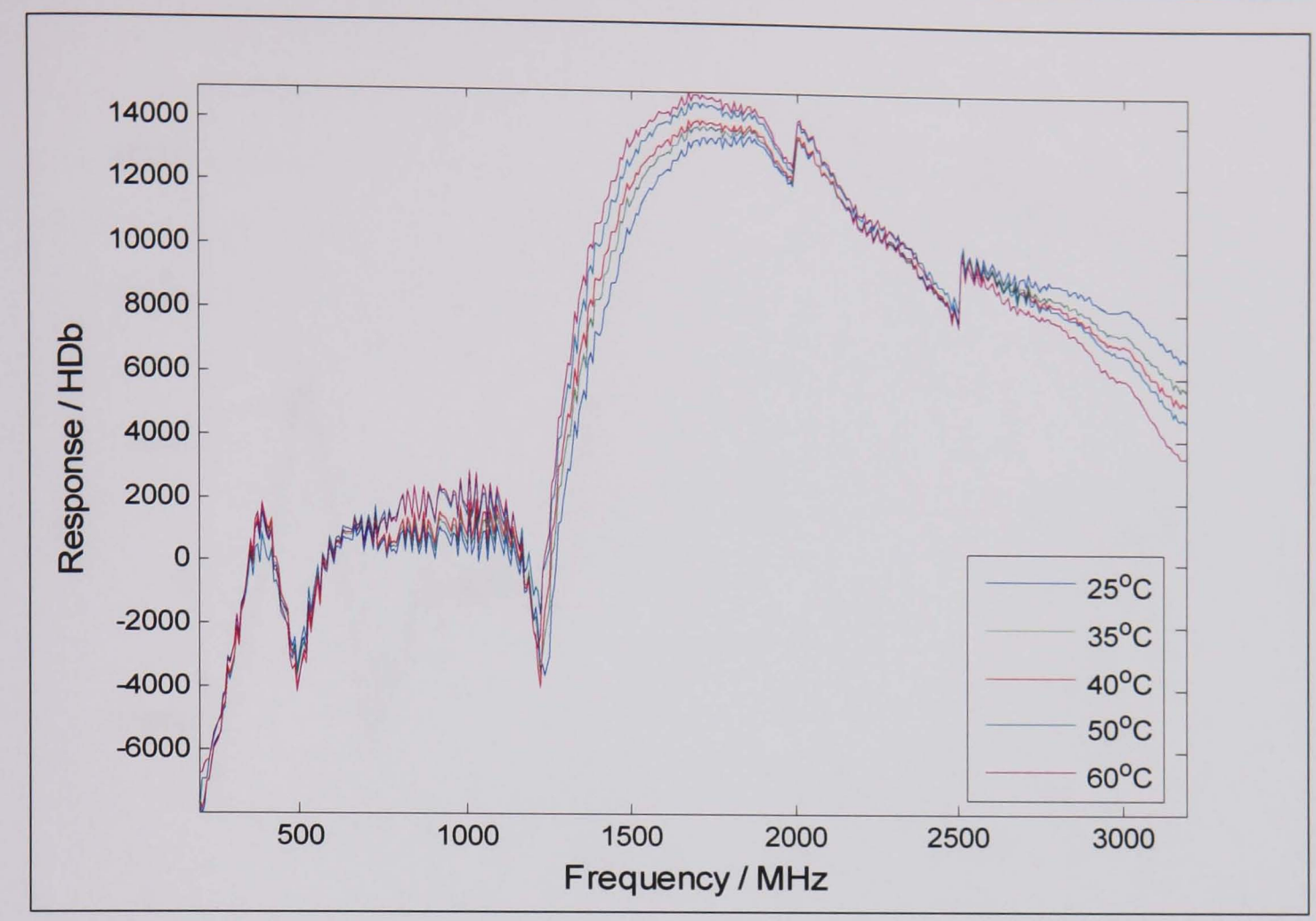

Figure 3.2.5: MW spectra of acetic acid, one of the reactants of the esterification reaction between butanol and acetic acid, at various temperatures.

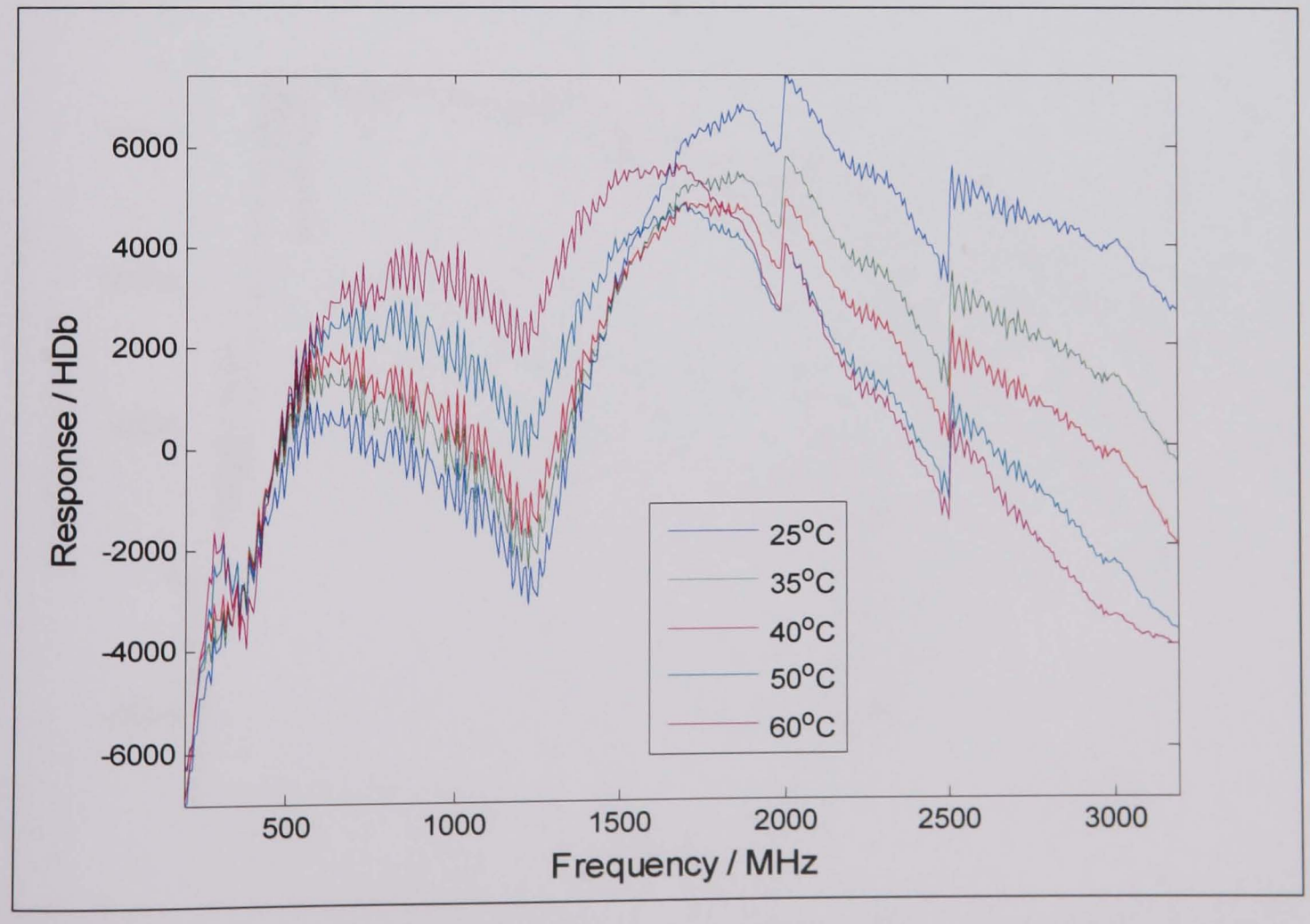

Figure 3.2.6: MW spectra of butanol, one of the reactants of the esterification reaction of butanol and acetic acid, at various temperatures.

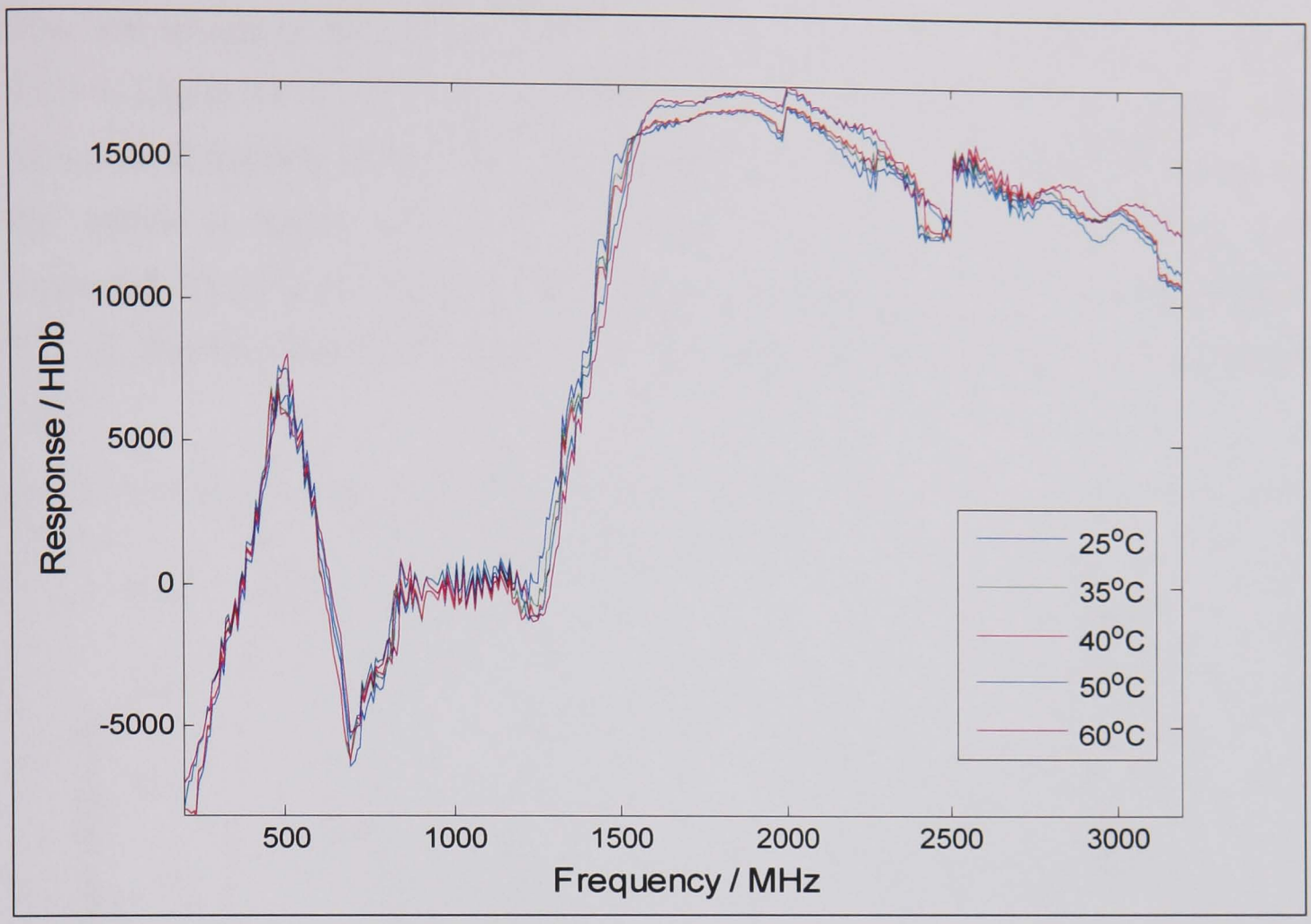

Figure 3.2.7: MW spectra of butyl acetate, one of the products of the esterification reaction of butanol and acetic acid, at various temperatures.

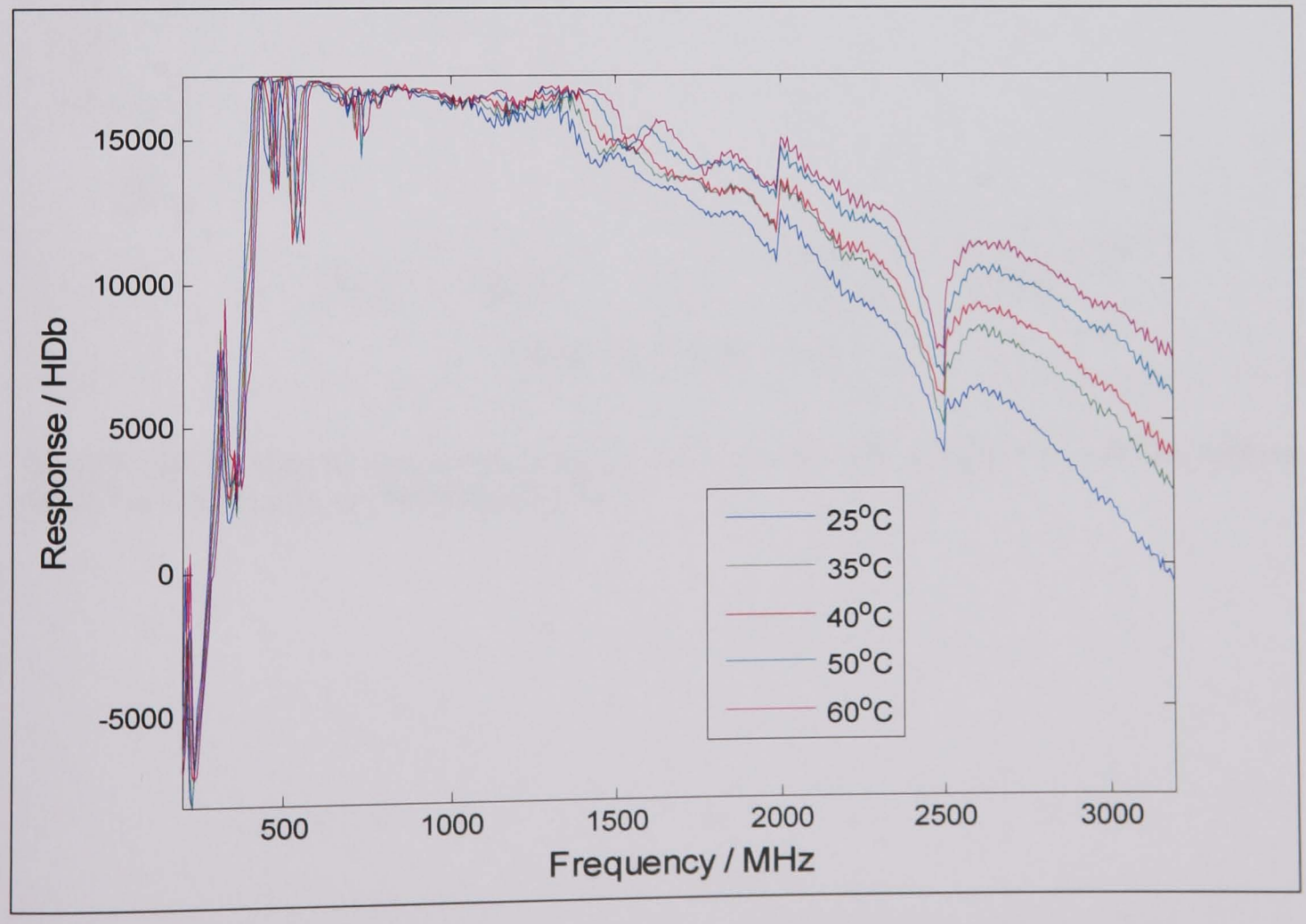

Figure 3.2.8: MW spectra of water, one of the products of the esterification reaction between butanol and acetic acid, at various temperatures.

The NIR spectra of the components of the esterification reaction are shown in Figure 3.2.9 to Figure 3.2.12. The change in NIR spectra due to temperature is very small, with only a small increase in absorbance seen with an increase in temperature. The change in the spectra is mainly seen in the baseline (9000 – 9500cm^{-1}) which shifts with increasing temperature. This baseline shift is at its greatest in the water spectra (Figure 3.2.12). Baseline shift in NIR spectra is a well known phenomenon and can be corrected for.

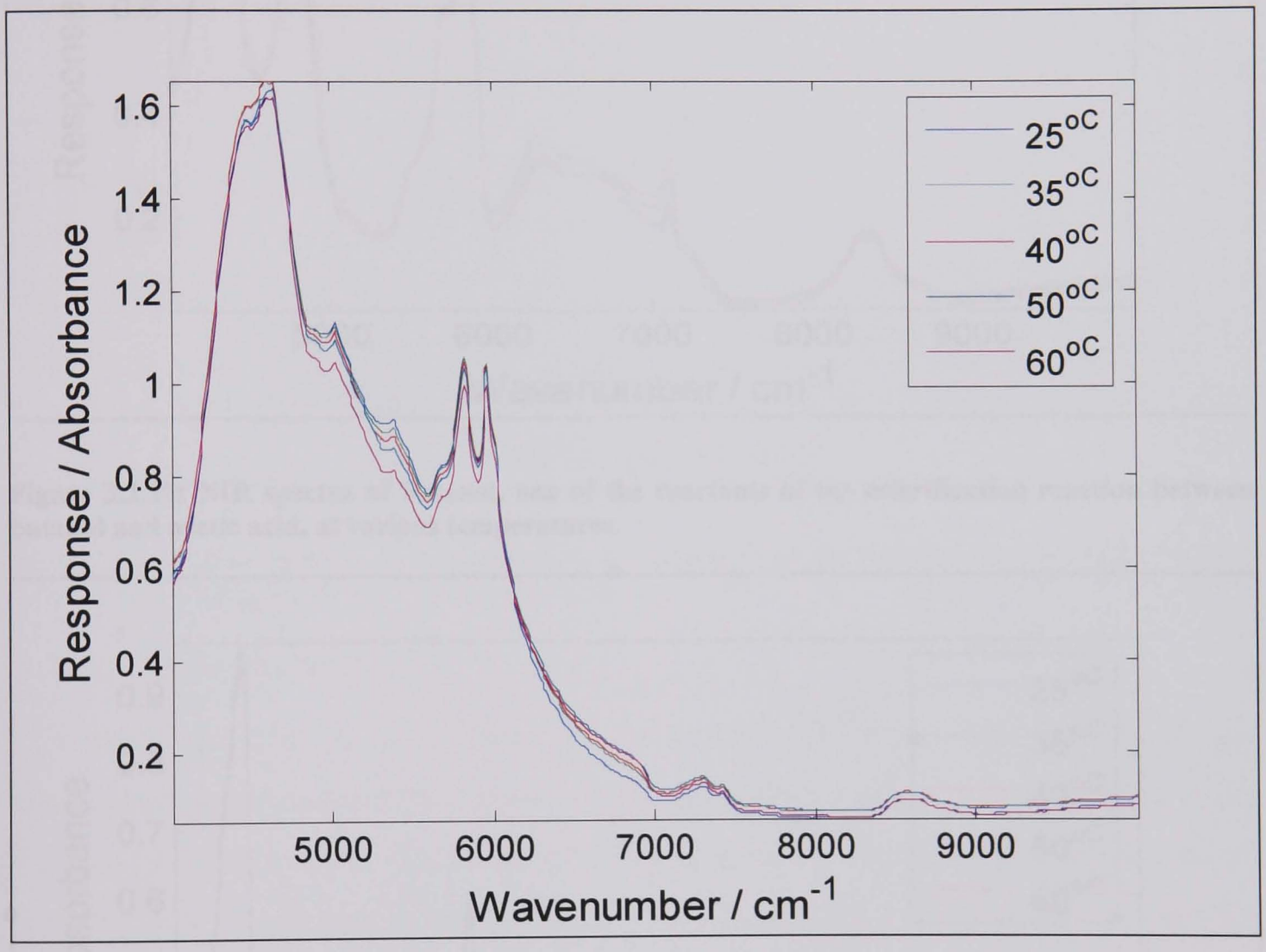

Figure 3.2.9: NIR spectra of acetic acid, one of the reactants of the esterification reaction between butanol and acetic acid, at various temperatures.

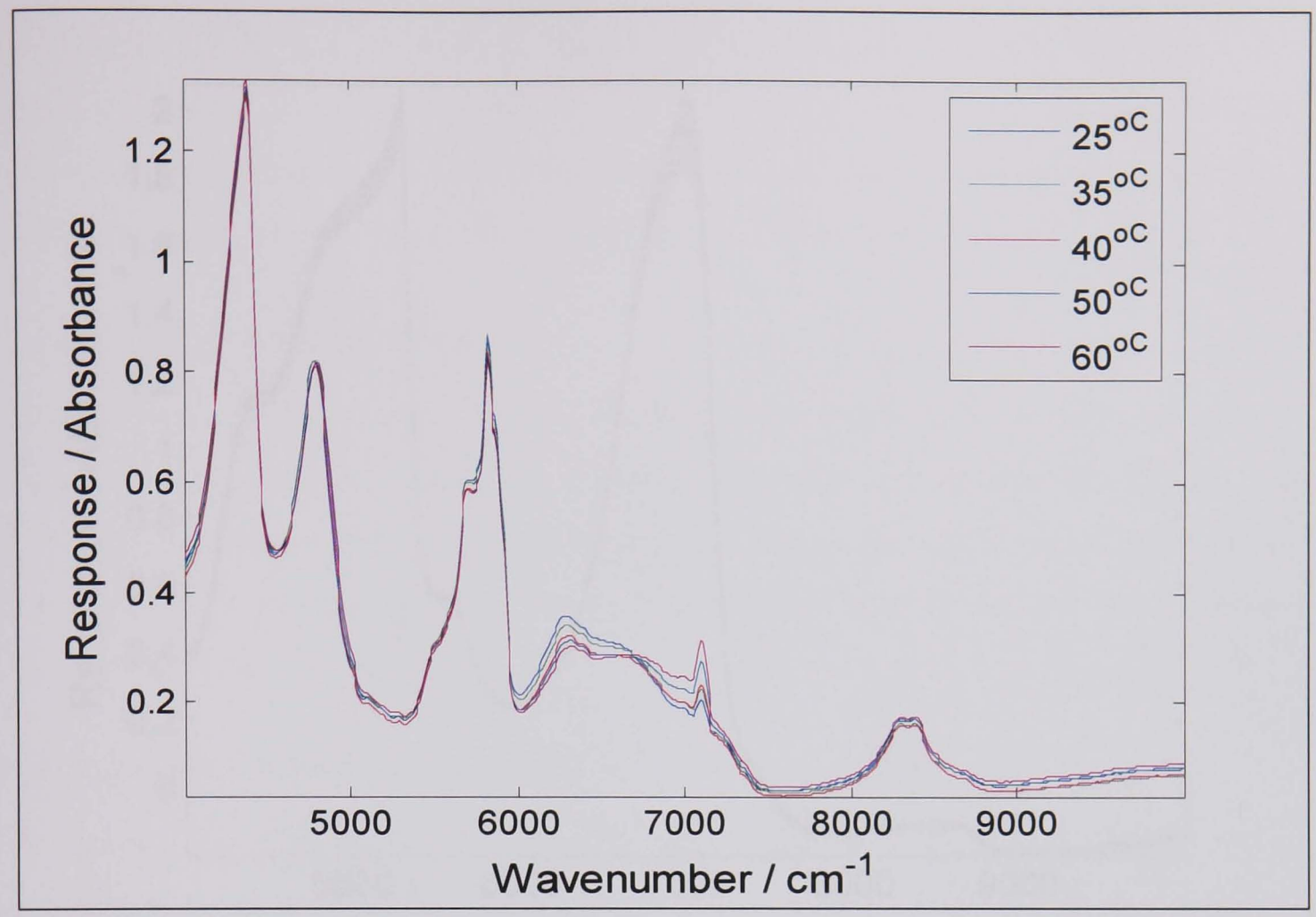

Figure 3.2.10: NIR spectra of butanol, one of the reactants of the esterification reaction between butanol and acetic acid, at various temperatures.

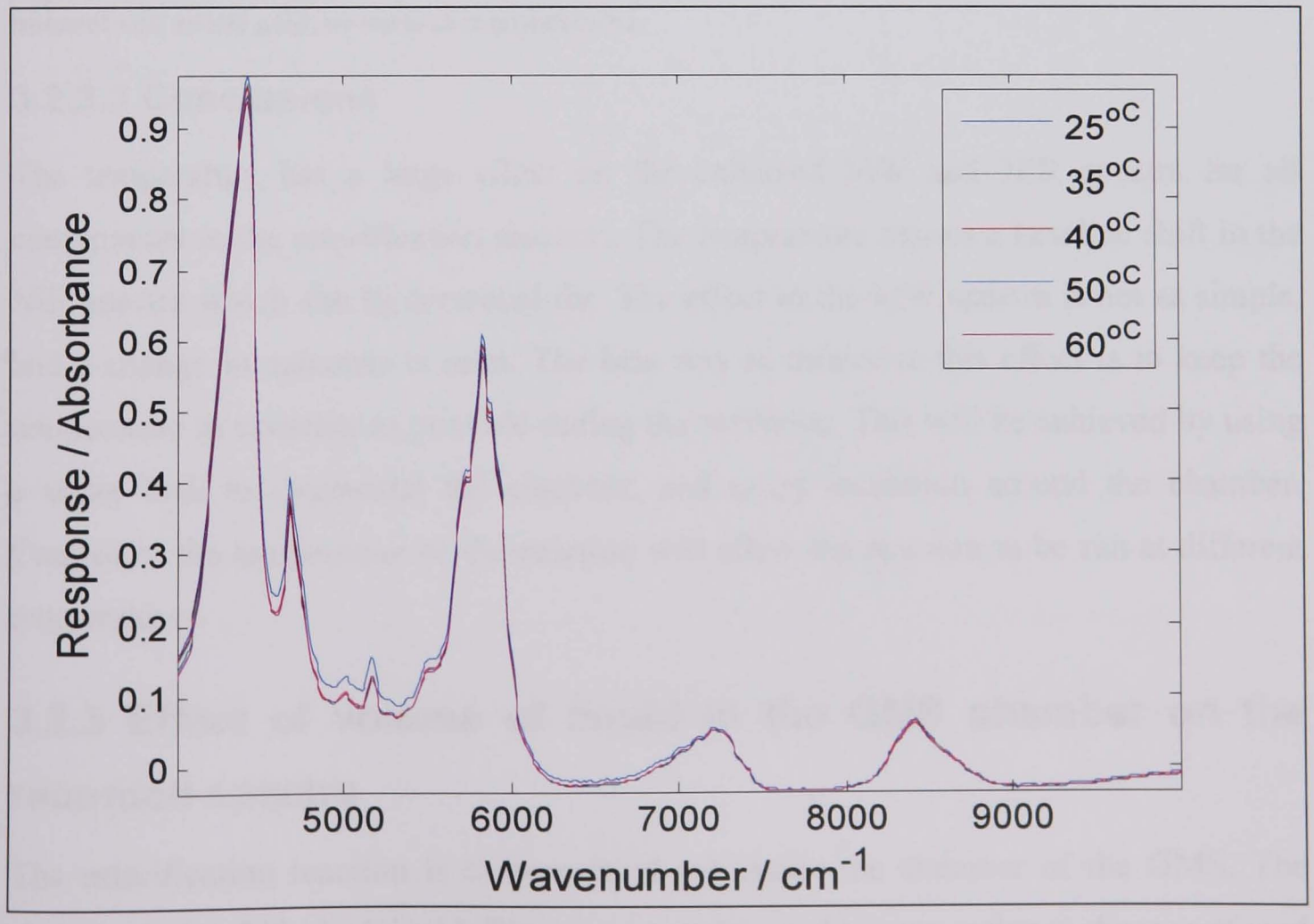

Figure 3.2.11: NIR spectra of butyl acetate, one of the products of the esterification reaction between butanol and acetic acid, at various temperatures.

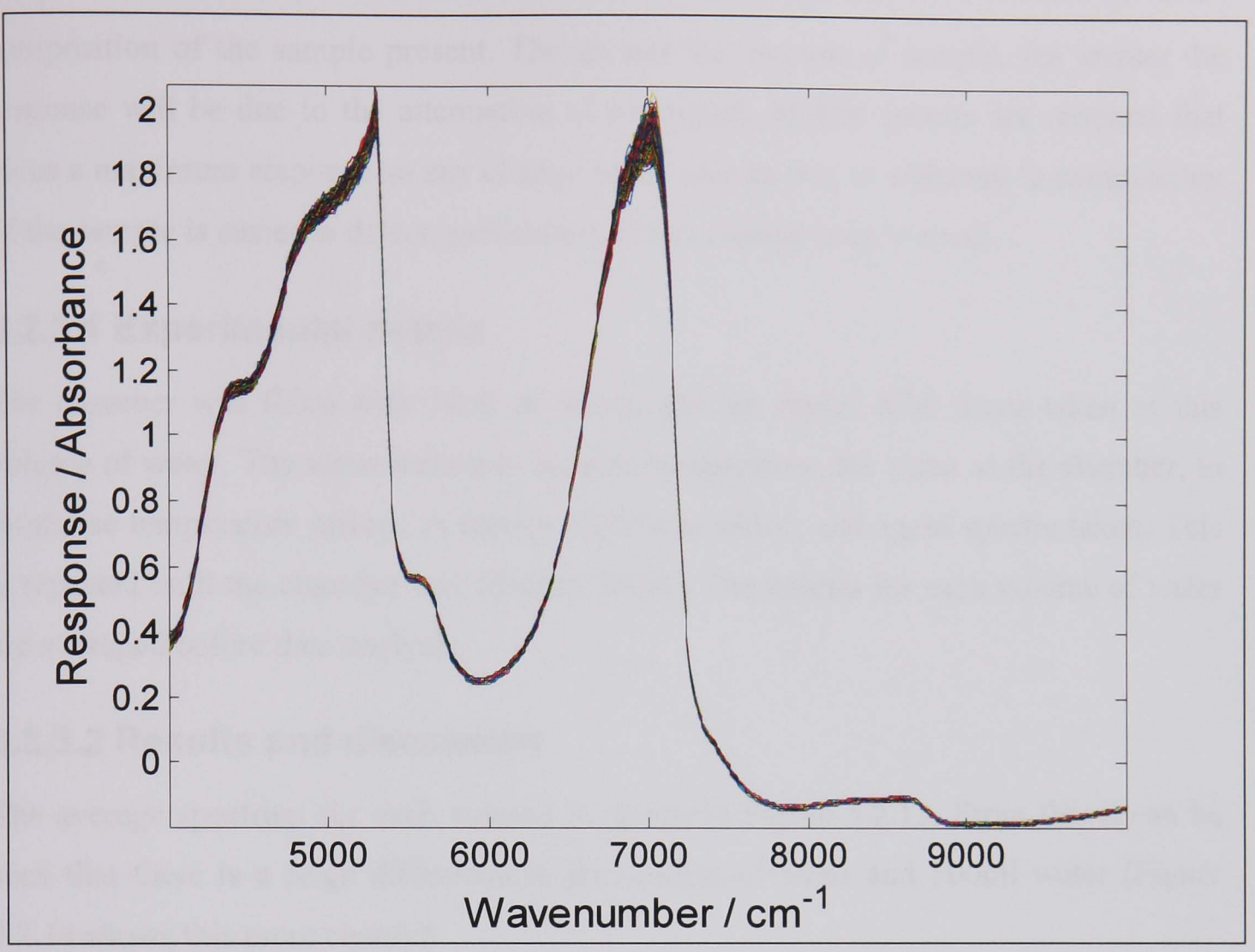

Figure 3.2.12: NIR spectra of water, one of the products of the esterification reaction between butanol and acetic acid, at various temperatures.

3.2.2.3 Conclusions

The temperature has a large effect on the collected MW and NIR spectra for all components in the esterification reaction. The temperature causes a baseline shift in the NIR spectra which can be corrected for. The effect in the MW spectra is not as simple, and a change in response is seen. The best way to minimise this effect is to keep the temperature as constant as possible during the reactions. This will be achieved by using a water bath to thermostat the chamber, and using insulation around the chamber. Control of the temperature of the reaction will allow the reaction to be run at different temperatures.

3.2.3 Effect of volume of liquid in the GMS chamber on the recorded spectra

The esterification reaction is to be carried out inside the chamber of the GMS. The chamber holds 540ml of liquid. The reagents to be used are expensive to dispose of, and are flammable. Therefore, ideally the total volume used should be minimised, whilst still giving representative MW spectra. The recorded MW spectra respond to the

composition of the sample present. The greater the amount of sample, the greater the response will be due to the attenuation of the signal. Ideally spectra are required that gives a maximum response so any change in the spectra due to a change in composition of the sample is easier to detect, particularly if this change is only small.

3.2.3.1 Experimental details

The chamber was filled with 50ml of water, and ten repeat MW scans taken of this volume of water. The water used was at room temperature, the same as the chamber, to minimise temperature effects. A further 50ml was added, and again spectra taken. This is repeated until the chamber was filled to 500ml. The spectra for each volume of water are averaged before data analysis.

3.2.3.2 Results and discussion

The average spectrum for each volume is shown in Figure 3.2.13. From this it can be seen that there is a huge difference in the spectra of 50ml and 500ml water (Figure 3.2.14 shows this more clearly).

As the volume of water increases, so does the response in the spectra. The maximum response is desirable to ensure any small change in the spectra due to a change in sample composition is detected. The spectra for 450ml of water gives a maximum response, no further increase is seen. 450ml and 500ml have similar spectra. This suggests the response is at maximum, so any further change in spectra may be missed. Therefore, a volume of 450ml should be used to maximise response.

3.2.3.3 Conclusions

Different volumes of sample in the GMS chamber will give different spectra as the spectra are related to the amount of sample present. A volume should be used that gives a maximum response so any small changes in the spectra due to composition change will be detected. 450ml of sample is to be used in the esterification reactions.

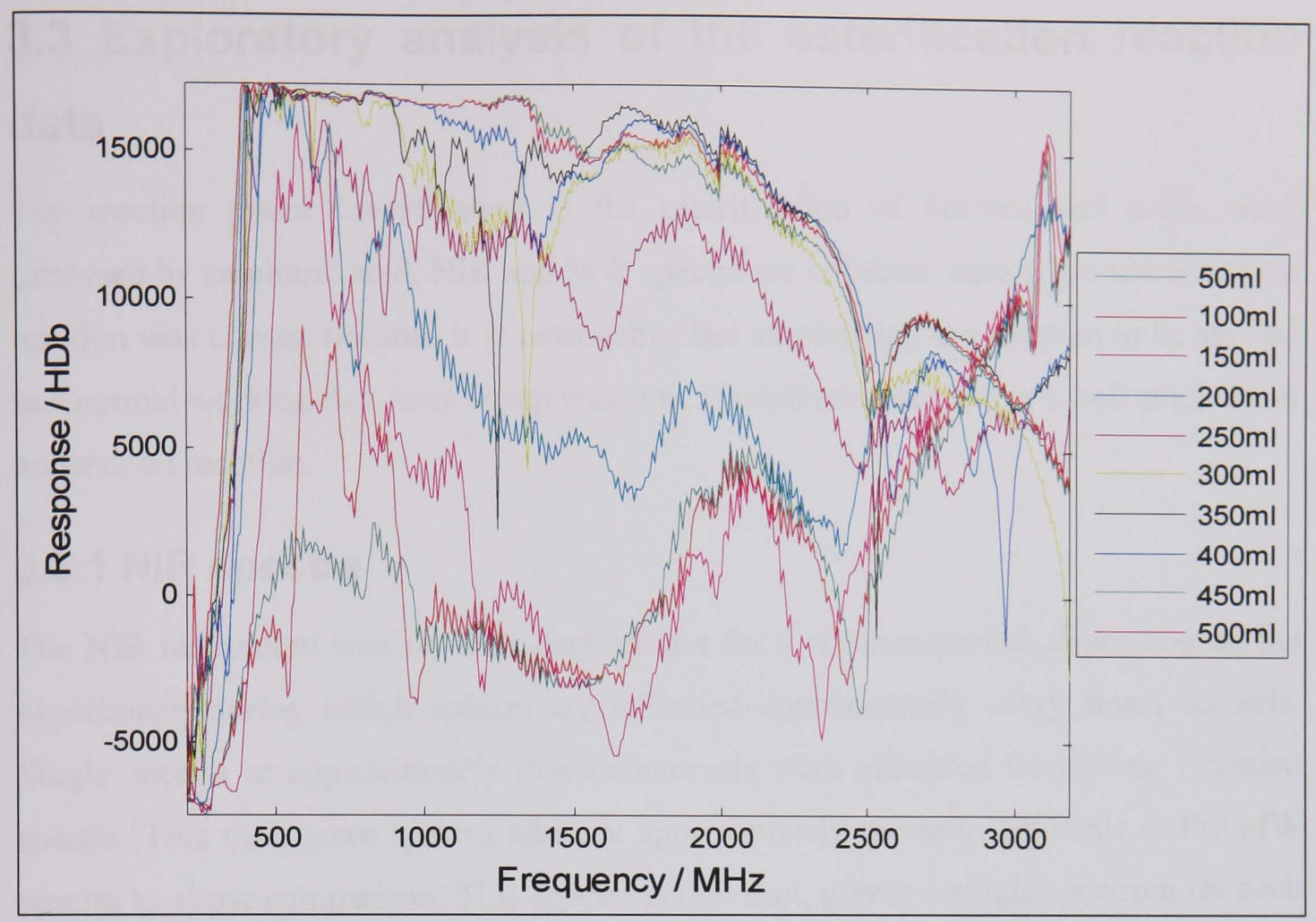

Figure 3.2.13: MW spectra of different volumes of water contained in the GMS chamber. The spectra are recorded at room temperature.

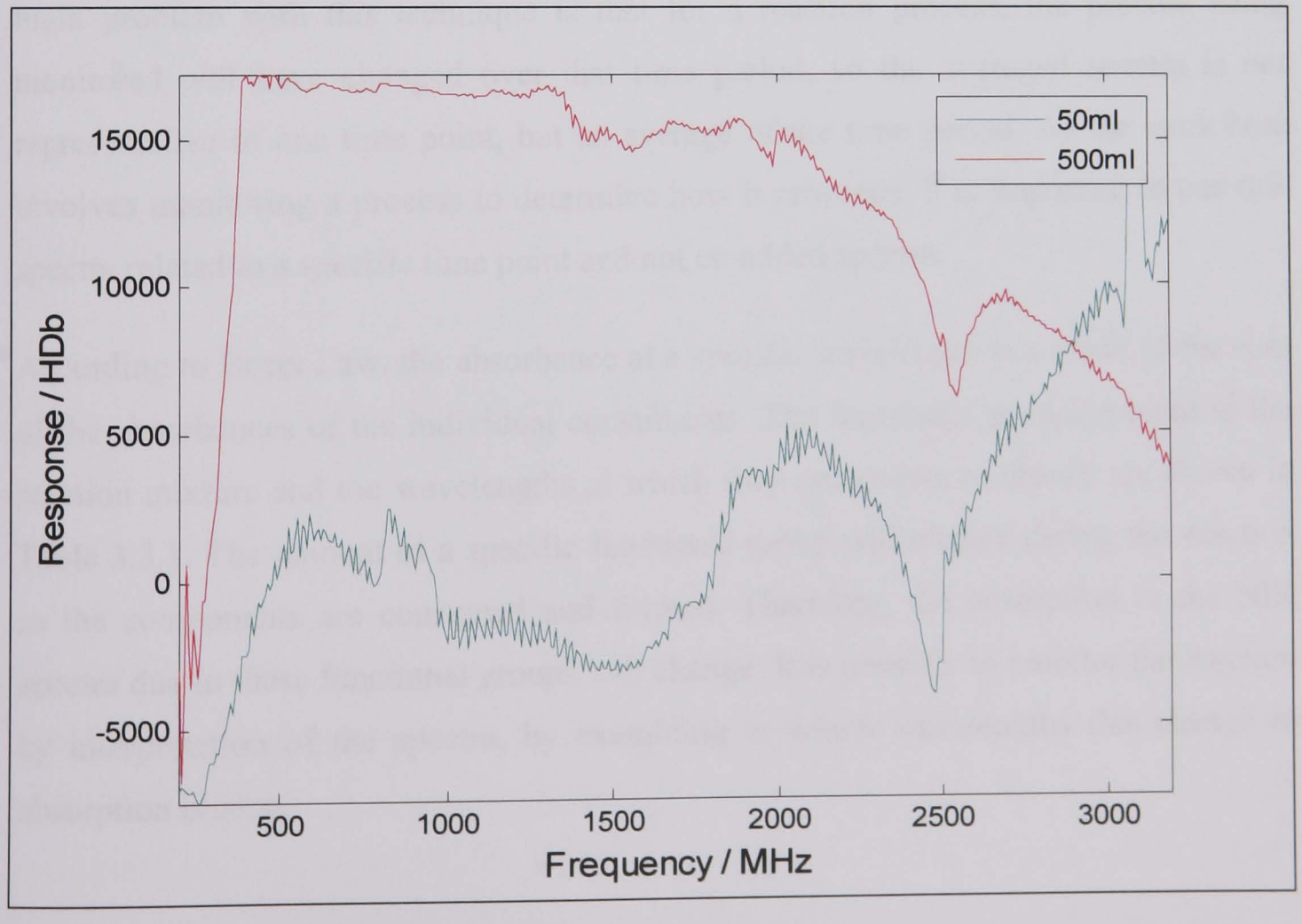

Figure 3.2.14: MW spectra of 50 and 500ml of water contained in the GMS chamber.

3.3 Exploratory analysis of the esterification reaction data

The reaction under investigation is the esterification of butanol and acetic acid, catalysed by sulphuric acid. NIR and MW spectra are collected during the reaction. This reaction was chosen because it is reasonably fast so allowing the reaction to be studied in a normal working day, uses cheap reagents, is relatively safe and is a well studied and understood reaction.

3.3.1 NIR spectra

The NIR instrument was set to collect spectra for a set time period, depending on the experiment, during which spectra are collected approximately every seven seconds. Single spectra at approximately minute intervals were extracted from these recorded spectra. This then gives spectra taken at approximately the same intervals as the MW spectra to allow comparison. This spectra is one-shot, giving a single spectrum for each sample. Traditionally, several NIR spectra may be recorded over a set time period of a couple of minutes. These are co-added, and are then averaged to give one spectrum. The main problem with this technique is that for a reaction process, the process being monitored will have changed over that time period, so the averaged spectra is not representative of one time point, but an average of the time period. As the work here involves monitoring a process to determine how it proceeds, it is important to use raw spectra related to a specific time point and not co-added spectra.

According to Beers Law, the absorbance at a specific wavelength is a result of the sum of the absorbances of the individual constituents. The functional groups present in the reaction mixture and the wavelengths at which they are known to absorb are shown in Table 3.3.1. The amount of a specific functional group will change during the reaction as the components are consumed and formed. Therefore, the absorption in the NIR spectra due to these functional groups will change. It is possible to monitor the reaction by interpretation of the spectra, by examining at which wavelengths this change in absorption is seen.

Table 3.3.1: Main absorptions expected to be seen in the NIR spectra due to the functional groups present in the esterification reaction.

	R-OH		RCOOH		RCOOR'		Water	
Combination bands / cm^{-1}	4785	4854	5236	5305	5025	5181	4435 5115	4464 5263
1st Overtone bands / cm^{-1}	6757	7067					7067	7112

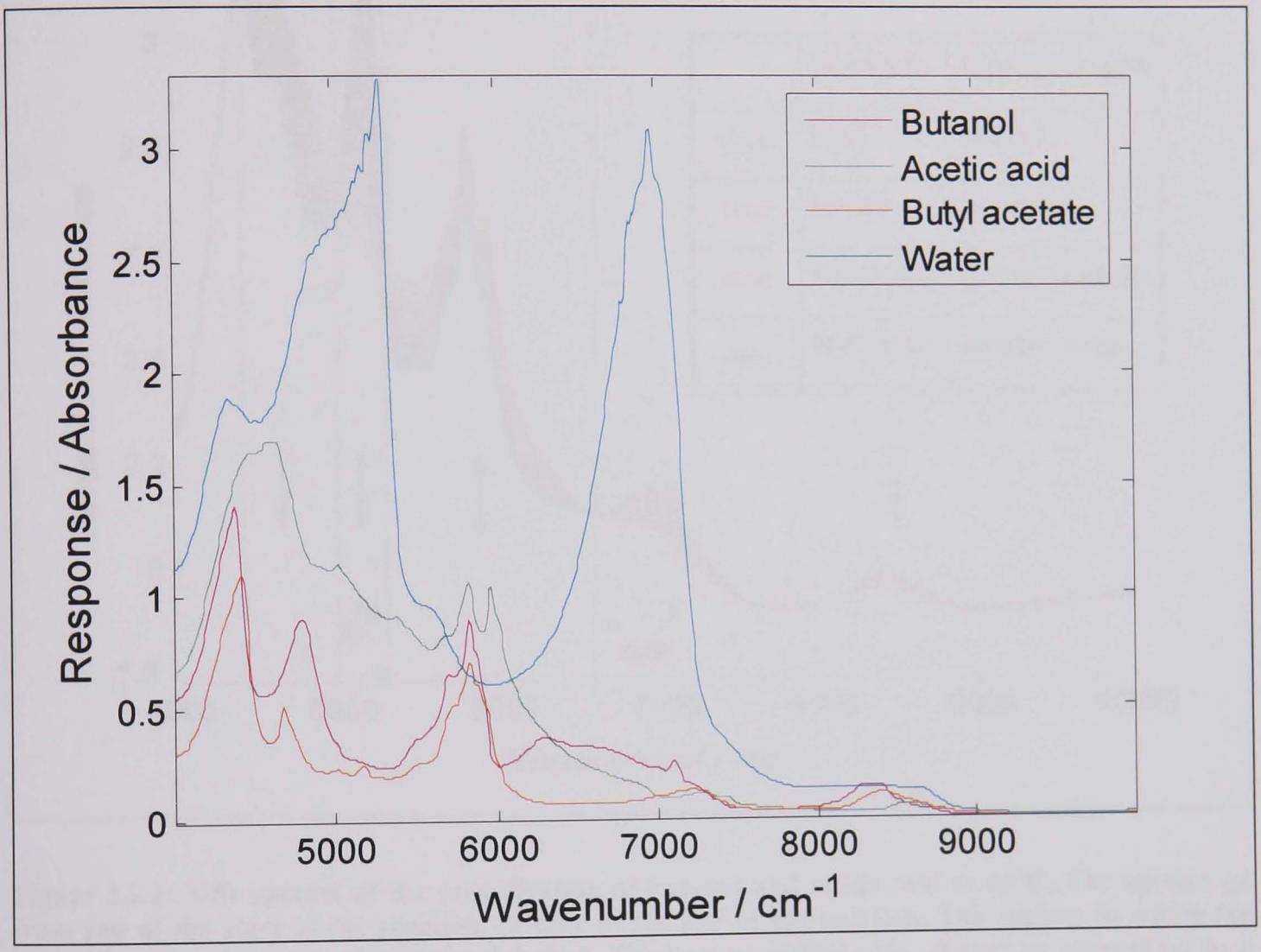

Figure 3.3.1: NIR spectra of the pure components used in the esterification reaction. Butanol and acetic acid are the reactants and butyl acetate and water are the products. The spectra are recorded at 40°C.

The spectra of the pure components show the regions in which those functional groups absorb (Figure 3.3.1). It is clear that the components all have different spectra, so it should be possible to monitor the formation and consumption of these during a reaction. These spectra were all recorded at 40°C, using 450ml of the component held in the GMS chamber, with the NIR transmission probe inserted. From the spectra it can be seen that the water is the strongest absorbing component, with two strong peaks at 5280 and 6972cm^{-1}, so it is expected that the formation of water during the reaction will dominate the spectra. Acetic acid has two distinct peaks at 5808 and 5952cm^{-1}. This first peak also exists in the butanol and butyl acetate spectra, so is not unique. Acetic

acid also has quite a strong absorption at 4620cm^{-1}. Butanol, butyl acetate and water all have a strong absorption at 4344cm^{-1}. Butanol has a unique absorption at 4788, and butyl acetate at 4680cm^{-1}. All components have similar absorption between 8000 to 9000cm^{-1}, so this region will not be useful to distinguish between them.

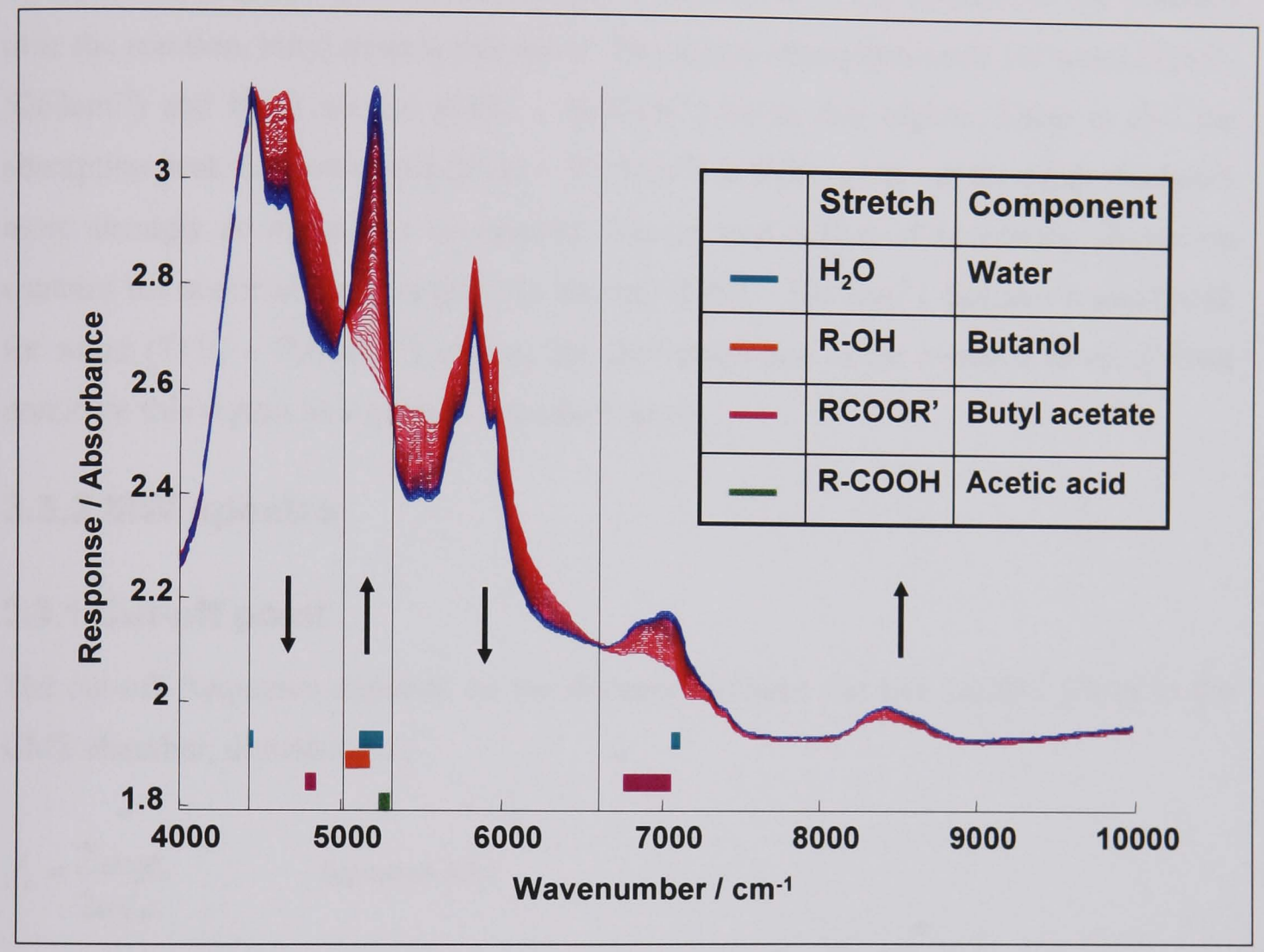

Figure 3.3.2: NIR spectra of the esterification of butanol and acetic acid at 40°C. The spectra go from red at the start of the reaction, to blue at the end of the reaction. The regions in which the major functional groups absorb are labelled. The arrows indicate the change in absorption in a particular region during the reaction.

Typical spectra recorded during a reaction are shown in Figure 3.3.2. The arrows indicate the change in absorption in that region. The coloured blocks relate to the typical absorption regions of the functional groups of components present as stated in Table 3.3.1.

Below 4440cm^{-1} no change in absorption is seen so this area can be ignored. Between 4440 and 5016, and 5316 and 6600cm^{-1}, there is a decrease in absorption. It is expected that these regions correspond to the reactants that are being used during the reaction, butanol and acetic acid. In the first region, there is an absorption band due to butanol (4785 - 4854cm^{-1}) and a very small one due to water (4435 – 4464 cm^{-1}). In the second region, there is no specific absorption band relating to a functional group. The region

may correspond to a general change in composition and is clearly useful for monitoring the change in reaction.

The regions between 5016 to 5316cm^{-1}, and 6600 to 10 000cm^{-1}, show an increase in absorption during the reaction. These can be correlated to the increase in the products over the reaction, butyl acetate and water. The major absorption areas for water (5115 - 5263cm^{-1}) and butyl acetate (5181 – 5025cm^{-1}) lie in this region. There is also the absorption peak for acetic acid (5236 – 5305cm^{-1}) in this region, but the products absorb more strongly so mask this component. The second region of increasing absorption contains the major absorption peak for alcohol (6757 – 7067cm^{-1}), and also a small peak for water (7112 – 7067cm^{-1}). Again, the absorption due to the increase in water must dominate this region as a general increase is seen.

3.3.2 MW spectra

3.3.1 Cut-off point

The cut-off frequency depends on the distance between the two parallel plates in the GMS chamber, dimension *a*:

$$f_c = \frac{v_{vacuum}}{2a\sqrt{\varepsilon'}} \qquad \textbf{Equation 3.3.1}$$

Where f_c = cut-off frequency, a = the distance separating the waveguides parallel surfaces, and $2a$ = cut-off wavelength.

The dielectric constant of a mixture depends upon the components present and the temperature. The dielectric constant for water is 80, giving a cut-off frequency of 360MHz. For most alcohols, ε' is between 20 and 40, giving a cut-off frequency between 715 and 505MHz. Only those wavelengths which are not cut-off should be used in the data analysis, as any below this point will not contain any information about the system, but may contain noise. For reactions at different temperatures, and molar ratios, the cut-off point may change. However, from examination of the spectra, it has been decided the change will be minimal and it is more important to make it uniform for all analysis. Therefore, all frequencies below 504MHz are to be discarded before data analysis. This can be seen in the spectra of the pure components (Figure 3.3.3), in which the spectra below 500MHz seem more noisy.

The spectra of the pure components are shown in Figure 3.3.3. These were recorded at 40°C, with 450ml of pure component in the GMS chamber. It can be seen that all the components give similar spectra above around 1750MHz, but at different intensities. These are quite distinct features at 2000 and 2500MHz present in all spectra. The spectra do not have features that are unique to the functional groups, so these cannot be identified. However, the spectra are all different, and have different levels of response, so as the reaction proceeds, and the composition changes, it is possible to see a change in spectra.

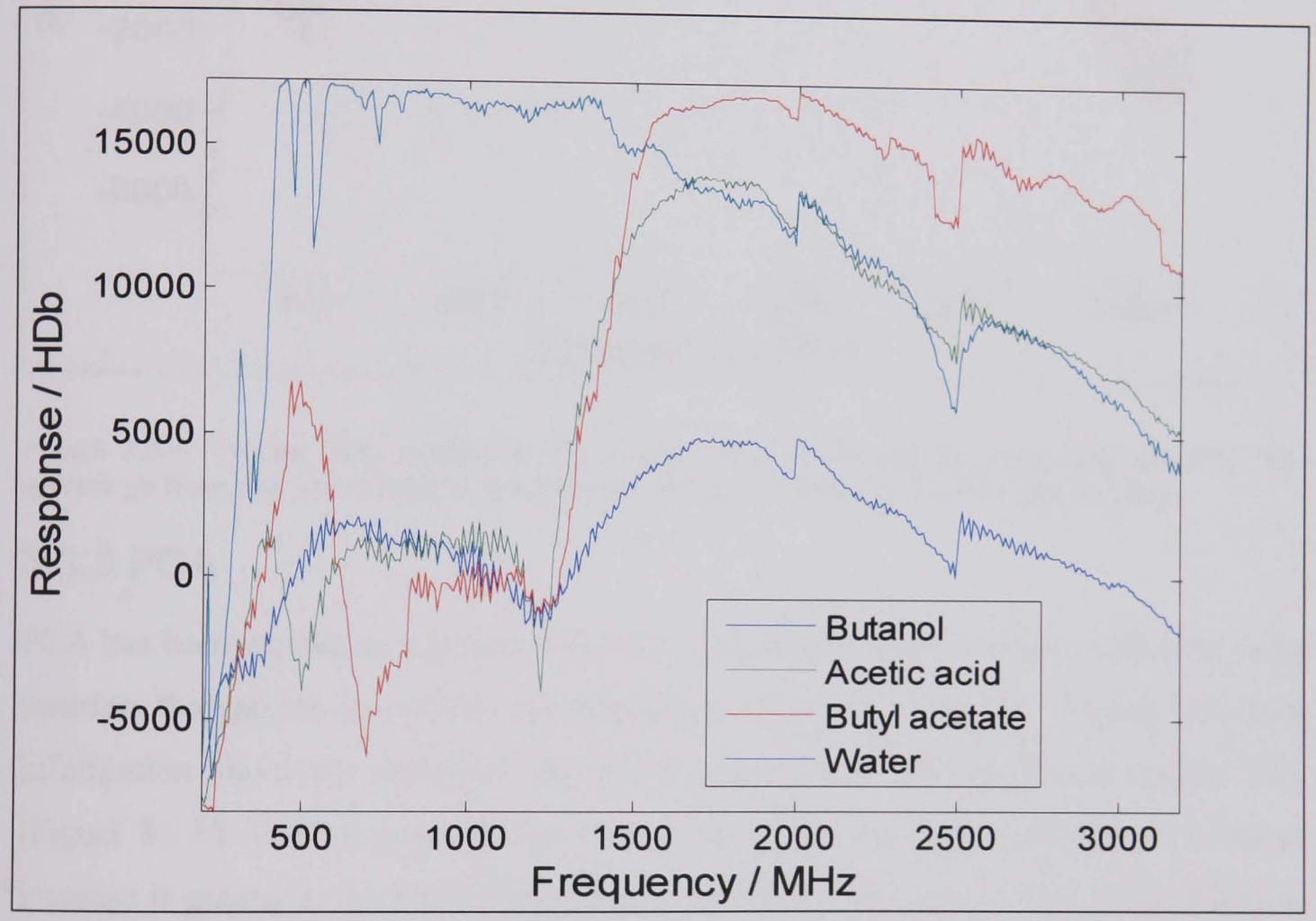

Figure 3.3.3: MW spectra of the pure components in the esterification of butanol by acetic acid. The spectra are recorded at 40°C.

Typical esterification reaction spectra are shown in Figure 3.3.4. The spectra show a general increase in response during the reaction. Over around 2750MHz there is a decrease in response. The spectra change over the whole frequency range. It is not possible to assign a specific region to a functional group. The spectra change due to the change in dielectric constant of the reaction mixture, which changes as the composition changes. MW spectra give much less information regarding the reaction from just examining them. Chemometric techniques are needed to follow the progress of the reaction.

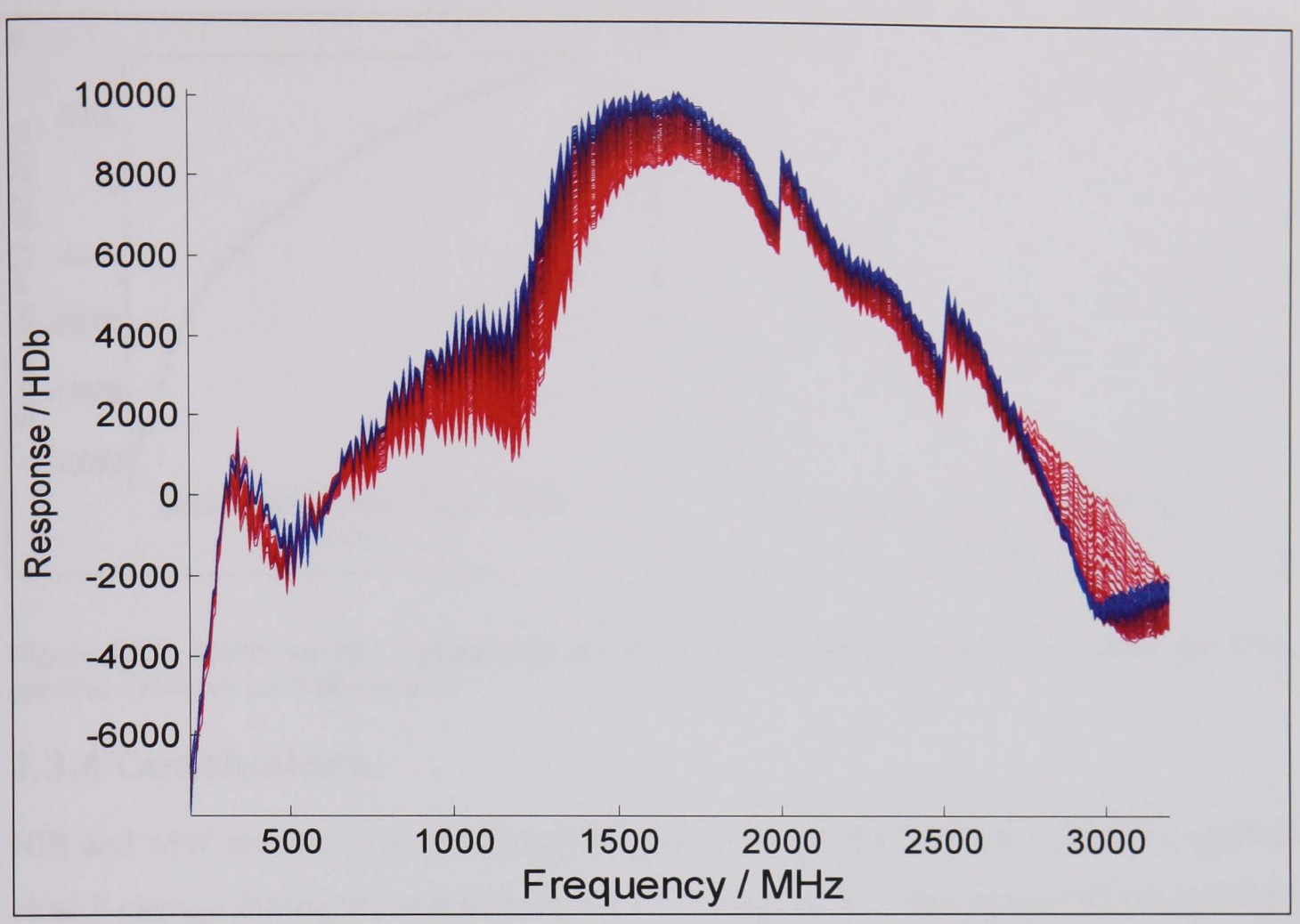

Figure 3.3.4: Typical MW spectra of the esterification of butanol by acetic acid at 40°C. The spectra go from red, at the start of the reaction, through to blue at the end of the reaction.

3.3.3 PCA

PCA has been applied to a typical data set for an esterification reaction, after first mean centring the spectra to remove the magnitude. The scores on PC1 contain the most information about the variation between the samples so this is plotted against time (Figure 3.3.5). There is a general increase in the scores during the reaction. The rate of increase is greater at the start of the reaction and slows down at the end of the reaction. This is a typical reaction profile as the reaction will start fast, and slow down as the end of the reaction is approached. It shows how the samples change relative to one another during the reaction, and give a good indication about the progression of the reaction. It shows that the sample spectra change as the reaction proceeds, so it should be possible to monitor the progress of the reaction using the spectra.

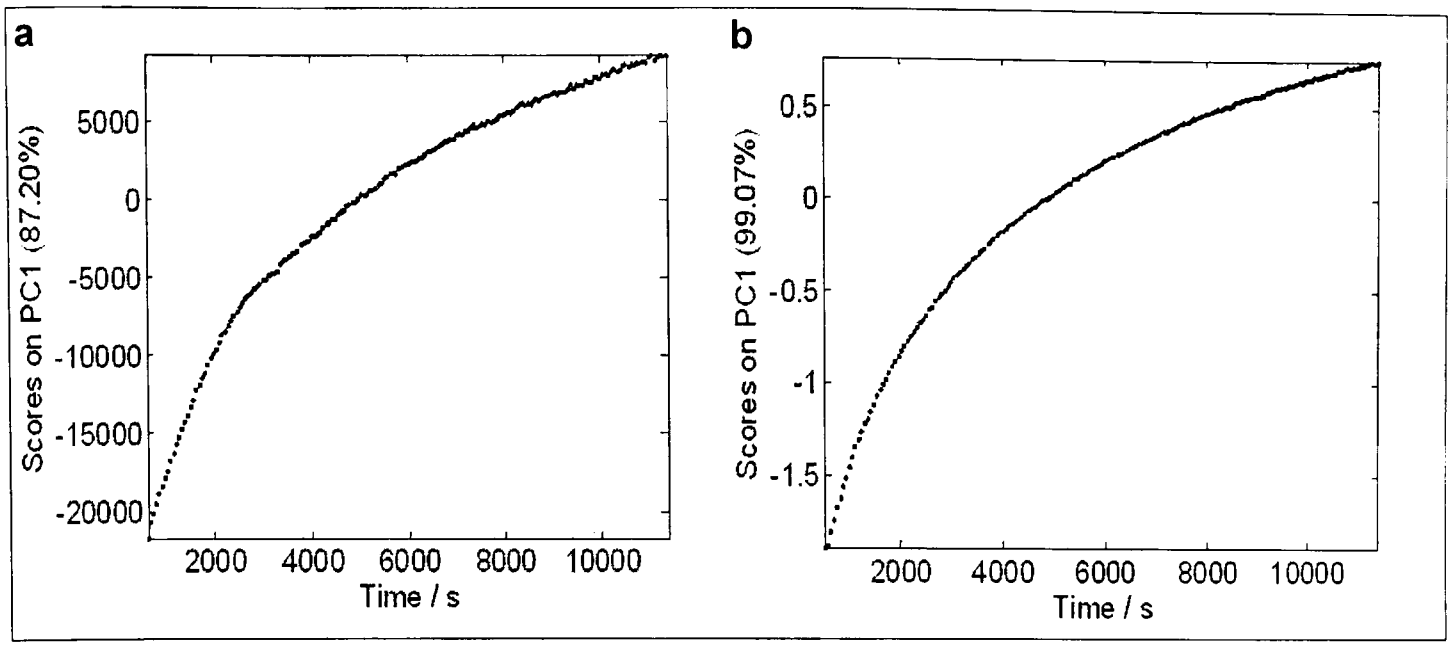

Figure 3.3.5: Scores on PC1 against time for a typical esterification reaction; a) scores for MW spectra; b) scores for NIR spectra.

3.3.4 Conclusions

NIR and MW spectra have been recorded during an esterification reaction. The spectra clearly change during the reaction due to the change in the composition of the reaction mixture.

NIR spectra record the change in absorption due to the components. As the relative amounts of the components change, a change in the recorded spectra is seen.

MW spectra record the change in dielectric constant of the reaction mixture as the reaction proceeds. Each component has a different dielectric constant, and as the concentrations of these change so does the relative dielectric constant of the mixture.

From the resulting spectra, it is clear to see the esterification reaction studied can be monitored by both MW and NIR spectroscopy. With the use of chemometric techniques combined with the spectra, it should be possible to monitor the reaction progress and make predictions of the concentrations of the individual components during the reaction and also the endpoint.

3.4 Monitoring of an esterification reaction

The main problem with monitoring reactions is finding a suitable reference method that is reliable, convenient and reproducible. For many reactions, analytical techniques such as GC and HPLC are used to measure the concentration of the reaction as it proceeds. These methods take time to develop. A sample must be removed from the reaction, which may not be completely representative of the reaction and there is a lag time between the sample being taken and the analytical results.

Spectroscopic techniques offer the advantage of monitoring a reaction without the need to remove a sample. The aim of this work was to use MW and NIR spectroscopy to monitor a simple esterification reaction, and determine if these methods are suitable to monitor the reaction in a reproducible way.

Curve resolution is a set of techniques that can be used with spectral data collected during a reaction. Concentration profiles and pure component spectra can be extracted without any reference method. Therefore it is a convenient way of monitoring reactions without the use of tedious reference methods. Multivariate curve resolution (MCR) has been used on MW and NIR spectral data collected during a simple esterification reaction of butanol and acetic acid.

To validate the curve resolution and ensure the extracted concentration profiles are a good representation of the real concentration profiles, a reference method must be used. In this work GC analysis has been used as it is a proven technique for measuring the concentrations of the components of the esterification reaction. Once MCR has been proved to extract reasonable concentration profiles, the method can be used on further reactions without the need for a reference method.

3.4.1 GC Set-up

3.4.1.1 Method development

A suitable method for GC analysis was initially developed. The components of the esterification reaction are acetic acid, butanol, butyl acetate and water. These components need to be separated during the GC analysis to allow measurement of the amount of each present. Water is not detected by the FID so only three components are to be calibrated for.

The components of the esterification reaction must be separated sufficiently to allow quantification using the peak area obtained from the GC trace. The temperature of the column affects the separation, as the higher the temperature the quicker the components move through the column to the detector. If the components come off the column too close together, the detected peaks may overlap so preventing accurate quantification of the individual components. Analysis time should be minimised by using a temperature that gives sufficient separation, but without too much wasted time between the detected peaks.

At 70°C it was found the components separated well, with a total analysis time of four minutes needed for all components to come off the column and be analysed. However, the chromatogram returned to the baseline for some time between each detected peak so it was felt a higher temperature could be used. 100°C was used and this gave an analysis time of three minutes. This was a good separation so was used for the calibrations.

3.4.1.2 Calibration

A range of suitable samples, covering the range of concentrations of each component expected to be sampled during a reaction, were used for the calibration of the GC (see section 2.3.5, Table 2.3). The samples were made up in methanol as this elutes at a different time from all the other components so does not interfere with the analysis, and is a good solvent for the dissolution of the water present in the samples.

The samples were made up with all four components present during the esterification reaction, along with 4-Methyl-2-pentanone as an internal standard to correct for any deviations in the amount of each sample injected. To do this, the peak area for each component is divided by the peak area of the internal standard to give the corrected peak area. It is this that is used in the calibration graph.

It is possible that some reaction may occur in these calibration samples due to the presence of both the reactants, but this should be a small amount as the esterification reaction requires an acid catalyst. However to minimise any reaction which may occur, the acetic acid was added last to the samples. The samples were used as quickly as possible once made, and stored in the fridge between analyses.

The samples were run in a random order in triplicate, to determine if the samples degrade over time. The analysis was repeated twice using freshly made samples to

determine the reproducibility of the calibration method. The analysis time was set to four minutes to ensure all components were resolved fully.

The corrected peak areas for each component have been plotted against the moles of that component for each sample for each of the replicate runs, to give a calibration graph, Figure 3.4.1. Samples with a peak area that appeared to be greatly different from the norm were removed as outliers. All three components show good correlation between the concentration of the component and the corrected peak areas. The r^2 values show how well the points fit on the line of best fit. All values exceed 0.98 showing a good fit to the linear model.

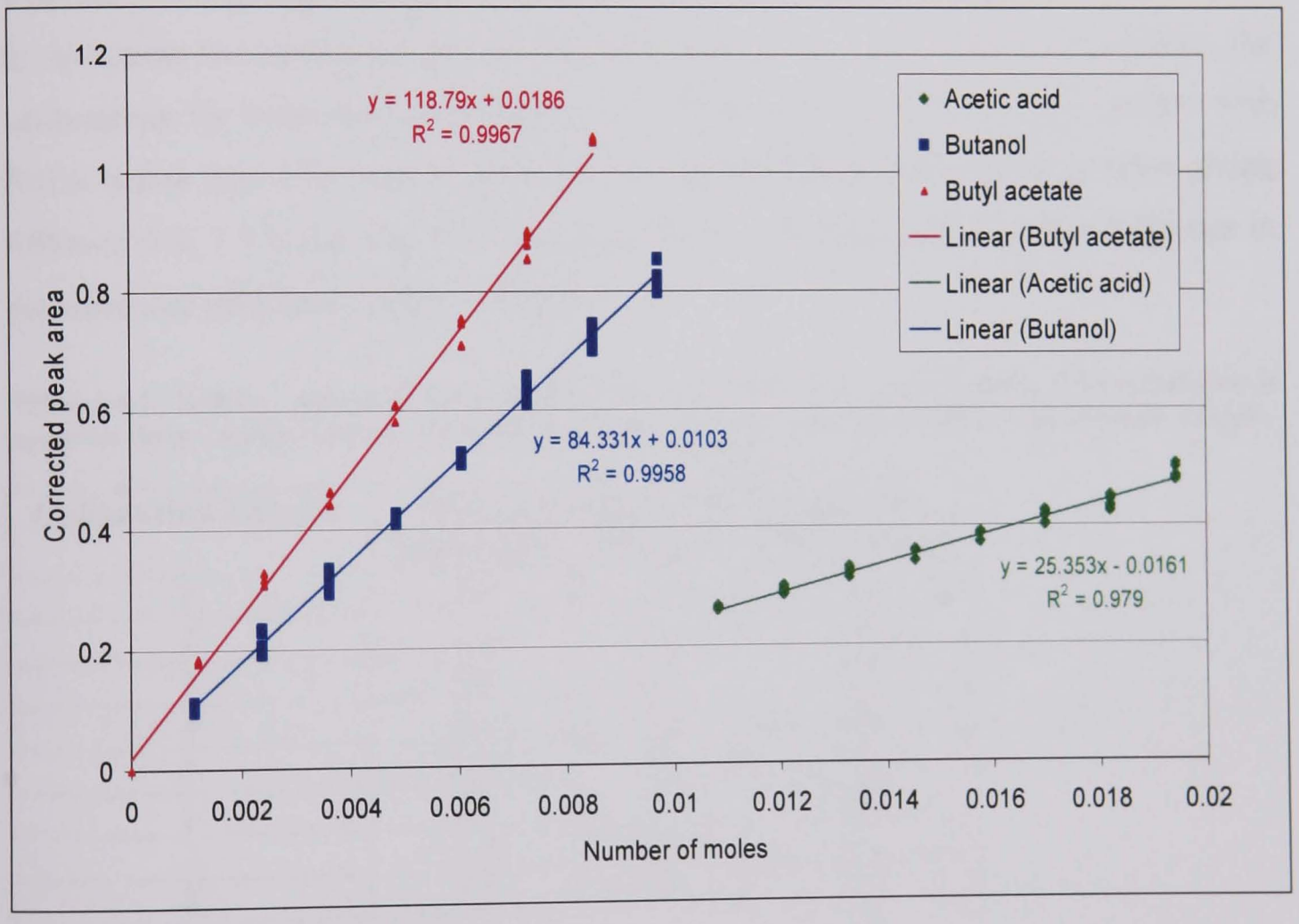

Figure 3.4.1: Calibration graph for the measurement of the concentration of the components of the esterification reaction using GC analysis.

The butanol corrected peak areas have a large variation between them. From closer inspection of the data, the peak area due to the butanol decreases over the repeat analysis of each sample. This suggests the actual amount of butanol in the sample decreases over time. If the butanol is reacting with the acetic acid then a corresponding decrease in the amount of acetic acid, and an increase in butyl acetate would be expected to be seen in the recorded peak area, but this is not the case. It is not known why the measured concentration of butanol decreases in these samples. Including more

repeats in the calibration will increase the robustness as more variation that may be seen in the real samples will be modelled. The effect seen in the calibration is minimal, so the measured concentration of the reaction samples should not be too greatly affected by this. Due to the nature of the reaction samples, the concentrations measured using the GC calibration is expected to be approximate as the samples will continue to react.

There is some difference seen in the replicate peak areas of the samples in the calibrations for the acetic acid and butyl acetate, but this is much less than seen in the butanol calibration. The relative standard deviation (RSD) has been calculated for each calibration sample using all three repeats of all three calibrations, after any outliers have been removed, giving a maximum of nine replicates used in the calculation. This is used to determine the reproducibility of the calibration, Table 3.4.1. From these values, the calibrations for both acetic acid and butyl acetate are shown to be reproducible with RSDs below 3%. The butanol shows lower reproducibility with three samples giving RSDs of 5.0, 7.9 and 6.1%. This was seen in the calibration graph by the difference in the corrected peak areas of the samples.

Table 3.4.1: Relative standard deviations (%) for each GC calibration sample. The calculation is based on three repeat calibrations, each of which comprises of three replicate runs for each sample.

Calibration Sample	Relative standard deviation / %		
	Acetic acid	Butanol	Butyl acetate
1	2.4	2.6	-
2	2.5	2.2	1.9
3	2.4	2.8	2.7
4	2.2	1.6	2.6
5	2.7	1.6	2.6
6	2.1	5.0	2.8
7	1.9	7.9	2.1
8	1.2	6.1	0.4

The average RSD for each component show the overall reproducibility of the calibrations. The acetic acid and butyl acetate are good reproducible calibrations with an average RSD of 2.2% for both. The butanol is also a good calibration with an average RSD of 3.7%.

These calibrations for butanol, acetic acid and butyl acetate have been used to measure the concentrations of reaction samples, allowing the reaction progress to be monitored.

3.4.1.3 Reaction monitoring

A series of esterification reactions have been followed by GC, NIR and MW spectroscopy. Samples were removed at 10 minute intervals and analysed by GC to measure the concentration of the reaction mixture at that time point. The reaction samples were put on ice immediately to lower the temperature as quickly as possible in an attempt to stop any further reaction taking place.

The esterification reactions followed by GC were carried out with a starting molar ratio of 1:2 butanol (200ml) to acetic acid (250ml). This gives initial starting concentrations of 4.9M butanol and 9.7M acetic acid. The reaction was carried out at 40°C numerous times to check reproducibility of using GC to monitor the reaction progress. It was found to be very difficult to get reproducible measurements. The reaction was monitored seven times, and only two of the repeats were found to give reproducible GC analysis.

Figure 3.4.2 shows three typical reactions. The first and second repeats are very reproducible, whereas the third one is quite different. This shows the difficulties that arose from using GC as a reference method. The inconsistencies may be due to problems with sampling, as the sample taken may not be representative of the reaction mixture, so reproducibility could be a problem. Also, some further reaction may have occurred in the removed sample. It is expected this would lead to a lower acetic acid and butanol concentration being determined, and a higher level of butyl acetate. In the third repeat, the butanol and acetic acid content has been measured lower, but the butyl acetate level appears to be similar.

The first and second reactions were carried out after several previous attempts to try to get a reproducible GC monitoring method. It appears that by this point the technique of removing samples from the reaction and analysing them by GC had been well practised. This led to much more reproducible results. The determined starting concentration of the acetic acid in both these reactions was around 10M, which corresponds fairly well to the known starting concentration of 9.7M. The starting concentration of butanol in both reactions was determined to be around 4.5M, which again corresponds reasonably well to the known starting concentration of 4.9M. From this it can be seen that the butanol concentration is measured at a slightly lower value and the acetic acid concentration

slightly higher than the actual values. This suggests no further reaction occurs in the sample, as a lower value of both reactants would be expected.

In the third repeat the initial starting concentrations were determined to be lower at around 7M acetic acid and 4M butanol. This is much lower than expected and shows the problems faced with the GC method used for the measurement of the reaction mixture composition.

There are errors in the initial determined values in the first two repeats when compared to the known initial concentrations, and this must be due to the calibration of the GC. The determined concentrations are acceptable as they are within the error of the calibration.

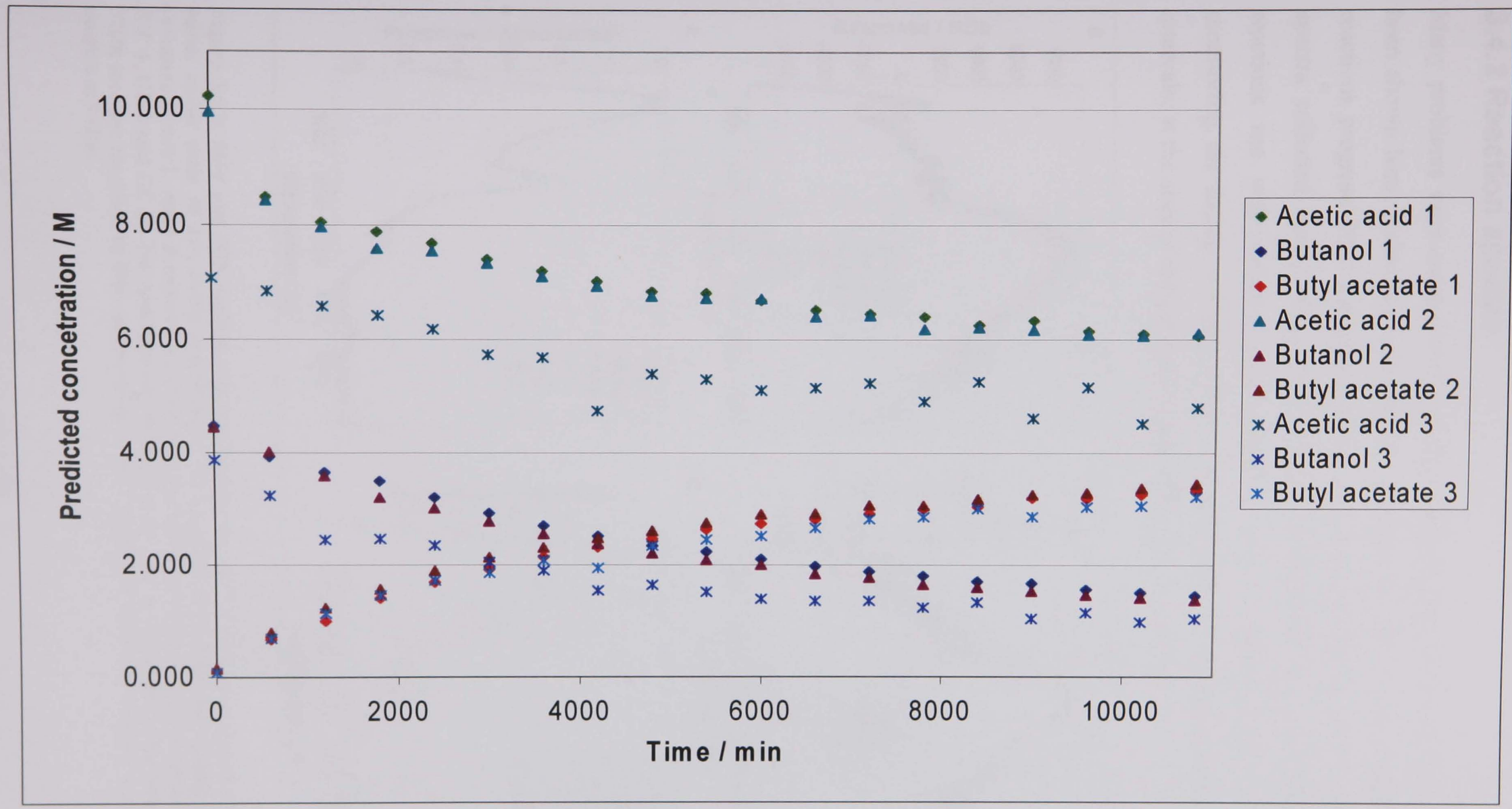

Figure 3.4.2: GC prediction of the reaction mixture concentration over time of esterification reactions carried out at 40°C with an initial starting molar ratio of 1:2, butanol (200ml) to acetic acid (250ml). The reaction was replicated three times.

3.4.2 Reaction spectra

Many problems were encountered with the reproducibility of the GC method, as has been shown here. Reference methods are often relied upon to allow monitoring of a reactions progress. MW and NIR spectra were recorded during these reactions. The spectra collected during these three repeat GC reactions, and also three replicate reactions run with identical experimental reaction conditions, but with no GC monitoring, are shown in Figure 3.4.3. The spectra shown were recorded at two time intervals; at the start of the reaction, t_0, and 9720s into the reaction.

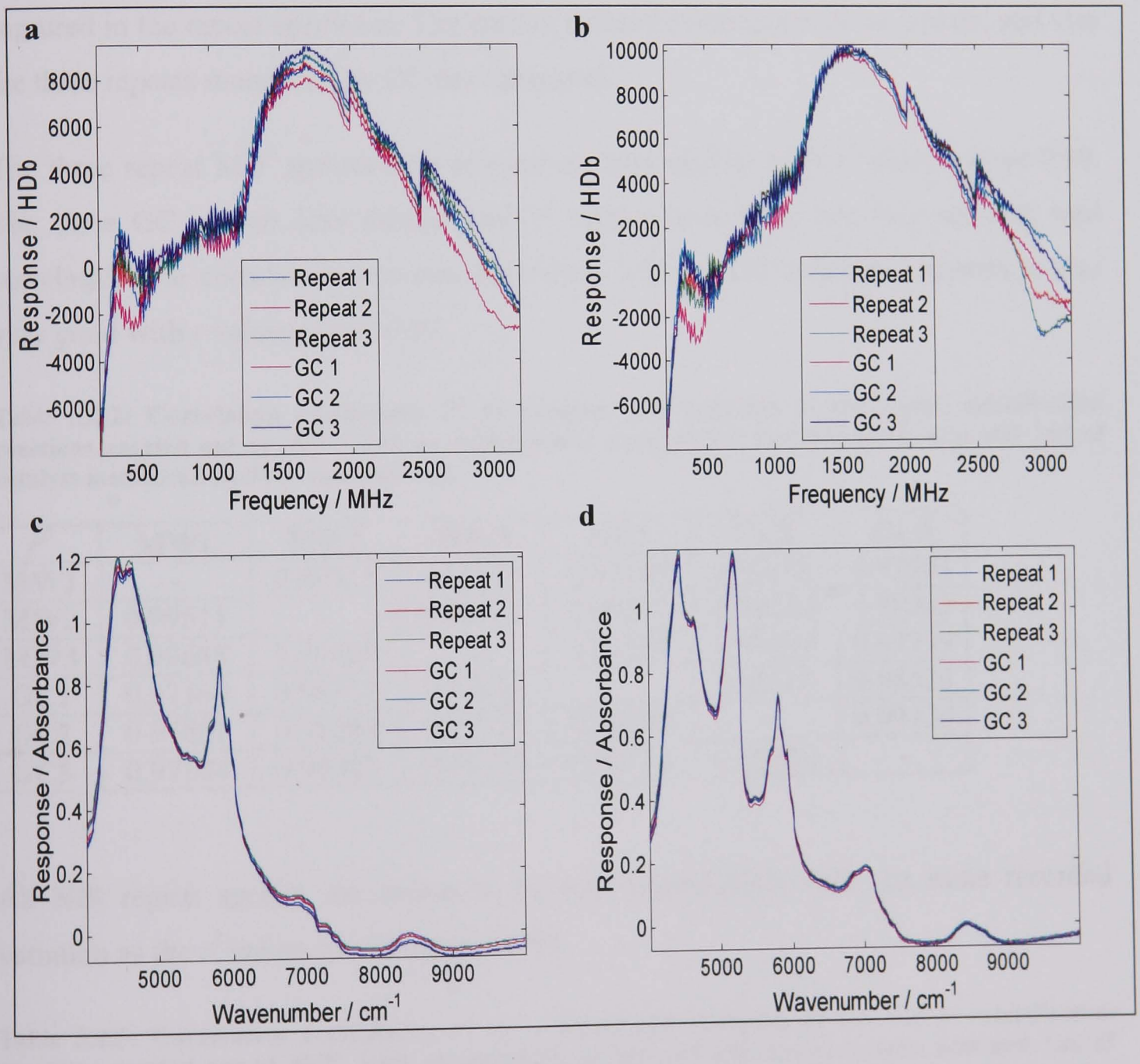

Figure 3.4.3: MW and NIR spectra collected during an esterification reaction at 40°C, with an initial molar ratio of 2:1, acetic acid:butanol. The spectra were collected during three repeat reactions (react 1, react 2 and react 3) and also during three repeat reactions monitored by GC (GC 1, GC 2 and GC 3). The spectra were recorded at two times, at the start of the reaction; t_0, and 9720s into the reaction; a) MW spectra at t_0; b) MW spectra at 9720s; c) NIR spectra at t_0; d) NIR spectra at 9720s.

These spectra show the reproducibility of the collected spectra. The NIR spectra (Figure 3.4.3c and d) are very similar for all reactions at both time intervals. There is some drift seen in the baseline, but this can be corrected for. The MW spectra (Figure 3.4.3a and b) are not as reproducible as the spectra appear to be slightly different. However, the spectra are very similar between 1250 and 2250 MHz.

The correlation coefficients, r^2, have been calculated for the repeat MW spectra (Table 3.4.2) and the repeat NIR spectra (Table 3.4.3). These are calculated by comparing the response of each spectrum in the data sets. This shows how reproducible the variation captured in the repeat spectra is. The spectra collected during the three repeats, and also the three repeats monitored by GC are compared.

The three repeat MW spectra data sets are all very similar with r^2 values above 0.99. The three GC repeats less similar with r^2 values over 0.97, but they are still well correlated. The correlation between the repeats and the GC monitored repeats is also very good with r values above 0.97.

Table 3.4.2: Correlation coefficients, r^2, to compare the variation of the repeat esterification reactions carried out at 40°C, with an initial molar ratio of 2:1, butanol:acetic acid and 1ml of catalyst monitored by MW spectroscopy.

r^2	MW1	MW2	MW3	GC1	GC2	GC3
MW1	-	0.99511	0.99688	0.97169	0.97601	0.97804
MW2	0.99511	-	0.99603	0.98312	0.98284	0.98303
MW3	0.99688	0.99603	-	0.97699	0.97374	0.97799
GC1	0.97169	0.98312	0.97699	-	0.98500	0.98520
GC2	0.97601	0.98284	0.97374	0.98500	-	0.99130
GC3	0.97804	0.98303	0.97799	0.98520	0.99130	-

All NIR repeat spectra are shown to be very reproducible with the same recorded variation as the r^2 values are all above 0.999.

Table 3.4.3: Correlation coefficients, r^2, to compare the variation of the repeat esterification reactions carried out at 40°C, with an initial molar ratio of 2:1, butanol:acetic acid and 1ml of catalyst monitored by NIR spectroscopy.

r^2	NIR1	NIR2	NIR3	GC1	GC2	GC3
NIR1	-	0.99991	0.99963	0.99925	0.99960	0.99988
NIR2	0.99991	-	0.99971	0.99921	0.99972	0.99980
NIR3	0.99963	0.99971	-	0.99970	0.99994	0.99959
GC1	0.99925	0.99921	0.99970	-	0.99960	0.99931
GC2	0.99960	0.99972	0.99994	0.99960	-	0.99953
GC3	0.99988	0.99980	0.99959	0.99931	0.99953	-

The GC results show the three GC repeat reactions are not reproducible as different reaction profiles were produced. The r^2 values show that the reactions are in fact reproducible, as the recorded spectra show the same variation for each of the repeats shown by the high correlation calculated above 0.999. This is a much more reproducible and reliable method of monitoring the reaction than the GC method has proved to be. Spectra can be used with chemometric methods to allowing monitoring of the reactions.

3.4.3 Prediction of k value

3.4.3.1 GC prediction

From the determined reaction profiles, the rate constant, k value, can be calculated. The esterification reaction studied is a second order reaction. The integrated rate equation is:

$$\frac{1}{[B]_0 - [A]_o} \ln\left(\frac{[A]_0[B]_t}{[B]_0[A]_t}\right) = kt \qquad \textbf{Equation 3.4.1}$$

Where A_0 and B_0 are the initial concentrations of butanol and acetic acid respectively, A_t and B_t the respective concentrations at time t, and k is the rate constant. Therefore, a plot of the left hand side of the equation against time should give a straight line with a slope equal to k.

The kinetic plot for the three repeats as previously discussed is shown in Figure 3.4.4. The three repeats give different kinetic plots. Runs 1 and 2 are the most similar. These kinetic plots should be a straight line if the reaction is truly second order. A straight line is fitted to the plots and the k value determined as the gradient of this straight line. The plots are not quite linear, so fitting a line will not give the true k value. Run 3 is the most non-linear. However, all three give similar gradients of 1.132×10^{-5}, 1.235×10^{-5} and 1.323×10^{-5} for runs 1, 2 and 3 respectively.

To overcome the non-linearity, a portion of the kinetic plot that is linear can be used to determine the k value. The first two more reproducible runs have been examined. The points below 3000s are discarded as these are furthest from the line of best fit. This can be seen in the kinetic plot, Figure 3.4.5. The k values determined by the slope are very similar as seen with the kinetic plot using the whole data set, 1.103×10^{-5} for run 1 and 1.142×10^{-5} for run 2, and are now more reproducible.

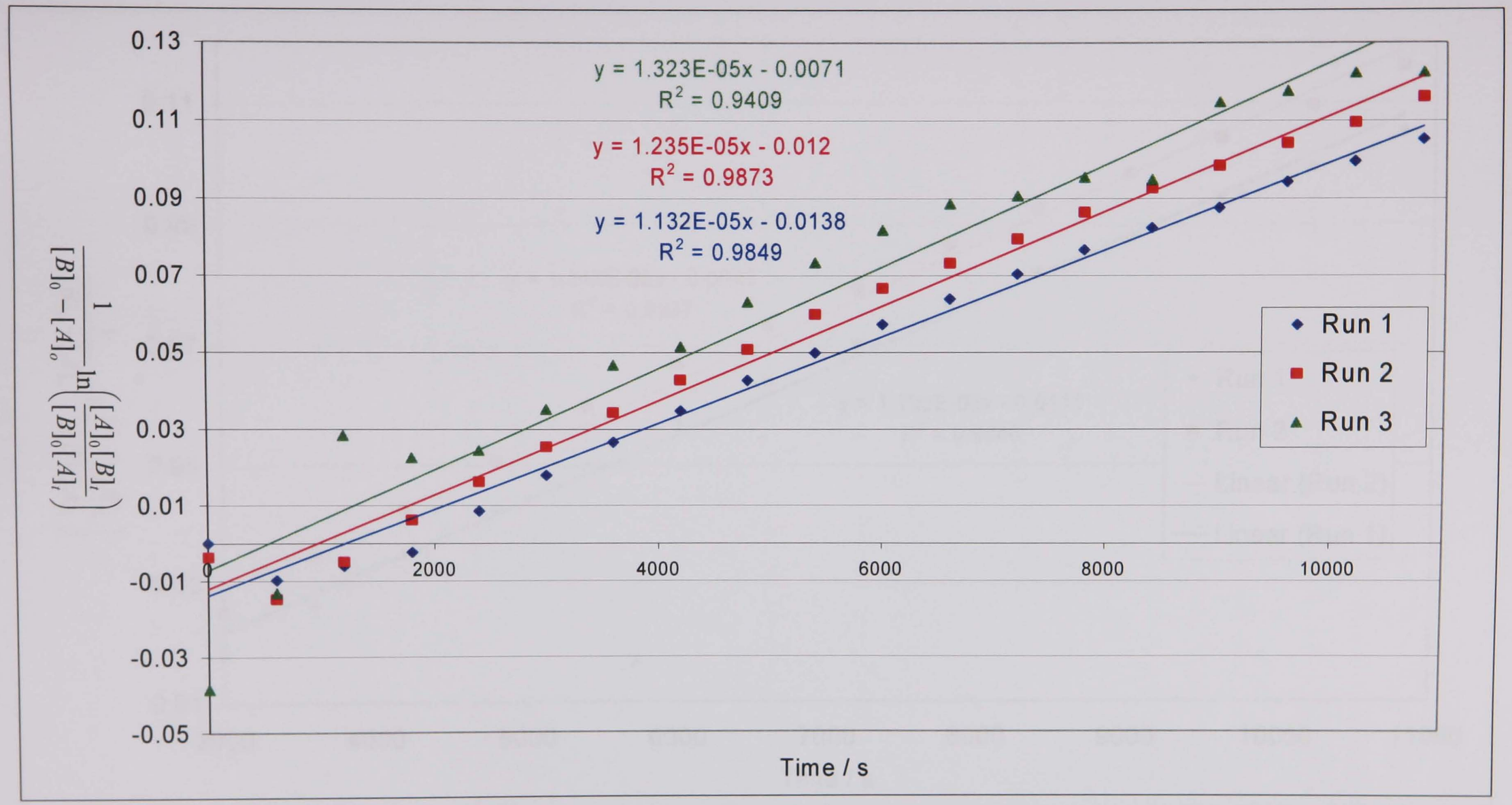

Figure 3.4.4: Kinetic plot of three repeat esterification reactions performed at 40°C, with an initial 2:1 acetic acid: butanol molar ratio, showing the relationship between the integrated form of a second-order reaction against time.

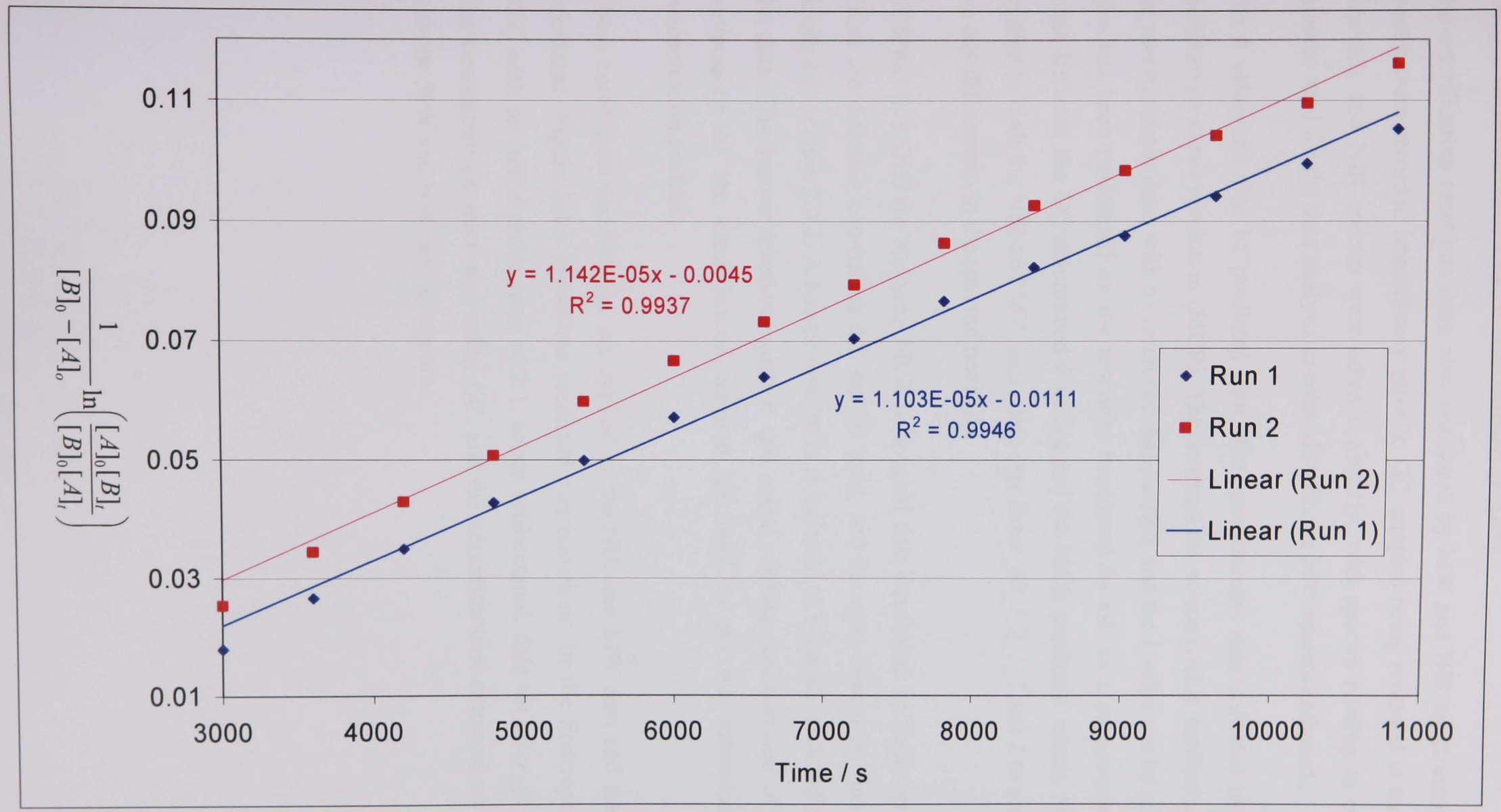

Figure 3.4.5: Kinetic plot of two repeat esterification reactions performed at 40°C, with an initial 2:1 acetic acid: butanol molar ratio, showing the relationship between the integrated form of a second-order reaction against a smaller time range.

3.4.3.2 Multivariate curve resolution (MCR)

The esterification reactions were also monitored by MW and NIR spectroscopy. MW spectra were recorded immediately prior to GC samples being removed at ten minute intervals, and NIR spectra were taken constantly, with spectra relating to every ten minutes used for the data analysis to coincide with the MW spectra collected.

The *k* value can also be predicted using the spectroscopic data collected along with multivariate curve resolution (MCR). This extracts the concentration profiles using just the spectroscopic data, with no reference data needed, and the *k* value can be calculated. This has been performed on the reactions monitored by GC so a comparison can be made between the GC determined *k* values and the MCR predicted values. MCR was applied to both the NIR and MW data, data sets *Ester_40_1:2_1_1* and *2* to see if there are any differences in the spectral methods.

GUIPRO is a GUI for applying MCR to spectral data developed by Paul Gemperline. There are different constraints that can be used, and the ones chosen for this data are detailed in section 2.4.2. A kinetic constraint is included to break the rank deficiency of the data. The known reaction equation and initial starting concentration of the four components of the esterification reaction are used to aid the extraction of the concentration profiles.

These constraints and settings are applied to the NIR and MW data and the *k* value calculated. Figure 3.4.6 shows the predicted concentrations for the first repeat run at 40°C with an initial molar ratio of 2:1, acetic acid:butanol, data set *ester_gc_40_1_1*. The concentrations measured using GC, and the concentrations extracted using MCR with the MW and NIR data are shown.

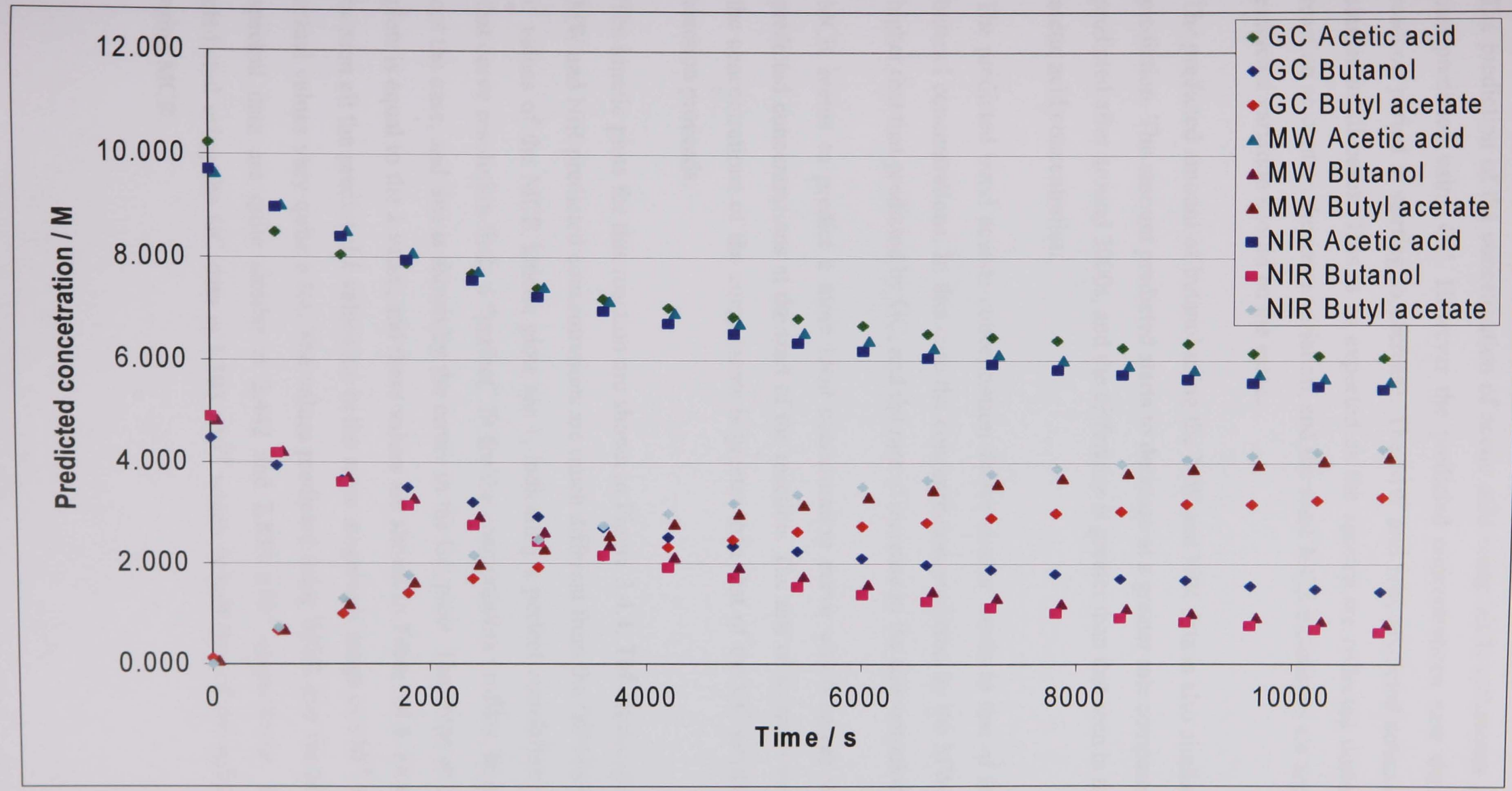

Figure 3.4.6: Predicted concentrations over time of the components of the esterification reaction of butanol and acetic acid, using GC measurements made every ten minutes and also the extraction of the concentration profiles using collected MW and NIR spectra, collected every ten minutes, along with MCR techniques. The reaction is carried out at 40°C with a 2:1, acetic acid:butanol starting molar ratio.

The prediction of the concentration of acetic acid using MCR techniques is similar to that predicted using GC. However the predicted concentrations near the end of the reaction period is starting to decrease. The MW and NIR predicted concentrations are similar in all cases. This is as expected as the spectra are collected during the same reaction so contain the same variation, and the same MCR techniques are applied, so the extracted variation should be the same.

The predicted amount of butanol using the MW and NIR data is also similar to the GC prediction. The amount predicted starts to decrease at a greater rate compared to the GC predicted after around 3000s, and the difference is greater than that seen in the predicted acetic acid concentration.

The predicted butyl acetate concentration shows similar trends to that of the predicted butanol concentrations. In this case the concentration predicted by the MW and NIR is higher that that predicted by GC, and the rate of increase in the concentration is greater.

MCR seems to predict a more ideal concentration curve which agrees with the GC predicted concentrations at the start of the reaction. The rate of increase or decrease of the concentrations of the components is greater than that of the GC predictions as the reaction proceeds.

The kinetic plots for this reaction are shown in Figure 3.4.4. The kinetic profiles of the MW and NIR predicted concentrations are much different from the GC kinetic plot. The r^2 values of the MCR kinetic plots are 1, indicating a perfect correlation. This shows that curve resolution finds a "perfect" fit for the concentration profiles. In reality this is not the case, and this is shown by the errors in the GC plots. The slope of these kinetic plots is equal to the *k* value, and these values are shown in Table 3.4.4. From this it can be seen all the predicted *k* values are in the same magnitude range of $x10^{-5}$, however the actual values vary quite a lot. The values predicted using MCR and the MW and NIR spectral data are quite similar at 2.442 and 2.833 $x10^{-5}$ respectively. The *k* value predicted using the GC data is 1.103 $x10^{-5}$ which is half that of the values predicted using MCR.

Table 3.4.4: Predicted *k* values using GC, and MW and NIR spectra along with MCR, for the esterification reaction of butanol and acetic acid at 40°C with an initial starting molar ratio of 2:1, acetic acid: butanol.

Data	Temp. / °C	Molar ratio	Predicted K value / $x10^{-5}$		
			GC	NIR	MW
Ester_gc_40_1_1	40	2:1	1.103	2.833	2.442

The differences seen in the predicted *k* values may be due to the different sampling methods. The main problem with the GC analysis is a small sample (~1ml) is removed from the total reaction volume (450ml). The reaction mixture is stirred to attempt to give a homogeneous mixture, but in reality the mixture may not be homogeneous so the sample removed for GC analysis may not be truly representative of the reaction. The "picture" of the reaction the GC samples capture may be different from that which the MW and NIR capture, so leading to a different *k* value being determined.

The MCR solution is not unique, and is an approximation of the component concentration profiles. This again may lead to incorrect *k* values. It is difficult to determine which answer is the correct one, if any of them really are.

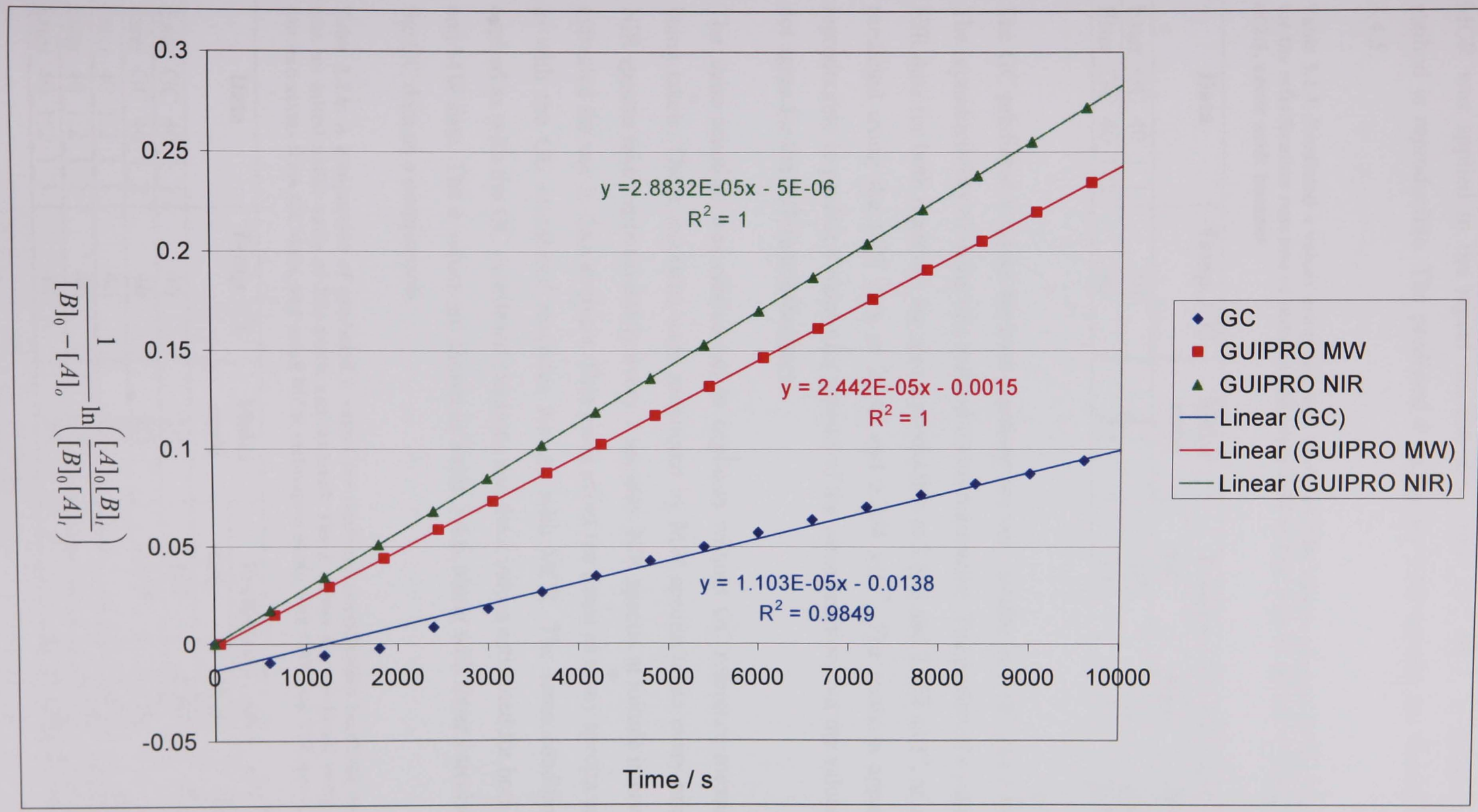

Figure 3.4.7: Kinetic plot of an esterification reaction performed at 40°C, with an initial 2:1 acetic acid: butanol molar ratio, showing the relationship between the integrated form of a second-order reaction against time as predicted by GC, and NIR and MW spectra recorded during the reaction used with MCR.

MCR was applied to the repeat reaction data, *ester_GC_40_2*, to determine if the method is reproducible. The predicted *k* values for both repeats are shown in Table 3.4.5.

Table 3.4.5: Predicted *k* values using GC, and MW and NIR spectra along with MCR techniques, for the esterification reaction of butanol and acetic acid at 40°C with an initial starting molar ratio of 2:1, acetic acid: butanol.

Data	Temp. / °C	Molar ratio	Predicted K value / $x10^{-5}$		
			GC	NIR	MW
Ester_GC_40_1_1	40	2:1	1.103	2.833	2.442
Ester_GC_40_1_2	40	2:1	1.142	2.752	2.204

The GC predicted *k* values for both reactions are very similar at 1.102 and 1.142 $x10^{-5}$. The reproducibility of using this method seems reasonable. The predicted *k* values using NIR data for both reactions are also reproducible at 2.833 and 2.752 $x10^{-5}$, as are those predicted using the MW data at 2.442 and 2.204 $x10^{-5}$. The methods appear to be reproducible to predict *k* values for repeats of the same reaction, but the values still do not agree for the different techniques.

The same reaction was carried out in triplicate without GC reference measurements being taken. These reactions were monitored by MW spectra taken every minute and NIR spectra taken approximately every 7 seconds. NIR spectra at minute intervals were extracted for use in data analysis. This gives about ten times as many spectra compared to with the GC monitored reactions for use with MCR. The same conditions were applied as with the GC monitored reactions and the *k* values estimated for both the NIR and MW data. The *k* values are shown in Table 3.4.6, along with those calculated from the GC data as a comparison.

Table 3.4.6: A comparison of predicted *k* values for replicate esterification reactions run at 40°C with an initial molar ratio of 2:1, acetic acid:butanol. The *k* values are predicted using predicted concentrations from GC data, and using MCR techniques along with MW and NIR spectral data.

Data	Temp. / °C	Molar ratio	Predicted *k* value / $x10^{-5}$		
			GC	NIR	MW
Ester_GC_40_1_1	40	2:1	1.103	2.833	2.442
Ester_GC_40_1_2	40	2:1	1.142	2.752	2.204
Ester_40_1:2_1_1	40	2:1	-	3.089	2.809
Ester_40_1:2_1_2	40	2:1	-	3.219	1.981
Ester_40_1:2_1_3	40	2:1	-	3.038	2.316

All *k* values predicted are in the same magnitude range of $x10^{-5}$. The three reactions monitored by MW and NIR only, give reproducible predicted *k* values from the collected NIR data of 3.089, 3.219 and 3.038 $x10^{-5}$. These are similar to the *k* values predicted using the NIR data for the two GC monitored reaction of 2.833 and 2.752 $x10^{-5}$.

The *k* values predicted using the MW data for the three reactions monitored by NIR and MW only vary quite a lot at 2.809, 1.981 and 2.316 $x10^{-5}$. These values are very different from those extracted from the NIR data. It appears that the method is not reproducible for the prediction of the *k* value from the predicted concentration profiles.

The MW and NIR data give different results so suggests the variation captured by each spectral method must vary. This could be due to the different methods, as the MW analyses the whole reaction volume so captures the true reaction progress, whereas the NIR spectra are collected using a probe so only a small volume of the total reaction volume is actually analysed. If the reaction in this region isn't representative of the whole batch, then different variation may be captured.

There are not any published literature values for the *k* value for the same reaction performed with identical reaction conditions. Blanco and Serrano [83] monitored the same reaction by NIR and GC analysis to predict the rate constant. The reactions were run with the same experimental conditions, at 40°C, with a 2:1 molar ratio, acetic acid:butanol. The integrated form of a second-order reaction was plotted in the same way as in this work, against time. The resulting plot did not give a straight line as is expected with a true second order reaction; therefore the *k* value was calculated based on the first ten points of the reaction. This results in an estimate of the *k* value at the start of the reaction. The *k* value was found to be 0.058. This is of a completely different magnitude from the values calculated in this work, but can be explained by the fact that the published *k* values are for the start of the reaction, and for this work they have been calculated for the entire reaction.

3.4.4 Conclusions

It is difficult to find a reference measurement that is suitable and reproducible to monitor a reaction. GC had been used to measure the concentration of the components of the esterification reaction studied. This has found to be a hard method to develop and

problems were found in the reproducibility of the method to monitor a reaction. There is a high error in this method.

The rate constants were determined using GC monitoring and also using MCR which extracts concentration profiles for the components without the need for reference data. The k values determined do not agree, and it is not known which of the calculated values is the true one for the reaction studied. There does not appear to be published rate constants for this reaction using exactly the same conditions.

The rate constant calculated is for a reaction assumed to be far from the equilibrium. In reality, the reaction studied seems to be reaching equilibrium at the end of the period it is monitored for, therefore this may be one of the reasons the k values calculated do not agree with each other.

The collected NIR spectra are affected by the change in hydrogen bonding during the reaction. This causes a change in the wavenumber at which a specific functional group absorbs, and may well affect the ability of MCR to extract the concentration profiles.

The values extracted using MCR from MW and NIR spectra collected for repeats of the reactions show reproducibility and some agreement between the two techniques. This suggests the reaction can be monitored by these techniques in a reproducible way. The calculated coefficients show that reproducible MW and NIR spectra can be collected for repeat reactions. The system has been proved to work and is reproducible. The spectra can be used with other chemometric techniques to determine other aspects of the reaction monitoring, such as endpoint determination and process upset detection.

3.5 Endpoint determination of an esterification reaction

The endpoint of a reaction is subjective. It can be defined as the point at which the reaction reaches equilibrium, or as it is reaching equilibrium when the formation of product is at such a slow rate that the reaction is costing more to maintain, than the value of the product being formed. The endpoint must first be defined before it can be determined for a process. For this work, an adaptive algorithm called caterpillar is demonstrated for its use in endpoint determination, and it is shown the parameters used in the algorithm can be altered to give a different determined endpoint according to needs.

3.5.1 Experimental set-up

All reactions were carried out within the GMS remote stainless steel cavity with a NIR transmission probe inserted into the chamber, as described in the experimental section (chapter 2), to allow MW and NIR spectra to be collected simultaneously. Spectra were collected at one minute intervals.

The reaction studied is the esterification of butan-1-ol and acetic acid which is catalysed by sulphuric acid. The reactions were carried out at different temperatures, with different molar ratios to give different endpoints for the reaction. Repeats of each reaction are carried out to examine the repeatability of the endpoint determination.

3.5.2 Results and discussion

All standard characterisation reactions can be used for endpoint determination. Repeats of the same reaction should have endpoints at the same time. Using different temperatures, molar ratios and amounts of catalyst will alter the rate of the reaction, and hence the endpoint.

Caterpillar is an adaptive algorithm which can be used to predict the endpoint of a reaction, by comparing the now variation to recent variation.

In caterpillar, two windows with a set window width size (WS) are placed in the data (see section 1.4.4) with an inter-window-distance (inter-WS) between them. A PCA model is calculated for the second, reference window, to describe the "now" variation of the samples in this window. This is compared to the old variation in the samples in the detection window. The windows are moved through the data stepwise, with the

model building repeated at each step, until a steady state in the variation is seen and this determined as the endpoint of the reaction. The windows are separated by an inter-window distance to ensure that a constant variation is due to the actual end-point of the reaction.

The variables within the algorithm, WS, inter-WS, stepsize, and number of PCs to use in the model must be defined. Once these are determined for a reaction with specific conditions, the same variables can be used for subsequent reactions with the same conditions.

3.5.2.1 Esterification reaction at 40°C, 1:2 initial molar ratio, 1ml catalyst

The mesh plots of the resulting spectra for these reactions are shown in Figure 3.5.1. Mesh plots show the spectra, plotted as response versus frequency or wavenumber, over time. This allows visualisation of the change in the spectra over time, to show the reaction profile. As can be seen, the spectra for each reaction are very similar as the reaction conditions were the same. The MW spectra for the second reaction (Figure 3.5.1c) has some differences from the others, particularly in the region below 1500MHZ, where there appears to be a greater response seen compared to the other two reactions. This spectra also appears to have a greater and more obvious increase in response over the time of the reaction. The NIR spectra are very similar, and there are no obvious differences between the spectra. This suggests all three NIR data sets should give the same determined endpoint.

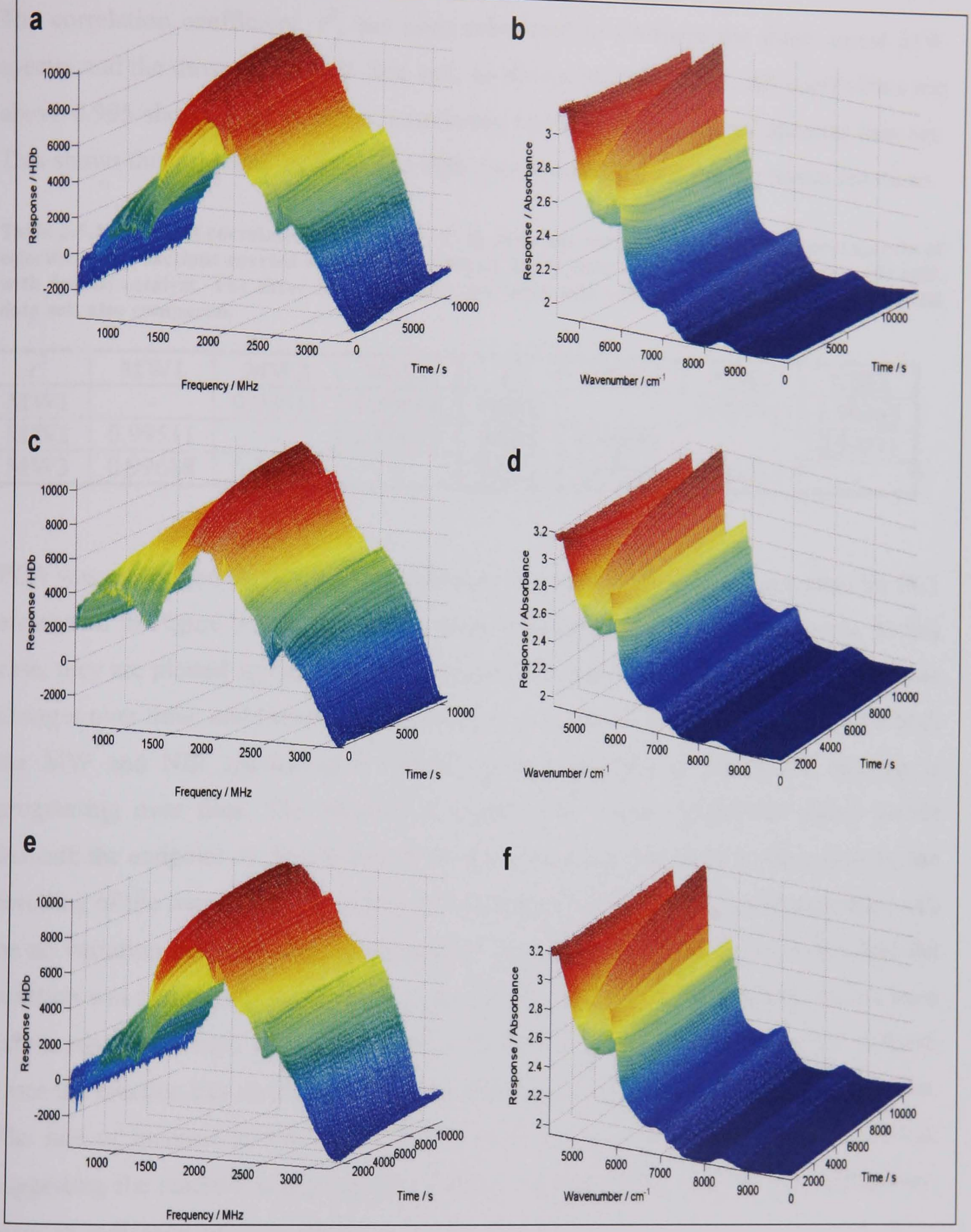

Figure 3.5.1: Mesh plots of the collected spectra for esterification reactions run at 40°C, using a molar ratio of 1:2, butanol to acetic acid, and 1ml of catalyst. The plots are the spectra (NIR or MW), response (Absorbance or HDb) against variable (wavenumber or frequency) plotted against time so the changes in the spectra over time can be clearly seen. The following data sets are shown: a) ester_40_1:2_1_1_MW; b) ester_40_1:2_1_1_NIR; c) ester_40_1:2_1_1_MW; d) ester_40_1:2_1_2_NIR; e) ester_40_1:2_1_3_MW; f) ester_40_1:2_1_3_NIR.

The correlation coefficient, r^2, has been calculated to compare the three repeat MW spectra and the three repeat NIR data sets, as shown in Table 3.5.1. All coefficients are above 0.995 showing an excellent correlation between the compared spectral data set. This shows that reproducible NIR and MW data is collected during the repeat reactions.

Table 3.5.1: Table of correlation coefficients, r^2, to show the variance between the repeat spectra of esterification reactions carried out at 40°C, with an initial molar ration of 1:2, butanol:acetic acid, with 1ml of catalyst. The three MW data sets are compared with each other, and the three NIR data sets also compared.

r^2	MW1	MW2	MW3	r^2	NIR1	NIR2	NIR3
MW1	-	0.99511	0.99688	**NIR1**	-	0.99991	0.99963
MW2	0.99511	-	0.99603	**NIR2**	0.99991	-	0.99971
MW3	0.99688	0.99603	-	**NIR3**	0.99963	0.99971	-

PCA was performed on the mean centred spectra, and the resulting scores plots for PC1 are shown in Figure 3.5.2. The scores show the relationship between samples. In this case, they are plotted against time so the plots show how the variation between samples changes over time, and hence how the reaction progresses. All the scores plots, for both the MW and NIR spectra, give typical reaction profiles in which the reaction is progressing over time. The reaction is expected to reach equilibrium which would indicate the endpoint of the reaction. It is expected to see this point in the scores by the levelling of the scores, as the reaction will no longer be proceeding and hence there will be no variation between samples. However, the scores increase for the entire time the reaction was monitored suggesting the reaction does not reach equilibrium. As has been previously mentioned, the endpoint of a reaction is subjective and must be defined. Once the reaction has slowed to almost equilibrium, this may be an acceptable endpoint. The rate of increase in the scores does slow down near the end of the time period, suggesting the reaction is nearing equilibrium. Looking at the scores plots in this way, gives an indication of the endpoint.

The scores for all three repeats of the reaction, for both MW and NIR, have similar profiles. This is to be expected as the reactions were carried out with the same reaction conditions, so should proceed in the same way.

The correlation coefficients, r^2, have been calculated, Table 3.5.2, to compare each of the scores on PC1 for each spectral data set, as shown in Figure 3.5.2. The r^2 values for all scores that have been compared are above 0.993, showing excellent correlation. This

shows that the NIR and MW spectra collected during the repeat reactions is reproducible, and the MW and NIR spectra are comparable. The MW and NIR capture the same process variation as can be seen on the scores which show the same variance in both the MW and NIR data.

Table 3.5.2: Correlation coefficients, r^2, to show the correlation between the scores on PC1 for esterification reactions carried out at 40°C, with an initial molar ration of 1:2, butanol:acetic acid, with 1ml of catalyst. Each repeat MW and NIR data sets are compared.

r^2	MW1	MW2	MW3	NIR1	NIR2	NIR3
MW1	-	0.99451	0.99633	0.99941	0.99896	0.99926
MW2	0.99451	-	0.99822	0.99419	0.99354	0.99485
MW3	0.99633	0.99822	-	0.99621	0.99563	0.99656
NIR1	0.99941	0.99419	0.99621	-	0.99988	0.99992
NIR2	0.99896	0.99354	0.99563	0.99988	-	0.99988
NIR3	0.99926	0.99485	0.99656	0.99992	0.99988	-

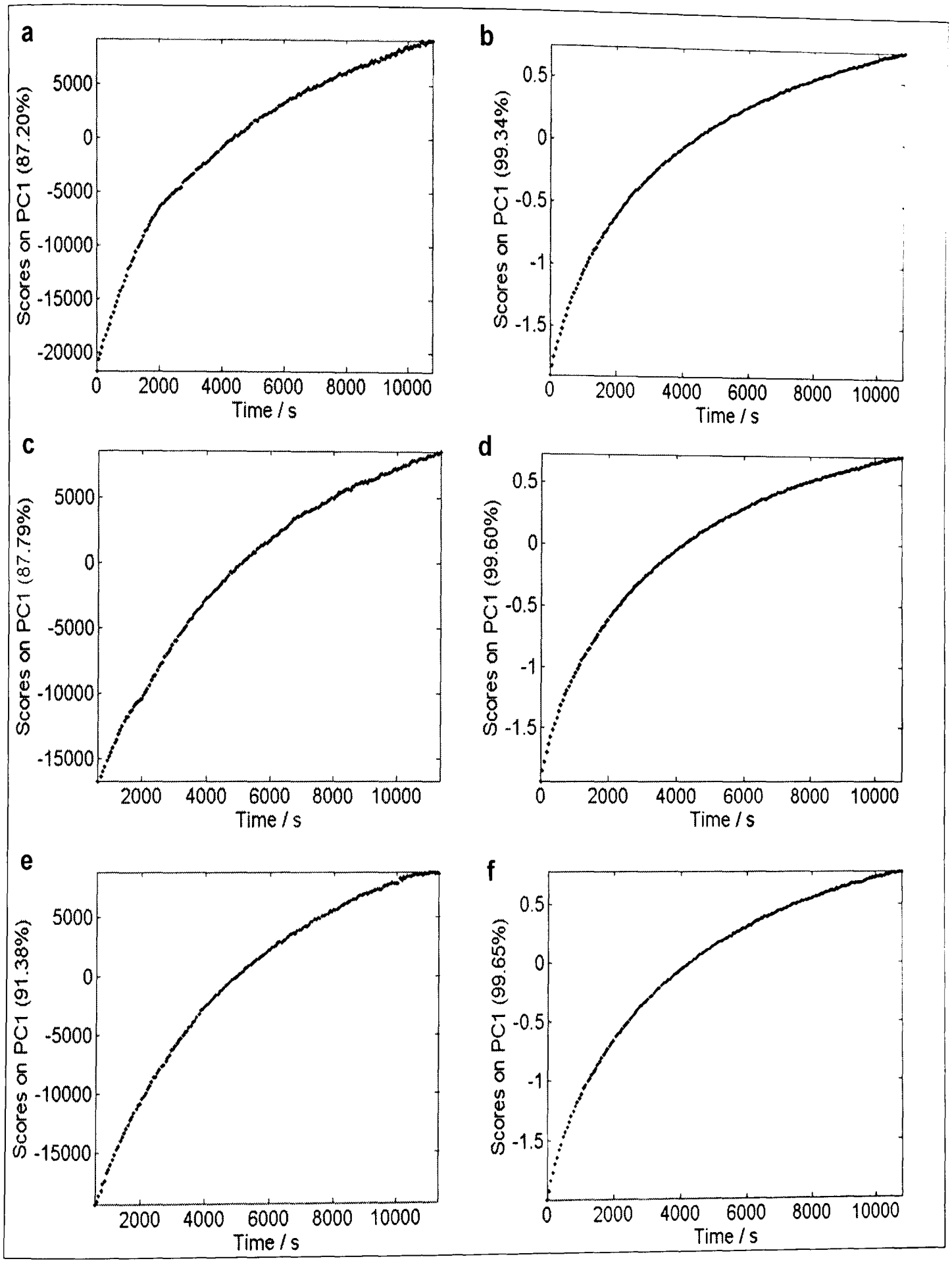

Figure 3.5.2: Scores on PC1 using the mean centred spectra for esterification reactions carried out at 40°C with an initial molar ratio of 1:2, butanol:acetic acid with 1ml catalyst; a) ester_40_1:2_1_1_MW; b) ester_40_1:2_1_1_NIR; c) ester_40_1:2_1_1_MW; d) ester_40_1:2_1_2_NIR; e) ester_40_1:2_1_3_MW; f) ester_40_1:2_1_3_NIR.

3.5.2.1.1 Endpoint detection

The spectra are analysed using the endpoint detection function within the caterpillar algorithm. As part of the function, the number of components to use in the PCA model, the window (WS) and the inter-window distance (inter-WS) can be altered to assist the determination of the endpoint of a reaction. Once these are determined for a reaction with specific conditions, the same variables can be used for subsequent reactions with the same conditions. The step-size of the movement of the windows through the data can also be changed. This is set to one for all analysis due to the data sets being relatively small (~180 samples). The significance level below which the reaction must fall before it is deemed to have reached stability and hence the endpoint, can also be altered. This is set to 0.99 for all analysis to ensure the reaction is truly at its endpoint.

The raw spectra are used in the algorithm with no pre-processing. This simplifies the analysis as choosing a pre-processing technique requires operator skill. The spectra are mean centred automatically within the algorithm.

These variables have been optimised using the *ester_40_12_1_3* MW and NIR data sets. All the combinations of the different variables to be used can be examined. A minimum WS of five and a maximum of ten, with a minimum inter-WS of ten and a maximum of 20 were examined. It is convenient to use an inter-WS double that of the WS.

MW spectra

The reactions comprise of four components, butanol, acetic acid, butyl acetate and water. However, two components increase at the same rate and two are consumed at the same rate, therefore there are effectively only two independent components. It is expected that only two components will be needed to describe the variation in the reaction data. Figure 3.5.3 shows the plot to determine the correct number of components to use. This is shown using a WS of five and inter-WS of ten. The components show the amount of variation described, and this will be the same for all combinations of WS and inter-WS, so it is reasonable to examine only one plot. From the plot, it is clear that almost all the variation in the spectra is described by the first component. The other components appear to contain a small amount of noise. A minimum of two components must be used in the algorithm to ensure all useful variance is captured, so two will be used as expected.

To choose the WS to use, a plot containing the results for each WS is examined, Figure 3.5.4. The results are only examined using an inter-WS of ten. Altering this does change the profiles, but only the relative intensities. For endpoint determination, the plots show how the reaction changes over time. At the start of the reaction, the variation between samples is great as the reaction is proceeding, and the reaction composition is altering. As the reaction proceeds, the variation between samples lessens until such a point at which the samples become similar as the reaction is reaching equilibrium. Within the endpoint determination plots, as in Figure 3.5.4, a high variation between samples should be seen at the start of the reaction as it is for all window sizes used in Figure 3.5.4. This variation should decrease until it reaches below the significance level, or endpoint level, which is set by the user, in this case at 0.99. Using a WS of five gives the lowest variation level at the end of the reaction, and this is expected to fall below the endpoint level. Using a WS of ten, gives quite a high level at the end, and this may not fall below the set endpoint level. The other window sizes all give similar variation profiles. Therefore, all window sizes are to be examined more closely.

Figure 3.5.3: Choosing the number of components to use in the PCA model in the endpoint detection caterpillar algorithm for MW spectra collected during an esterification reaction run at 40°C with an initial molar ratio of 1:2, butanol:acetic acid, data set *ester_40_12_1_3_MW*.

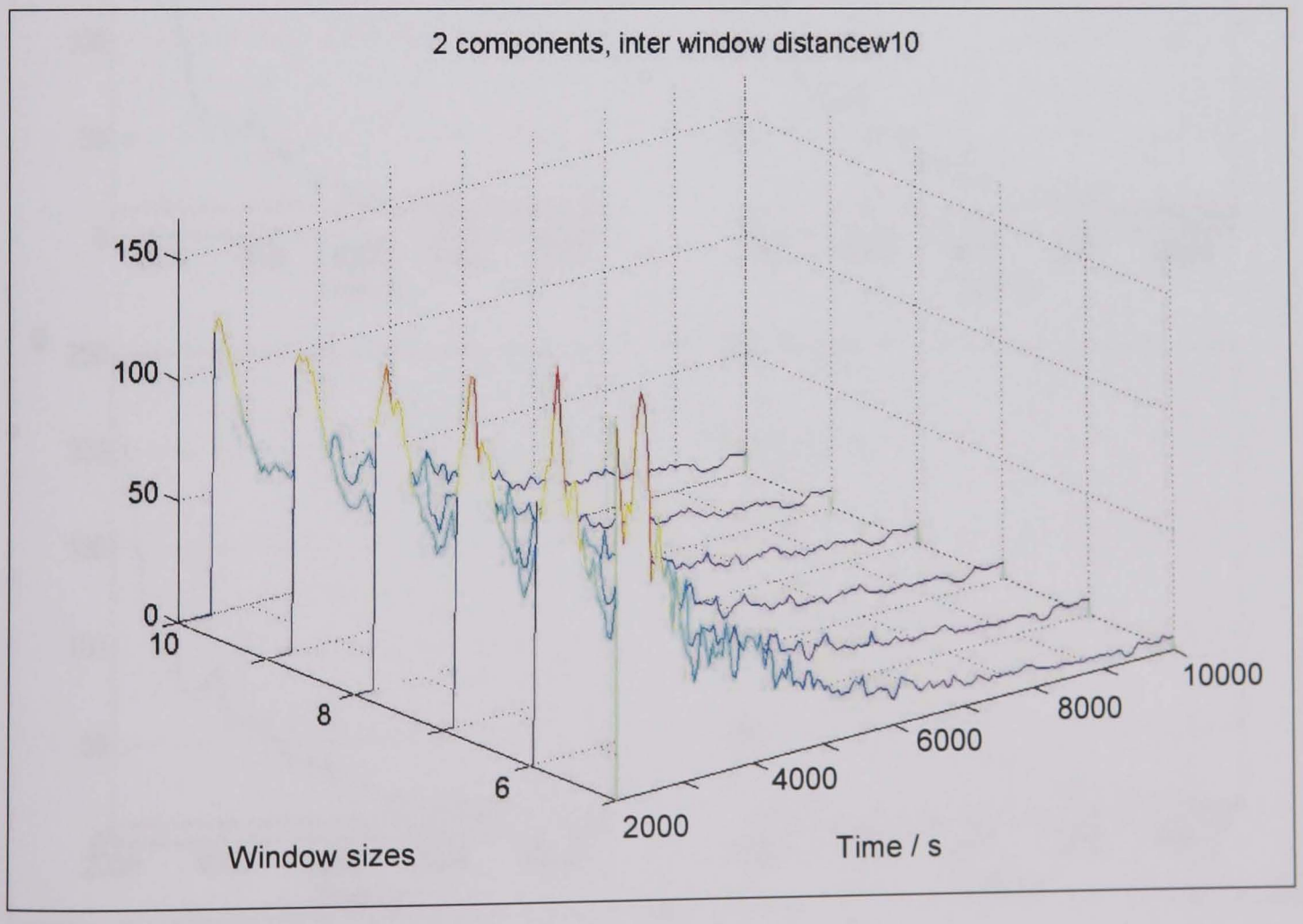

Figure 3.5.4: Choosing the window size to use in the endpoint detection caterpillar algorithm for MW spectra collected during an esterification reaction run at 40°C with an initial molar ratio of 1:2, butanol:acetic acid, data set *ester_40_12_1_3_MW*.

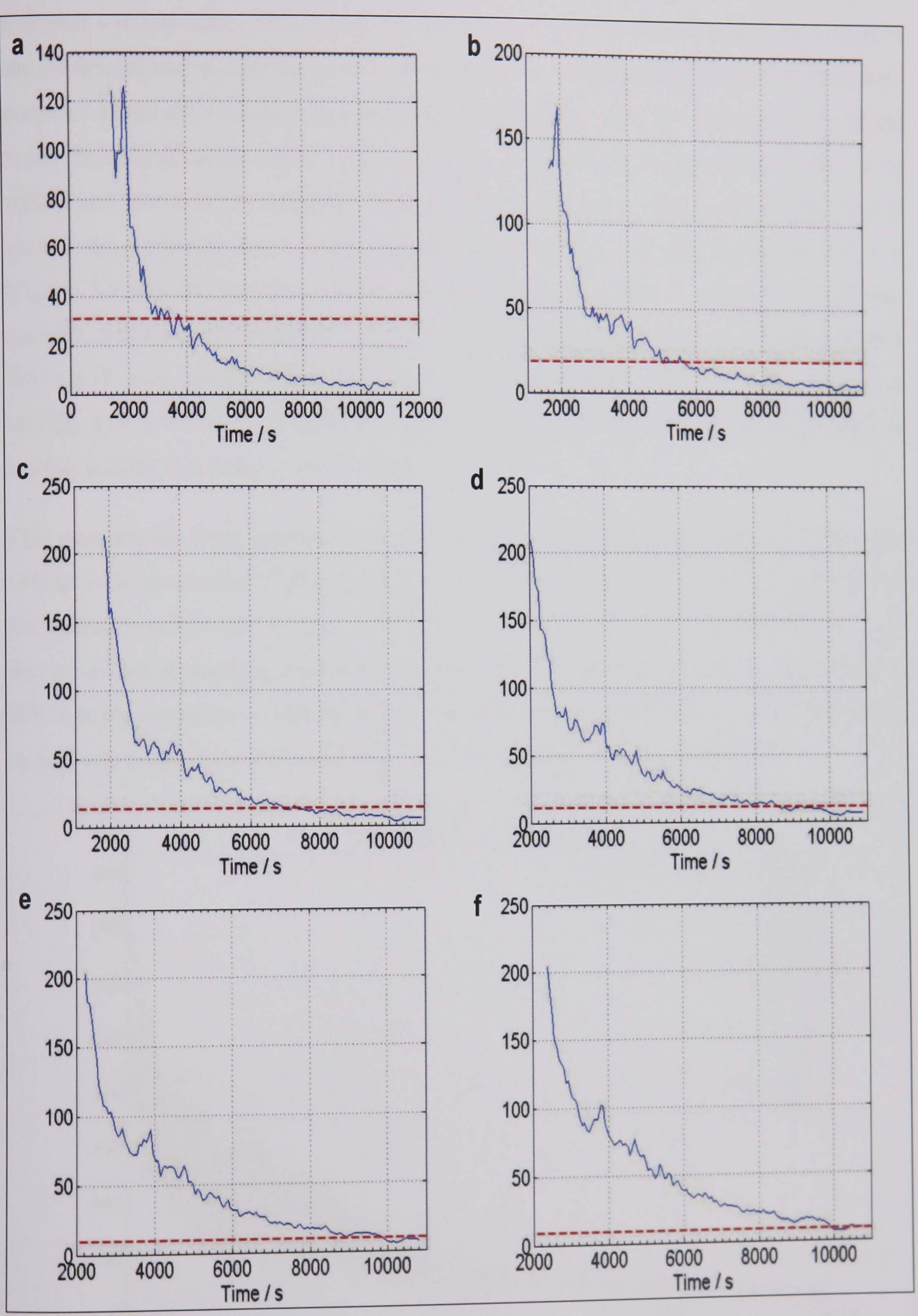

Figure 3.5.5: Determination of window size (WS) to use in the endpoint determination function in caterpillar, using data set *ester_40_12_1_3_MW* data, and an inter-window distance of 10. The significance level (0.99), below which the reaction should fall, is indicated by the dashed line. a) WS=5; b) WS=6; c) WS=7; d) WS=8; e) WS=9; f) WS=10.

Figure 3.5.5 shows the resulting plot for the endpoint determination when using the different window sizes. This shows that depending on the variables chosen, the endpoint can be determined at different times. Therefore, it is important to define when the actual endpoint is, to allow correct identification. In the plots, once the reaction has reached below the significance level, indicated by the dashed line, the reaction is said to be stable, and hence at the endpoint. Using WS = 5 (Figure 3.5.5a), the reaction hovers around the endpoint line briefly, and has fallen below it by 4000s. Using WS = 6 (Figure 3.5.5b), the endpoint is determined at 6000s. For WS = 7 (Figure 3.5.5c), the reaction crosses the significance level at 7000s, and is truly below it at 8000s. With a WS = 8 (Figure 3.5.5d), the endpoint is around at 9000s and WS = 9 (Figure 3.5.5e) at 10000s. For a WS = 10 (Figure 3.5.5f), the reaction is around the significance level at around 10000s, but it isn't clearly below it.

This reaction has been carried out at 40°C, and it is reasonable to assume the reaction will be over by around 7200s (2 hours). It has been decided to use a WS = 7 in which the endpoint is between around 7000-8000s. The reaction has clearly slowed down at this point and is reaching equilibrium as the variation between samples is small. Using WS = 6, the endpoint is determined at around 6000s, some 20 min earlier. Depending on how the endpoint is defined by the user, this may be a suitable endpoint.

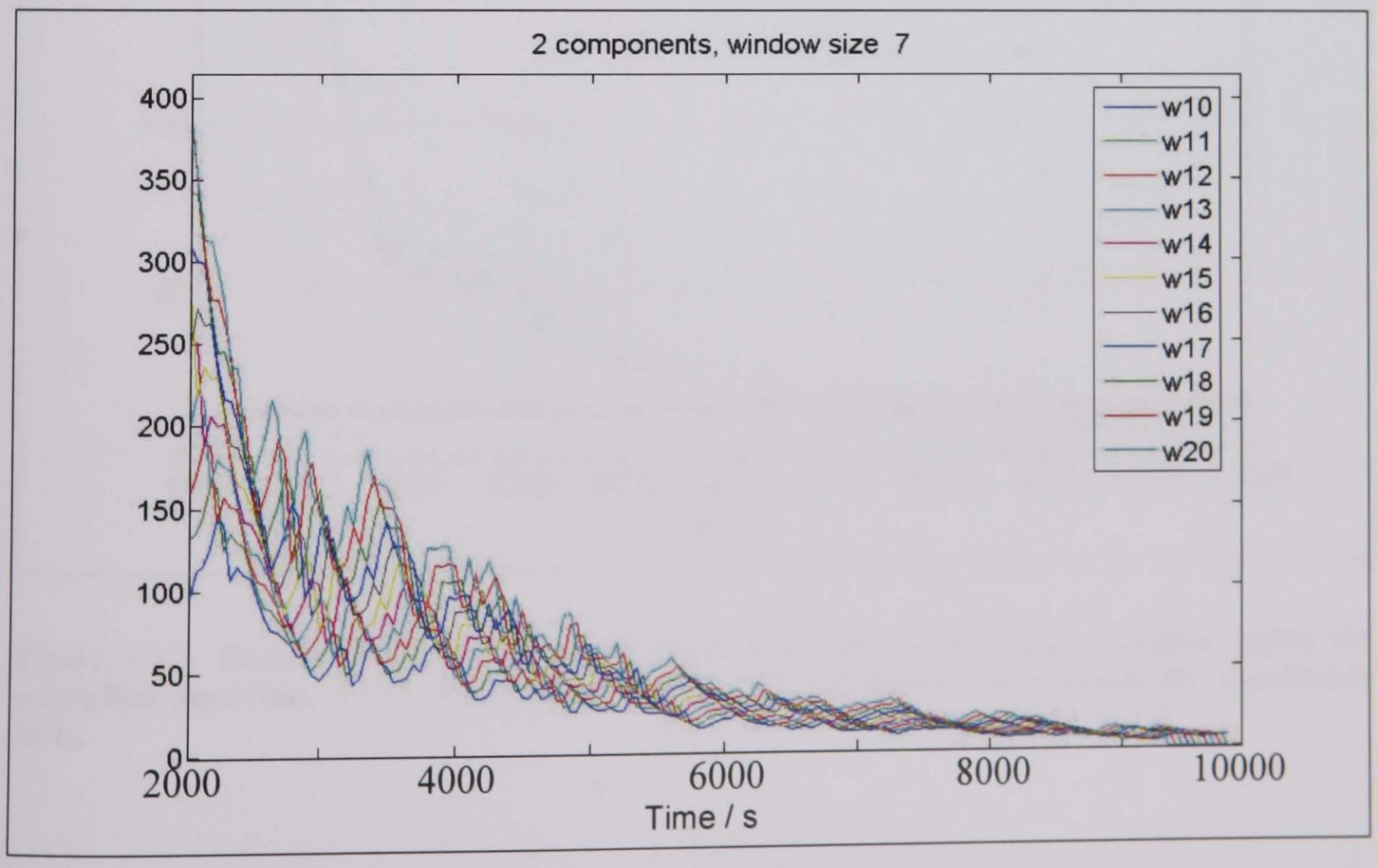

Figure 3.5.6: Plot of different inter-window sizes in the endpoint determination using data set ester_40_12_1_3_MW. 2 PCs are used in the algorithm with a WS=7.

From the inter-WS plot (Figure 3.5.6) it can be seen that changing this variable does have an effect on the determined endpoint. However, between time points 7000 to 8000s, there is only a small difference in the plots. Therefore, only a small difference will be seen in the determined endpoint of the reaction when using different inter-window sizes. From this, it has been decided to always use twice the size of the chosen WS for the inter-WS, to simplify the procedure for choosing the variables to use.

The resulting determination of the endpoint using the chosen variables is shown in Figure 3.5.7. The reaction reaches the significance level at 7000s, and is clearly below it at 7500s, so this is to be determined as the endpoint. The other reactions, run under the same conditions, can now be analysed using the same variables to ensure the same endpoint is achieved.

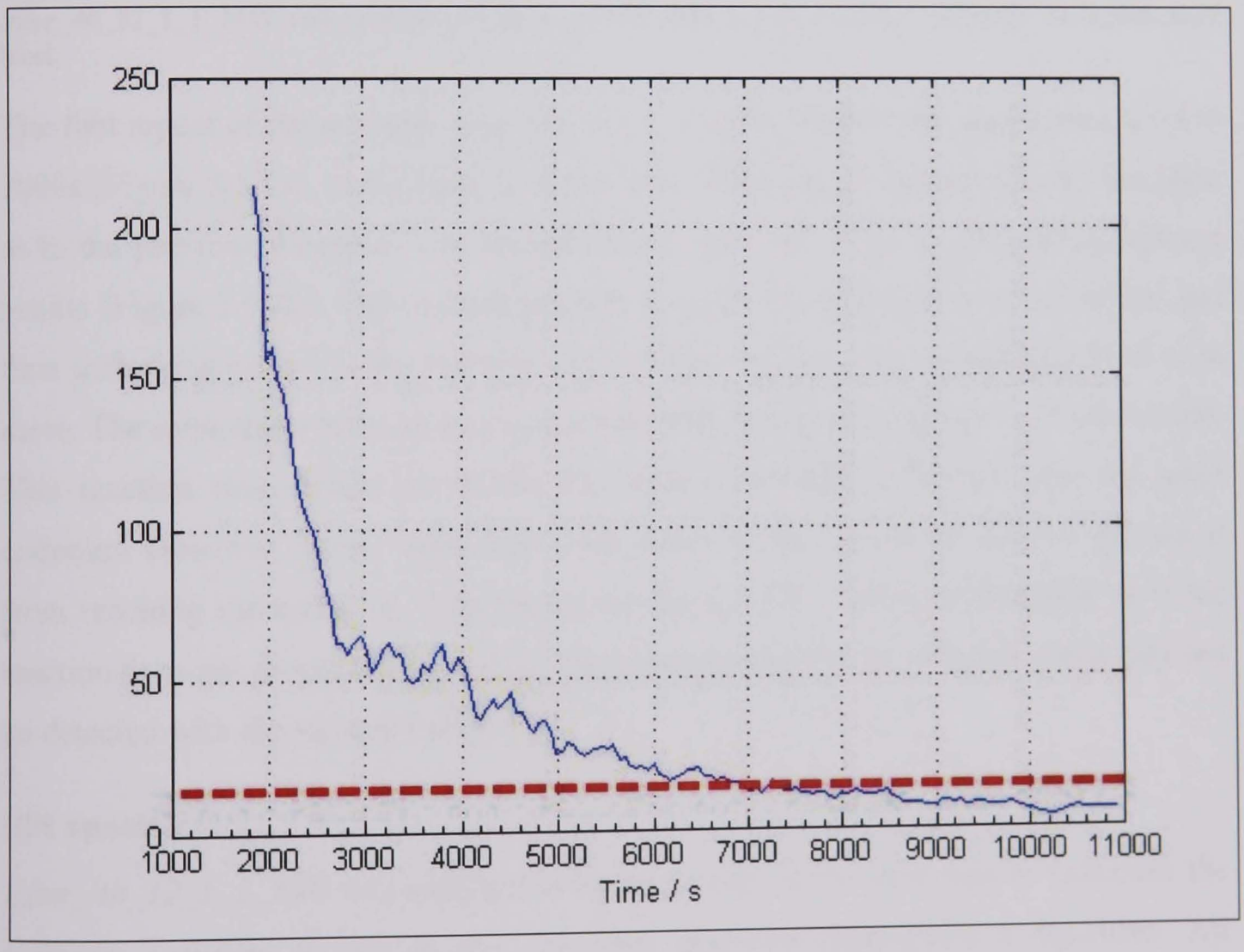

Figure 3.5.7: Endpoint detection for ester_40_12_1_3_MW, using chosen variables within the caterpillar algorithm: PC=2, ES=7, inter-WS=14. The red dashed line indicates the significance level.

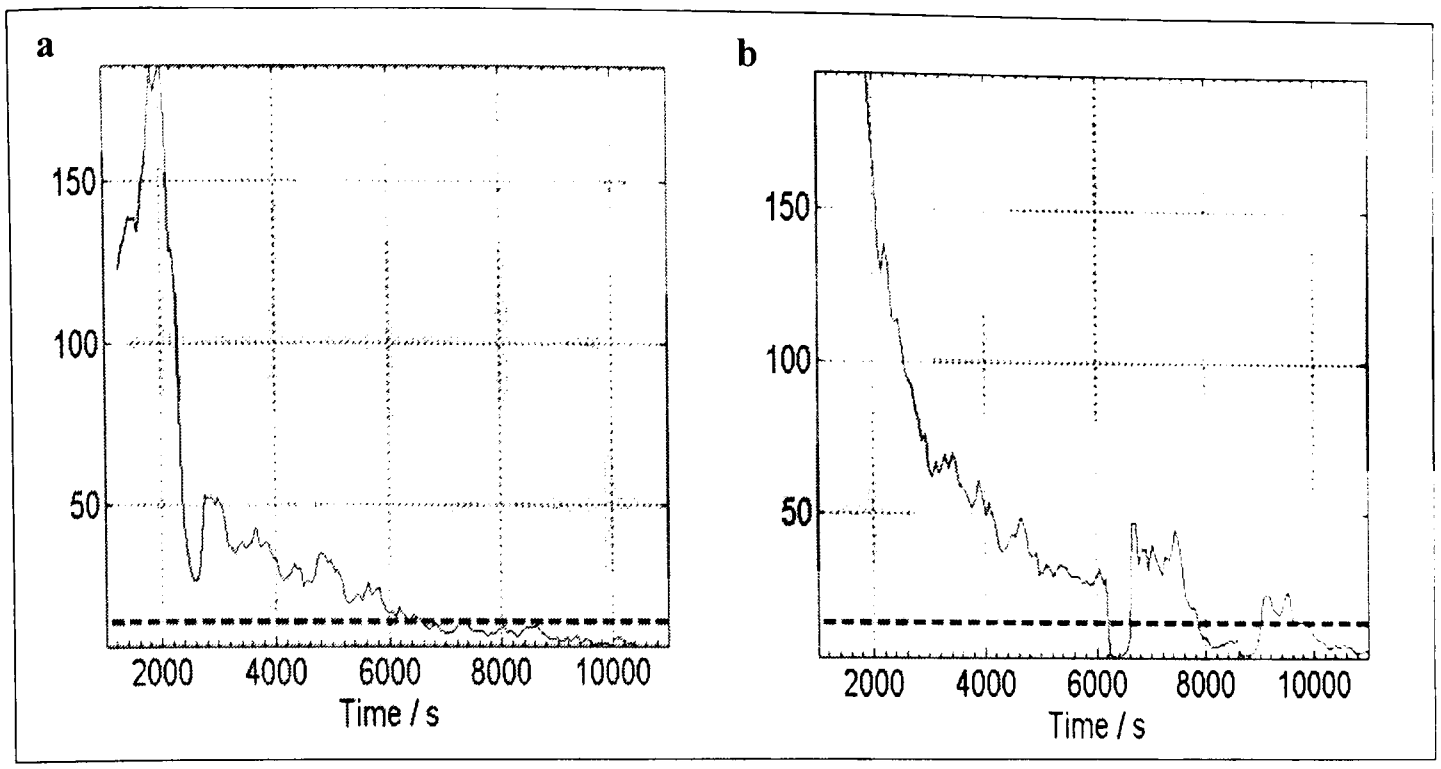

Figure 3.5.8: Endpoint determination using PC=2, WS=7, inter-WS=14 for: a) ester_40_12_1_1_MW and b) ester_40_12_1_2_MW. The red dashed line indicates the significance level.

The first repeat of the reaction, *ester_40_12_1_1_MW*, reaches the significance level at 7000s (Figure 3.5.8a), and clearly is below it at 7500s, so giving an endpoint the same as in the previous example. The second repeat, *ester_40_12_1_2_MW*, gives different results (Figure 3.5.8b). The reaction appears to reach the endpoint at around 6000s, but then something occurs in the reaction and it proceeds above the significance level once more. The same thing happens again at around 8000s, so the endpoint is not determined. This reaction was carried out under the same conditions so should give the same endpoint. However, some upset must have occurred during the reaction to prevent it from reaching the endpoint. This shows the limits of the endpoint detection as if the reaction does not proceed as expected, the true endpoint will be changed, and it may not be detected with the variables chosen.

NIR spectra

Ester_40_12_1_3_NIR was analysed in the same way as the MW data to determine the optimum variables to use in the caterpillar endpoint determination algorithm. All variation is captured in the first two PCs and so two were used. A WS of five gives an endpoint in the reaction at around the time expected, and so a corresponding inter-WS of ten was used.

Figure 3.5.9 shows the resulting endpoint determination plots for each repeat reaction using the optimised variables in the caterpillar algorithm. In the first repeat (Figure

3.5.9a) the endpoint is seen just before 8000s, but the reaction still hovers around the significance level. In repeat 2 (Figure 3.5.9b) the endpoint is also seen just before 8000s, and this stays clearly below the significance level for the remainder of the reaction. In repeat 3 (Figure 3.5.9c) the endpoint is just before 8000s.

The endpoint is reproducible in these three repeats, but it has been determined slightly later at 8000s, then the 7500s determined with the corresponding MW data. This could be due to the localised sampling nature of the NIR probe used, which may have a delay in seeing the reaction progress.

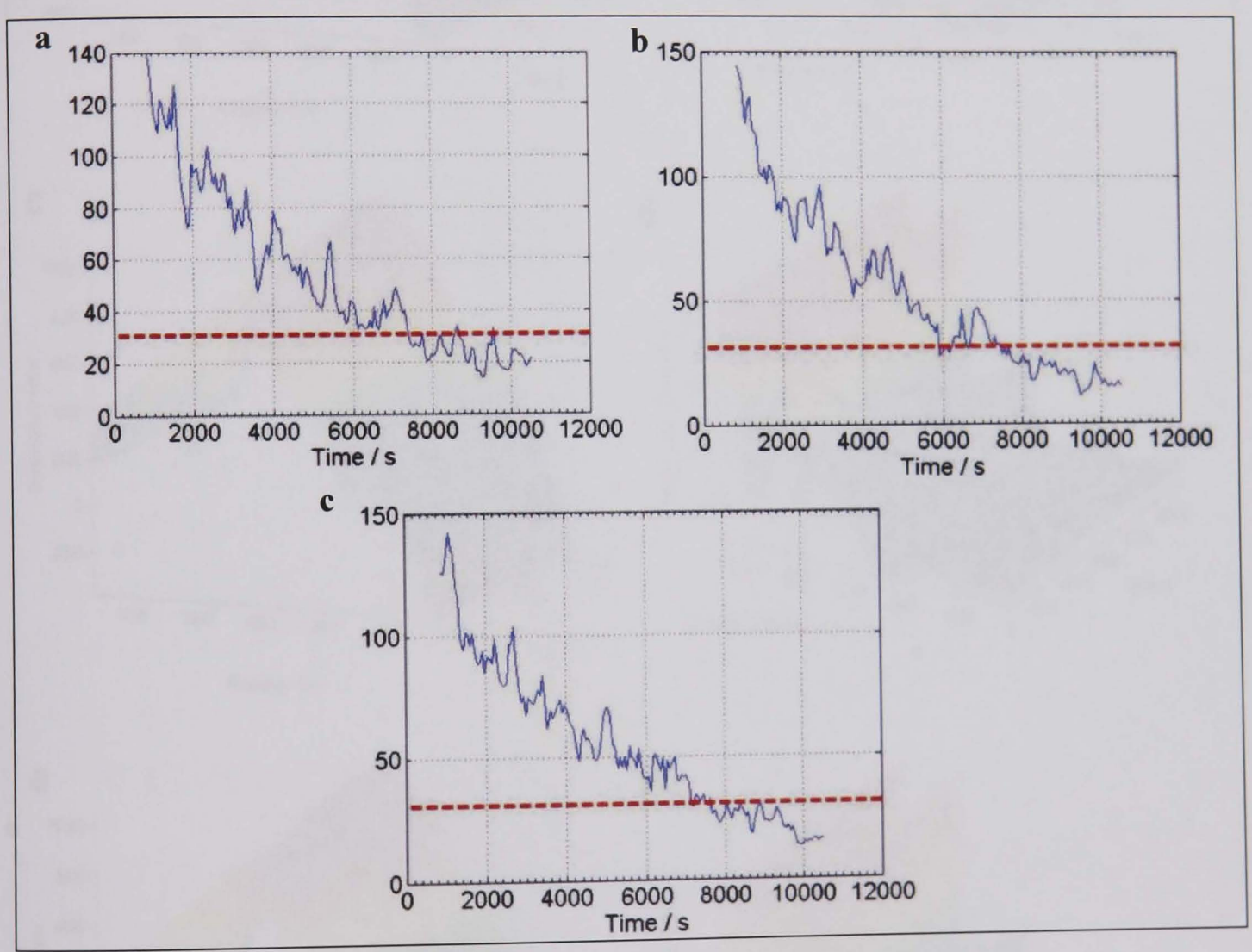

Figure 3.5.9: Endpoint determination using the caterpillar algorithm with variables PC=2, WS=5, inter-WS=10. a) ester_40_12_1_1_NIR; b) ester_40_12_1_2_NIR; c) ester_40_12_1_3_NIR. The red dashed line indicates the significance level.

3.5.2.2 Esterification reaction at 50°C, 1:0.25 initial molar ratio, 1ml catalyst

The collected NIR and MW spectra are shown in Figure 3.5.10. From this it can be seen that the spectra are very smooth and are reproducible over the repeat reactions.

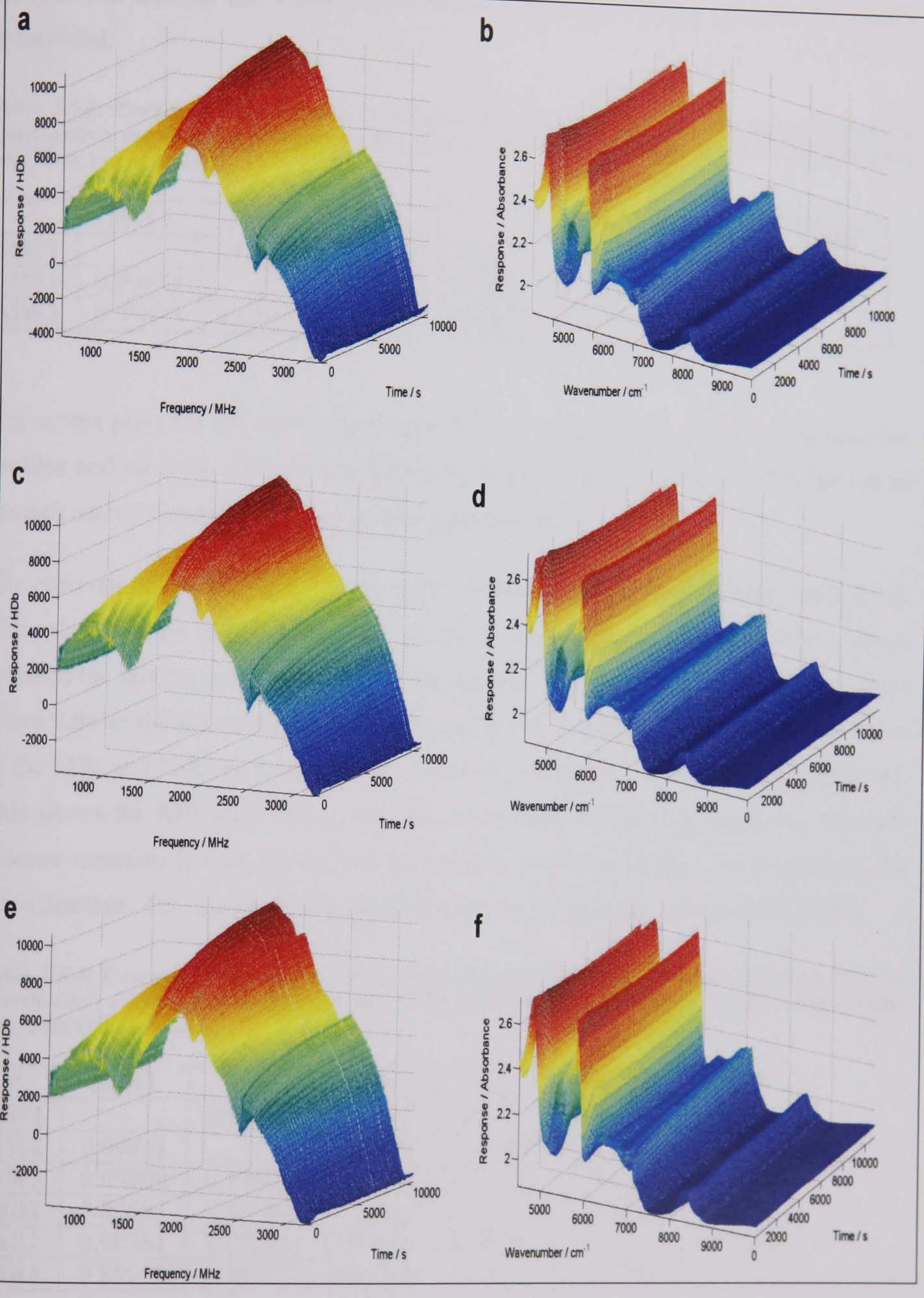

Figure 3.5.10: Mesh plots of esterification reaction carried out at 50°C with a molar ratio of 1:0.25, butanol:acetic acid, and 1ml of catalyst; a) ester_50_1:025_1_1_MW; b) ester_50_1:025_1_1_NIR; c) ester_50_1:025_1_1_MW; d) ester_50_1:025_1_2_NIR; e) ester_50_1:025_1_3_MW; f) ester_50_1:025_1_3_NIR.

The correlation coefficients, r^2, are shown in Table 3.5.3 to show the reproducibility of the recorded spectra. The values are all above 0.998 showing very reproducible spectra is recorded.

Table 3.5.3: Correlation coefficients, r^2, to show the correlation between the repeat spectra for esterification reactions carried out at 50°C, with an initial molar ration of 1:0.25, butanol:acetic acid, with 1ml of catalyst.

r^2	MW1	MW2	MW3	r^2	NIR1	NIR2	NIR3
MW1	-	0.99875	0.99893	**NIR1**	-	0.99868	0.99967
MW2	0.99875	-	0.99925	**NIR2**	0.99868	-	0.99915
MW3	0.99893	0.99925	-	**NIR3**	0.99967	0.99915	-

The scores plots for the MW data (Figure 3.5.11a, c and e) have very smooth reaction profiles and are very reproducible. The NIR scores (Figure 3.5.9b, d and f) are not as smooth reaction profiles, but they appear reproducible.

The correlation coefficients, r^2, have been calculated for each set of data, Table 3.5.4. The values for the MW data sets are all above 0.998, showing there is little variance between the scores, so the spectra are reproducible. The NIR repeat spectra have values above 0.94 so the scores show more variance but are still reproducible. When the scores of the MW and NIR are compared, r^2 values of between 0.0.85 and 0.92 are achieved. This shows the MW and NIR spectra are much less comparable, suggesting different process variation is seen by the two techniques, even though they are monitoring the same reaction. This may be due to the difference in the way the spectra are recorded.

Table 3.5.4: Correlation coefficients, r^2, to show the correlation between the scores on PC1 for esterification reactions carried out at 50°C, with an initial molar ration of 1:0.25, butanol:acetic acid, with 1ml of catalyst.

r^2	MW1	MW2	MW3	NIR1	NIR2	NIR3
MW1	-	0.99841	0.99809	0.87883	0.90781	0.85952
MW2	0.99841	-	0.99925	0.87980	0.91735	0.86232
MW3	0.99809	0.99925	-	0.87543	0.91616	0.85758
NIR1	0.87883	0.87980	0.87543	-	0.94482	0.99510
NIR2	0.90781	0.91735	0.91616	0.94482	-	0.95466
NIR3	0.85952	0.86232	0.85758	0.99510	0.95466	-

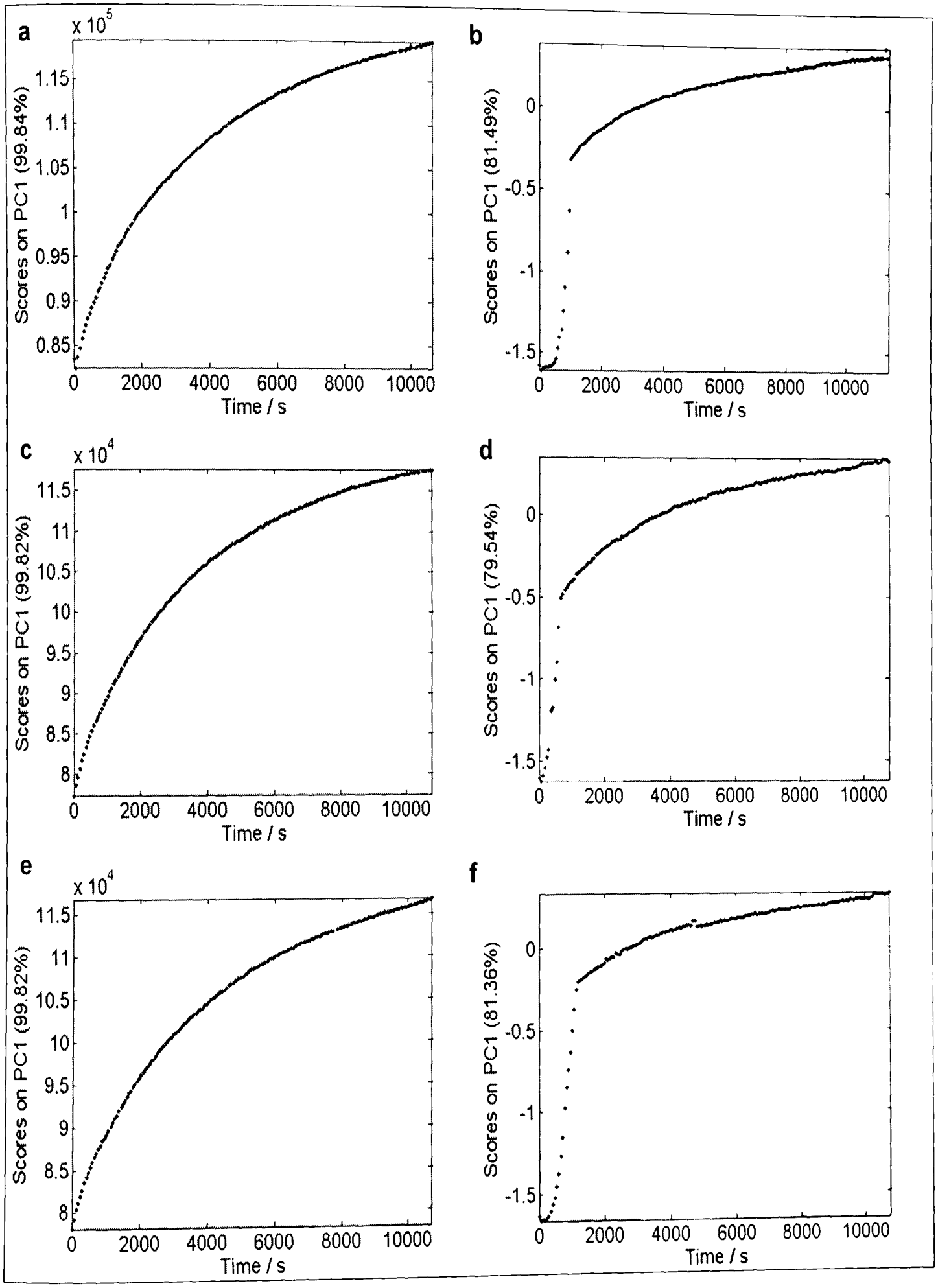

Figure 3.5.11: Scores on PC1 using the mean centred spectra for esterification reactions carried out at 50°C with an initial molar ratio of 1:0.25, butanol:acetic acid, and 1ml of catalyst: a) ester_50_1:0.25_1_1_MW; b) ester_50_1:0.25_1_1_NIR; c) ester_50_1:0.25_1_1_MW; d) ester_50_1:0.25_1_2_NIR; e) ester_50_1:0.25_1_3_MW; f) ester_50_1:0.25_1_3_NIR.

The spectra has been analysed using the endpoint determination function in the caterpillar algorithm, using PC = 2, WS = 5, and an inter-WS = 10. The resulting endpoint determination plots are shown in Figure 3.5.12. The endpoints detected are not reproducible. In these reactions, a molar ratio of 1:0.25, butanol to acetic acid. has been used so they will have a different endpoint to the reactions looked at previously. The molar ratio used does not favour equilibrium, so it is expected the endpoint will be late in the reaction.

The MW data for the first repeat (Figure 3.5.12a) does not give a clear endpoint. The reaction appears to reach the endpoint at 5000s, but quickly moves back above the significance level, suggesting the reaction stopped proceeding for a short while. The reaction hovers around the endpoint at the end of the reaction, so it is not clear if it has been reached. For the second repeat (Figure 3.5.12c) a more obvious endpoint is determined at about 9250s. With the third repeat (Figure 3.5.12e) there is also a clear endpoint at 8000s, although the reaction does move back towards the significance level nearer the end of the reaction. The determined endpoint is not reproducible for these reactions.

With the NIR data, the endpoint appears to be very early on in the reaction. This is not expected as the reaction conditions do not favour equilibrium. However, on closer inspection of the plot for the first repeat (Figure 3.5.12b), the reaction does not actually reach the endpoint, but hovers around the line for the length of the reaction. With the second repeat (Figure 3.5.12d), the reaction nears the significance level for some time and actually only goes below it at 8000s, and the reaction goes back over the line at the end of the time period. On closer inspection of repeat 3 (Figure 3.5.12f) the reaction does not actually reach the endpoint.

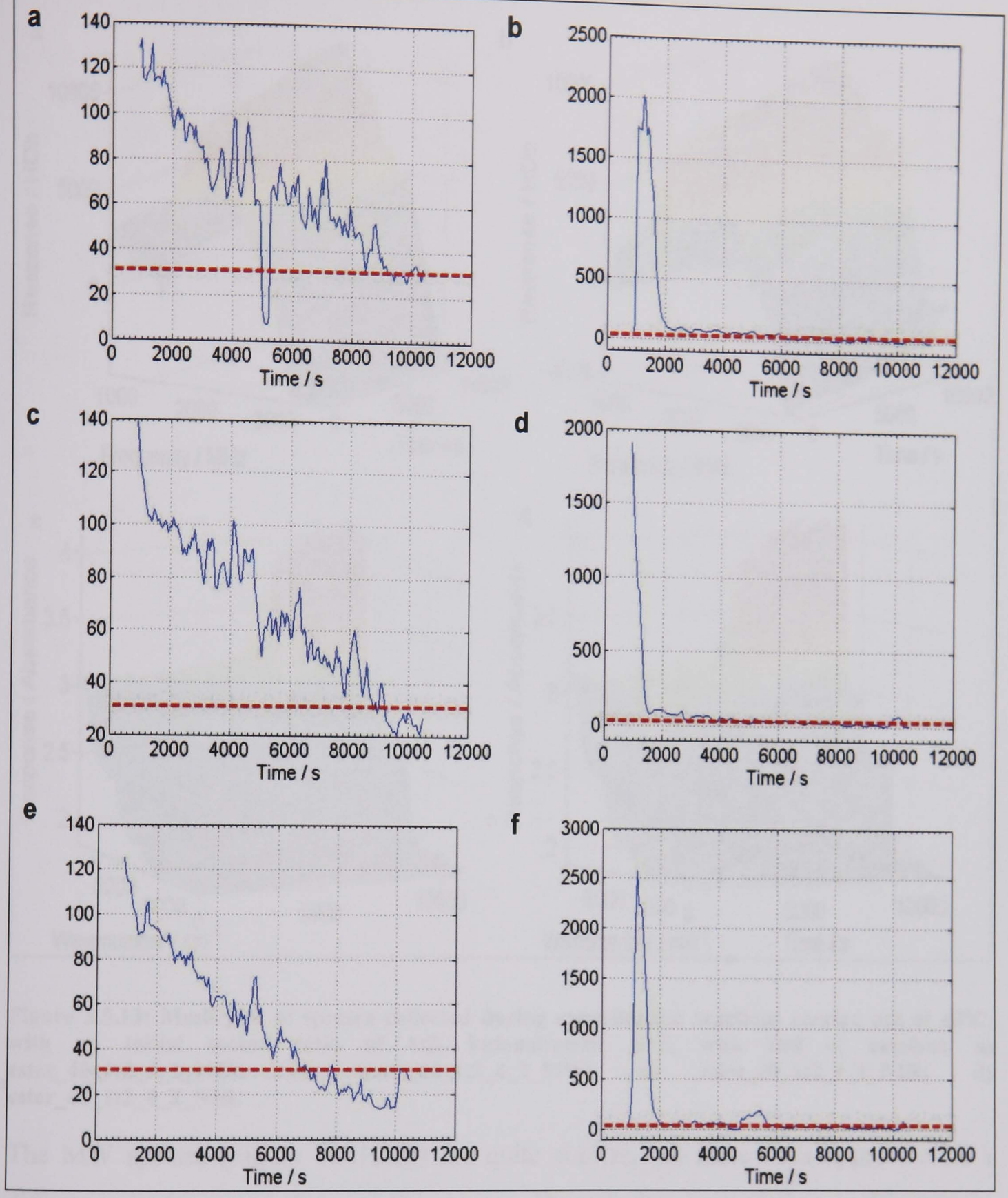

Figure 3.5.12: Endpoint determination plots for esterification reactions carried out at 50°C, with an initial molar ratio of 1:0.25, butanol:acetic acid, and 1ml of catalyst, using PC=2, WS=5, inter-WS=10 in caterpillar algorithm: a) ester_50_1:0.25_1_1_MW; b) ester_50_1:0.25_1_1_NIR; c) ester_50_1:0.25_1_1_MW; d) ester_50_1:0.25_1_2_NIR; e) ester_50_1:0.25_1_3_MW; f) ester_50_1:0.25_1_3_NIR. The red dashed line indicates the significance level.

3.5.2.3 Esterification at 40°C, 1:2 initial molar ratio, 4ml catalyst

These two reactions were carried out under the same conditions, so it is expected they will have similar endpoints. The resulting spectra are shown in Figure 3.5.13. From these it can be seen that the reactions carried out are similar as similar spectra result, however, there are differences in the spectra.

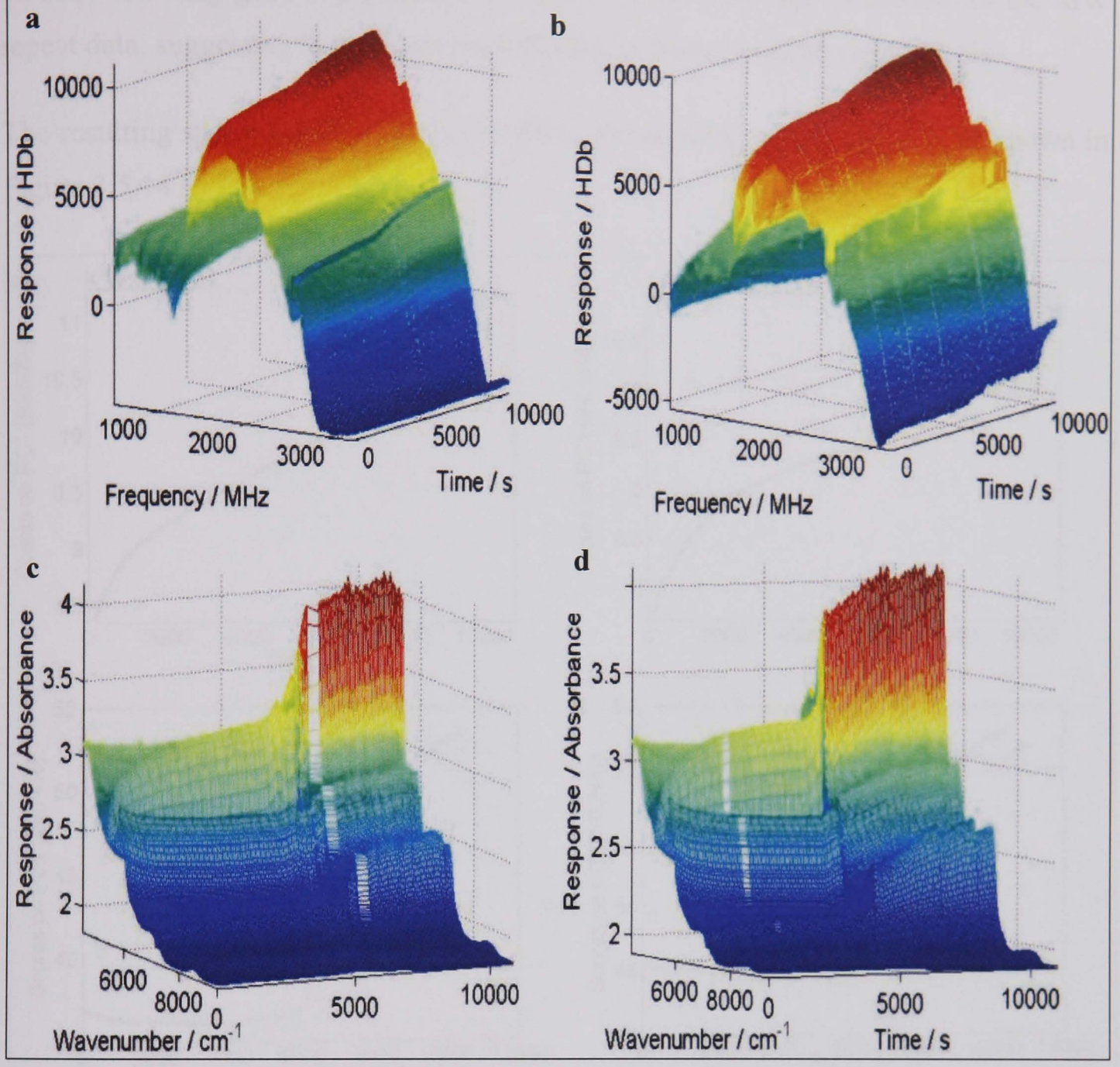

Figure 3.5.13: Mesh plot of spectra collected during esterification reactions carried out at 40°C, with an initial molar ratio of 1:2, butanol:acetic acid, with 4ml of catalyst; a) ester_40_1:2_4_1_MW; b) ester_40_1:2_4_2_MW; c) ester_40_1:2_4_1_NIR; d) ester_40_1:2_4_2_NIR.

The MW spectra (Figure 3.5.13a,b) are quite similar, but there does appear to be a difference in the actual shape of the spectra. The calculated correlation coefficients, *r*, for the two repeat spectral data sets is 0.95531 showing a high reproducibility of the repeat spectra. However, this is lower than the values seen for the other repeat reactions looked at which have been above 0.99.

The NIR spectra (Figure 3.5.13c,d) are quite similar. The spectra change gradually, in a typical reaction profile manner. Then, between 5000 and 6000s, the spectra change dramatically. This point could be due to something occurring during the reaction that results in a sudden increase in absorption of the NIR. However, it is seen in both reactions, so appears to be a reproducible change. The *r* value for these two repeats is

0.99307 showing good reproducibility. This is higher than that calculated for the MW repeat data, suggesting in this case the NIR data collected is more reproducible.

The resulting spectra were analysed by PCA, the resulting scores on PC1 are shown in Figure 3.5.14 .

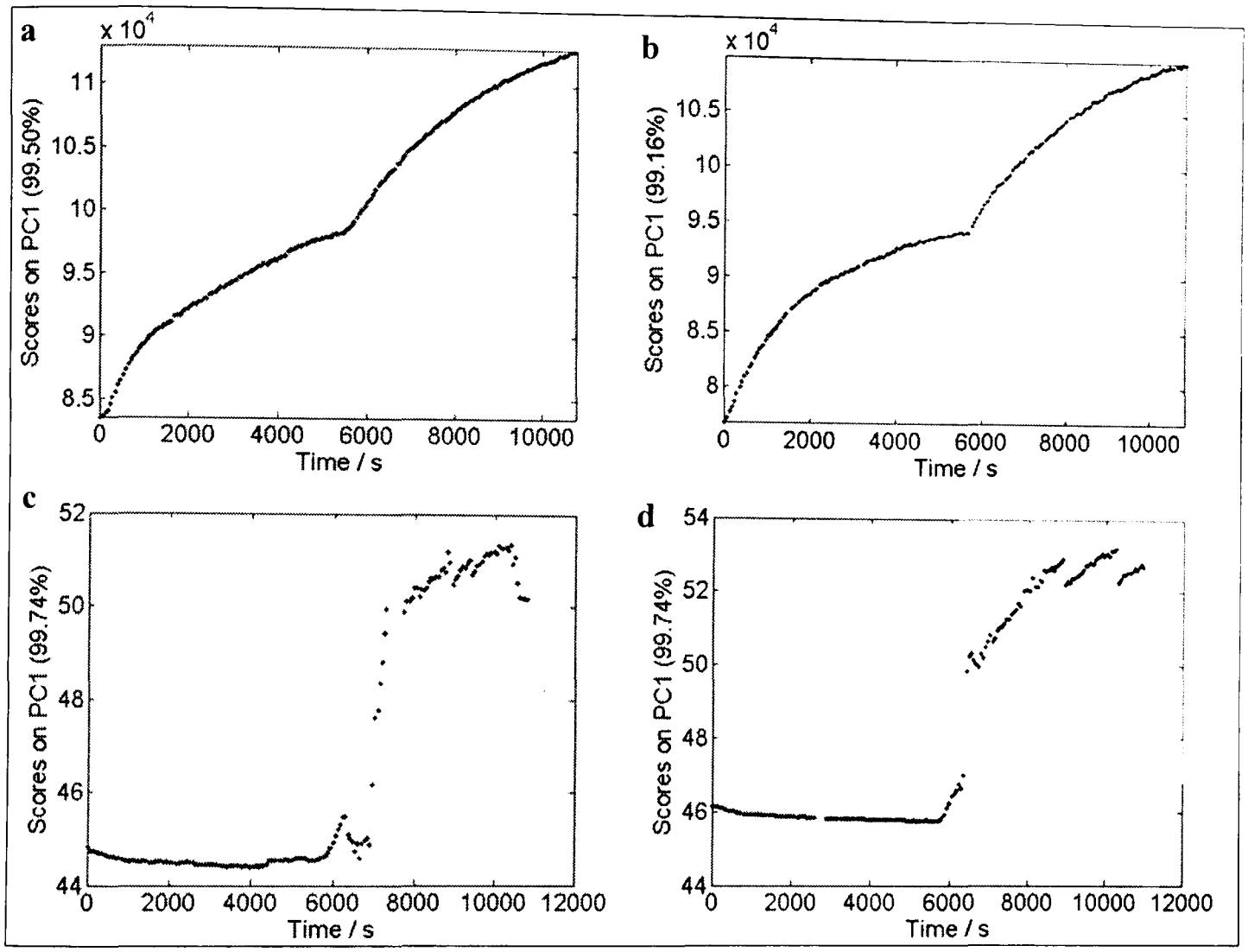

Figure 3.5.14: Scores on PC1 vs. time for a) ester_40_1:2_4_1_MW; b) ester_40_1:2_4_2_MW; c) ester_40_1:2_4_1_NIR; d) ester_40_1:2_4_2_NIR.

The scores on PC1 show the greatest variation seen in the spectra during the reaction. The scores plots show how the samples change over time, and so give a profile of the reaction as it progresses. The scores plots for the MW spectra for both reactions (Figure 3.5.14a,b) have a very similar reaction profile. This is to be expected as the same reaction is studied. In a normal reaction profile, it is expected to see the variation change between the samples to be quite large at the start, and then slow down as the reaction reaches equilibrium, as the samples are changing less rapidly. This profile is not seen here. There is a dip in the scores at around 6000s, which suggests something occurs in the reaction. This is reproducible in both reactions. Looking at the NIR scores (Figure 3.5.14c,d) a typical reaction profile is not evident. The scores are fairly level until around 6000s, suggesting the samples change very little. This would suggest that

the reaction is not proceeding. The NIR probe only measures a small area of the reaction mixture, suggesting it does not see the true reaction picture. The samples then change dramatically after 6000s, and the reaction appears to have slowed down by 9000s. This relates to the large increase seen in the spectra at the same time period (Figure 3.5.13). The scores plots do not give much useful information about the reaction progress, and do not help with the prediction of the end point of the reaction.

The r^2 values have been calculated to compare each of the data sets, Table 3.5.5. The scores for the two repeat MW data sets show little variance with an r^2 value of 0.99873. The two NIR data sets are also fairly reproducible with an r value of 0.95335. The NIR and MW scores show greater variance with r^2 values of between 0.88 and 0.92, indicating the two techniques do not capture the same process variation.

Table 3.5.5: Correlation coefficients, r^2, for the PCA scores on PC1 for the repeat MW and NIR spectra recorded during an esterification reaction carried out at 40°C, with an initial molar ratio of 1:2, butanol:acetic acid, with 4ml of catalyst.

r^2	MW1	MW2	NIR1	NIR2
MW1	-	0.99873	0.89352	0.92049
MW2	0.99873	-	0.88613	0.91108
NIR1	0.89352	0.88613	-	0.95335
NIR2	0.92049	0.91108	0.95335	-

The data was then analysed using the caterpillar algorithm and the optimum variables to be used determined. It was decided to use PC = 2, WS = 5 and inter-WS = 10 for both the NIR and MW data. However, with all possible combinations, the endpoint is not determined in the reactions, and so these variables are used to illustrate the example.

Figure 3.5.15 shows the endpoint determination plots for both the MW and NIR data sets for the *ester_40_12_4_1* and *2* data sets. Its clear from these plots that an endpoint is not determined for the reaction and that something abnormal occurs during the process.

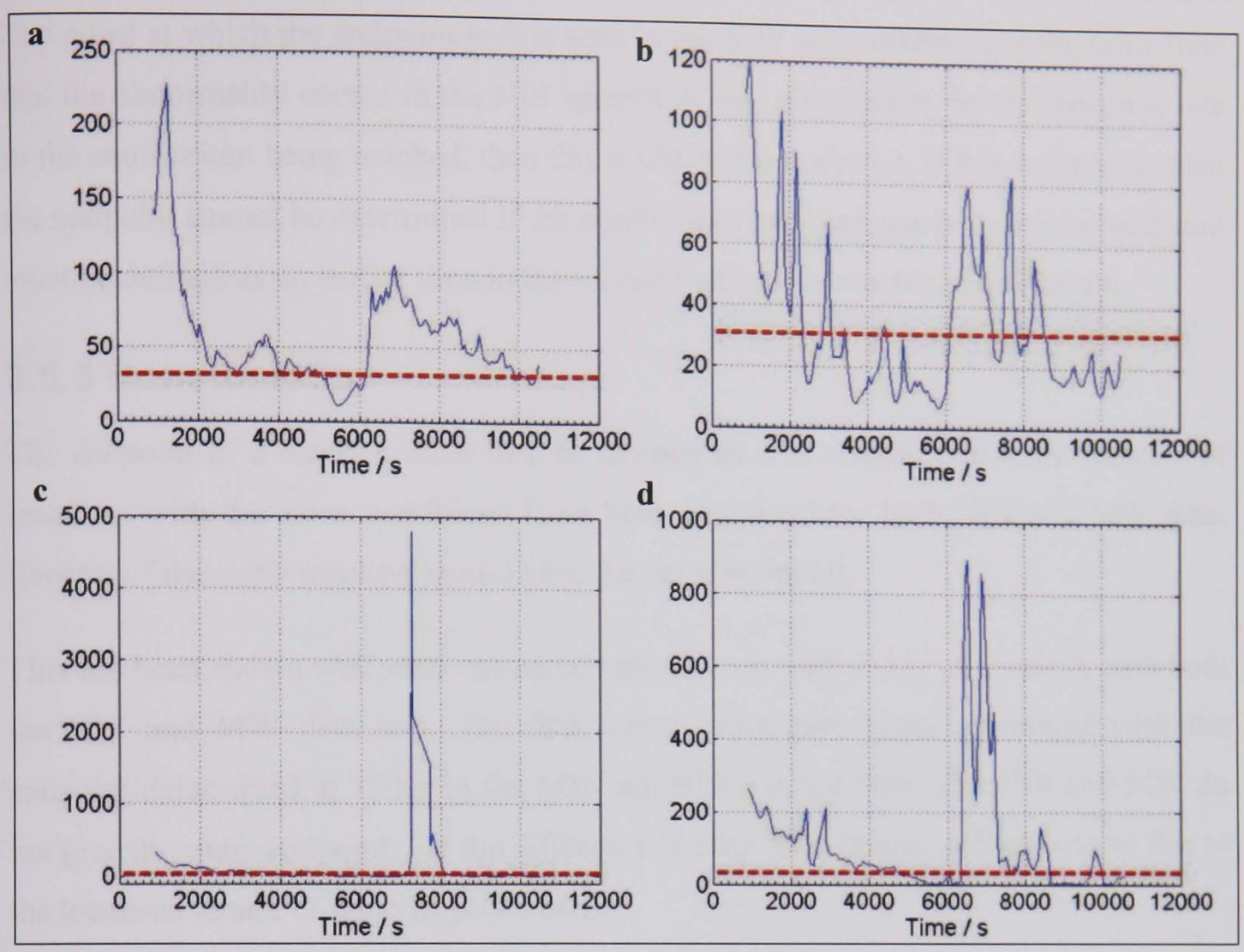

Figure 3.5.15: Endpoint determination using the caterpillar algorithm with variables PC=2, WS=5, inter-WS=10. for an esterification reaction carried out at 40°C, with an initial molar ratio of 1:2, butanol:acetic acid, with 4ml of catalyst; a) ester_40_12_4_1_MW; b) ester_40_12_4_2_MW; c) ester_40_12_4_1_NIR; d) ester_40_12_4_2_NIR. The red dashed line indicates the significance level.

In the MW data of the first reaction (Figure 3.5.15a) there appears to be an endpoint at 5000s, but then the reaction goes above the significance level again after 6000s, and slowly moves down towards the endpoint by the end of the reaction. This "dip" below the endpoint line correlates to the dip seen in the corresponding scores (Figure 3.5.14a) at around 6000s. A similar thing is seen in the MW data for the second reaction (Figure 3.5.15b) in which the reaction appears to reach the endpoint but moves above the significance level again. The reaction appears to be very erratic after this point. The NIR data for the first reaction (Figure 3.5.15c) does not show anything about the reaction. The NIR data for the second reaction (Figure 3.5.15d) also shows very little with no endpoint detected for the reaction.

As the endpoint is not determined for either of the reactions run under the same conditions, it suggests that the caterpillar algorithm cannot be used in this situation. It seems unlikely that an occurrence would happen in both reactions to prevent the determination of the endpoint.

The point at which the endpoint is first seen in the MW data, 6000s, is at the same time that the abnormality occurs in the NIR spectra. If this abnormality in the spectra is due to the equilibrium being reached, then this could be the endpoint. If this is the case, then the endpoint cannot be determined if the equilibrium has been reached, and the endpoint must be defined as an earlier time in the reaction when it is reaching equilibrium.

3.5.3 Conclusions

The endpoint of a reaction must first be defined as it is a subjective term. Repeats of reactions with the same conditions have been examined for both NIR and MW data. Repeats of the same reaction should have the same endpoint.

This has been shown well with one set of repeats, *ester_40_1:2_1_1, 2* and *3*, with both the NIR and MW data sets. The first two repeats gave good agreement with the endpoint determined at 7500s in the MW and 8000s in the NIR. The NIR and MW do not give the same endpoint, but the difference is only 500s (8 min). This could be due to the localised nature of the NIR probe used.

The second example using *ester_50_1:0.25_1_1,2* and *3*, does not give as good results. An endpoint is not determined for the first repeat, and the determined endpoints do not agree for the second and third repeats. The second data set gave an endpoint of 9250s with the MW and 8000s with the NIR. The third repeat gave an endpoint of 8000s for the MW, and no endpoint was detected in the NIR. The molar ratio used does not favour equilibrium, so this shows the limits of the reaction studied which may have not reached endpoint in the time studied.

The last example uses data set *ester_40_1:2_1* and *2*. In these reactions a larger amount of catalyst is used, 4ml compared to 1ml used in the other examples. No endpoint was determined in either the NIR or MW data. The NIR spectra showed some abnormalities in the collected spectra. This may be due to the reaction actually reaching equilibrium within the studied time, as these reactions are expected to proceed at a faster rate. This shows the limit of using caterpillar to detect the endpoint once the equilibrium has been reached. The endpoint must be defined as the reaction reaching equilibrium, and not the actual equilibrium point.

3.6 Detection of process upsets during an esterification reaction

A process upset is defined as anything which disturbs the progress of a reaction. It is important to detect such upsets during a reaction, and if possible identify the nature of the upset to allow correction of it and ensure the reaction proceeds as expected.

Caterpillar is an adaptive algorithm which can be used to determine the endpoint of a reaction. It can also be adapted to detect upsets during a reaction. The "now" variation is compared to the recent variation, and any major change in variation is identified as an upset as the reaction is no longer proceeding as expected.

In this work, several upsets have been stimulated during an esterification reaction monitored by MW and NIR spectroscopy. The caterpillar algorithm has been used to identify these upsets.

3.6.1 Experimental set-up

All reactions were carried out within the GMS remote stainless steel cavity with a NIR transmission probe inserted into the chamber, as described in the experimental section (section 2.4), to allow MW and NIR spectra to be collected simultaneously. Spectra were collected at one minute intervals.

Reactions were carried out with process upsets stimulated, similar to those expected to be seen in an industrial setting (section 2.5.5).

3.6.2 Results and discussion

The caterpillar algorithm can be used to detect process upsets in a reaction. This works in a similar way to the endpoint determination, but this time the windows are placed side by side (section 1.4.4). The first window is used as a reference window and the second as a detection window. A PCA model is calculated for the reference window to describe the variation of the samples in this window. The newest samples, contained in the detection window, are then compared to this model. If several of the samples in the prediction window are significantly different from the reference PCA model, this is interpreted as process change. Both windows are moved through the data stepwise allowing the reference model to adapt to any process changes. This means the caterpillar algorithm will detect the onset of new phases in the process data as they occur.

The variables of window size (WS) and number of components (PCs) to use in the PCA model must be optimised to ensure correct determination of process upsets. It is important that only true process upsets are detected and not normal reaction variation as this would lead to false alarms.

Once the optimum variables have been chosen, the algorithm can be performed on spectra collected from reactions with stimulated process upsets to determine if these process upsets can be detected.

3.6.2.1 Determination of window size and number of components

The characterisation reaction spectra, data sets *ester_40_4_1* and *ester_40_4_2*, were used to determine the WS and the number of PCs to be used in the PCA model within the caterpillar algorithm. These are set so that upsets are determined and normal process change is not identified as an upset. This data is representative of the reactions performed and contains only normal process variation. The reference reaction profiles can be seen in the mesh plots of the spectra over time (Figure 3.6.1a and b). The MW spectra changes very little over time. The NIR spectra changes more dramatically, particularly at around 7000s, when something appears to occur in the reaction. This is a reproducible change, seen in most of the reactions carried out, and is possibly related to the endpoint of the reaction and due to the local nature of the NIR measurements.

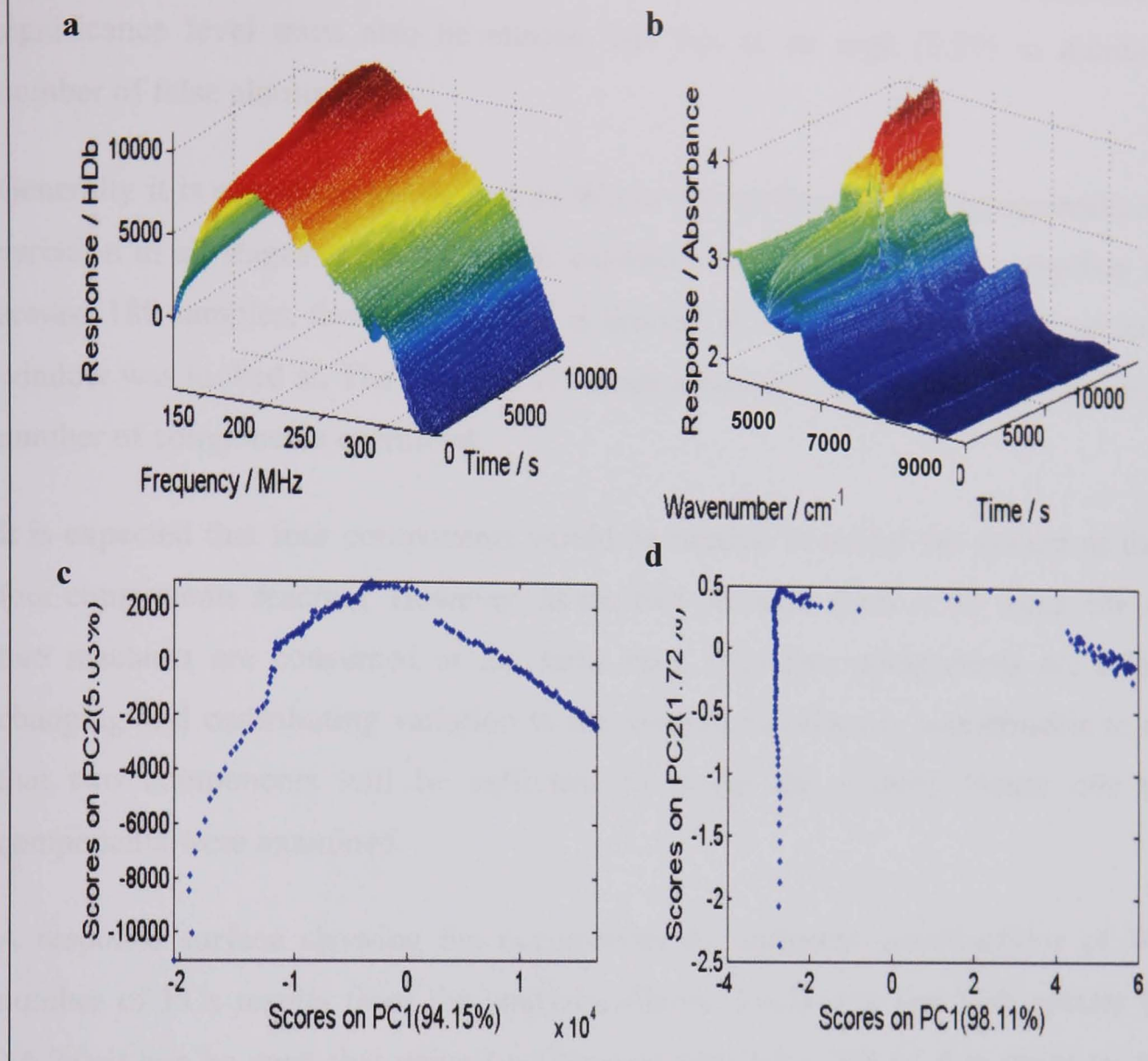

Figure 3.6.1: Mesh plots for reference esterification reaction carried out at 40°C, with an initial molar ration of 1:2, butanol:acetic cid, and no process upsets stimulated. The resulting scores plots, PC1 vs PC2, from PCA are also shown; a) MW spectra) NIR spectra; c) MW scores; d) NIR scores.

PCA has been performed on the mean-centred spectra. The scores plots for the MW spectra (Figure 3.6.1c) show how PCA can be used to visualise the progression of a reaction. The scores have a typical reaction profile in which the reaction appears to progress rapidly at the start, and proceeds towards equilibrium. However, the NIR scores (Figure 3.6.1d) do not show the progression of the reaction in the same way.

The reference data is analysed using a range of window sizes and number of PCs. The "now" variation is compared to the recent variation and any atypical samples, i.e. those which are significantly different, are determined for each combination. The number of atypical samples is counted and displayed in an occurrence plot. This gives easy viewing of the state of the reaction. Occurrences greater than zero indicate atypical samples have been detected in the process, and hence a process upset. The number of atypical samples should be none for an ideal system with only normal process variance.

Therefore, a WS and number of PCs is chosen that gives no occurrences. The significance level must also be chosen, but this is set high (0.99) to minimise the number of false alarms.

Generally it is suggested to use a wide WS to ensure that the best representation of the variation in all stages of the process is captured. The data examined comprises of only around 180 samples, therefore the WS is limited. A range of five to ten samples in the window was looked at. The smallest WS must always be one greater than the maximum number of components examined.

It is expected that four components would be needed to model the system as there are four components reacting. However, as the two products form at the same rate and the two reactants are consumed at the same rate, only two components are effectively changing and contributing variation to the system, therefore it is reasonable to assume that two components will be sufficient to model the system. Hence one to four components were examined.

A response surface showing the occurrences for different combinations of WS and number of PCs results from the analysis (Figure 3.6.2). For the MW spectra (Figure 3.6.2a) it can be seen that using two components and a WS of five gives no atypical samples i.e. no occurrences are detected. Using four components with a WS of five also gives no occurrences. However, it is considered that two components should suffice to model all the relevant information, and using four might lead to the inclusion of noise in the system. Looking at the PCA scores, 99.18% of the variance is captured in the first two components, and including more is not adding anything to the model.

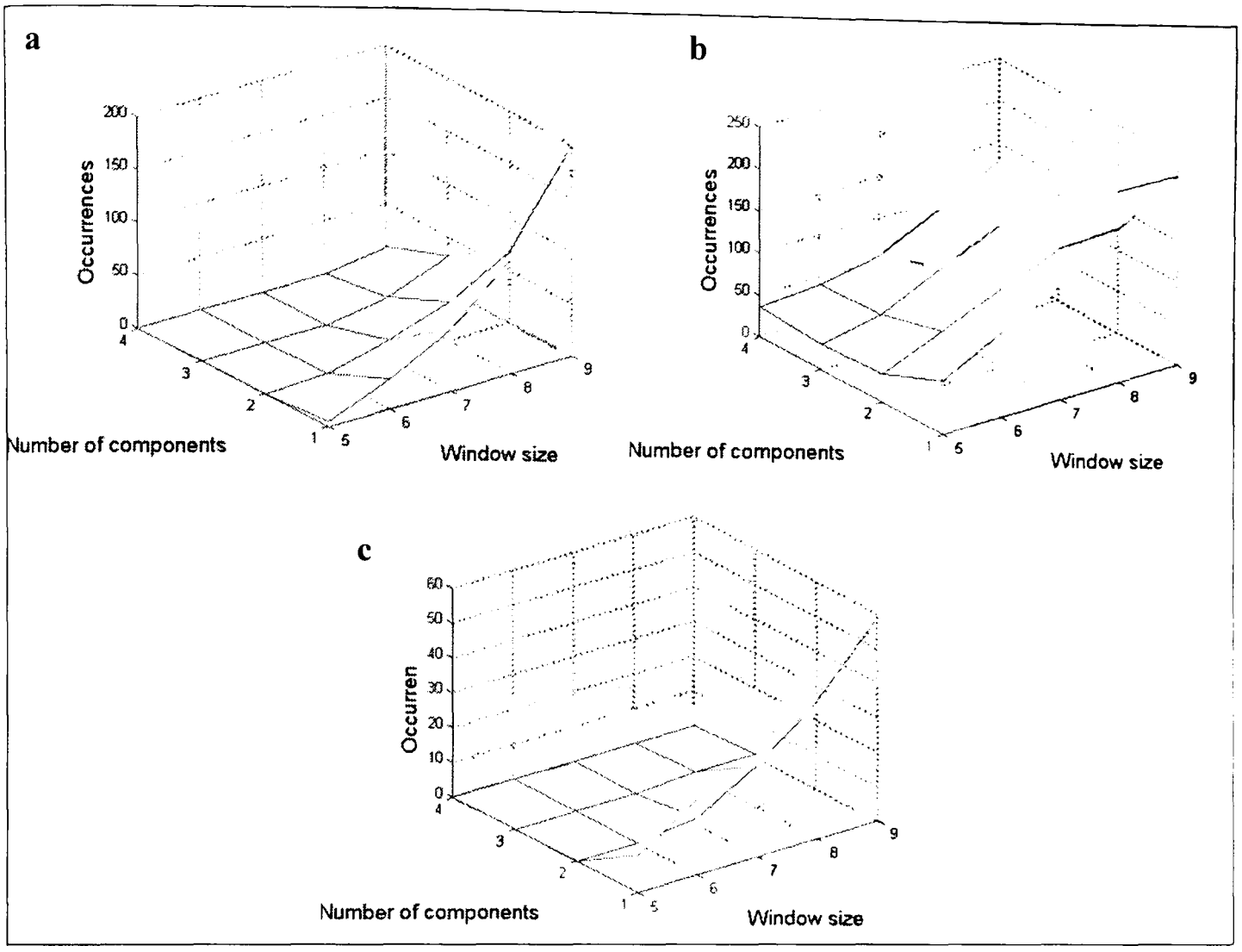

Figure 3.6.2: The response surface plot shows the occurrences for different combinations of window size, *WS*, and number of components, *PCs*, for the reference data set. Results for; a) MW spectra; b) NIR spectra; c) NIR spectra using just the first 1.5 hours of reaction data.

The NIR spectra were analysed in the same way. Using the full 3 hour, 10 800s, data set there are occurrences of greater than one for all combinations, implying atypical samples are detected (Figure 3.6.2b). Examination of the spectra (Figure 3.6.2b) shows the process does seem to change dramatically around 7000s into the reaction. This could be the endpoint of the reaction which may prove to be a problem when trying to identify process upsets if the end of the reaction is itself seen as an upset. Due to the nature of the probe, only one small area of the reaction mixture is analysed and so the true reaction progress may not be seen. When analysing the first half of the reaction, around 1.5 hours, 5400s, (Figure 3.6.2c) a WS of five and two components can be used to give no atypical samples. This shows the limits of using NIR data for process upset detection as the endpoint of the reaction seems to be detected as process change.

It was decided to analyse all reactions using two components in the PCA model, with a WS of five, in the caterpillar algorithm. The WS is equivalent to five minutes as the spectra are taken at one minute intervals. The window is moved through the data one spectra at a time. The atypical sample due to a process upset is detected in the next

spectrum that is recorded giving a lag before the upset is identified. Therefore, the more frequently spectra are taken, the quicker the upset will be identified.

3.6.2.2 Addition of catalyst

The reaction was carried out in the way described, but with 1.0ml catalyst added at the start, data set *Ester_upset_cat*. Further additions of catalyst (1.0ml) were added at 1790, 3590 and 5450s into the reaction, to give a total of 4.0ml of catalyst. This reaction is to simulate problems with charging of catalyst. Figure 3.6.3a and b show the resulting MW spectra and NIR spectra respectively. The MW spectra show clear changes at the points the catalyst is added (as indicated by arrows). The NIR spectra show no such change, but do show a dramatic change near the end of the reaction.

The spectra were analysed with the caterpillar process upset algorithm using a WS of five, two PCs and significance level of 0.99. The resulting occurrence plots are shown in Figure 3.6.3c, and d.

In the occurrence plot, the "new" samples that are statistically different from the reference samples are counted and shown as an occurrence. The three additions of catalyst are clearly identified as occurrences in the MW spectra (Figure 3.6.3c), at 1800, 3600 and 5450s. An occurrence of one is seen at the start of the upset. This indicates one of the five samples in the window is atypical. This builds up to an occurrence of five after five minutes, so now all five samples are atypical. This shows a clear process upset, and not just a false alarm. False alarms are likely to be seen as single events with a low occurrence, so are clearly identifiable as false alarms.

The only occurrence identified in the NIR spectra (Figure 3.6.3d) is at around 8250s. This does not relate to the addition of catalyst, but perhaps indicates the endpoint of the reaction analogous to the observation in the reference data (Figure 3.6.3b). As mentioned previously, if the endpoint of the reaction is identified as an upset in the NIR spectra, then this is not a suitable method to detect process upsets.

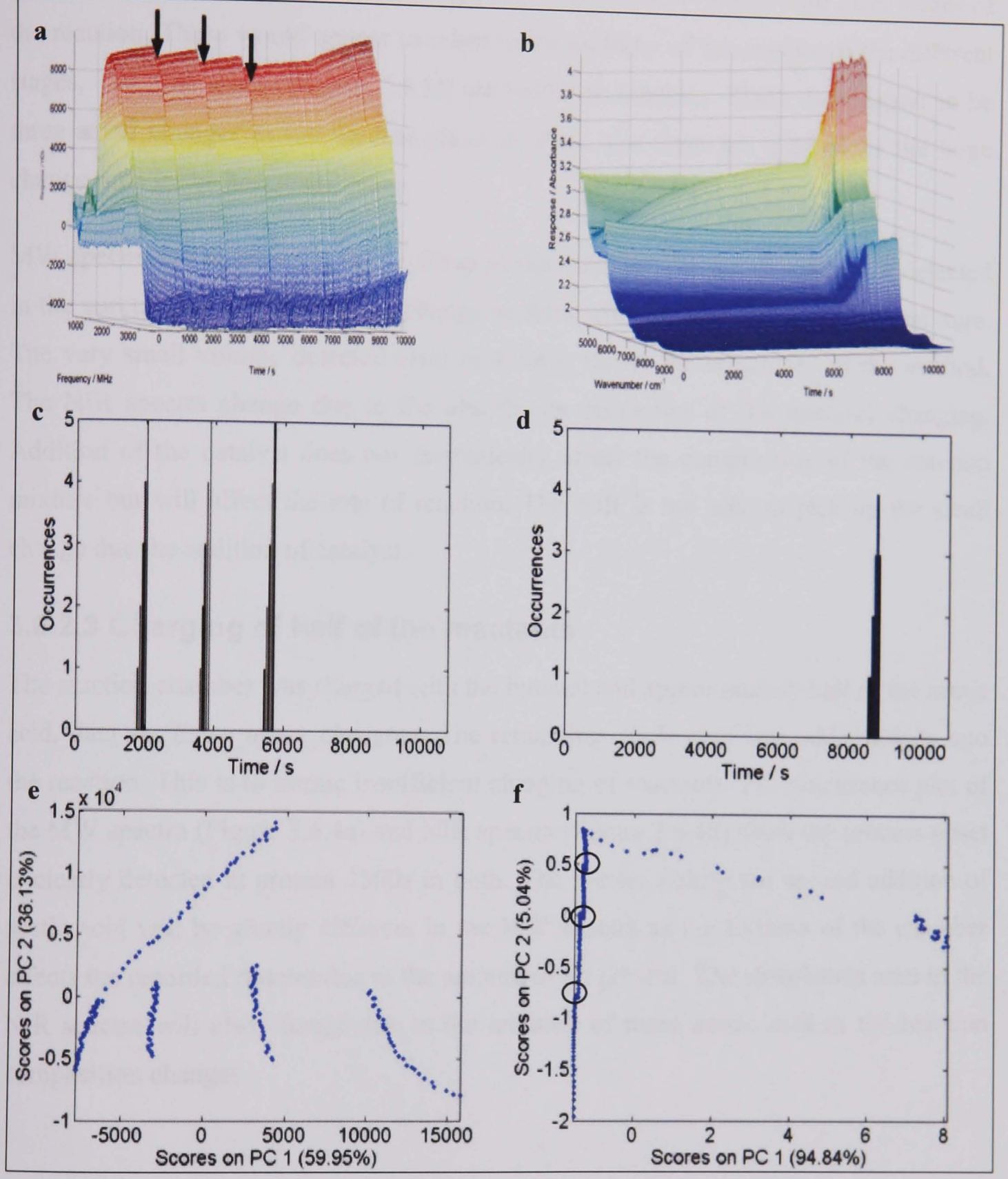

Figure 3.6.3: Esterification reaction with addition of catalyst at 1790, 3590 and 5450s to stimulate a process upset; a) Resulting MW spectra. The arrows indicate the addition of catalyst. It can be clearly seen the effect this has on the spectra; b) Resulting NIR spectra; c) Occurrence plot for MW spectra; d) Occurrence plot for NIR; e) Scores plot of PC1 vs. PC2 for MW spectra; f) Scores plot of PC1 vs. PC2 for NIR spectra. The three circles indicate a change in the scores due to the addition of catalyst.

PCA was carried out on the mean centred MW and NIR spectra to examine the reaction progress. The scores plot for the MW spectra (Figure 3.6.3e) shows four clear stages of the reaction. These would appear to relate to the addition of the catalyst at the different stages. The NIR scores (Figure 3.6.3f) are harder to interpret. There does appear to be three small changes in the vertical plane (circled), but these are masked by the large change seen in the horizontal plane.

MW spectra are sensitive to the addition of the catalyst. The actual catalyst is detected in the spectra due to the resulting change in dielectric constant of the reaction mixture. The very small volume detected (1ml in 450ml) shows the sensitivity of the method. The NIR spectra change due to the absorbance properties of the material changing. Addition of the catalyst does not dramatically affect the composition of the reaction mixture but will affect the rate of reaction. The NIR is not able to pick up the small change due the addition of catalyst.

3.6.2.3 Charging of half of the reactants

The reaction chamber was charged with the butanol and approximately half of the acetic acid, data set *Ester_upset_charging*. The remaining acetic acid was added 2460s into the reaction. This is to mimic insufficient charging of reactants. The occurrence plot of the MW spectra (Figure 3.6.4a) and NIR spectra (Figure 3.6.4b) show the process upset is clearly detected at around 2500s in both. The spectra before the second addition of acetic acid will be greatly different in the MW spectra as the fullness of the chamber affects the recorded spectra due to the amount of air present. The absorbance seen in the NIR spectra will also change due to the addition of more acetic acid as the reaction composition changes.

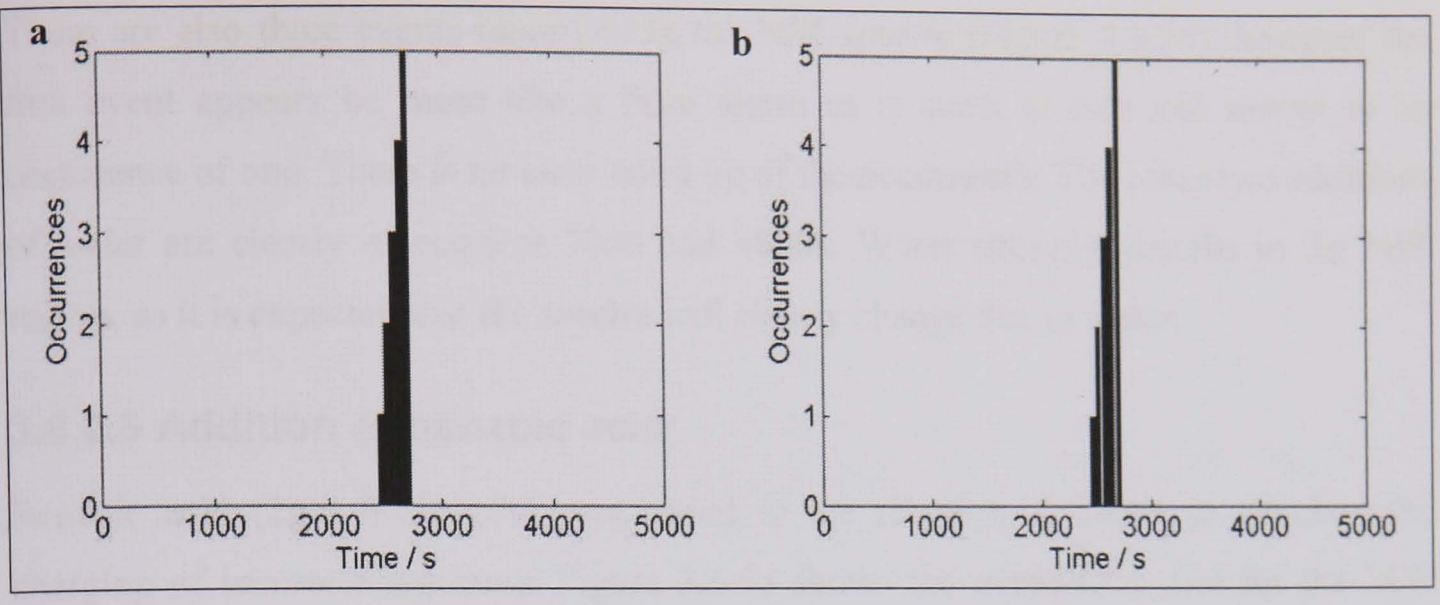

Figure 3.6.4: Occurrence plots for an esterification reaction with charging of half the reagents, and addition of the second half at 2460s to stimulate a process upsets; a) using MW spectra; b) using NIR spectra.

3.6.2.4 Addition of water

In this reaction, *Ester_upset_water_1*, water was added to the reaction at 1800 (5ml), 2990 (7.5ml) and 4790s (10ml). This is to simulate a leaking cooling pipe in industry. All three additions of water are detected as process upsets in the MW spectra (Figure 3.6.5a) at 1900, 2990 and 4800s. The first event appears slightly after the actual addition of the water, around two minutes later. The MW spectra seem to have trouble detecting such a small amount of water. The addition of the water will change the dielectric constant of the reaction composition, which affects the resulting MW spectra. The MW spectra are very sensitive to small amounts of water - 7.5 ml in 450 ml, 1.7% by volume, is detected.

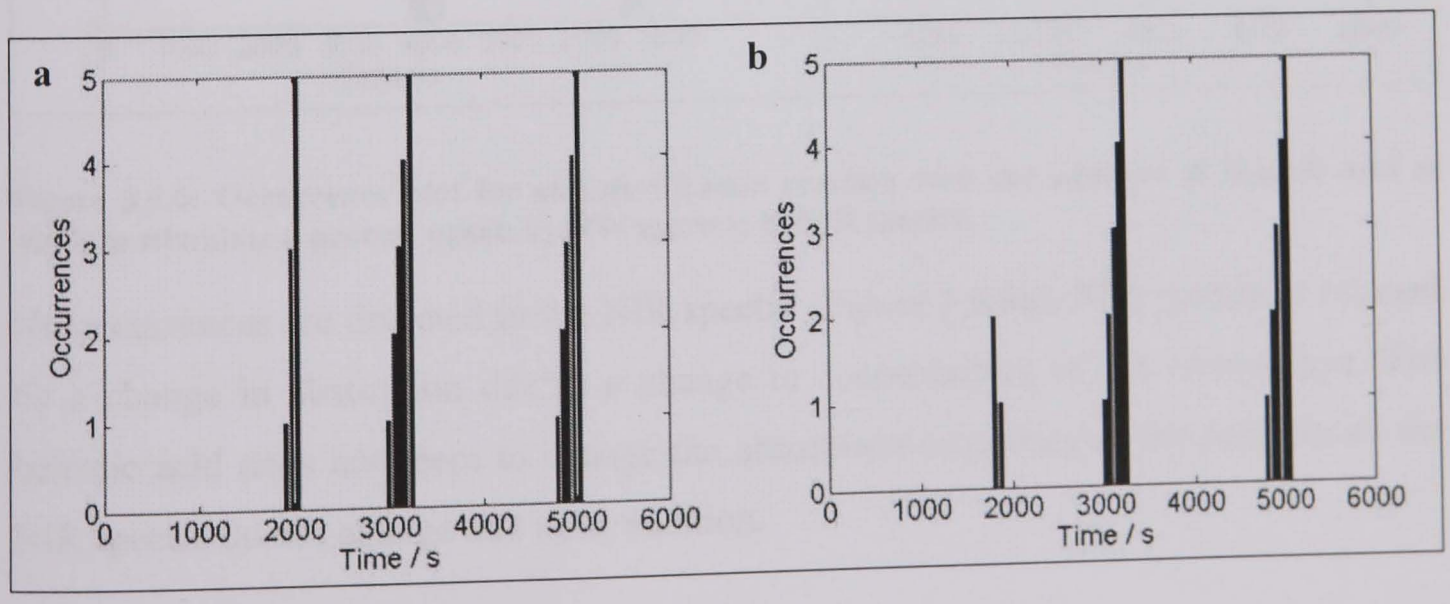

Figure 3.6.5: Occurrence plot for an esterification reaction with the addition of water at 1800 (5ml), 2990 (7.5ml) and 4790s (10ml) to stimulate a process upset; a) using MW spectra; b) using NIR spectra.

There are also three events identified in the NIR spectra (Figure 3.6.5b), however the first event appears be more like a false alarm as it starts at two and moves to an occurrence of one. There is no clear build up of the occurrence. The other two additions of water are clearly detected at 3000 and 4800s. Water strongly absorbs in the NIR region, so it is expected that the spectra will clearly change due to water.

3.6.2.5 Addition of benzoic acid

Benzoic acid (2g / 0.45%w/v) was added to the reaction at 3800s to simulate the charging of incorrect reactants. Figure 3.6.6a shows the occurrence plot for the MW spectra. The addition of benzoic acid is seen as an upset at around 3800s. There is also an event detected later in the reaction. This was not a stimulated upset, but could perhaps be due to a secondary effect of the addition of the benzoic acid. The benzoic acid is added as a solid so it may take time to dissolve and have an effect on the reaction. The addition of the benzoic acid will change the dielectric constant of the reaction mixture, and hence the MW spectra recorded.

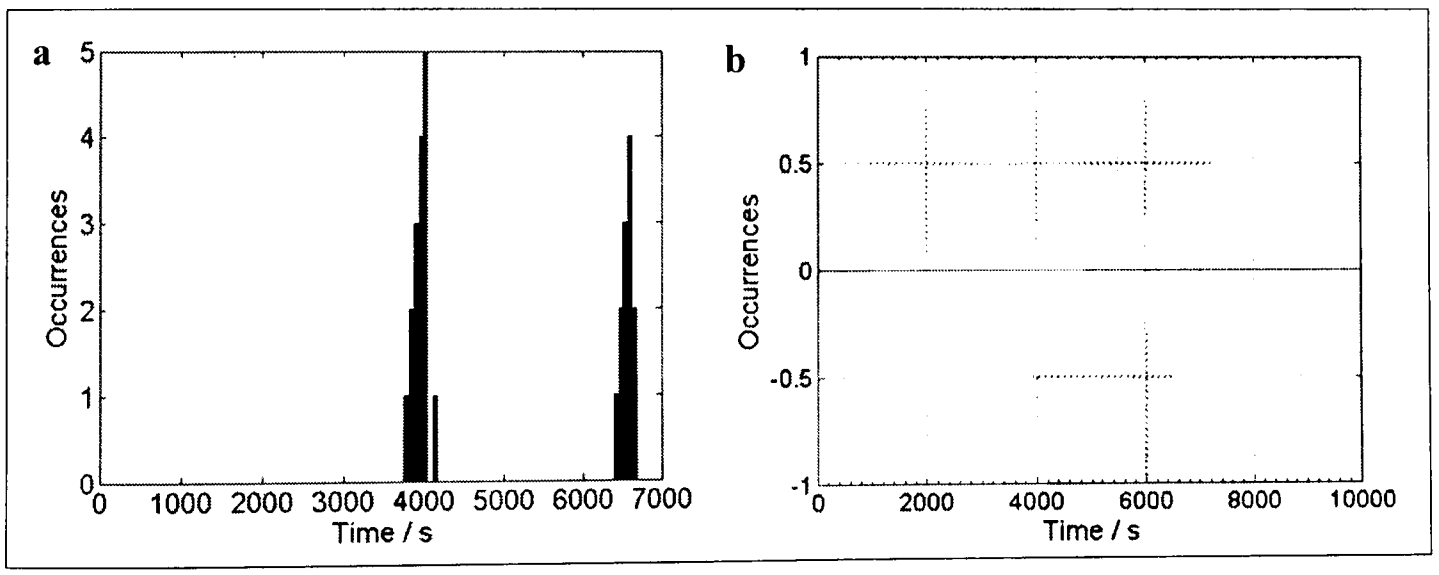

Figure 3.6.6: Occurrence plot for an esterification reaction with the addition of benzoic acid at 4000s to stimulate a process upset; a) MW spectra; b) NIR spectra.

No occurrences are detected in the NIR spectra (Figure 3.6.6b). NIR spectra is affected by a change in absorption due to a change in concentration of the components. The benzoic acid does not seem to change the absorption properties of the mixture, so the NIR spectra do not change due to its addition.

3.6.2.6 Disturbance of stirrer

Two reactions were carried out in which the stirrer is disturbed. In the first, *Ester_upset_stirrer_1*, the following disturbances occurred:

Table 3.6.1: Disturbance cause by altering the stirrer during the esterification reaction *ester_upset_stirrer_1*.

Time / s	Disturbance
1500	stirrer switched off
1860	stirrer switched on
2460	stirrer turned up to 2
3180	stirrer turned down to 1
5400	stirrer switched off
6000	stirrer switched on

When using a WS of five and two PCs, no occurrences are seen in the MW data. When looking at the occurrences for the NIR data (Figure 3.6.7), an occurrence is seen at 2550s, but this appears to be a false alarm as it only reaches an occurrence of one. There is another upset at 6000s, and at 6450s. Neither of these coincide with a stimulated process upset. It could be that a lag occurs before the effect of switching off the stirrer is seen, but this seems unlikely.

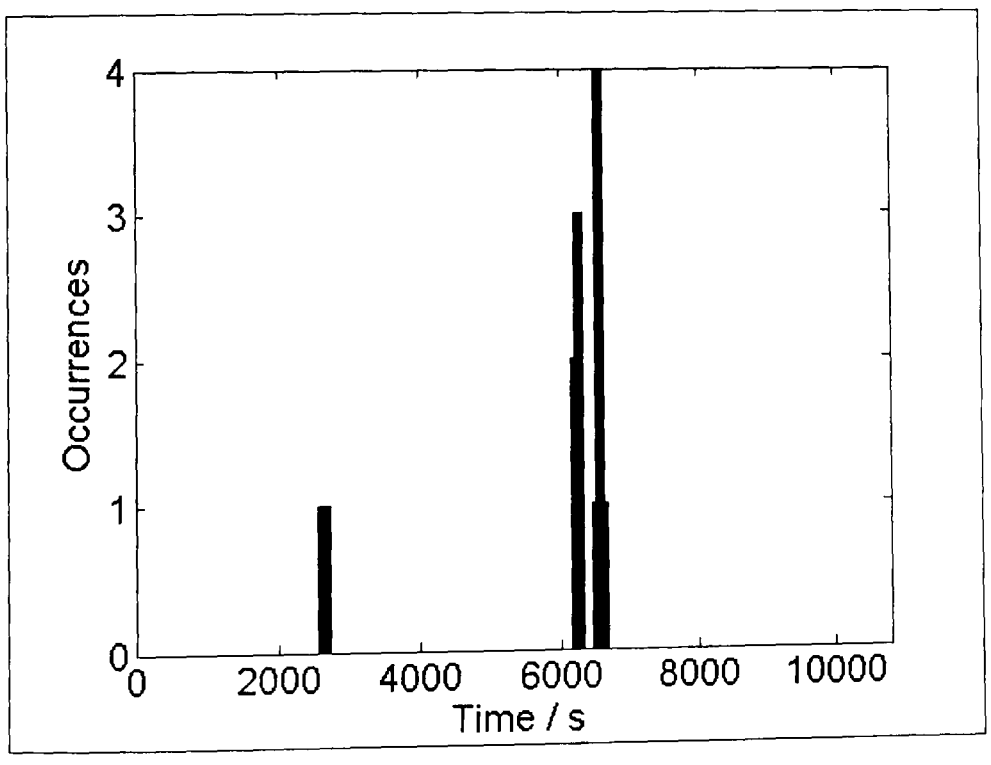

Figure 3.6.7: Occurrence plot for the esterification reaction with stirrer disturbance as a stimulated upset for NIR spectra.

The reaction was repeated in which the stirrer was switched off for longer periods to see if it could be identified as a process upset. In the second reaction, *Ester_upset_stirrer_2*, the following disturbances occurred:

Table 3.6.2: Disturbance cause by altering the stirrer during the esterification reaction *ester_upset_stirrer_2*.

Time / s	Disturbance	
600	stirrer switched off	stirrer off for 3 min
780	stirrer switched on	
1380	stirrer switched off	stirrer off for 5 min
1680	stirrer switched on	
2280	stirrer switched off	stirrer off for 6 min
2640	stirrer switched on	
3240	stirrer switched off	stirrer off for 7 min
3660	stirrer switched on	
4260	stirrer switched off	stirrer off for 8 min
4740	stirrer switched on	
5360	stirrer switched off	stirrer off for 9 min
5880	stirrer switched on	
6660	stirrer switched off	stirrer off for 10 min
7260	stirrer switched on	
7860	stirrer switched off	stirrer off for 15 min
8760	stirrer switched on	

This time the stirrer was switched off for increasing lengths of time. The resulting occurrences are shown in Figure 3.6.8.

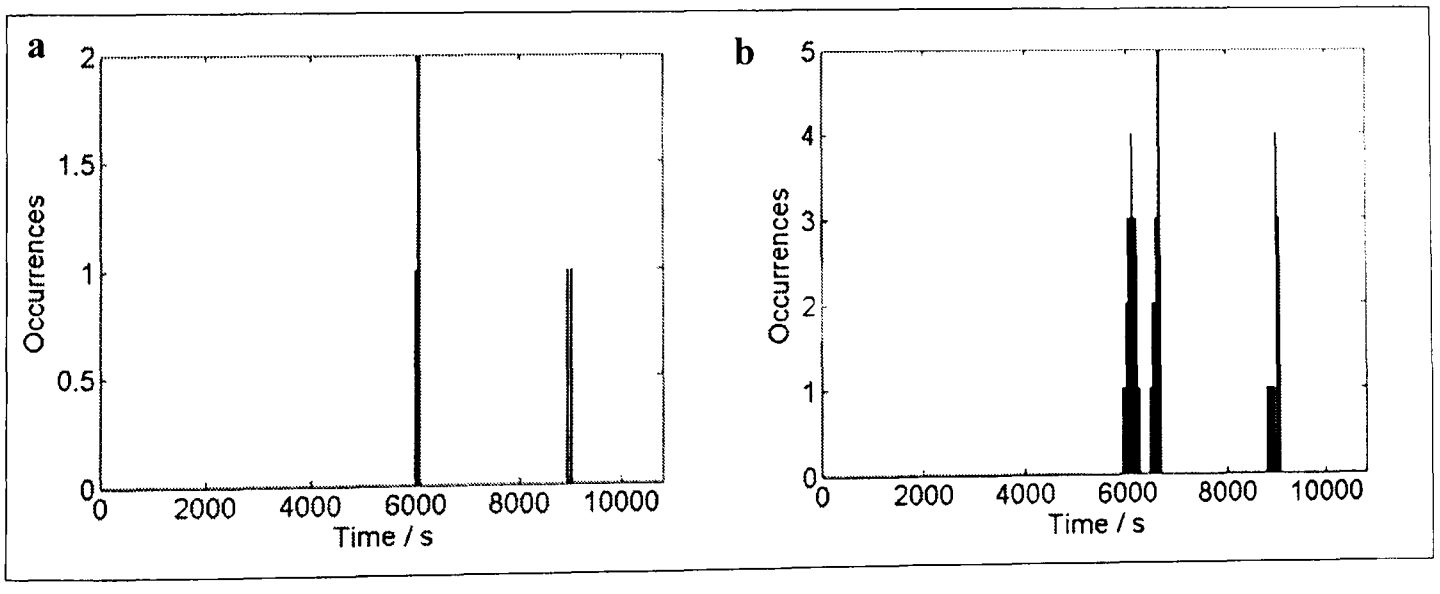

Figure 3.6.8: Occurrence plot for the disturbance of stirrer process upset a) MW spectra, b) NIR spectra.

From the MW spectra (Figure 3.6.8a) only false alarms are detected as the greatest number of atypical samples detected is two out of five. In the NIR spectra (Figure 3.6.8b) more obvious process upsets are identified. The first is seen at 5900s which coincides with the stirrer being switched back on after 9 minutes. The second is at 6450s, which does not coincide with any of the stimulated upsets. The third is at 8800s, which is just after the stirrer was switched on after 15 minutes. This would mean that no

effect was seen when the stirrer was switched off for 10 minutes. It therefore appears that the effect of the stirrer being switched on and off is not detected, but some other interference in the reaction.

It was not expected that the disturbance of the spectra can be identified as a process upset. For an upset to be determined it must affect the spectra, and cause atypical variation. The disturbance of the stirrer will not affect the spectra as it does not alter the composition of the reaction.

3.6.3 Conclusions

In this work, the esterification of butanol by acetic acid has been monitored by NIR and MW spectroscopy. Various process upsets have been stimulated, and the resulting spectra analysed using a new algorithm called caterpillar. This is an adaptive algorithm which can be used to identify such process upsets. This has the advantage of being suitable for dynamic processes as the algorithm analyses the spectroscopic data directly and no static model is built.

The use of caterpillar has been demonstrated using MW spectra to identify the incorrect addition of catalyst, addition of water, insufficient charging of reactants and the addition of an interferant, benzoic acid, as process upsets during the reaction. Caterpillar has also been used with NIR spectra of the same process, which only picks up some of these upsets, but not all, so has limited use in this application. Neither technique was able to detect disturbances to the stirrer. MW spectroscopy has been shown to be much more sensitive to small variation in the process, and has the advantage that the entire reaction volume is monitored. The occurrence of an upset can be detected, but not the cause of the upset. Other techniques are needed to determine the cause of the upset and allow identification of the remedial action necessary.

4.0 Conclusions

In this work guided microwave spectroscopy (GMS) and near infrared (NIR) spectroscopy have been used to monitor two typical industrial processes namely drying of a solid material, and the monitoring of an esterification reaction. Both processes have monitoring issues, but the main issue is that of sampling. The process must be sampled in such a way as to give a sample that is representative of the entire process.

Traditional techniques may involve removing a sample from the process and analysing it off-line. This is especially difficult in drying and so methods involving analysis of the off-gases have been developed. It takes time between sampling and the analytical results, so these methods are generally used to check the final product is within specification and not to control the process. Process analytical techniques, such as NIR and MW spectroscopy produce no waste, are quicker, safer and measurements are made on-line, in real-time so can be used to monitor and control the process.

NIR spectra record the change in absorption due to the components present. As the relative amounts of the components change, a change in the recorded spectra is seen. Microwave (MW) spectra record the change in dielectric constant of the reaction mixture as the reaction proceeds. Each component has a different dielectric constant, and as the concentrations of these change so does the relative dielectric constant of the mixture, therefore these techniques are suitable for monitoring evolving processes.

NIR spectroscopy is a widely used and well understood technique, and many examples exist of applications of NIR in the field of process analysis. It is relatively easy to relate the spectra of a process to how the process is proceeding. GMS has only been used for a couple of process analysis applications, and the technique is less understood. The process spectra are much harder to interpret and relate to the process. It was hoped using both techniques to monitor these processes would give a reference method, NIR, to which the MW spectra could be compared to aid interpretation of the process from the MW spectra.

4.1 Drying

The drying process was initially simulated by wetting a material with solvent to show the possibility of monitoring a drying process. Calibration models were built using the recorded MW spectra and NIR spectra to predict the amount of solvent present in the material.

The MW spectra were successfully used to predict the amount of solvent in a sample down to very low amounts (below 1% w/w) using a global model built with spectra pre-processed with auto-scaling followed by Box-Cox logarithmic transformation. This worked well for the prediction of water in sand and propanol in ascorbic acid, which gave prediction errors of 5% and 2% respectively. The global models were not as successful for the prediction of ethanol in salicylic acid which gave a prediction error of 32% for the global model. This could be due to problems in reproducibility of the experiments. This was seen in the PCA scores which show a large variation between the repeat experiments. It seems more likely that the limits of detection have been reached, and the method is not sensitive to such a low amount of ethanol. This would appear to be the case as the use of a local model for above 2% solvent gave much better errors of only 2% when using the auto-scaling and Box-Cox logarithmically transformed spectra. Models below 2% gave 23% error using Box-Cox logarithmically scaled data.

The NIR spectra collected were not representative of the process as a diffuse reflectance probe was used. This only measures a small area of the sample and is reliant on the solvent spreading through the sample to the area the probe is measuring. The NIR should be capable of measuring a true drying process as the solvent is being removed in a more continuous manner. Unfortunately the NIR probe could not be used to monitor the drying process due to limitations of space within the GMS chamber.

During the wetting process, the solvent is added in steps and it must then seep though the material. Effectively two processes are occurring and both are monitored successfully by the GMS. The wetting experiments have shown the possibility of building calibration models to predict the amount of solvent present.

An actual drying process was also monitored by MW spectroscopy to show that the true process can be monitored. These experiments lack reference concentration data, so can only give an indication of the possibility of monitoring the process. The use of the PCA

scores plotted against time and the calculated residual spectra showed the possibility of monitoring the drying process using MW spectroscopy. These experiments did not reach completion, but do show the possibility of the technique. Drying is a continuous process and has been shown to be monitored successfully.

Industrial drying processes involve either fluid bed dryers or pressure filtration units. Both have problems of monitoring the process due to huge cakes of material being dried. Visual inspection of the material may be carried out to determine if it is dry, but only the top layer of the material can be seen so this is not a good way to determine if it is dry. A sample may be removed and analysed, but this is unlikely to be representative of the entire process. York *et al.* [91] have used electrical tomography to provide a 3D model of the drying process. This involves the use of sensors located around the vessel to monitor the process. Green *et al.* [93] have used NIR to monitor drying, and found that sampling is the main issue.

MW spectroscopy has the advantage over these methods as the whole sample is analysed so a truly representative model is produced of the drying process. MW provides quick, non-invasive and non-destructive analysis, so is much better than analysing a sample by wet chemistry as traditionally is done. Also the MW has been proved to measure very small amounts of solvent in the sample, down to 1% w/w so can monitor a sample until it is almost completely dry. This process has only been monitored using small amounts of powder, less than 150g. True industrial drying processes are on huge scales. Further work is needed to determine how large a sample can be analysed, and if it is possible to simply attach the microwave antenna to either side of a process vessel to monitor the process.

4.2 Esterification reactions

The set-up of the equipment was examined to ensure the optimum conditions to collect reproducible spectra were used. The volume of sample in the GMS chamber was examined and it was found the GMS chamber should be as full as possible, and the volume used kept constant as the amount of air present affects the spectra. It is also important to regulate the temperature to give reproducible spectra.

During this work it was found difficult to find a reference measurement that was suitable and reproducible to monitor the studied reaction. GC had been used to measure

the concentration of the components of the esterification reaction of butanol and acetic acid studied in this work. This was found to be a hard method to develop and problems were found in the reproducibility of the method to monitor a reaction. There is a high error in this method.

The rate constants, *k*, were determined using GC monitoring and also from MW and NIR spectra using multivariate curve resolution (MCR). This extracts concentration profiles for the reaction components without the need for reference data. The *k* values determined by the different techniques do not agree, and it is not known which of these calculated values is the true one for the reaction studied. There does not appear to be published rate constants for this reaction using exactly the same rate constants. The *k* values calculated for repeat reactions are fairly reproducible for each technique. This indicates the MW and NIR spectra recorded are reproducible as the underlying variation can be used to extracted reproducible *k* values using MCR. The system has been proven to work and very reproducible spectra can be collected.

Traditional monitoring systems involve building a model to calibrate the spectra to concentration data to allow the process progress to be monitored [83, 97]. Model building is a long process and the model is only valid whilst the process is operating under the same conditions. The model is only as good as the samples used to build it. Samples are often made up in the laboratory which may not be fully representative of the process. Ideally real process samples should be used but these rely on a reliable, reproducible reference method. Methods such as GC may be used to provide this reference concentration data.

MCR methods can extract concentration profiles from spectral reaction data without the need for reference concentration data so has the advantage over traditional methods in that no tedious model must be built. This gives a reaction profile to allow monitoring of the progress of the reaction, and the endpoint can be determined. These methods can be use in real-time and are batch independent as a model is not built, but concentration profiles are extracted from the underlying spectral variation. Within this work, MCR has been used to extract the concentration profiles, but due to an unreliable reference method it is not known which of these are the true profiles. The potential for the use of MCR has been proved as reproducible profiles can be extracted from repeat spectra.

Previous work proves that MCR is a reliable method for monitoring reactions by extraction of reaction profiles. For example, Richards *et al.* [100] used MCR-ALS with IR spectra to extract the concentration profiles of a reaction The extracted results showed good agreement with the reference HPLC data. Blanco *et al.* [98] used MCR to monitor an esterification reaction by NIR, and found the extracted concentration profiles showed good agreement with the GC reference data.

The endpoint of a reaction must first be defined as it is a subjective term. Repeats of reactions with the same conditions have been examined for both NIR and MW data and an adaptive algorithm, caterpillar, used to determine the endpoint of the reaction. Repeats of the same reaction should have the same endpoint.

The endpoint was determined reproducibly from the MW spectra for one set of repeat spectra. The NIR spectra gave a slightly later endpoint, around 500s later, and it is thought this could be due to the localised nature of the NIR probe used. The endpoint was not determined reproducibly for another set of reactions which were carried out using a molar ratio that doesn't favour equilibrium. This shows the limits of the algorithm with the reaction studied, which may have not reached the endpoint.

The calibration free method used is caterpillar which does not require a static model to be built so can be used to monitor reactions and determine endpoints much quicker. It is adaptive so it is not necessary to build a new model should the reaction conditions change. This makes it a much more suitable method for monitoring dynamic processes than traditional model building.

During the esterification reaction, various process upsets were stimulated, and the resulting spectra analysed using the caterpillar algorithm. The use of caterpillar has been demonstrated using MW spectra to identify the incorrect addition of catalyst, addition of water, insufficient charging of recants and the addition of an interferant, benzoic acid, as process upsets during the reaction. Caterpillar has also been used with NIR spectra of the same process, which only picks up some of these upsets, but not all, so has limited use in this application. Neither technique was able to detect disturbances to the stirrer. MW spectroscopy has been shown to be much more sensitive to small variations in the process, and has the advantage that the entire reaction volume is monitored. The occurrence of an upset can be detected, but not the cause of the upset.

Other techniques are needed to determine the cause of the upset and allow identification of the remedial action necessary.

Previous methods for fault detection during processes include the use of SIMCA [84]. This involves building a static model to model the normal operating state of a process. New samples are compared to this model and any deviations from the model interpreted as a process change or upset. However, this may interpret normal process variation as an upset, so is only suitable for steady state reactions.

Caterpillar is an adaptive algorithm that is batch independent, so normal process variation is not identified as process upsets. This is a suitable algorithm for dynamic processes, and reduces the number of false alarms. Also no static model is needed to be built, so time is saved in this way. Once the method is optimised on a reaction with only normal process variation, it can be used in real-time to allow monitoring of the reaction and upsets can be corrected for.

Previous monitoring for esterification reaction has involved the use of Raman spectroscopy [18]. The main problem with this technique is that fluorescence interferes with the spectra, masking the variation due to the process. NIR and MW do not have these problems so the spectra are easy to relate to the process. Also, water is virtually invisible to Raman, so cannot be used to monitor the water production during the esterification reaction unlike NIR and MW [26].

4.3 Overall conclusions

The original aim of the work was to use well understood NIR spectra which can easily be related to reaction progress as a reference method to aid interpretation and correlation of MW spectra to the process variation. In fact MW spectroscopy has been found to provide more information regarding a process, mainly due to it measuring the entire sample so giving a representative measurement of the process. MW spectroscopy has been found to be a more sensitive technique for detection of process upsets. It can measure both chemical and physical properties of a reaction so can provide more information about a process than NIR, which only provides chemical information.

The main error in calibration is in sampling. Without representative samples, the sampling error typically amounts to 10-100 times the analytical errors associated with the chemical analysis [19]. If the need for sampling can be removed, then the error will

be reduced. It has been proved in this work that both MW and NIR can provide reproducible spectra relating to the variation seen in the process. The quality of the data collected is not a problem, but sampling is still an issue.

GMS removes the need for sampling as the whole process sample is measured. The microwaves penetrate into the sample and are reflected by the stainless steel walls of the sampling chamber. This ensures the entire sample is measured. NIR has low analytical error and this can be seen in the spectra collected during this research which has been found to be highly reproducible. However, the main issue with NIR is sampling as a probe must be used which only sample a small area.

NIR is a limited technique due to its sensitivity to hydrogen bonding which affects the spectra by changing the wavenumber at which a species absorbs. This appears to make the spectra harder to relate to the process, and deconvolute into its principal parts of concentration and spectral profiles.

Both techniques provide quick, non-destructive methods for analysis. Real-time measurement can be made to allow the process to be monitored and corrected for if necessary to ensure the batch is right first time. If samples are removed from the process, time is wasted waiting for the analytical results, and the results are used retrospectively to provide the quality of the process, and not used to control it.

Traditional model building involves building models using reference data which may be difficult to obtain and takes time. In this work the use of the calibration free techniques of MCR and caterpillar have been demonstrated to be useful in the monitoring of a simple esterification reaction. MCR extracts concentration profiles from reaction data without the need for reference concentration data. Caterpillar is an adaptive algorithm which can detect process upsets and the endpoint of a reaction. No model is built so time is saved, and the algorithm appears to be batch independent.

5.0 Further work

All processes were monitored in a rectangular chamber. This may present problems for homogenous mixing, which may be a reason for the NIR probe used not capturing the same process variation as the MW. The NIR only samples a small area of the process, so if it is not homogenous then it will not capture the true process, whereas the MW measures the whole sample so homogeneity is not an issue. To ensure the process is homogenous a round bottom flask should be used which can encompass the NIR probe and the MW antenna to ensure a homogenous process is measured.

Temperature control was a problem within the GMS sample chamber due to it being made of stainless steel. Design of a new reaction vessel would include better temperature control. This would allow the effect of temperate to be more easily studied.

Multivariate curve resolution has been used to extract concentration profiles to allow monitoring of an esterification reaction using MW and NIR spectra. This was compared to GC data but due to this method being difficult to develop, the methods are not comparable. The GC method was not found to be reproducible, so it is unknown which of the methods, if any, provide the correct reaction profiles. Further work is necessary to determine the true reaction profiles. This would involve developing a much more reliable reference method, and also ensuring that the samples removed from the reaction are representative, and no further reaction occurs once removed.

The processes investigated here have been on small laboratory scales. The drying process has involved amounts of sample below 150g, and the esterification reactions were run on a 450ml scale. GMS has been shown to be a useful process analyser for these processes as it analyses the whole process to give a reproducible model. In industry these reactions are carried out on much larger scales. Therefore further work is needed to determine how large a scale of process could be monitored by GMS. The GMS chamber can be used as a process pipe to allow the monitoring of a process as it is passed through the pipe. Ideally the GMS antenna should simply be placed at either side of a vessel to allow monitoring of the process.

The drying process monitored did not reach completion. Further work is needed to design a better system to mimic a drying process. The process should be monitored to completion to ensure the full process can be monitored using MW spectroscopy.

6.0 References

[1] Y. Kim, M. Singh, and S.E. Kays, *Near-infrared spectroscopy for measurement of total dietary fiber in homogenized meals*, Journal of Agricultural and Food Chemistry, **2006** 54(2), p292-298.

[2] S. Kasemsumran, N. Kang, A. Christy, and Y. Ozaki, *Partial least squares processing of near-infrared spectra for discrimination and quantification of adulterated olive oils*, Spectroscopy Letters, **2005** 38(6), p839-851.

[3] M. Sohn, D.S. Himmelsbach, D.E. Akin, and F.E. Barton, *Fourier transform near-infrared spectroscopy for determining linen content in linen/cotton blend products*, Textile Research Journal, **2005** 75(8), p583-590.

[4] T. Norris, and P.K. Aldridge, *End-point determination on-line and reaction co-ordinate modelling of homogeneous and heterogeneous reactions in principal component space using periodic near-infrared monitoring*, Analyst, **1996** 121(8), p1003-1008.

[5] M. Blanco, and M. Alcala, *Content uniformity and tablet hardness testing of intact pharmaceutical tablets by near infrared spectroscopy - A contribution to process analytical technologies*, Analytica Chimica Acta, **2006** 557(1-2), p353-359.

[6] L. Liang, R.C. Anantheswaran, M.J. Bradley, and B.R. Long, *Characterization of guided microwave spectrometry using water-ethanol mixtures*, Journal of Microwave Power and Electromagnetic Energy, **2002** 37(1), p3-13.

[7] P. Worsfold, A. Townshend, and C. Poole, *Encyclopaedia of analytical science 2nd edition*, Elsevier Academic Press: Oxford, (2005).

[8] J.B. Callis, D.L. Illman, and B.R. Kowalski, *Process analytical chemistry*, Analytical Chemistry, **1987** 59(9), p624A-637A.

[9] Center for Process Analytical Chemistry website, *http://www.cpac.washington.edu*, Viewed on 15.3.06.

[10] Centre for Process Analytics and Control Technologies website, *http://www.cpact.com*, Viewed on 15.3.06.

[11] D.A. Burns, and E.W. Ciurczak, *Handbook of near-infrared analysis*, Mercel Dekker Inc.: New York, (2001).

[12] M.T. Riebe, and D.J. Eustace, *Process analytical chemistry - an industrial perspective* Analytical Chemistry, **1990** 62(2), p65A-71A.

[13] N.S. Sahni, T. Isaksson, and T. Næs, *The use of experimental design methodology and multivariate analysis to determine critical control points in a process*, Chemometrics and Intelligent Laboratory Systems, **2001** 56, p105-121.

[14] D.L. Massart, B.G.M. Vandeginste, L.M.C. Buydens, S.E. De Jong, P.J. Lewi, and J. Smeyers-Verbeke, *Handbook of chemometrics and qualimetrics: Part A*, Elsevier: Amsterdam, (1997); Vol. 20A.

[15] M. Koch, *Reasons behind the current trends in process analysis*, Process control and quality, **1994** 6(1), p3-7.

[16] J.J. Workman, D.J. Veltkamp, S. Doherty, B.B. Anderson, K.E. Creasy, M. Koch, J.F. Tatera, A.L. Robinson, L. Bond, L.W. Burgess, G.N. Bokerman, A.H. Ullman, G.P. Darsey, F. Mozayeni, J.A. Bamberger, and M.S. Greenwood, *Process analytical chemistry*, Analytical Chemistry, **1999** 71(12), p121R-180R.

[17] R. Kellner, J.-M. Mermet, M. Otto, and H.M. Widmer, *Analytical chemistry*, Wiley-VCH: Weinheim, (1998).

[18] R.J. Ampiah-Bonney, and A.D. Walmsley, *Monitoring of the acid catalysed esterification of ethanol by acetic acid using Raman spectroscopy*, The Analyst, **1999** 124, p1817-1821.

[19] L. Peterson, P. Minkkinen, and K.H. Esbensen, *Representative sampling for reliable data analysis: Theory of Sampling*, Chemometrics and Intelligent Laboratory Systems, **2005** 77(1-2), p261-277.

[20] K.J. Clevett, *Process analytical chemistry - Industry perspectives - Trends in applications and technology*, Process control and quality, **1994** 6(2-3), p81-90.

[21] D. Hassell, and E.M. Bowman, *Process analytical chemistry for spectroscopists*, Applied Spectroscopy, **1998** 52(1), p18A-29A.

[22] M. Amrhein, B. Srinivasan, D. Bonvin, and M.M. Schumacher, *Calibration of spectral reaction data*, Chemometrics and Intelligent Laboratory Systems, **1999** 46, p249 - 264.

[23] F. McLennan, and B.R. Kowalski, *Process analytical chemistry*, Chapman & Hall: Glasgow, (1995).

[24] A.C. Quinn, P.J. Gemperline, B. Baker, M. Zhu, and D.S. Walker, *Fiber-optic UV / visible composition monitoring for process control of batch reactions*, Chemometrics and Intelligent Laboratory Systems, **1999** 45, p199-214.

[25] C.C. Felicio, L.P. Bras, J.A. Lopes, L. Cabrita, and J.C. Menezes, *Comparison of PLS algorithms in gasoline and monitoring with MIR and NIR*, Chemometrics and Intelligent Laboratory Systems, **2005** 78(1-2), p74-80.

[26] E.N.M. van Sprang, H.J. Ramaker, H.F.M. Boelens, J.A. Westerhuis, D. Whiteman, D. Baines, and I. Weaver, *Batch process monitoring using on-line MIR spectroscopy*, Analyst, **2003** 128(1), p98-102.

[27] R. Belchamber, Acoustics - a process analytical tool, *Spectroscopy Europe Process Column*, 2003; Vol. 15(6).

[28] G.R. Flåten, and A.D. Walmsley, *Tracking process changes in a fluidised bed using acoustic sensors*, Chemometrics and Intelligent Laboratory Systems, **IN PRESS**.

[29] J.C. Lindon, G.E. Tranter, and H.J. L., *Encyclopaedia of spectroscopy and spectrometry, vol. 2*, Academic Press: (2000).

[30] M.C. Yappert, *Near Infrared (NIR) spectroscopy in the undergraduate chemistry curriculum* Journal of Chemical Education, **1999** 76(3), p315–316.

[31] W.F. McClure, *Near-infrared spectroscopy: The giant is running strong*, Analytical Chemistry, **1994** 66(1), p43A - 51A.

[32] I. Zilberman, and J. Bigman, *Use of telecommunications for real-time process control*, Hydrocarbon Processing, **1996** 75(5), p91 - 95.

[33] L. Kane, and S. Romanow-Garcia, *Fiber optics improves NIR process analysis*, Hydrocarbon Processing, **1995** 74(11), p37 -38.

[34] N.K. Afseth, V.H. Segtnan, B.J. Marquardt, and J.P. Wold, *Raman and near-infrared spectroscopy for quantification of fat composition in a complex food model system*, Applied Spectroscopy, **2005** 59(11), p1324-1332.

[35] A.S. El-Hagrasy, and J.K. Drennen, *A Process Analytical Technology approach to near-infrared process control of pharmaceutical powder blending. Part III: Quantitative near-infrared calibration for prediction of blend homogeneity and characterization of powder mixing kinetics*, Journal of Pharmaceutical Sciences, **2006** 95(2), p422-434.

[36] R. Liu, B. Deng, W.L. Chen, and K.X. Xu, *Next step of non-invasive glucose monitor by NIR technique from the well controlled measuring condition and results*, Optical and Quantum Electronics, **2005** 37(13-15), p1305-1317.

[37] Y. Zhang, L.N. Lu, and K.X. Xu, *Research on non-invasive blood glucose measurement with simulate sample by NIR spectroscopy*, Spectroscopy and Spectral Analysis, **2005** 25(4), p512-515.

[38] J.C. Pickup, F. Hussain, N.D. Evans, and N. Sachedina, *In vivo glucose monitoring: the clinical reality and the promise*, Biosensors & Bioelectronics, **2005** 20(10), p1897-1902.

[39] R. Liu, W.L. Chen, X.Y. Gu, R.K.K. Wang, and K.X. Xu, *Chance correlation in non-invasive glucose measurement using near-infrared spectroscopy*, Journal of Physics D-Applied Physics, **2005** 38(15), p2675-2681.

[40] H.Y. Zhang, D. Ding, L.Q. Song, L.N. Gu, P. Yang, and Y.G. Tang, *Achievement of the non-invasive measurement for human blood glucose with NIR diffusion reflectance spectrum method*, Spectroscopy and Spectral Analysis, **2005** 25(6), p882-885.

[41] A. Townshend, and P.J. Worsfold, *Encyclopaedia of analytical science*, Academic Press: London, (1995).

[42] C.E. Cleeton, and N.H. Williams, *Electromagnetic waves of 1.1 cm. wave length and the absorption spectrum of ammonia* Physical Review, **1934** 45, p234-237.

[43] D.J.E. Ingran, *Spectroscopy at radio and microwave frequencies, Second edition*, Butterworths: London, (1967).

[44] F. Thompson, *Non-destructive moisture measurement using microwaves*. Materials Science Forum, **1996** 210, p85-92.

[45] W. Meyer, and W. Schilz, *A microwave method for density independent determination of the moisture content of solids*, Journal of Physics D: Applied Physics, **1980** 13, p1823-1830.

[46] M. Kent, and W. Meyer, *A density-independent microwave moisture meter for heterogeneous foodstuffs*, Journal of Food Engineering, **1982** 1, p31-42.

[47] S. Trabelsi, and S.O. Nelson, *Non-destructive sensing of bulk density and moisture content in shelled peanuts from microwave permittivity measurements*. Food control, **2006** 17, p304-311.

[48] H. Kaarianinen, M. Rudolph, D. Schaurich, K. Tulla, and H. Wiggenhauser, *Moisture measurements in building materials with microwaves*, NDT & E International, **2001** 34(6), p389-394.

[49] A.D. Walmsley, and V.C. Loades, *Determination of acetonitrile and ethanol in water by guided microwave spectroscopy with multivariate calibration*, Analyst, **2001** 126(4), p417-420.

[50] A.D. Dane, G.J. Rea, A.D. Walmsley, and S.J. Haswell, *The determination of moisture in tobacco by guided microwave spectroscopy and multivariate calibration*, Analytica Chimica Acta, **2001** 429(2), p185-194.

[51] J.L. Danielwicz, *Improved on-line measurement of water content and other product mixture ratios using microwave spectrum analysis*, Advances in Instrumentation and Control, **1992** 47, p617-632.

[52] Thermo Electron Corporation website, *http://www.thermo.com*, Guided Microwave Spectrometer guide, Viewed on 21.2.06.

[53] K. Kupfer, A. Kraszewski, and R. Knochel, *RF and microwave sensing of moist materials, food and other dielectrics*, Wiley-VCH: Weinheim, (2000); Vol. 7.

[54] *Epsilon Industrial Inc. Guided Microwave Spectroscopy Series Analyser Instruction Manual*, (1996).

[55] H. Martens, and T. Næs, *Multivariate calibration*. John Wiley & Sons: Chichester, (1989).

[56] H. Swierenga, F. Wulfert, O.E. de Noord, A.P. de Weijer, A.K. Smilde, and L.M.C. Buydens, *Development of robust calibration models in near infra-red spectrometric applications*, Analytica Chimica Acta, **2000** 411, p121 - 135.

[57] J.N. Miller, and J.C. Miller, *Statistics and chemometrics for analytical chemists - Fourth Edition*, Prentice Hall: Harlow, (2000).

[58] R.G. Brereton, *Chemometrics: Data analysis for the laboratory and chemical plant*, Wiley: Chichester, (2003).

[59] A. de Juan, and R. Tauler, *Chemometrics applied to unravel multicomponent processes and mixtures - Revisiting latest trends in multivariate resolution*, Analytica Chimica Acta, **2003** 500(1-2), p195-210.

[60] A. de Juan, Y.V. Heyden, R. Tauler, and D.L. Massart, *Assessment of new constraints applied to the alternating least squares method*, Analytica Chimica Acta, **1997** 346, p307-318.

[61] P.J. Gemperline, and E. Cash, *Advantages of soft vs. hard constraints in self-modeling curve resolution problems - Alternating Least-Squares with Penalty functions (P-ALS)*, Analytical Chemistry, **2003** 75, p4236-4243.

[62] M.J. Rodriguez-Cuesta, R. Boque, F.X. Rius, J.L.M. Vidal, and A.G. Frenich, *Development and validation of a method for determining pesticides in groundwater from complex overlapped HPLC signals and multivariate curve resolution*, Chemometrics and Intelligent Laboratory Systems, **2005** 77(1-2), p251-260.

[63] E. Pere-Trepat, S. Lacorte, and R. Tauler, *Solving liquid chromatography mass spectrometry coelution problems in the analysis of environmental samples by multivariate curve resolution*, Journal of Chromatography A, **2005** 1096(1-2), p111-122.

[64] M. Wasim, and R.G. Brereton, *Application of multivariate curve resolution methods to on-flow LC-NMR*, Journal of Chromatography A, **2005** 1096(1-2), p2-15.

[65] A. Pasamontes, and M.P. Callao, *Sequential injection analysis linked to multivariate curve resolution with alternating least squares*, Trac-Trends in Analytical Chemistry, **2006** 25(1), p77-85.

[66] M. Garrido, I. Lazaro, M.S. Larrechi, and F.X. Rius, *Multivariate resolution of rank-deficient near-infrared spectroscopy data from the reaction of curing epoxy resins using the rank augmentation strategy and multivariate curve resolution alternating least squares approach*, Analytica Chimica Acta, **2004** 515(1), p65-73.

[67] L.A. Mercado, M. Galla, J.A. Reina, M. Garrido, M.S. Larrechi, and F.X. Rius, *Reactivity of silicon-based epoxy monomers as studied by near-infrared spectroscopy and multivariate curve resolution methods*, Journal of Polymer Science Part a-Polymer Chemistry, **2006** 44(4), p1447-1456.

[68] B. Mertens, M. Thompson, and T. Fearn, *Principal component outlier detection and SIMCA - a synthesis*, Analyst, **1994** 119(12), p2777-2784.

[69] B.G.M. Vandeginste, D.L. Massart, L.M.C. Buydens, S.E. De Jong, P.J. Lewi, and J. Smeyers-Verbeke, *Handbook of chemometrics and qualimetrics: Part B*, Elsevier: Amsterdam, (1997); Vol. 20B.

[70] B.K. Lavine, *Chemometrics*, Analytical Chemistry, **2000** 72, p91R-97R.

[71] A.R. de Carvalho, M.D. Sanchez, J. Wattoom, and R.G. Brereton, *Comparison of PLS and kinetic models for a second-order reaction as monitored using ultraviolet visible and mid-infrared spectroscopy*, Talanta, **2006** 68(4), p1190-1200.

[72] D. Cozzolino, and A. Moron, *Potential of near-infrared reflectance spectroscopy and chemometrics to predict soil organic carbon fractions*, Soil & Tillage Research, **2006** 85(1-2), p78-85.

[73] M.C. Ortiz, L. Sarabia, R. Garcia-Rey, and M.D.L. de Castro, *Sensitivity and specificity of PLS-class modelling for five sensory characteristics of dry-cured ham using visible and near infrared spectroscopy*, Analytica Chimica Acta, **2006** 558(1-2), p125-131.

[74] Y. Ozaki, S. Sasic, and J.H. Jiang, *How can we unravel complicated near infrared spectra? - Recent progress in spectral analysis methods for resolution enhancement and band assignments in the near infrared region*, Journal of Near Infrared Spectroscopy, **2001** 9, p63 - 95.

[75] M.B. Seasholtz, and B. Kowalski, *Short communication: The effect of mean centring on prediction in multivariate calibration*, Journal of Chemometrics, **1992** 6, p103-111.

[76] G.E.P. Box, and D.R. Cox, *An analysis of transformations*, Journal of the Royal Statistical Society: Series B, **1964** 26, p211-252.

[77] G.R. Flåten, and A.D. Walmsley, *A design of experiment approach incorporating layered designs for choosing the right calibration model*, Chemometrics and Intelligent Laboratory Systems, **2004** 73, p55-66.

[78] F. Dieterle, S. Busche, and G. Gauglitz, *Different approaches to multivariate calibration of nonlinear sensor data*, Analytical and Bioanalytical Chemistry, **2004** 380(3), p383-396.

[79] S. Wold, H. Antti, F. Lindgren, and J. Őhman, *Orthogonal signal correction of near-infrared spectra*, Chemometrics and Intelligent Laboratory Systems, **1998** 44, p175-185.

[80] T. Fearn, *On orthogonal signal correction*, Chemometrics and Intelligent Laboratory Systems, **2000** 50, p47-52.

[81] M.A. Sharaf, D.L. Illman, and B.R. Kowalski, *Chemometrics*, Wiley-Interscience: New York, (1986); Vol. 82.

[82] G.R. Flåten, and A.D. Walmsley, *Using design of experiments to select optimum calibration model parameters*, Analyst, **2003** 128(7), p935-943.

[83] M. Blanco, and D. Serrano, *On-line monitoring and quantification of a process reaction by near-infrared spectroscopy. Catalysed esterification of butan- 1-ol by acetic acid*, Analyst, **2000** 125(11), p2059-2064.

[84] K. De Braekeleer, R. De Maesschalck, P.A. Hailey, D.C.A. Sharp, and D.L. Massart, *On-line application of the orthogonal projection approach (OPA) and the soft independent modelling of class analogy approach (SIMCA) for the detection of the end point of a polymorph conversion reaction by near infrared spectroscopy (NIR)*, Chemometrics and Intelligent Laboratory Systems, **1999** 46(2), p103-116.

[85] T. Kourti, and J.F. MacGregor, *Tutorial: Process analysis, monitoring and diagnosis, using multivariate projection models*, Chemometrics and Intelligent Laboratory Systems, **1995** 28, p3-21.

[86] B.M. Wise, and N.B. Gallagher, *The process chemometrics approach to process monitoring and fault detection*, Journal of Process Control, **1996** 6(6), p329-348.

[87] C. Undey, S. Ertunc, E. Tatara, F. Teymour, and A. Cinar, *Batch process monitoring and its application to polymerization systems*, Macromolecular Symposia, **2004** 206, p121-134.

[88] G.R. Flåten, R. Belchamber, M. Collins, and A.D. Walmsley, *Caterpillar - an adaptive algorithm for detecting process changes from acoustic emission signals*, Analytica Chimica Acta, **2005** 544, p280-291.

[89] University of Manchester website, *http://www.tomography.manchester.ac.uk/procemon_filtration.shtml*, Industrial process tomography at Manchester, Viewed on 1.3.06.

[90] B.D. Grieve, M. R., and T.A. York, The Application of 3-D electrical resistance tomography to production-scale solid-liquid pressure filters, *presented at APACT '03*, York, 2003.

[91] T.A. York, J.L. Davidson, L. Mazurkiewich, R. Mann, and B.D. Grieve, *Towards process tomography for monitoring pressure filtration*, IEEE Sensors Journal, **2005** 5(2), p139-152.

[92] Barr-Rosin website, *http://www.barr-rosin.com/english/products/fluid-bed-dryer.htm*, Fluid bed dryer, Viewed on 1.3.06.

[93] R.L. Green, G. Thurau, N.C. Pixley, A. Mateos, R.A. Reed, and J.P. Higgins, *In-line monitoring of moisture content in fluid bed dryers using near-IR spectroscopy with consideration of sampling effects on method accuracy*, Analytical Chemistry, **2005** 77(14), p4515-4522.

[94] P. Dallin, Obtaining process analytical information from drying processes using spectroscopic monitoring?, *presented at APACT '05*, Birmingham, 2005.

[95] P. Shering, Engineering a system to enable spectroscopy in a filter dryer. *Spectroscopy Europe Process Column*, 2005; Vol. 17(6).

[96] J. Daintith, *Oxford Dictionary of Chemistry, Third Edition*, Oxford University Press: (1996).

[97] C.A. McGill, A. Nordon, and D. Littlejohn, *Comparison of in-line NIR, Raman and UV-visible spectrometries, and at-line NMR spectrometry for the monitoring of an esterification reaction*, Analyst, **2002** 127, p287 - 292.

[98] M. Blanco, M. Castillo, R. Beneyto, and M. Porcel, *Use of multivariate curve resolution to monitor an esterification react by near-infrared spectroscopy*. Spectroscopy Letters, **2005** 38, p825-837.

[99] P. Gemperline, User's guide for GUIPRO, *http://personal.ecu.edu/gemperlinep/Research/gemper_software.html*, Viewed on 3.2.06.

[100] S. Richards, M. Ropic, D. Blackmond, and A. Walmsley, *Quantitative determination of the catalysed asymmetric hydrogenation of 1-methyl-6,7-dimethoxy-3,4-dihydroisoquinoline using in situ FTIR and multivariate curve resolution*. Analytica Chimica Acta, **2004** 519(1), p1-9.